Head Office: Università degli Studi di Padova

Department of Biology

Ph.D. COURSE IN: BIOSCIENCE

CURRICULUM: BIOCHEMISTRY AND BIOTECHNOLOGY

SERIES: XXX°

Genetic engineering approaches to increase microalgae light use efficiency

PhD work supported by

"Centro studi di economia e tecnica dell'energia Giorgio Levi Cases", Università di Padova

Coordinator: Ch.mo Prof. Ildikò Szabò

Supervisor: Ch.mo Prof. Tomas Morosinotto

Ph.D. student : Alessandra Bellan

Ai miei genitori e a Sara

TABLE OF CONTENTS

ABSTRACT

In the next fifty years world population will reach 9-10 billion of people. This increment will drastically increase energy and food demand. The current global food and energy supply chain is not sustainable and it causes increasing CO_2 emissions, exacerbating the greenhouse effect and the climate change, whose effects we are already experiencing. The Climate Change conference hold in Paris in 2015 showed a global consensus on the need to drastically reduce carbon emissions to avoid the environmental disaster, which is leading to many negative effects like desertification, animal and plants species extinction and ocean acidification.

In order to face this challenge different strategies are under study and development. Microalgae are emerging as an interesting possibility for the production of energy and food. Being photosynthetic organisms, algae biomass is produced from CO_2 fixation, and contains proteins, and lipids exploitable as food or fuel.

Despite their potential, microalgae production on a large scale is still not competitive on the food and energy market. One of the main limitation is that photosynthetic efficiency at the industrial scale is reduced, negatively affecting growth and biomass accumulation. All first attempts of algae large scale cultivation have been pursued cultivating wild type strains (WT) that evolved in an environment extremely different and thus they are not adapted to have a maximal productivity in the industrial system. As done with crops domestication, there is the need to modify genetically strains in order to adapt them to grow in industrial systems and increase productivity. There are different algal species that are emerging as promising candidates for food and fuel production and among them the largest part of this work is focused on *Nannochloropsis gaditana*, a marine microalga able to accumulate lipids and molecules like β-carotene interesting for nutraceutical purposes.

After a general introduction, chapter 2 described the generation of a collection of random mutants of *N.gaditana* exploiting two different mutagenic approaches, one based on the use of the mutagen compound Ethyl Methane Sulfonate (EMS) and the other one based on random insertion of a resistance cassette to zeocin. The collection was screened for strains altered in the photosynthetic apparatus using a multiple steps *in vivo* fluorescence analysis. In Appendix 1 I collaborated in evaluation of the productivity for one of these strains (E2) in a fed batch system mimicking an industrial culture. E2 was selected for a reduction in the chlorophyll content and also in the PSII antenna size. One of the

limitations in algae mass cultures is that light penetration negatively affects growth and thus a strain with a reduction in the light absorption capacity could have a productivity advantage. This work indeed showed that the strain E2 had increased productivity with respect to WT, but also highlighted the seminal influence of the cultivation parameters on strains performances.

Most of the PhD work was then invested on the characterization of two promising insertional strains. The first strain presented in chapter 3 is I29. This is a low chlorophyll (Chl) content mutant with no difference in the antenna size of PSII. In flask culture I29 showed a reduction of 20% in the Chl content respect to the WT, which leaded also to a higher electron transport rate (ETR). The site of insertion of the resistance cassette was identified but there was no apparent effect on transcription level of closest genes. The full genome of the strain was thus re-sequenced revealing a point mutation in a key gene involved in the chlorophyll biosynthetic pathway, a highly likely candidate to justify the phenotype. I29 in lab scale PBR was also assessed evidencing an increase in productivity of 14% with respect to the WT.

An analogous work was done in chapter 4 for the characterization of another interesting mutant from the collection isolated in chapter 2, the mutant I48. This mutant has a severe reduction in the non-photochemical quenching (NPQ) activation. The site of insertion was not identifiable because of the presence of tandem insertions and again the strain genome was re-sequenced highlighting the presence of point mutations due to electroporation. Among these we found an interesting one in the gene codifying for the protein LHCX1. This is a stress-related antenna protein which in other species like *Phaeodactylum tricornutum* has already been recognized as a key component of the fast NPQ response. The loss of the protein accumulation was confirmed by Western Blot. Strain response to different illumination conditions was also evaluated highlighting the ability of the mutant to grow also in high light condition. The last part of the characterization was devoted to productivity evaluation since a depletion of NPQ could be advantageous in an industrial condition of a dense culture, where only the external layer are exposed to intense light. A low NPQ phenotype can avoid undesired energy dissipation in the internal layers. We observed a 24% higher productivity for I48 respect to the WT but, as discussed in Appendix 1 this was dependent from growing conditions.

In diatoms NPQ has been associated not only to the high light response but also to the fluctuating light (FL) response, which is a condition easily experienced in outdoor

cultivation system. We take advantage from the isolation of this mutant with a severe reduction in NPQ to verify what can be the impact of NPQ in *N.gaditana* response. In chapter 5 we set up an experiment in which we exposed the cultures to 150 μmol of photons $m^{-2}s^{-1}$ but in the control sample the light intensity was constant, in FLs it was the result of a combination of a low light exposition with high light flashes given with different frequencies and duration. We found that those FL treatments caused a severe growth reduction in WT but I48 showed no increased sensitivity. The growth reduction was proportional to the flash frequency and stronger with higher flash frequency. An analysis of photosynthetic apparatus functionality evidenced that in FL PSII activity is not affected while PSI is largely inactivated. This suggests that alternatives electron transport around PSI, that are active in avoiding its over-excitation, are not as efficient in *N.gaditana* as in other organisms.

These first 5 chapters highlight the potential of microalgae engineering to find new strains more productive respect to the WT. FL experiment not only adds new knowledge about NPQ role in *N.gaditana*, but taking in count that FL is a condition easily found if we want to exploits sunlight in industrial system, it can be the starting point to find new gene targets to improve productivity. This work started with an insertional approach that in principle should facilitate identification of the genes responsible of the phenotype. In this case this advantage is impaired by the frequent presence of tandem insertions and accumulation of point mutations during transformation. Alternative strategies are thus more suitable and will be pursued in the future.

In chapter 6 we tested the chemical mutagenesis and the screening method set up for *N.gaditana* with *Scenedesmus obliquus* to evaluate if the approach could be generally applied to any species of interest. Indeed at least a strain with interesting properties was isolated (SOB17). In this work we also evaluated productivity in a flat panel in continuous mode. Indeed the geometry of a flat panel leads to a better light distribution and homogeneity respect to other system like the bottles. Moreover the continuous mode provides a stable culture continuously producing. This culture showed remarkable stability for more than 30 weeks and SOB17 showed a higher productivity in one of the conditions tested but, as observed for *Nannochloropsis gaditana* strains also in this case operational conditions were shown to have a fundamental influence on strains performances.

In addition to the Appendix 1 described above, other two appendix sections are also included in the thesis. They are the results of two different collaboration in which some of the experimental techniques exploited in this work were applied with different aims.

In Appendix II, there is the published work "Genetic Engineering of algae photosynthetic productivity using mathematical models" that describes the development of a mathematical model to evaluate the key factors influencing algae biomass productivity in PBR. The model was shown to be able to predict the effect of genetic modifications on algae performances in an industrial context, thus providing a valuable tool to identify the genotypes with the best advantages for productivity.

In Appendix III is reported the collaboration with Prof. Angela Falciatore (Diatom Functional Genomics team, at the UPMC-Paris). A screening procedure similar to those one set up for *N.gaditana* was adapted to search photosynthetic alterations in a collection of *Phaeodactylum tricornutum* transgenic lines genetically modified by the RNA interference approach, in order to modulate the expression of transcription factors (TF). Thank to this screening procedure we found some promising correlation between the genetic modulation of a class of TFs and the photosynthetic phenotype of mutants strains isolated. Now this correlation phenotype-TF expression level is under validation by confirming the screening phenotype and evaluating the transcripts level.

RIASSUNTO

Si stima che nei prossimi 50 anni la popolazione mondiale aumenterà fino a raggiungere i 9-10 miliardi di persone. Un incremento di queste proporzioni porterà inevitabilmente ad una maggior richiesta di produzione di cibo ed energia. L'attuale metodo di approvvigionamento di queste risorse non è sostenibile in quanto è la causa principale dell'aumento delle emissioni di CO_2 in atmosfera, le quali stanno alimentando il cambiamento climatico. Nella conferenza che si è tenuta a Parigi nel 2015 sul cambiamento climatico è emersa chiaramente la necessità di un cambio di tendenza per poter evitare il collasso ambientale, che sta già portando alla desertificazione di molti terreni un tempo fertili, all'estinzione di massa di specie animali e vegetali e all'acidificazione degli oceani. Per invertire questa tendenza quindi bisogna rivedere il nostro sistema di produzione alimentare ed energetica. Tra le possibilità al vaglio le microalghe stanno emergendo come un interessante candidato sia per la produzione di energia che di cibo. Infatti le microalghe sono organismi fotosintetici che producono biomassa fissando CO_2. Molte specie sono ricche di proteine e lipidi utilizzabili come nutrimento o come matrice per la produzione di biodiesel. Tuttavia nonostante le loro potenzialità le microalghe non sono ancora utilizzate su larga scala perché la loro produzione continua ad aver un costo troppo elevato a fronte di produttività insufficienti. Uno dei maggiori limiti è legato al calo di efficienza fotosintetica che si registra nel passaggio in scala industriale, la quale impatta negativamente sulla crescita delle microalghe e quindi sulla produzione di biomassa. Tuttavia bisogna tenere conto che ad ora si stanno coltivando ceppi *wild type*, che quindi si sono evoluti ed adattati per crescere al meglio in un ambiente naturale estremamente diverso da quello industriale. Perciò come si è fatto con la domesticazione delle piante per uso alimentare, sarà necessario un passaggio di ingegnerizzazione dei ceppi parentali per ottenere dei nuovi ceppi più adatti alle condizioni industriali e quindi più produttivi una volta coltivati su larga scala.

Ci sono svariate specie algali al vaglio come candidati per la produzione alimentare ed energetica, ma questo lavoro si focalizza principalmente su *Nannochloropsis gaditana*. Questa è una microalga marina capace di accumulare sia lipidi sia molecole di interesse per la nutraceutica come il β-carotene. Dopo una introduzione generale, nel capitolo 2 viene descritto l'ottenimento di una collezione di mutanti casuali generati attraverso due diversi approcci di mutagenesi. Il primo è un approccio di mutagenesi chimica, che utilizza come agente mutageno l'etil-metano-sulfonato (EMS) e il secondo è un approccio

di mutagenesi inserzionale che sfrutta l'inserimento casuale nel genoma di DNA esogeno che conferisca al ceppo la resistenza per la zeocina. Da questa collezione si sono isolati solo i mutanti alterati nell'apparato fotosintetico utilizzando cicli progressivi di selezione attraverso misure di fluorescenza in vivo. In Appendice 1 è riportata la collaborazione nella valutazione delle produttività di uno dei mutanti ottenuti con EMS (E2), in condizioni di semi continuo che mimano una coltura industriale. E2 è stato selezionato perché presentava un ridotto contenuto di clorofilla abbinato anche ad una riduzione del numero di proteine antenna legate al PSII. Infatti uno dei maggiori problemi su scala industriale è la scarsa penetrazione della luce, dovuta alle densità elevate raggiunte dalle colture, la quale ha un impatto negativo sulla produzione. Un mutante con una ridotta capacità di assorbimento della luce può essere vantaggioso perché migliora la distribuzione della luce nel sistema con un conseguente incremento nella crescita. Questo lavoro infatti dimostra come E2 sia più produttivo del WT, ma sottolinea anche che le condizioni di coltura sono fondamentali per utilizzare al meglio il potenziale del ceppo mutato.

La maggior parte di questa tesi è stata poi dedicata alla caratterizzazione di due ceppi promettenti ottenuti per mutagenesi inserzionale. Il primo è I29 ed è presentato nel capitolo 3. Questo mutante è stato selezionato perché presentava un ridotto contenuto di clorofilla anche se il numero di proteine antenna per PSII è analogo al WT. In beuta la coltura di I29 mostra un 20% in meno di clorofilla rispetto al WT, che si accompagna con un trasporto elettronico che si satura ad intensità di luce maggiori (maggiore ETR *electron transport rate*). Il sito di inserzione della cassetta è stato identificato come singolo, ma sembra non influenzare i livelli di trascrizione dei geni vicini. Il completo ri-sequenziamento del genoma ha evidenziato una mutazione puntiforme in un gene chiave nella biosintesi della clorofilla, che può essere un promettente candidato per giustificare il fenotipo di I29. Di questo mutante si è valuta anche la produttività e si è visto un incremento del 14% rispetto al WT.

Un lavoro analogo è stato fatto per il mutante I48, isolato sempre nel capitolo 2. Questo mutante ha una importante riduzione nell'attivazione dei meccanismi di dissipazione dell'eccesso di energia luminosa come calore (NPQ). Non è stato possibile individuare il sito di inserzione a causa della presenza di inserzioni multiple in tandem, perciò anche in questo caso il genoma è stato ri-sequenziato. Il sequenziamento ha evidenziato nuovamente la presenza di mutazioni puntiformi dovute al protocollo di trasformazione.

Tra queste è emersa una mutazione nel gene codificante per la proteina LHCX1. Questa è una proteina antenna coinvolta nella risposta allo stress luminoso, il cui ruolo chiave nella risposta rapida del NPQ è già stato evidenziato in altre specie come *Phaeodactylum tricornutum*. Il mancato accumulo di questa proteina è stato confermato attraverso *Western Blot*. Si è valutata la capacità di questo ceppo di crescere in diverse condizioni luminose. È emerso che I48 è in grado di crescere anche in alta luce nonostante questa riduzione nella risposta di NPQ. L'ultima parte della caratterizzazione ne ha valutato invece la produttività. Infatti una riduzione nel NPQ può essere vantaggiosa in condizioni industriali in quanto in una coltura densa solo lo strato esterno è esposto a luci intense. Perciò un NPQ ridotto può evitare una dissipazione indesiderata di energia negli strati più interni dove la luce è già limitante. I48 ha mostrato un aumento di produttività del 24% rispetto al WT, ma come già discusso in Appendice 1 questo è strettamente dipendente dalle condizioni di coltura.

Nelle diatomee il NPQ è stato associato non solo alla risposta ad alta luce ma anche a quella alla luce fluttuante (FL), una condizione facilmente sperimentabile nei sistemi di coltura all'esterno.

Abbiamo sfruttato questo mutante con una marcata riduzione nel NPQ per verificare qual è l'impatto di questi meccanismi nella risposta di *N.gaditana* alla luce FL. Nel capitolo 5 quindi è stato messo a punto un esperimento in cui le colture sono state esposte ad una intensità luminosa di 150 μmol di fotoni $m^{-2}s^{-1}$, i quali nel controllo sono somministrati in modo costante, mentre nelle FL sono frutto di una combinazione di una bassa luce di base inframmezzata da flash di alta luce, dati con frequenze e durate diverse. Il risultato è un forte impatto delle FL sulla crescita del WT. Il difetto di crescita è proporzionale alla frequenza dei flash ed è più marcato alle frequenze maggiori. Tuttavia I48 non mostra una sensibilità maggiore a questo genere di trattamento rispetto al WT, perciò il NPQ non sembra essere coinvolto in modo significativo nella risposta di *N.gaditana* alla luce FL. Approfondite analisi sulla funzionalità dell'apparato fotosintetico hanno evidenziato che l'attività del PSII non è compromessa, bensì è il PSI ad essere pesantemente inattivato. Questo risultato suggerisce che i trasporti alternativi attorno al PSI, che in altri organismi fotosintetici sono attivati per evitare la sovraeccitazione del PSI, non sono così efficienti in *N.gaditana*.

I primi 5 capitoli quindi hanno evidenziato il potenziale dell'ingegnerizzazione delle microalghe per trovare ceppi più produttivi rispetto al WT. Gli esperimento in FL in

particolare non solo hanno aiutato a chiarire il ruolo del NPQ in questa microalga, ma tenendo conto che la FL è una condizione facilmente trovabile in sistemi industriali che utilizzano la luce del sole come fonte di energia, può fornire un punto di partenza per trovare nuovi targets di ingegnerizzazione per aumentare la produttività. Inizialmente ci siamo focalizzati su un approccio inserzionale, perché avrebbe dovuto facilitare l'identificazione dei geni responsabili del fenotipo. In questo caso la frequente presenza di inserzioni in tandem e l'accumulo di mutazioni puntiformi ha vanificato questo vantaggio, perciò strategie alternative sono in fase di ottimizzazione per il futuro.

Nel capitolo 6 abbiamo invece testato l'approccio di mutagenesi chimica ed il protocollo di selezione, ottimizzati per *N.gaditana*, su un'altra specie: *Scenedesmus obliquus*, per valutare se questo metodo può essere applicato con successo a qualsiasi specie di interesse. Almeno un ceppo promettente è stato isolato (SOB17). In questo lavoro si è messo a punto anche un diverso sistema di valutazione delle produttività, attraverso un pannello messo in coltura in continuo. Infatti la geometria del pannello migliora la distribuzione della luce, rendendola più omogenea rispetto ad altri sistemi come la bottiglia. Inoltre la coltura in continuo fornisce una coltura stabile che ha una produzione continua di biomassa. Questa coltura ha avuto una buona stabilità nel tempo, arrivando ad essere, mantenuta per più di 30 settimane e SOB17 ha mostrato anche una maggiore produttività in una delle condizioni testate, anche se di nuovo come si era visto per *N.gaditana*, le condizioni di coltura sono fondamentali per ottenere il miglior risultato da ogni ceppo.

In aggiunta all'Appendice 1 descritta prima, altre due appendici sono incluse nella tesi. Queste sono il risultato di due diverse collaborazioni in cui gli approcci sperimentali messi a punto in questa tesi sono stati applicati con fini diversi.

In Appendice 2 è riportato il lavoro già pubblicato *"Genetic Engineering of algae photosynthetic productivity using mathematical models"* che descrive lo sviluppo di un modello matematico per valutare i fattori che influenzano la produttività delle microalghe nei fotobioreattori. Il modello è in grado di predire gli effetti di modifiche genetiche in un contesto di produzione industriale, fornendo uno strumento per identificare i genotipi più vantaggiosi in termini di produttività.

In Appendice 3 è riportata una collaborazione con la Prof.ssa Angela Falciatore (*Diatom Functional Genomics team, UPMC-Paris*). In questo lavoro è stato adattato il protocollo di selezione ottimizzato per *N.gaditana* per trovare fenotipi fotosintetici in una collezione

di mutanti di *Phaeodactylum tricornutum*, ottenuti per RNA *interference* così da modulare l'espressione di diversi fattori di trascrizione. Con questo approccio è stato possibile stabilire alcune promettenti correlazioni tra fenotipo e modulazione di una determinata classe di fattori di trascrizione, che ora saranno validati con un'analisi approfondita del fenotipo di questi mutanti e dei livelli di trascrizione in questi ceppi mutati.

CHAPTER 1:

Introduction

MICROALGAE: GREAT POTENTIAL IN SMALL ORGANISMS

The global population is expected to increase by over a third by 2050 reaching ≈ 10 billion people (fig 1). Such a drastic population growth will inevitably lead to an even larger increment in food and energy demand, estimated to increase by 70% (Godfray et al. 2010; Outlook 2016). This is clearly a major challenge, also considering the long term unsustainability of our food and energy production systems (British Petroleum Corp. 2016). Indeed terrestrial agriculture already requires approximately 75% of the total global freshwater supply and fossil fuels exploitation results in the greenhouse effect caused by carbon dioxide release from combustion of fossil oil, which led to the anthropogenic climate change over the past 20 years (Rodolfi et al. 2009; Wallace 2000). In a natural environment already compromised such a massive increase in food and energy production is clearly not sustainable. This issue is now widely recognized and in the climate conference held in Paris in 2015, 196 countries adopted the Paris Agreement which established a global warming goal below 2°C with respect to pre-industrial averages (Note 2015). In the same year European Commission decided that by 2050, the European Union should cut emissions to 80% below 1990 levels. Reaching these major goals without drastically impairing our lifestyle, however, requires the development of new food and energy feedstocks, which will need to be renewable and more environmental friendly.

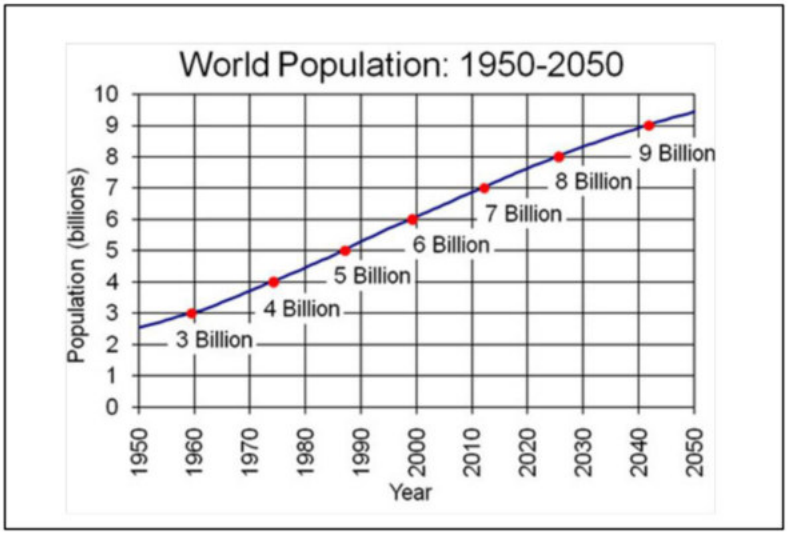

Figure 1: World population growth estimation from 1950 till 2050. Adapted from UE Census Bureau International Database 2011.

Microalgae are a group of unicellular microscopic photosynthetic organisms counting more than 200.000 species (Bleakley and Hayes 2017). Microalgae evolved to tolerate a wide variety of environmental conditions. Indeed they account for about 50% of global carbon fixation so they already have a major impact on CO_2 levels (Palma et al. 2017).
In the last few years microalgae are emerging as promising candidates as biomass source potentially exploitable both for food and energy production. If we consider food production some species of microalgae are potentially interesting for their high protein levels, similar to those of traditional protein sources, such as meat, eggs, soybean, and milk and they can be even richer in essential amino acids. Several algae species produce compounds, such as carotenoids, polyunsaturated fatty acid (PUFA), astaxanthin and lutein, widely used in the nutraceutical industry (I-Son et al. 2017).
Considering instead the energy market some microalgae species show the ability to accumulate high amount of oil (20-50% w/w) that can be converted into liquid fuels (Chisti 2007). With respect to plants, microalgae present some advantages, for example:

- they convert captured solar energy into biomass with efficiencies that generally exceed those of terrestrial plants (an efficiency of 3% reported for marine microalgae compared with 0.2–2% for terrestrial plants) (Stephenson et al. 2011);
- as unicellular organisms the allocation of energy and resources for the production of heterotrophic tissues is avoided (Palma et al. 2017);
- they do not need arable land to be cultivated, so they do not compete with food production (Ishika, Moheimani, and Bahri 2017);
- they do not need freshwater for their cultivation. On the contrary wastewaters can be used as source of nitrogen and phosphorous, coupling the bioremediation processes with industrial production (Salama et al. 2017).

Despite these advantages several limitations for microalgae industrial production are still present. Especially for biofuels production cultivation costs are still too high, making the product not economically competitive. According to some recent estimations the cost of a barrel of algae-based fuel using current technology is around US$300, compared with petroleum which is available at US$40 to 60 per barrel (I-Son et al. 2017). So to explore microalgae possibilities in next years the goal for the scientific community will be to find a way to increase the production while also reducing costs.

CONVERSION OF LIGHT INTO CHEMICAL ENERGY IN OXYGENIC PHOTOSYNTHESIS

Microalgae potential as sustainable source of biomass for food and fuel applications is strictly connected with their ability to perform oxygenic photosynthesis. Algae as photosynthetic organisms exploit oxygenic photosynthesis to covert light energy into ATP and NADPH that are then used to fix CO_2, producing also molecular oxygen as secondary product. The process can be divided into a light and dark phase (fig 2-A). During the light phase the solar energy is used to oxidize water and produce ATP and NADPH. During the dark phase ATP and NADPH are involved in CO_2 fixation by Calvin-Benson cycle (Bassham, Benson, and Calvin 1950).

In eukaryotes photosynthesis takes place in specialized organelles called chloroplasts. Two external membranes separate a compartment called stroma, that contains all the enzymes involved in dark reaction, plastidial DNA, RNA and ribosomes. Within the stroma there are also the thylakoid membranes, which form a three dimensional network around thylakoids lumen. Four major protein complexes are localized in the thylakoids membrane and catalyze the processes of the light phase: Photosystem II, cytochrome b6f complex, Photosystem I and ATP synthase (fig 2-B). Photosynthetic process starts with light absorption by a pigment, chlorophyll, that uses excitation energy for a charge separation. Primary electron donor during this process is water. O_2 is generated as secondary product after water oxidation.

Water oxidation releases on the lumenal side of thylakoid membrane 4 protons. These protons are translocated through the thylakoid membrane during the so called Q-cycle, which involves the reduction and oxidation of plastoquinone/plastoquinol pool. Plastoquinone reduction to plastoquinol is due to Cytb6f, which oxidizes two plastoquinols, reduces one plastoquinone, and translocates 3 H^+ for every 2 electrons transported to PSI. The formation of a proton gradient across the thylakoid membrane leads to the generation of free energy and reducing power, in the form of ATP and NADPH + H^+.

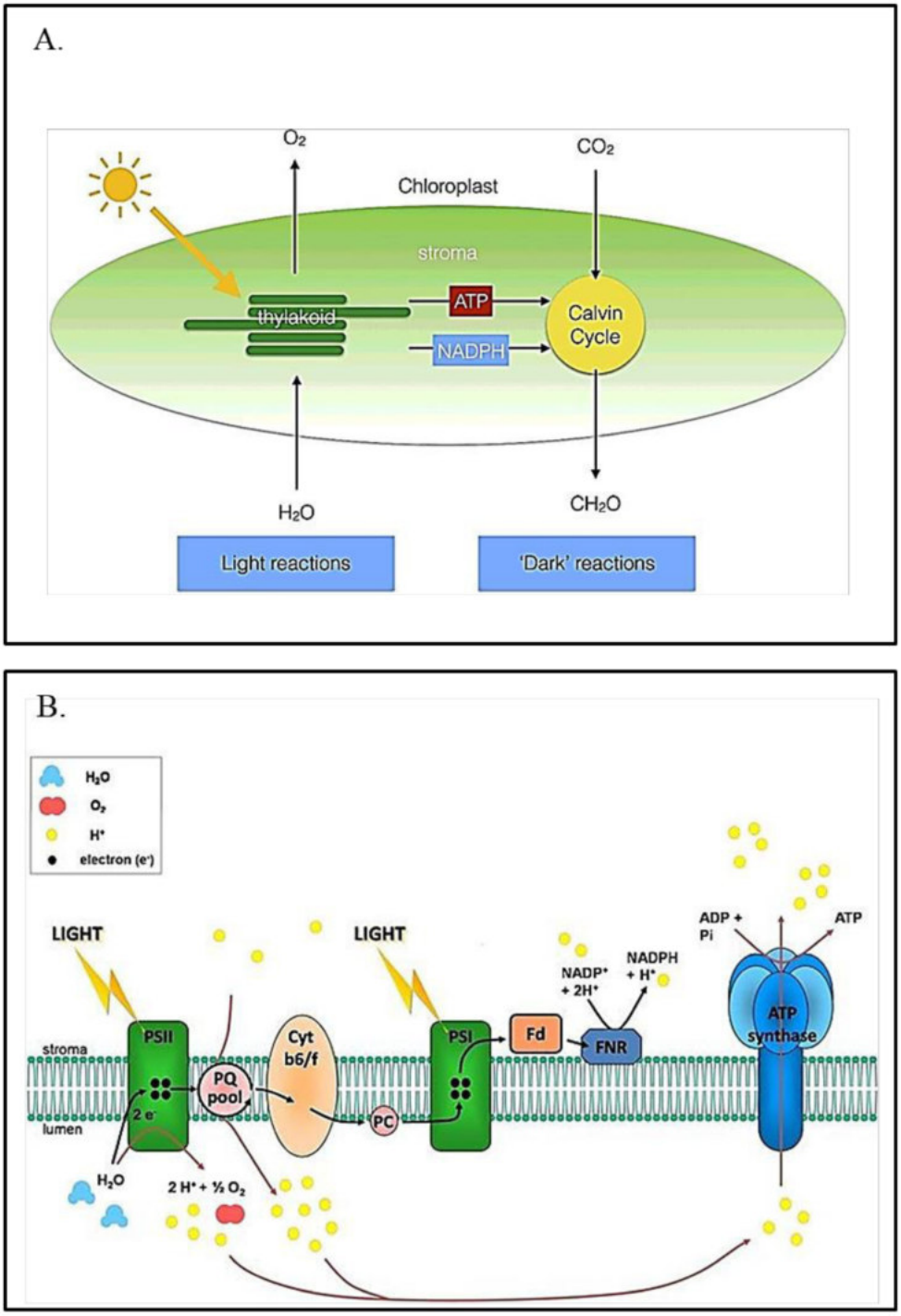

Figure 2: In A is shown a schematic representation of the light and dark phases of photosynthesis, adapted from (Johnson 2016). In B is reported a picture of the photosynthetic electron transport chain adapted from (Michelet et al. 2013)

ATP and NADPH produced during light reaction are exploited to reduce CO_2 in the Calvin-Benson cycle. It consists in the net synthesis of one glyceraldehyde 3-phospate

(GAP) from three CO_2 molecules and in the regeneration of Ribulose 1,5-bisphospate (RuBP). Nine ATP and six NADPH are consumed for the production of one GAP.

MOLECULAR BASES OF LIGHT HARVESTING

The first step of photosynthesis is light harvesting by pigments, namely chlorophyll and carotenoids (Koziol et al. 2007). Chlorophyll is the major light harvesting pigment, its structure comprises a phytol tail and a porphyrin ring. The former appears dissolved in the membrane lipids of the chloroplast. The alternating single and double bonds of the porphyrin moiety act as antenna to capture light with the magnesium atom at the center carrying the electrons necessary for the photosynthesis reactions to take place (Carvalho et al. 2011). Carotenoids instead are isoprenoids compounds with a variable structure. They are not only involved in light harvesting but also in stress response. They have an antioxidant function which can reduce the oxidative damage due to reactive oxygen species (ROS) formation in stress condition.

These pigments are bound to pigment protein complexes found in both photosystems. In eukaryotes most of the pigments are bound to members of Light Harvesting Complex (LHC). LHC are a multigene family evolved from an internal gene duplication/unequal crossing-over of tandem genes (Engelken, Brinkmann, and Adamska 2010). They are nuclear genes but their products are then directed to the chloroplast by an N-terminal signal peptide. In the chloroplast they associate with pigments and they are inserted into the thylakoid membrane (Koziol et al. 2007). Antenna proteins possess three α-helical transmembrane regions, connected by stroma and lumen exposed loops (fig 3). LHCs are divided in several subfamilies. For example there are LHCAs and LHCBs that are found in green algae and they form PSI and PSII supercomplexes. FCPs also called LHCfs bind fucoxanthin or violaxanthin and they are mainly found in brown algae and Heterokonts (Koziol et al. 2007; Litvin et al. 2016; Nield, Redding, and Hippler 2004). There are also LHCRs and LHCARs, which are found in red algae and in secondary endosymbiont like diatoms. These ones bind Chl a/c, zeaxanthin and β-carotene. Instead LHCSRs or LHCXs are stress induced chlorophyll binding proteins (fig 3), which play a role in the response to the excess of light called Non Photochemical Quenching (NPQ) (Bailleul et al. 2010; K. K. Niyogi and Truong 2013).

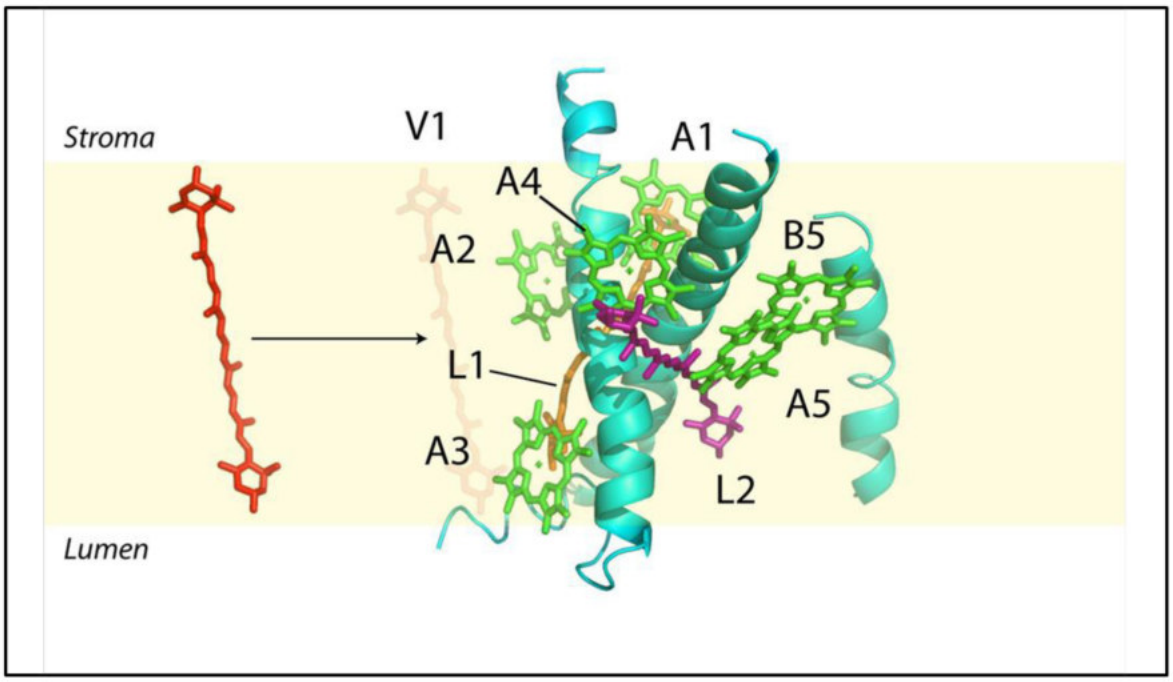

Figure 3: The model shows the structure of member of LHCSR family, with Chl and xanthophyll chromophores bound, adapted from (Bonente et al. 2011).

REGULATION OF LIGHT USE EFFICIENCY: NON PHOTOCHEMICAL QUENCHING

Light harvesting supports photosynthetic organisms metabolism, but when available excitation energy exceeds their photosynthetic capacity, it drives to the dangerous formation of oxidative reactive species (ROS).

In order to avoid oxidative stress photosynthetic organisms evolved different mechanisms, which contribute to the safe dissipation of excess excitation energy as heat. These mechanisms have been on the whole defined as Non Photochemical Quenching (NPQ).

NPQ has been shown to be composed of different components (fig 4):

- the fast high-energy-state quenching qE, which is the most rapid component in algae and plants NPQ and it depends on the decrease of pH in the lumen (Muller, Li, and Niyogi 2001);
- the zeaxanthin dependent component qZ, which is due to zeaxanthin synthesis via xanthophyll cycle (Nilkens et al. 2010);

- the slow photo inhibitory quenching qI, which is correlated with the accumulation of photo-damaged photosystems (Muller, Li, and Niyogi 2001);

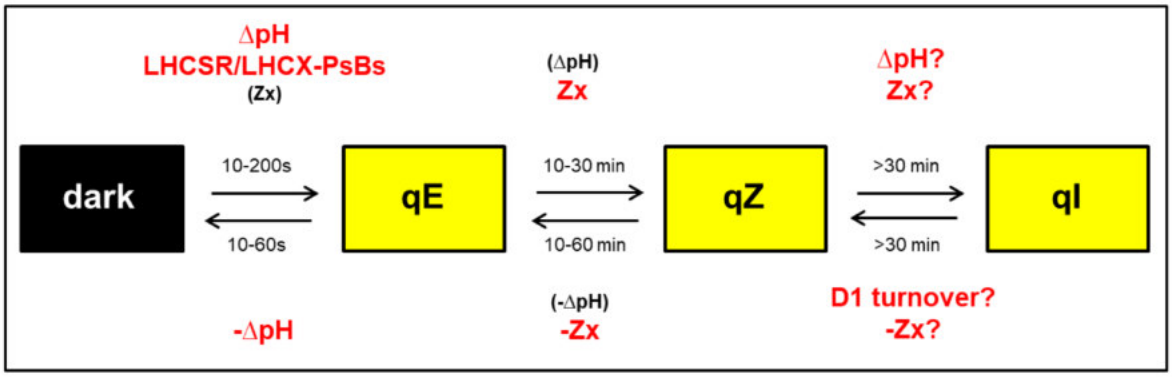

Figure 4: This is a model adapted from (Nilkens et al. 2010) for the NPQ components activation and de-activation. qE is the fast components, it is formed in 10-200 s and it is mainly due to the ΔpH and LHCSR/LHCX antenna proteins or PsBs protein (marked in red). It seems to play a minor role in its formation also zeaxanthin synthesis. qZ is the slower component (10-30 min to be activated) and it depends mainly from the conversion of violaxanthin to zeaxanthin, which is in any case linked with pH variation. The last component is qI which is activated after a long light exposure and it is not still clear its activation and de-activation mechanism.

The key regulatory signal of light excess response is the proton gradient generated between the thylakoid lumen and the chloroplast stroma during light exposure (ΔpH). The decrease in pH within the thylakoid lumen is a signal that metabolism activity is slower than electron transport rate and it triggers the feedback regulation of light harvesting by NPQ (Muller, Li, and Niyogi 2001). This fast response in algae depends from the activity of stress related antenna proteins of the light-harvesting complexes LHCSR or LHCX, mentioned before but it is also enhanced by zeaxanthin synthesis via xanthophyll cycle (K. K. Niyogi and Truong 2013; Peers et al. 2009).

LHCSRs bind several chlorophylls and xanthophylls, and they have an unusually short chlorophyll fluorescence lifetime *in vitro* that is even shorter at low pH (Bonente et al. 2011). This suggests that these proteins have high capacity to dissipate energy as heat. This activity is presumably enhanced by protonation of acidic residues (aspartate and/or glutamate) on the lumen-facing side of the protein. LHCSR proteins are present in green algae, mosses, haptophytes, photosynthetic stramenopiles (diatoms, brown algae, eustigmatophytes), and the photosynthetic apicomplexan *Chromera velia*. On the other hand, LHCSRs appear to be absent in red algae and higher plants (fig 5).

In higher plants another protein called PSBS was found to be responsible for qE activation. PSBS is a four-helix integral membrane protein that does not appear to bind pigments. Instead, it functions as a sensor of lumen pH and it induces a still unclear reorganization of antenna proteins. Although the biochemical mechanism is not yet understood, protonation of PSBS seems to promote a rearrangement of the PSII supercomplex in grana that is necessary for rapid induction of NPQ (Goss and Lepetit 2015).

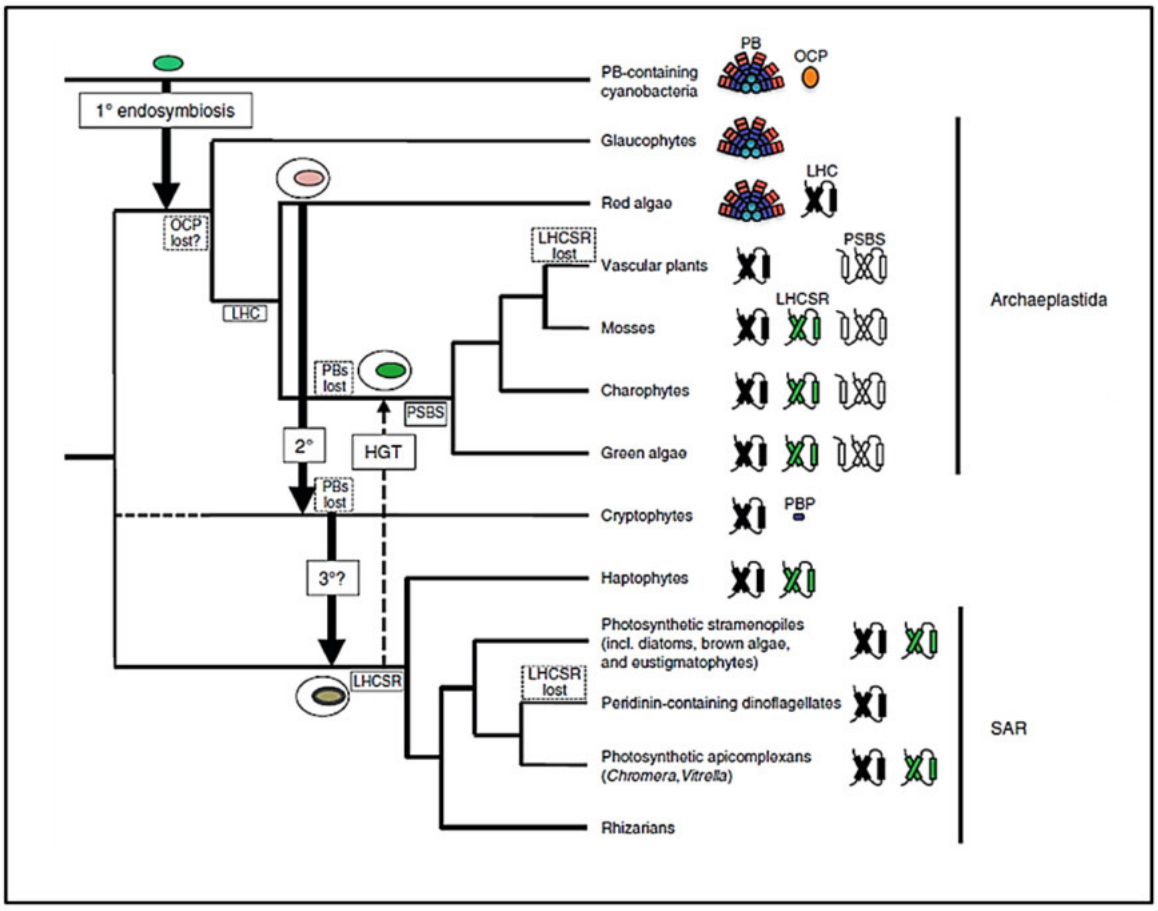

Figure 5: Phylogenetic analysis of stress related antenna proteins distribution during the evolution of photosynthetic organisms. It has been adapted from (K. K. Niyogi and Truong 2013).

LHCSR and PSBS have been identified as the molecular responsible for NPQ activation. NPQ activity however also is strongly enhanced by xanthophyll cycle. Xanthophylls are a diverse group of oxygenated carotenoids with varied structures and multiple functions (K. Niyogi, Bjorkman, and Grossman 1997). In almost all photosynthetic eukaryotes, the majority of xanthophylls are bound with chlorophyll (Chl) molecules to LHCs proteins.

Indeed xanthophylls can function as accessory light-harvesting pigments but are especially important for the protection of photosynthetic organisms from the potentially toxic effects of light (Havaux and Niyogi 1999). Specific xanthophylls are involved in the de-excitation of singlet Chl that accumulates in the LHC under conditions of excessive illumination. Xanthophylls avoid the triplet state chlorophyll formation. Indeed this triplet state is quite instable and tends to react with the oxygen resulting in the formation of reactive oxygen species (ROS).

The development of NPQ correlates with the synthesis of zeaxanthin (Z) and antheraxanthin (A) from violaxanthin (V), via the xanthophyll cycle (fig 6). In high light V is converted to Z, which switches a PSII unit into a quenched state, dissipating the excess of light energy as heat (Goss and Jakob 2010).

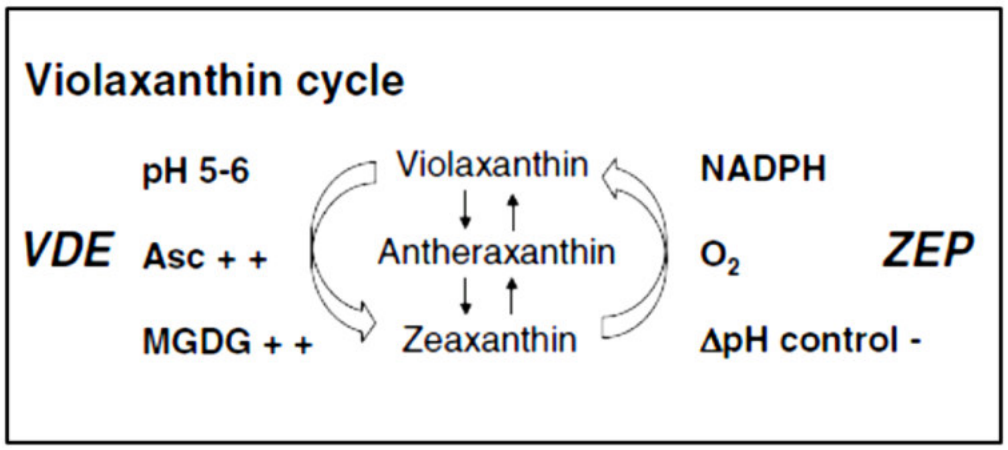

Figure 6: Schematic representation of violaxanthin cycle, adapted from (Goss and Jakob 2010).

THE CHALLENGE OF LIGHT USE EFFICIENCY IN ALGAE INDUSTRIAL CULTIVATION

Microalgae exposed to light can experience three different conditions (fig 7):

- light excess, when the light adsorbed is higher respect to that one exploitable for photochemistry. To reduce the production of harmful reactive oxygen species photoprotection mechanisms are activated to dissipate excess excitation energy as heat;

- optimal light, which means that the light adsorbed is in largest part used for the photochemistry, ensuring the best photosynthetic performance;
- limiting light, which means that light is too low to sustain the photochemistry at the maximum of the photosynthetic organism possibilities.

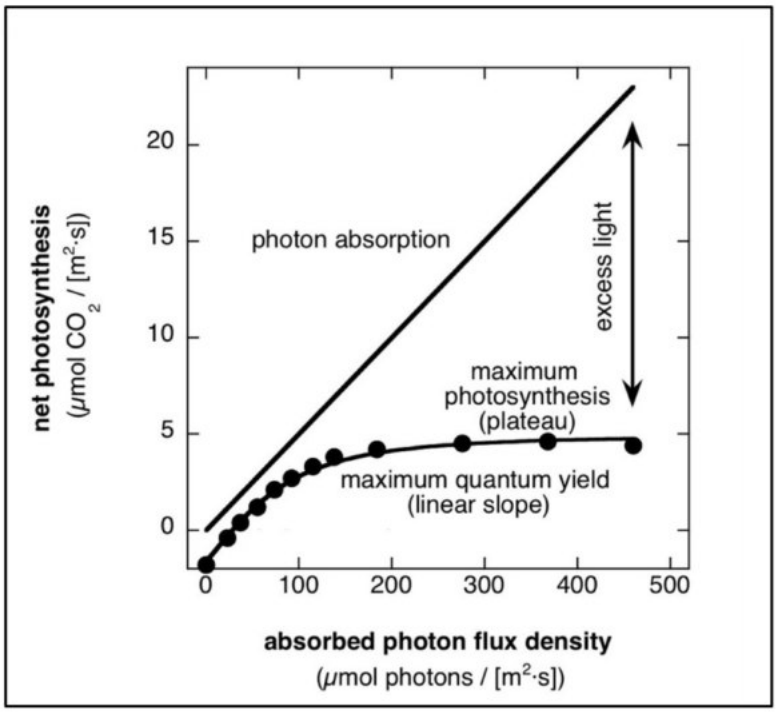

Figure 7: It is reported the correlation between photosynthesis and the adsorbed photon flux density. As it is shown with the circles, photosynthesis reaches a plateau, so an higher photon flux density does not result in a higher photosynthetic yield. Instead photons absorption is linear with the photon flux density (solid line). This leads to an excess of light energy absorbed (marked by the arrow) that has to be dissipated to avoid ROS formation. The picture was adapted from: https://www.intechopen.com/books/thermodynamics-systems-in-equilibrium-and-non-equilibrium/photosynthetic-productivity-can-plants-do-better.

One major limitation in microalgae growth and metabolite production is their ability to use sunlight efficiently. The reason is that they evolved in a natural environment extremely different from the artificial. Indeed in natural environment light is in general limiting, so microalgae evolved large light-harvesting complexes for maximizing light absorption and to compete with other organisms for this limiting resource (Kirst and Melis 2014). In their natural environment this characteristic confers an advantage with respect to the other organisms, but in a photobioreactor it decreases the overall productivity. Due to the high light-harvesting efficiency of chlorophyll, microalgae absorb essentially all light that reaches them. So the external layer tends to adsorb the

largest fraction of the available light, leaving the internal one in a condition of limitation. Approximately 10% of full light sunlight saturates photosynthetic apparatus, so the excess adsorbed is then dissipated as heat rather than be exploited to the growth (Simionato, Basso, et al. 2013). The concept of light dilution is frequently employed to optimize light distribution by increasing its surface area per unit of reactor volume (De Mooij et al. 2014).

As alternative/complementary approach to light dilution there is the genetic engineering of microalgae cells to reduce the chlorophyll content and thus their light absorption capacity in the external layer (fig 8). The aim is reached using different strategy both affecting chlorophyll biosynthesis and antenna proteins accumulation (Mussgnug et al. 2007; Polle et al. 2000). A lot of work was done on the model genus *Chlamydomonas reinhardtii* (Beckmann et al. 2009; Bonente et al. 2011; Nakajima and Ueda 2000). The isolated strains have a higher maximum photosynthetic rate in lab scale evaluations, but in some case strains tested in large scale PBRs showed contrasting results (De Mooij et al. 2014).

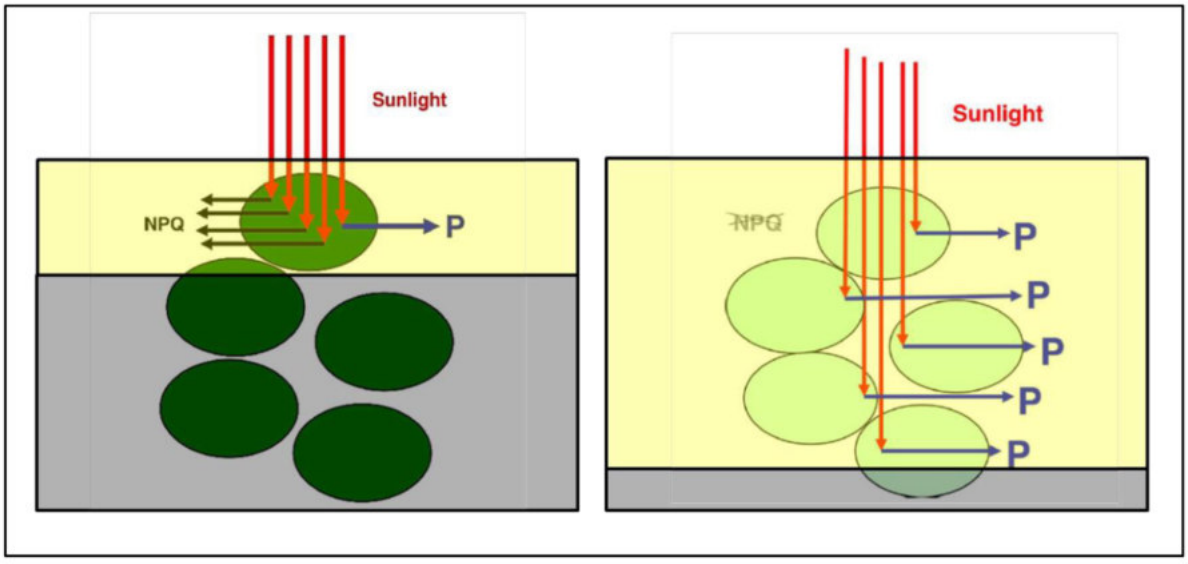

Figure 8: Exemplification of the possible effect in the light penetration due to a reduction in the chlorophyll content. P stays for photochemistry, adapted from (Melis 2009).

Nannochloropsis gaditana, A SPECIES WITH APPLIED POTENTIAL

Nannochloropsis gaditana is a marine microalga with spherical or slightly ovoid cells of 2-4 µm in diameter (fig 9-A). In recent years, species belonging to the *Nannochloropsis* genus have gained increasing interest for their potential exploitation for biodiesel production, reflecting the rapid growth rate, with a maximum specific growth rate of 0.56 day^{-1} at 23°C, and accumulation of lipids in these species.

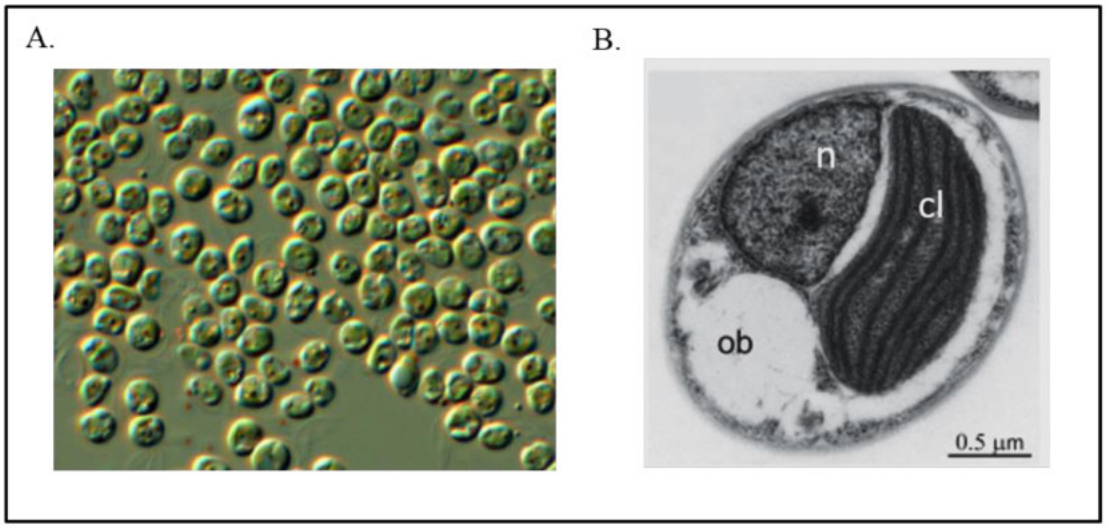

Figure 9: In A is shown an optical microscopy image from Provasoli-Guillard National Center for Marine Algae and Microbiota. In B is shown a transmission microscopy image of a *Nannochloropsis gaditana* cell. Organelles are indicated as, n, nucleus; cl, chloroplast; ob, oil body. The image was taken in N-deplete conditions, adapted from (Simionato, et al. 2013)

Indeed *N.gaditana* has the ability to accumulate large amount of lipids (over 60% of its dry weight in nitrogen starvation) and long chain poly-unsatured fatty acids (LC-PUFA), at least in specific environmental conditions (fig 9-B) (Radakovits et al. 2012; Simionato et al. 2013). This microalga belongs to the class of Eustigmatophyceae within Heterokonts, a group which also includes diatoms and brown algae (Basso et al. 2014). These species originated from a secondary endosymbiotic event in which a eukaryotic host cell engulfed a red alga (Archibald 2009).

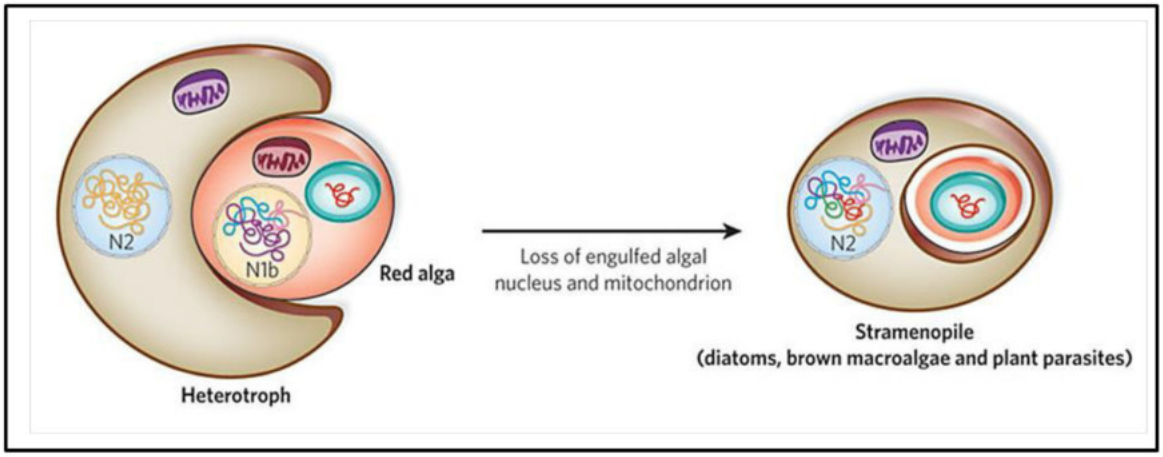

Figure 8: Schematic representation of the secondary endosymbiotic event from which *N.gaditana* originated. Adapted from (Armbrust 2009).

They are unicellular microorganisms with polysaccharides wall and they contain only one chloroplast. *Nannochloropsis* has a peculiar photosynthetic apparatus composition. The only chlorophyll present is chlorophyll a and the main accessory pigments are violaxanthin and vaucheraxanthin esters (Basso et al. 2014; Litvin et al. 2016). Also the cell wall is peculiar and it contains algaenans, a term that likely encompasses several lipid-related species. Algaenans are highly resistant to alkali/acid hydrolysis and aqueous/organic solubilization. Their biochemical characterization has been considered tentative since isolation procedures may have induced chemical alterations (Scholz et al. 2014). The genome of several *Nannochloropsis* species was completely sequenced. *N.gaditana* nuclear genome size is 28.5 Mbp including repeated and telomeric regions and it is organized in 30 chromosomes. Genome sequencing prediction revealed a density of one gene every 2.6 kbp in the *N.gaditana* nuclear genome. On average, coding sequences have a length of 1.2 kbp and they are interrupted by fewer than two short introns per gene (Corteggiani et al. 2014; Jinkerson, Robert E, Randor Radakovits 2013). Thanks to the interest around these species a lot of work was done in the last few years to set up genetic tools in order to engineering the WT strain to increase biomass and lipids productivity.

REFERENCES

Archibald, John M. 2009. "The Puzzle of Plastid Evolution." *Current biology* 19(2): 81–88.

Armbrust, E Virginia. 2009. "The Life of Diatoms in the World 's Oceans." *Nature* 459(14): 185–92.

Bailleul, Benjamin et al. 2010. "An Atypical Member of the Light-Harvesting Complex Stress-Related Protein Family Modulates Diatom Responses to Light." *Proceedings of the National Academy of Sciences* 107(42): 18214-18219

Bassham, A, A Benson, and M Calvin. 1950. "THE PATH IN PHOTOSYNTHESIS." *Journal of Biological Chemistry* (2).

Basso, Stefania et al. 2014. "Characterization of the Photosynthetic Apparatus of the Eustigmatophycean Nannochloropsis gaditana: Evidence of Convergent Evolution in the Supramolecular Organization of Photosystem I." *Biochimica et biophysica acta* 1837(2): 306–14.

Beckmann, J et al. 2009. "Improvement of Light to Biomass Conversion by de-Regulation of Light-Harvesting Protein Translation in Chlamydomonas Reinhardtii." *Journal of biotechnology* 142(1): 70–77.

Bleakley, Stephen, and Maria Hayes. 2017. "Algal Proteins: Extraction, Application and Challenges Concerning Production." *Foods* 6(33): 1–34.

Bonente, Giulia et al. 2011. "Analysis of LHcSR3, a Protein Essential for Feedback de-Excitation in the Green Alga Chlamydomonas Reinhardtii." *PLoS Biology* 9(1):1-17.

British Petroleum Corp. 2016. "BP Statistical Review of World Energy."

Carvalho, Ana P, Susana O Silva, José M Baptista, and F Xavier Malcata. 2011. "Light Requirements in Microalgal Photobioreactors: An Overview of Biophotonic Aspects." *Applied microbiology and biotechnology* 89(5): 1275–88.

Chisti, Yusuf. 2007. "Biodiesel from Microalgae." *Biotechnology advances* 25(3): 294–306.

Corteggiani, Elisa et al. 2014. "Chromosome Scale Genome Assembly and Transcriptome

Profiling of Nannochloropsis gaditana in Nitrogen Depletion." *Molecular Plant* 7(2): 323–35.

Engelken, Johannes, Henner Brinkmann, and Iwona Adamska. 2010. "Taxonomic Distribution and Origins of the Extended LHC (light-Harvesting Complex) Antenna Protein Superfamily." *BMC evolutionary biology* 10(1): 233-248

Godfray, H.Charles J. et al. 2010. "Food Security : The Challenge of Feeding 9 Billion People." *Science* 327: 812–19.

Goss, Reimund, and Torsten Jakob. 2010. "Regulation and Function of Xanthophyll Cycle-Dependent Photoprotection in Algae." *Photosynthesis research* 106(1-2): 103–22.

Goss, Reimund, and Bernard Lepetit. 2015. "Biodiversity of NPQ." *Journal of Plant Physiology* 172: 13–32.

Havaux, Michel, and Krishna K. Niyogi. 1999. "The Violaxanthin Cycle Protects Plants from Photooxidative Damage by More than One Mechanism." *Plant Biology* 96: 8762–67.

Ishika, Tasneema, Navid R Moheimani, and Parisa A Bahri. 2017. "Sustainable Saline Microalgae Co-Cultivation for Biofuel Production : A Critical Review." *Renewable and Sustainable Energy Reviews* 78: 356–68.

I-Son, Ng. et al. 2017. "Recent Development on Genetic Egineering of Microalgae for Biofuels and Bio-Based Chemicals." *Biotechnology Journal*: 1–50.

Jinkerson, Robert E, Randor Radakovits, Matthew Posewitz. 2013. "Genomic Insights from the Oleaginous Model Alga." *Bioengineered* 4(1): 1–7.

Johnson, Matthew P. 2016. "Photosynthesis An Overview of Photosynthesis." *Essays in Biochemistry* 60: 255–73.

Kirst, Henning, and Anastasios Melis. 2014. "The Chloroplast Signal Recognition Particle (CpSRP) Pathway as a Tool to Minimize Chlorophyll Antenna Size and Maximize Photosynthetic Productivity." *Biotechnology Advances* 32(1): 66–72.

Koziol, Adam G et al. 2007. "Tracing the Evolution of the Light-Harvesting Antennae in Chlorophyll a / b Containing Organisms." *Plant Physiology* 143: 1802–16.

Litvìn, Radek, David Bi-na, Miroslava Herbstova, and Zdenko Gardian. 2016. “Architecture of the Light-Harvesting Apparatus of the Eustigmatophyte Alga Nannochloropsis Oceanica.” *Photosynthesis Research* 130(1-3): 137–50.

Melis, Anastasios. 2009. “Solar Energy Conversion Efficiencies in Photosynthesis: Minimizing the Chlorophyll Antennae to Maximize Efficiency.” *Plant Science* 177(4): 272–80.

Michelet, Laure et al. 2013. “Redox Regulation of the Calvin-Benson Cycle : Something Old , Something New."*Frontiers in Plant Science* 4: 1–21.

De Mooij, Tim et al. 2014. “Antenna Size Reduction as a Strategy to Increase Biomass Productivity : A Great Potential Not yet Realized.” *Journal of Applied Phycology*.

Muller, Patricia, Xiao-ping Li, and Krishna K Niyogi. 2001. “Non-Photochemical Quenching. A Response to Excess Light Energy .” *Update on Photosynthesis* 125: 1558–66.

Mussgnug, Jan H et al. 2007. “Engineering Photosynthetic Light Capture: Impacts on Improved Solar Energy to Biomass Conversion.” *Plant biotechnology journal* 5(6): 802–14.

Nakajima, Yuji, and Ryohei Ueda. 2000. “The Effect of Reducing Light-Harvesting Pigment on Marine Microalgal Productivity.” *Journal of Applied Phycology* 12(3-5): 285–90.

Nield, Jon, Kevin Redding, and Michael Hippler. 2004. “Remodeling of Light-Harvesting Protein Complexes in Response to Environmental Changes.” *Eukaryotic Cell* 3(6): 1370–80.

Nilkens, Manuela et al. 2010. “Identification of a Slowly Inducible Zeaxanthin-Dependent Component of Non-Photochemical Quenching of Chlorophyll Fluorescence Generated under Steady-State Conditions in Arabidopsis.” *Biochimica et Biophysica Acta - Bioenergetics* 1797(4): 466–75.

Niyogi, Krishna K, Olle Bjorkman, and Artur R. Grossman. 1997. “Chlamydomonas Xanthophyll Cycle Mutants Identified by Video Imaging of Chlorophyll Fluorescence Quenching.” *The Plant cell* 9(8): 1369–80.

Niyogi, Krishna K., and Thuy B. Truong. 2013. “Evolution of Flexible Non-Photochemical Quenching Mechanisms that Regulate Light Harvesting in Oxygenic Photosynthesis.” *Current Opinion in Plant Biology* 16(3): 307–14.

Note, Briefing. 2015. “The Paris Agreement Summary.” (December): 1–6.

Outlook, International Energy. 2016. “IEO2016 World Chapter.” 2016: 7–17.

Palma, H. et al. 2017. “Assessment of Microalga Biofilms for Simultaneous Remediation and Biofuel Generation in Mine Tailings Water.” *Bioresource Technology* 234: 327–35.

Peers, Graham et al. 2009. “An Ancient Light-Harvesting Protein is critical for the Regulation of Algal Photosynthesis.” *Nature* 462(7272): 518–21.

Polle, J E, J R Benemann, a Tanaka, and a Melis. 2000. “Photosynthetic Apparatus Organization and Function in the Wild Type and a Chlorophyll b-Less Mutant of Chlamydomonas Reinhardtii. Dependence on Carbon Source.” *Planta* 211(3): 335–44.

Radakovits, Randor et al. 2012. “Draft Genome Sequence and Genetic Transformation of the Oleaginous Alga Nannochloropis gaditana.” *Nature Communications* 3: 610–86.

Rodolfi, Liliana et al. 2009. “Microalgae for Oil : Strain Selection , Induction of Lipid Synthesis and Outdoor Mass Cultivation in a low cost photobioreactor.” *Biotechnology and bioengineering* 102(1): 100–112.

Salama, El-sayed, Mayur B Kurade, Reda A I Abou-shanab, and Marwa M El-dalatony. 2017. “Recent Progress in Microalgal Biomass Production Coupled with Wastewater Treatment for Biofuel Generation.” *Renewable and Sustainable Energy Reviews* 79: 1189–1211.

Scholz, Matthew J et al. 2014. “Ultrastructure and Composition of the Nannochloropsis gaditana Cell.” *Eukaryotic Cell* 13(11): 1450–64.

Simionato, Diana, et al. 2013. “The Response of Nannochloropsis gaditana to Nitrogen Starvation Includes de Novo Biosynthesis of Triacylglycerols, a Decrease of Chloroplast Galactolipids, and Reorganization of the Photosynthetic Apparatus.” *Eukaryotic Cell* 12(5): 665–76.

Simionato, Diana, Stefania Basso, Giorgio M. Giacometti, and Tomas Morosinotto. 2013. "Optimization of Light Use Efficiency for Biofuel Production in Algae." *Biophysical Chemistry* 182: 71–78.

Stephenson, Patrick G et al. 2011. "Improving Photosynthesis for Algal Biofuels : Toward a Green Revolution." *Trends in Biotechnology* 29(12): 615–23.

Wallace, J S. 2000. "Increasing Agricultural Water Use Efficiency to Meet Future Food Production." *Agriculture Ecosystems & Environment* 82: 105–19.

CHAPTER 2:

Generation of random mutants to improve light-use efficiency of *Nannochloropsis gaditana* cultures for biofuel production

Authors name and affiliations

Giorgio Perin[2], Alessandra Bellan[1], Anna Segalla[1], Andrea Meneghesso[1], Alessandro Alboresi[1] and Tomas Morosinotto[1]

1-PAR-Lab_Padua Algae Research Laboratory, Department of Biology, University of Padova, Via U. Bassi 58/B, 35121 Padova, Italy.

2- Department of Life Sciences, Imperial College London, Sir Alexander Fleming Building, London, SW7 2AZ, UK.

THIS CHAPTER WAS PUBLISHED IN BIOTECHNOGY FOR BIOFUELS JOURNAL (2015)

The format is different from the main chapters because it is that one required by the journal.

CONTRIBUTION:

In this chapter AB the mutagenesis screenings and the physiological characterization of the insertional mutant strains.

ABSTRACT

Background: The productivity of an algal culture depends on how efficiently it converts sunlight into biomass and lipids. Wild type algae in their natural environment evolved to compete for light energy and maximize individual cell growth; however, in a photobioreactor, global productivity should be maximized. Improving light use efficiency is one of the primary aims of algae biotechnological research, and genetic engineering can play a major role in attaining this goal.

Results: In this work, we generated a collection of *Nannochloropsis gaditana* mutant strains and screened them for alterations in the photosynthetic apparatus. The selected mutant strains exhibited diverse phenotypes, some of which are potentially beneficial under the specific artificial conditions of a photobioreactor. Particular attention was given to strains showing reduced cellular pigment contents, and further characterization revealed that some of the selected strains exhibited improved photosynthetic activity; in at least one case, this trait corresponded to improved biomass productivity in lab-scale cultures.

Conclusions: This work demonstrates that genetic modification of *Nannochloropsis gaditana* has the potential to generate strains with improved biomass productivity when cultivated under the artificial conditions of a photobioreactor.

KEYWORDS

Photosynthesis, *Nannochloropsis*, mutants, EMS, insertional mutagenesis, biodiesel, algae

LIST OF ABBREVIATIONS

Abbreviations used are: Chl, Chlorophyll; DCMU, 3-(3,4-dichlorophenyl)-1,1-dimethylurea; EMS, Ethyl Methane Sulfonate; ETR, Electron Transport Rate; GMO, Genetically Modified Organism; LHC, Light Harvesting Complex; NPQ, Non-Photochemical Quenching; PBR, Photobioreactor; PS, Photosystem; ROS, Reactive Oxygen Species; TLA, Truncated Light Harvesting; WT, Wild Type.

INTRODUCTION

Biodiesel production using microalgae biomass represents one interesting alternative for replacing fossil liquid fuels and reducing emission of greenhouse gasses into the atmosphere. Several thousand different algae species exist in nature, and thus far, few of them have been identified as being particularly suitable for these types of applications [1]. Species of the *Nannochloropsis* genus are included in the list of biodiesel production candidates due to their ability to accumulate large amounts of lipids, especially during nutrient starvation [2, 3].

Algae are photosynthetic organisms and thus depend on sunlight for energy to support their metabolism [4]. Solar light is an abundant resource, but it is also distributed on a very large surface, making the average amount of energy available per unit area relatively low (1,084 x 10^{16} J/km^2 [5]). Consequently, algae growing in outdoor ponds and photobioreactors (PBR) are commonly limited by light availability, and their efficiency in converting light into biomass substantially influences overall productivity [6, 7]; this limitation is particularly true for photoautotrophs, such as the species belonging to the *Nannochloropsis* genus [8]. To make algae-based products competitive on the market it is therefore imperative that biomass production be maximized by optimizing the light use efficiency of these organisms in industrial-scale cultivation systems [6, 7].

One of the major problems associated with growing algae in any large scale PBR (or pond) is that cultures have high optical densities, resulting in strongly inhomogeneous light distributions [9, 10]. Consequently, most of the available light is absorbed by superficial cells, which easily absorb energy exceeding their photochemical capacity. This surplus excitation leads to oxidative damage and photoinhibition, which can be avoided in part by dissipating a fraction of the absorbed energy as heat through a photoprotective mechanism known as Non-Photochemical Quenching (NPQ) [11]. NPQ effectively protects cells from photoinhibition, but it can drive the dissipation of up to 80 % of the absorbed energy as heat, strongly decreasing the light use efficiency of cells exposed to excess irradiation [12–14]. While the external cells absorb most of the available energy and use it with low efficiency, cells underneath are strongly light-limited, reducing the overall accumulation of biomass. Due to this inhomogeneous light distribution, algae grown in large scale PBRs are significantly less productive than algae grown under laboratory conditions [15–17].

The large antenna system of the algae photosynthetic apparatus binds hundreds of chlorophyll molecules (Chl) per reaction center. These pigments maximize light-harvesting efficiency as an evolutionary adaptation to a natural environment where solar radiation is often limiting for growth, and competition with other organisms for light is essential [5, 18]. In contrast, in a large scale PBR, such large antenna systems limit light penetration into algal cultures and the capacity for competition exists at the expense of overall productivity. In this artificial environment, an "ideal" organism should harvest only the amount of light that it can use with high efficiency, without removing useful energy that other cells could use; such a domesticated strain would have reduced fitness in a natural context but improved productivity in the artificial environment of a PBR [16, 19].

Following on this hypothesis, genetically engineered strains have been generated in past years with altered composition and regulation of the photosynthetic apparatus to reduce their competitive capacity, for example with reduced cell pigment content [6, 16, 20]. Reduction of culture light harvesting efficiency is indeed conceivable and it has been suggested that only approximately 50/350 and 90/300 of the chlorophyll molecules found in Photosystems II (PSII) and PSI (PSI), respectively, in *Chlamydomonas reinhardtii* are strictly necessary, while the rest are bound to light-harvesting complexes (LHC) and are, in principle, dispensable [19, 21]. The mutations responsible for Chl content reduction should bear two positive effects: first, a cell will harvest less light when exposed to strong irradiation, reducing the need for the activation of energy dissipation mechanisms, and second, light will be better distributed in the culture volume, making more energy available to support the growth of biomass in cells in the internal light-limited layers [16]. Several recent reports have demonstrated that it is possible to isolate algae mutant strains with reduced Chl content and/or reduced antenna size, defined as TLA (truncated light-harvesting) mutant strains, especially in the model organism *Chlamydomonas reinhardtii* [15, 22–25]. These modifications were achieved by altering genes that are involved in the chlorophyll biosynthetic pathway [26] and genes that encode LHC proteins [27], as well as factors involved in their co- or post-translational regulation [28] or in their import into the chloroplast [18, 29]. Some of these TLA mutant strains have been shown increased maximum photosynthetic rates and a greater photosynthesis light saturation [28]; however, strains with reduced antenna systems might also exhibit enhanced photosensitivity under high light conditions because the pigment-binding complexes

function not only in harvesting light but also in photoprotection and NPQ activation [11, 30, 31].

Despite promising results obtained in lab-scale experiments, TLA mutant strains produced contrasting results with regards to the improvement of biomass productivity when tested in a larger scale PBR [25, 32, 33], likely because the mutations can carry negative consequences, such as the aforementioned increased sensitivity to light stress. To effectively improve productivity, it is therefore necessary to find the optimal compromise between the benefits of reducing light harvesting and the disadvantages associated with the potential reduction in photo-protection [34].

Here, we isolated and characterized mutant strains with photosynthetic apparatus alterations that were generated by chemical and insertional random mutagenesis in *Nannochloropsis gaditana*, an interesting model organism for biofuel production and large scale cultivation [35]. Such a collection of strains will facilitate the search for mutant strains with reduced competitive capacity that could potentially provide positive advantages in the artificial environment of a PBR. We also characterized those strains with reduced cellular Chl contents in greater detail, identifying strain E2 as having a reduced PSII antenna size, improved photosynthetic activity and improved productivity in lab-scale fed-batch cultures, representing a promising starting point in the search for improved productivity outdoors.

MATERIAL AND METHODS

Microalgae growth.

Nannochloropsis gaditana (strain 849/5) from the Culture Collection of Algae and Protozoa (CCAP) were used as the WT strain for the generation of mutant strains. Cells were grown in sterile F/2 media with sea salts (32 g/L, Sigma Aldrich), 40 mM Tris-HCl (pH 8) and Guillard's (F/2) marine water enrichment solution (Sigma Aldrich) in Erlenmeyer flasks with 100 μmol photons m^{-2} s^{-1} illumination and 100 rpm agitation at 22 ± 1 °C in a growth chamber. Fed-batch cultures were grown in 5 cm diameter Drechsel's bottles with a 250 ml working volume and bubbled using air enriched with 5 % CO_2 (v/v); in this case, F/2 growth media was enriched with added nitrogen, phosphate and iron sources (0.75 g/L $NaNO_3$, 0.05 g/L NaH_2PO_4 and 0.0063 g/L $FeCl_3$•6 H_2O final concentrations). Illumination at 400 μE m^{-2} s^{-1} was provided by a LED Light Source SL

3500 (Photon Systems Instruments, Brno, Czech Republic). The pH of the fed-batch cultures was set to 8.00 and fresh media was added every other day to restore the starting cell biomass concentration of 1 gr/L. Algal growth was measured by the change in optical density at 750 nm (OD_{750}; Cary Series 100 UV–VIS spectrophotometer, Agilent Technologies) and cells were counted using a cell counter (Cellometer Auto X4, Nexcelom Bioscience). The biomass concentration was measured gravimetrically as a dry weight (DW) by filtering 5 ml of culture that had been diluted 1:5 to dissolve salts using 0.45 µm pore size cellulose acetate filters. The filters were then dried at 70 °C for at least 24 h and the dry weights were measured in grams per liter. Biomass productivity was then calculated as $([C_f] - [C_i]) / (t_f - t_i)$, where C is the final or initial biomass concentration of the culture and t is the day number.

Chemical mutagenesis

To generate the mutant collection, mutagenesis conditions were set to induce 90 % cell mortality, ensuring a high mutation frequency. Microalgae suspensions ($2 * 10^7$ cells/mL) in the late exponential growth phase were mutagenized using 70 mM EMS (Sigma Aldrich) for 1 h in darkness at room temperature with mild agitation. The treated cells were then centrifuged at 5000 g for 8 min, washed four times with sterile F/2 media to remove excess EMS and then plated on F/2 agar dishes. Plates were cultured at 22 ± 1 °C with 20 µmol photons m^{-2} s^{-1} illumination until algae colonies emerged (5 and 8 weeks after mutagenesis).

Insertional mutagenesis.

A library of insertional mutant strains was generated via transformation of the *N. gaditana* strain CCAP 849/5 with the *Sh-ble* gene (from *Streptoalloteichus hindustanus*, kindly provided by Prof. Matthew Posewitz [35]) conferring resistance to zeocin. The DNA cassette (approximately 1.3 kb) containing the *Sh-ble* gene with an endogenous UBIQUITIN promoter and the FCPA terminator [35], was digested from the pPha-T1-UEP vector and purified on an agarose gel (0.8 % (w/v)). For transformations, $5 * 10^8$ *N. gaditana* cells were washed four times with 375 mM sorbitol at 4 °C and resuspended in 100 µl 375 mM cold sorbitol. Cells were then incubated with 5 µg DNA for 10 minutes on ice and then electroporated in a 2 mm cuvette using an ECM630 BTX electroporator set (500 Ω, 50 µF and 2400 V). Following electroporation, the cells were maintained on ice for 5 minutes, resuspended in 10 ml F/2 media and recovered for 24 hours at 22 ± 1

°C with agitation and 20 µmol photons m^{-2} s^{-1} before plating onto F/2 plates containing 3.5 µg/ml zeocin. Resistant colonies were detected after 3 weeks and picked after 4-5 weeks.

Mutant selection and in vivo fluorescence-based high-throughput screening.

Approximately 5-6 weeks after mutagenesis or transformation, colonies were collected and transferred. Colonies were then analyzed by *in vivo* fluorescence using a FluorCam FC 800 video-imaging apparatus (Photon Systems Instruments, Brno, Czech Republic) to identify those with mutations affecting the regulation of the photosynthetic apparatus. The selected mutant strains were retained if they were positively selected in at least three successive screening rounds.

Pigment content analysis.

Chlorophyll a and total carotenoids were extracted from cells after 4 days of growth at the end of exponential phase using a 1:1 biomass to solvent ratio of 100 % N,N-dimethylformamide (Sigma Aldrich) [43]. Pigments were extracted at 4 °C in the dark for at least 24 h. Absorption spectra were determined between 350 and 750 nm using a Cary 100 spectrophotometer (Agilent Technologies) to spectrophotometrically determine pigment concentrations using specific extinction coefficients [43].

Absorption values at 664 and 480 nm were used to calculate the concentrations of Chlorophyll a and total carotenoids, respectively.

Measurements of photosynthetic activity and PSII functional antenna size.

Oxygen evolution activity was recorded using a Clark-type O_2 electrode (Hansatech, Norfolk, UK) at 25 °C. Cell suspensions (1.3 ml) containing 325 * 10^6 cells were illuminated with a halogen lamp (KL 1500, Schott, Germany) after a 5 minutes dark adaptation. The concentrations of Chl a were determined after pigment extraction. PSII functionality was assessed *in vivo* by measuring Chl fluorescence using a PAM 100 fluorimeter (Heinz-Walz, Effeltrich, Germany) after a 20' dark adaptation. Samples were treated with increasingly intense light up to 2000 µmol photons m^{-2} s^{-1}, and the light was then switched off to evaluate NPQ relaxation. NPQ and ETR values were calculated as previously described [38].

PSII antenna sizes were determined at the end of exponential phase (4^{th} day of growth) using a JTS10 spectrophotometer. Samples (200 * 10^6 cells/ml final concentration) were

adapted to the dark for 20 minutes and then incubated with 80 µM DCMU for 10 minutes. Fluorescence induction kinetics were then monitored upon excitation with 320 µmol photons m^{-2} s^{-1} of actinic light at 630 nm. The $t_{2/3}$ values obtained from the induction curves were then used to calculate the size of the PSII functional antenna.

SDS-PAGE electrophoresis and western blotting

Samples for western blotting analysis were collected from 4 day cultures in the late exponential phase. Cells were lysed using a Mini Bead Beater (Biospec Products) at 3500 RPM for 20 s in the presence of glass beads (150–212 µm diameter), B1 buffer (400 mM NaCl, 2 mM $MgCl_2$, and 20 mM Tricine–KOH, pH 7.8), 0.5% milk powder, 1 mM PMSF, 1 mM DNP-ε-amino-n-caproic acid and 1 mM benzamidine. Broken cells were then solubilized in 10% glycerol, 45 mM Tris (pH 6.8), 30 mM dithiothreitol, and 3% SDS at RT for 20 min. Western blot analysis was performed by transferring the proteins to nitrocellulose (Bio Trace, Pall Corporation) and detecting them with alkaline phosphatase-conjugated antibodies. The antibodies recognizing D2, LHCf1 and LHCX1 proteins were produced by immunizing New Zealand rabbits with purified spinach protein [UniProt: P06005 for D2] or recombinant proteins obtained from cDNA overexpression in *E. coli* [UniProt: W7T4V5 for LHCf1, and Uniprot: K8YWB4 for LHCX1].

RESULTS AND DISCUSSION

Isolation of a collection of Nannochloropsis mutant strains with alterations in the photosynthetic apparatus.

A *Nannochloropsis gaditana* culture in the late exponential growth phase was treated with ethyl methane sulfonate (EMS) to induce random genomic mutations. EMS is an alkylating agent that causes a high frequency of nucleotide substitutions and has been largely employed to induce mutations in various organisms. In recent years, EMS mutagenesis has also been employed in algae, e.g., to induce the over-production of metabolites such as astaxanthin, carotenoids and eicosapentaenoic acid [36]. Unlike other approaches, chemical mutagenesis avoids the issues connected with the outdoor cultivation of genetically modified organisms (GMOs), and generates strains that are

readily applicable to large-scale systems; however, chemical mutagenesis readily induces multiple mutations (typically point mutations), making the identification of the gene(s) responsible for the phenotype complex and time-consuming. For this reason, we also generated a second insertional mutant collection in parallel by transforming *Nannochloropsis gaditana* cells by electroporation and selecting transformants on plates containing zeocine [35]. Colonies surviving the antibiotic treatment contained at least one copy of the resistance gene integrated in the genome, and this was verified using PCR (Supplementary Figure S1). In principle, the insertion of exogenous DNA occurs randomly throughout the genome and can thus alter the expression of a wild type (WT) gene to generate a mutant. The probability of gene disruption is expected to be very high in *N. gaditana* due to the high density of genes in its nuclear genome (10646 genes in 27.5 Mbp, approximately 387 genes/Mbp) compared with that of *Chlamydomonas reinhardtii* (17741 genes in 111.1 Mbp, approximately 160 genes/Mbp [37]).

Following EMS and insertional mutagenesis, independent colonies (7 and $5x10^3$, respectively) were screened by measuring *in vivo* Chl fluorescence, which is a powerful approach for assessing the presence of changes to the composition and/or regulation of the photosynthetic apparatus [38]. This widely-used technique is based on the principle that once light is absorbed by a chlorophyll molecule within an algal cell, excitation energy can take three alternative pathways: it can drive photochemical reactions, be dissipated as heat or be re-emitted as fluorescence. These three processes compete for the same excited states and although only a relatively small amount of energy is re-emitted as fluorescence (1-2 % of the absorbed light), this fluorescence can be measured and used to gather indirect information about the other pathways [38].

To gather information about possible changes in photosynthesis, we measured the Chl fluorescence of algal mutant collections on agar plates using a video-imaging apparatus (Figure 1).

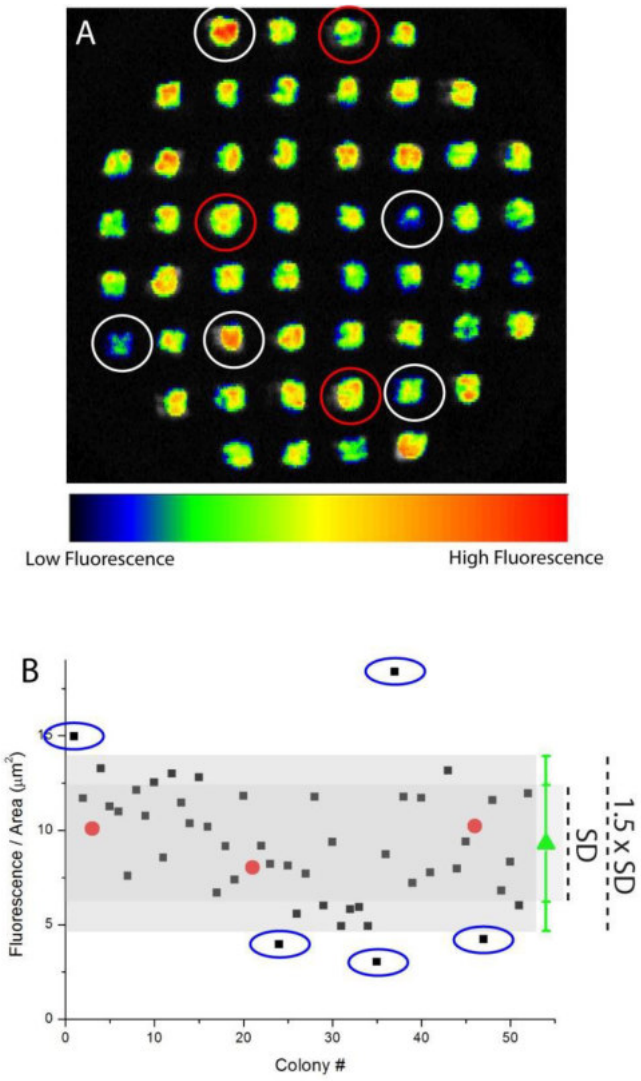

Figure 1. Example of screen for altered fluorescence intensity. A) Fluorescence imaging (F_0) of an F/2 agar plate with 52 *Nannochloropsis gaditana* colonies generated by insertional mutagenesis. Three WT colonies are circled in red, and five colonies selected for either decreased or increased fluorescence signals are circled in white. B) Chl signal quantification (fluorescence intensity/colony area) of the samples shown in A. WT colonies are circled in red, and the average of all 52 colonies ± SD is indicated with green triangles. Strains that were selected for their altered fluorescence intensities are circled in blue.

Several parameters were monitored during screening to facilitate the selection of various phenotypes (Table S1). The first parameter was the fluorescence of dark-adapted cells (F_0); when normalized to the colony area, this metric provides an estimate of the cellular Chl content, allowing the identification of mutant strains with potentially reduced pigment contents. As shown by the false color image in figure 1A, a few colonies had fluorescence signals that were either more or less intense than the others. Quantification of the fluorescence signal per area (Figure 1B) facilitated the selection of potentially interesting mutant strains with altered pigment contents. Because most of the cells in the

plate are not likely to have an altered photosynthetic apparatus, the average value for all of the colonies on the plate was used as a reference. This method was preferable over direct comparison with WT colonies present on the plate as it allowed a more reliable evaluation of variability and this choice was validated by the fact that WT colonies fell close to the average value of the screened population, as shown in figure 1B. Fluorescence intensity signals have substantial variability, and we observed that the standard deviations for each plate were between 20 and 35% of the average (33% for the plate shown in figure 1A). We used the average value ± 1.5 SD as a threshold and selected mutant strains falling outside of that interval for further investigation (e.g., the five mutant strains highlighted in figure 1A). An incontrovertible problem with this screening approach is the selection of several false positive strains during the first round analysis for simple statistical reasons. Using more stringent selection criteria would have reduced their number but would have also yielded only those strains with the strongest phenotypes, which are undesirable as extensive alterations in the photosynthetic apparatus would most likely negatively affect productivity.

Other parameters determined from *in vivo* Chl fluorescence measurements were used to identify mutant strains with additional alterations in the photosynthetic apparatus (Supplementary Table S1). The maximum quantum yield of PSII (ΦPSII, or Fv/Fm) estimates the fraction of absorbed light used for photochemistry [38] and therefore quantifies the maximum photochemical capacity of dark-adapted cells. When deviating from WT values, this metric suggests the existence of alterations in the cell's photochemical reactions. The same parameter can also be monitored in cells that have been exposed to an actinic light (ΦPSII', or Fm'-F/Fm'); in this case, its value decreases in part due to the oxidation of PS reaction centers, making them unavailable for photochemistry (the so-called "closed" state). Light-sensitive strains will show a greater decrease in PSII quantum yield, while strains with higher potential photochemical capacity will have greater ΦPSII' values.

The same fluorescence measurements after cell illumination can also be used to evaluate the mutant's capacity to regulate photosynthesis through NPQ. In natural environments, the loss of heat dissipation mechanisms would be detrimental [11]; however, these strains are potentially interesting for use in PBRs as they do not waste energy under light-limited conditions [19].

As mentioned above, all of the strains selected for one or more parameters (approximately 10 % of the initial number) were subjected to a second round of screening to identify

those showing reproducible alterations to reduce the number of false positives. At this stage, the relative number of mutant strains was theoretically enriched and WT colonies grown on the same plate were used as a reference instead of the average value of all colonies.

In several cases, differences in colony size or density affected fluorescence measurements, leading to the use of a third round of screening. All strains were homogenously spotted onto solid media (Supplementary Figure S2) at equal cellular concentrations (OD_{750} = 0.2). Although homogenizing the inoculum is time-consuming for a large number of colonies, it is extremely helpful for increasing screening sensitivity, as colony heterogeneity often prevents the detection of mutant strains with weak phenotypes [24]. Following this third round of screening, the strains exhibiting confirmed phenotypes were retained for further characterization; examples of the identified phenotypes are shown in figure 2.

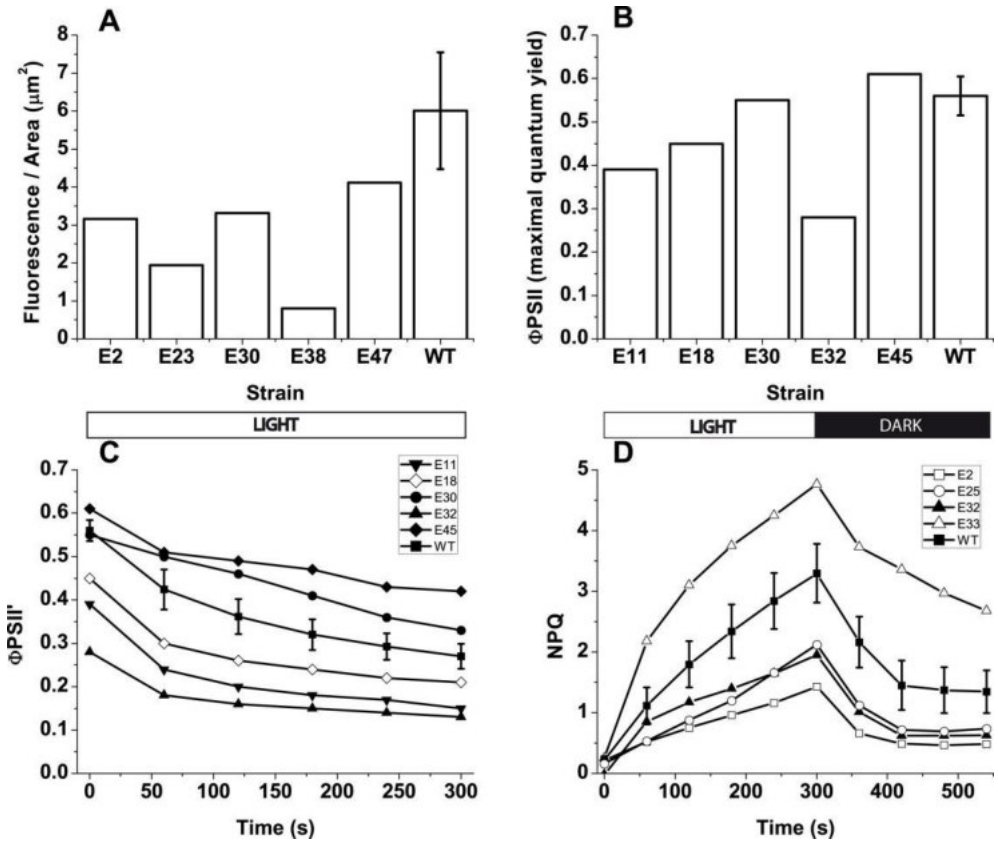

Figure 2. Examples of selected mutant strains with altered fluorescence parameters. Cells were diluted to the same cell density (OD_{750} = 0.2) prior to measurements, and examples of EMS-induced mutant strains exhibiting significant variation from WT are shown in each panel. A) F_0/Area; B) PSII quantum yield in dark-adapted colonies; C) PSII quantum yield in colonies illuminated with 450 µmol photons m^{-2} s^{-1}; D) NPQ induction and recovery (light was switched off after 300 seconds). WT n = 9.

In total, 48 were selected from the collection of insertional mutant strains (named I1-48) and 49 were selected from the EMS mutant strains (named E1-49) (Supplementary Figure S3). This screen identified mutant strains with altered fluorescence density, PSII quantum yield in dark-adapted and illuminated cells, and NPQ kinetics (Figures 2A, 2B, 2C and 2D, respectively). Selection according to the first parameter led to the isolation of mutant strains exhibiting potential alterations in their cellular Chl contents compared with the WT strain, that could be advantageous in an artificial growth system through improved light penetration in the entire culture volume. The second parameter was used to isolate strains with either improved or unaltered PSII maximum quantum yield compared with WT. The third parameter identifies strains that can saturate photosynthesis at higher irradiances than WT. The NPQ kinetics were instead useful for identifying those strains that were unable to constitutively activate excess energy dissipation, which may be valuable when grown in photobioreactor regions that are heavily light-limited. It is worth underlining that at this stage all mutants showing reproducible phenotypes were retained even if their phenotype, such in the case of strains exhibiting larger NPQ than the WT are likely not advantageous for industrial applications. In some cases (figure 2), the same strain (e.g., clone E32) was altered in more than one parameter; this feature was expected, as the parameters are not entirely independent.

Isolation of Nannochloropsis strains with reduced pigment contents.

The work described thus far produced a collection of mutant strains carrying a broad spectrum of alterations in the photosynthetic apparatus that was useful for isolating strains with a specific phenotype of interest. For all mutant strains, the mutation's effect on cell growth is key piece of information. *Nannochloropsis gaditana* is a strict photoautotroph and we can assume that some photosynthesis mutant strains may also have growth defects that would prohibit their use in large-scale cultivation applications.

For this reason, we tested all selected strains for growth in liquid media; it should be noted that the cells were grown in flasks containing F/2 media, under conditions in which the duplication rate is largely limited by CO_2 and nutrient availability rather than light use efficiency [39]. Consequently, these tests did not facilitate the identification of mutant strains with improved biomass productivity but rather the elimination of those with growth defects.

Cellular Chl contents were monitored during the late exponential phase (4th day of growth) to highlight alterations in the composition of the photosynthetic apparatus. The overall results obtained for strains produced by chemical mutagenesis are reported in figure 3.

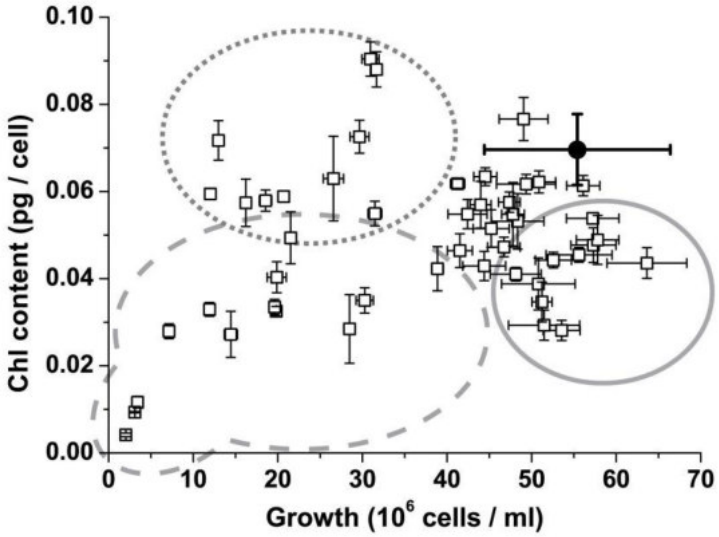

Figure 3. Growth rates and pigment contents of selected strains. Selected mutant strains produced by chemical mutagenesis were tested in liquid cultures and monitored for growth and cellular pigment content at the end of exponential phase (4th day of growth, see methods for details). Mutant strains with reduced cellular pigment content but unaffected growth compared to WT are circled with a continuous line. Mutant strains exhibiting both reduced pigment content and growth compared with WT colonies are circled with a dashed line. Strains with unaltered pigment content but with reduced growth are circled with a dotted line. WT (n = 7) is shown as black circle; mutant strains n = 2.

There was a group of mutant strains with altered growth but not altered cellular Chl content; for these strains, the reduced growth rate caused a reduction in cell concentration and a consequent decrease in fluorescence signal, leading to their selection during the screening stage even without a change in the cellular pigment content (e.g., E1 and E4 in Supplementary Figure S2). This result is reasonable considering that *N. gaditana* is an obligate phototroph and its growth depends entirely on photosynthesis [8], therefore any growth impairment, even if independent of photosynthesis, will result in reduced fluorescence.

Another group of mutant strains exhibited a reduced growth rates that were accompanied by a reduced cellular pigment contents. These mutant strains, whose phenotypes are particularly severe in some cases (e.g., I1 and E3 in Supplementary Figure S2), likely

carry mutations that impair the photosynthetic apparatus but also drastically affect growth and are therefore of limited interest for biotechnological applications.

A third group of strains exhibited growth rates and pigment contents that were indistinguishable from WT. There were a few residual false positives within this group; however, this group also contained mutant strains with altered fluorescence parameters (e.g., NPQ and/or Fv/Fm) without significant effects on either growth rates or pigment contents.

Finally, the fourth group includes mutant strains with reduced cellular pigment contents but not growth defects (Figures 3 and S2, E2, I2 and I3). These mutant strains are interesting for applied research as they could potentially drive improved light distribution and productivity in large-scale cultures.

Similar analysis of the insertional mutant strains produced comparable results even though the growth conditions used in the two experiments were slightly different (Supplementary Figure S4). One difference between the two strategies was that for the insertional mutant strains, strains with increased fluorescence levels were retained, leading to the isolation of strains with increased Chl contents. Another difference between the two experiments is that no insertional mutant strains had dramatically impaired growth as observed for the chemical mutant set (Figure 3). One possible explanation for this observation is that in the case of chemical mutagenesis, mutant strains were chosen for screening over a longer interval (up to 8 weeks), therefore even slowly growing mutant strains could form detectable colonies and be screened. In contrast, the insertional mutant colonies were all collected between 4 and 5 weeks to standardize the fluorescence imaging screening, leading to the elimination of the slowest growing colonies. Furthermore, the EMS-induced mutant strains likely carry many mutations and their combined effects can cause dramatic growth phenotypes.

Characterization of mutants with reduced pigment contents.

The collection of mutant strains described thus far includes strains with various photosynthetic properties from which smaller groups of mutant strains with the desired phenotypes can be selected. We focused on selecting mutant strains with reduced cellular Chl contents that may improve light distribution in mass cultures [19]. To this end, 7 strains from both screens were identified as being the most promising due to their unchanged growth rates and reduced pigment contents; these mutant strains were then

analyzed in greater detail. Repetition of the growth curve analysis confirmed that these strains have between 45 and 80% of the WT cellular Chl content (Figure 4A), with no change in growth rate under the tested conditions (Figure 4B).

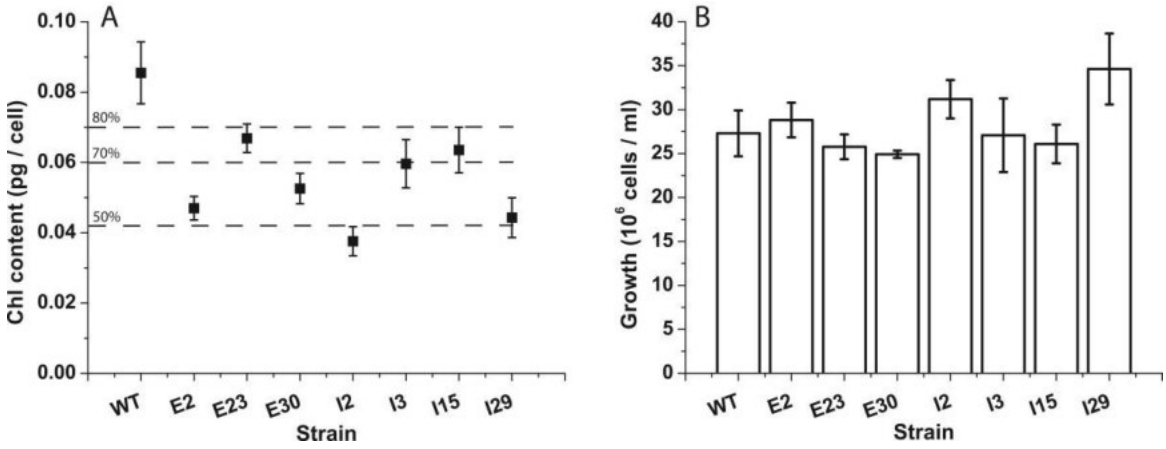

Figure 4. Validation of Chl contents and growth rates of mutant strains selected for reduced Chl contents. The phenotypes of seven mutant strains selected for their reduced Chl contents regardless of the mutagenesis method, were validated by measuring Chl content (A) and growth rate (B). Growth rates were evaluated using the concentrations of cells on the 4th day when the cells were still growing exponentially. The data are expressed as the mean ± SD, n = 6; all mutant strains exhibited significantly different Chl contents compared with WT (ANOVA, p-value < 0.05).

As previously stated, the cultures were grown in flasks with CO_2 and nutrient-limiting conditions, potentially minimizing the growth differences between WT and mutant strains; regardless, this step was useful in confirming the reduced cellular Chl contents of the selected mutant strains.

First, we used western blotting to test whether two highly expressed pigment-binding proteins present in the *Nannochloropsis gaditana* photosynthetic apparatus were responsible for the selected phenotype. We used antibodies recognizing LHCf1 and LHCX1, the major antenna proteins of *N. gaditana*, which are expected to bind a significant fraction of the Chl molecules within the cell [40, 41]. Western blotting analysis revealed that five of the seven mutant strains exhibited consistently reduced LHCf1 levels compared with WT (E2, E23, E30, I2 and I29; Figure 5A). In some cases (I2 and I29), this reduction was also accompanied by a reduction in a major PSII core subunit, D2, suggesting that PSII was reduced overall in these cells. For two other strains, E23 and E30, D2 levels were instead close to WT levels, suggesting a specific decrease in the LHCf1 antenna. For strain E2, D2 levels appeared to be greater than in WT,

emphasizing the reduction in LHCf1 levels. In contrast, the two other strains selected for their reduced Chl contents (I3 and I15) exhibited increased LHCf1 levels.

The levels of another major antenna protein, LHCX1, were also reduced in five of the seven strains (E2, E23, I15, I2, and I29). For strains E2 and I15, D2 levels were maintained or even increased compared with WT, suggesting specific reductions in LHCX1 subunits (Figure 5B).

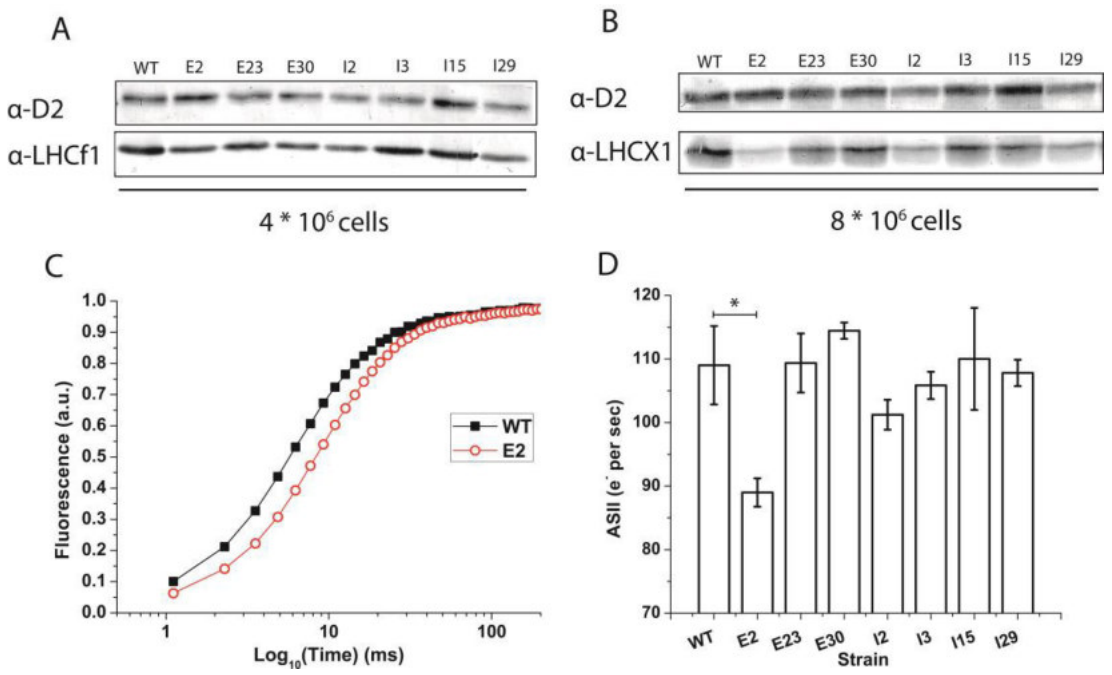

Figure 5. Evaluation of alterations in the composition of the photosynthetic apparatus of selected mutant strains. Western blot quantifications of LHCf1 (A) and LHCX1 (B), two major antenna proteins of the Nannochloropsis gaditana photosynthetic apparatus. As a control, the PSII core subunit D2 was also detected on the same membrane. Equivalents of 4 and 8 * 10^6 cells were loaded for the detection of LHCf1 and LHCX1, respectively; C) Representative traces of fluorescence induction kinetics for WT and E2 DCMU-treated cells. On the 4th day of growth, 200 * 10^6 cells in late exponential phase were used for fluorescence measurements following excitation with 320 µmol photons m^{-2} s^{-1} of actinic light at 630 nm; D) Fluorescence induction curve $t_{2/3}$ values were used to calculate the size of the PSII functional antenna. The data are expressed as the mean ± SD, n = 4; values that significantly differ from wild-type are marked with an asterisk (ANOVA, p-value < 0.05).

Together, these results clearly suggest that reductions in the pigment contents of various strains are caused by different molecular alterations to the photosynthetic apparatus. Among the identified strains, I2 and I29, exhibited a clear general decrease in the levels of all three tested proteins, suggesting a global reduction in the accumulation of all of the photosynthetic complexes. Two other strains, E2, and less obviously, E30, exhibited

reduced LHCf1 and LHCX1 levels while the reaction center contents were more stable, suggesting specific effects on the antenna proteins. In contrast, strains I15 and I3 exhibited more specific effects on LHCX1 while the other two proteins were present at levels that were similar to or even greater than in WT.

Complementary information on the light-harvesting efficiency of the photosynthetic apparatus can be obtained using fluorescence induction kinetics to estimate PSII functional antenna size *in vivo*. In cells treated with 3-(3,4-dichlorophenyl)-1,1-dimethylurea (DCMU), electron transport from PSII is inhibited, and PSII reaction centers are saturated upon illumination, resulting in an increase in the emitted fluorescence over time (figure 5C). The time required to completely saturate all of the reaction centers depends on the number of pigments that are harvesting light and transferring energy; consequently, fluorescence kinetics provide an estimate of the number of antenna complexes associated with each PS [2, 24]. In the case of strain E2, the fluorescence rise was clearly slower than for WT (Figure 5C), suggesting a specific reduction in antenna proteins in this strain and confirming the above western blotting results. In contrast, the functional antenna sizes of the other mutant strains, e.g., E23, E30, I2, I3, I15 and I29, are very similar to WT, suggesting that the pigment content reductions in these strains are not due to specific effects on the antenna complexes, or at least on those associated with PSII (Figure 5D). This result is also consistent with our biochemical data, with the exception of strain E30, for which it is possible that other antennas compensate for the decrease in LHCf1 levels.

Photosynthetic efficiency and productivity of strains with reduced pigment contents.

Photosynthesis functionality in all strains was verified using a PAM fluorimeter to measure Chl fluorescence kinetics (see methods for details). First, we analyzed PSII maximum quantum yield [38]; this parameter was not reduced for strains with reduced cellular Chl contents compared to the WT strain, suggesting that their mutations were not deleterious to photosynthesis. Four strains (E2, I2, I15 and I29) even exhibited increased PSII maximum quantum yield compared with the WT strain (Figure 6A). Second, we analyzed the photosynthetic electron transport rate (ETR), which can be estimated by monitoring the PSII quantum yield of cells treated with increasingly intense light [38]. For WT *Nannochloropsis*, ETR progressively increased with increased illumination up to 540 µmol photons m^{-2} s^{-1} (Figures 6B and C). At this point, photosynthesis reached

saturation and further increases in light intensity did not induce an increase in ETR; in contrast, ETR began to decline (Figures 6B and C). Most mutant strains behaved like the WT strain, while some showed an increase in maximal ETR (E2, E30, E23, I2 and I29), and two also reached saturation at higher light intensities (E2 and E30), which is a desired phenotype that could lead to increased productivity (Figures 6B and C).

Another important feature of photosynthetic organisms is their ability to dissipate light energy as heat, a property that strongly influences algal light use efficiency [6]. This ability was quantified using an NPQ parameter, and the data revealed that most of the mutant strains did not significantly differ from WT, with the exception of E23, I2 and I29, which exhibited a small but reproducible reduction in NPQ activation. Strain E2 exhibited the strongest reduction in NPQ activation kinetics (Figure 6D) enhancing its potential utility in large scale cultivation systems as it could also use light much more efficiently in the inner PBR layers that are often light-limited. It is worth emphasizing that this reduction in NPQ agrees with our western blotting results (Figure 5B) showing a reduction in LHCX1 protein levels in E2 compared with the WT strain. This analysis suggests a role for LHCX proteins in protection from light stress, similar to what has been observed for other algae species [42]. In contrast, strain E30 showed greater NPQ when exposed to strong illumination; in this case, it is worth noting that strong NPQ did not result from photoinhibition, as it was rapidly deactivated after the light was switched off (Figure 6E).

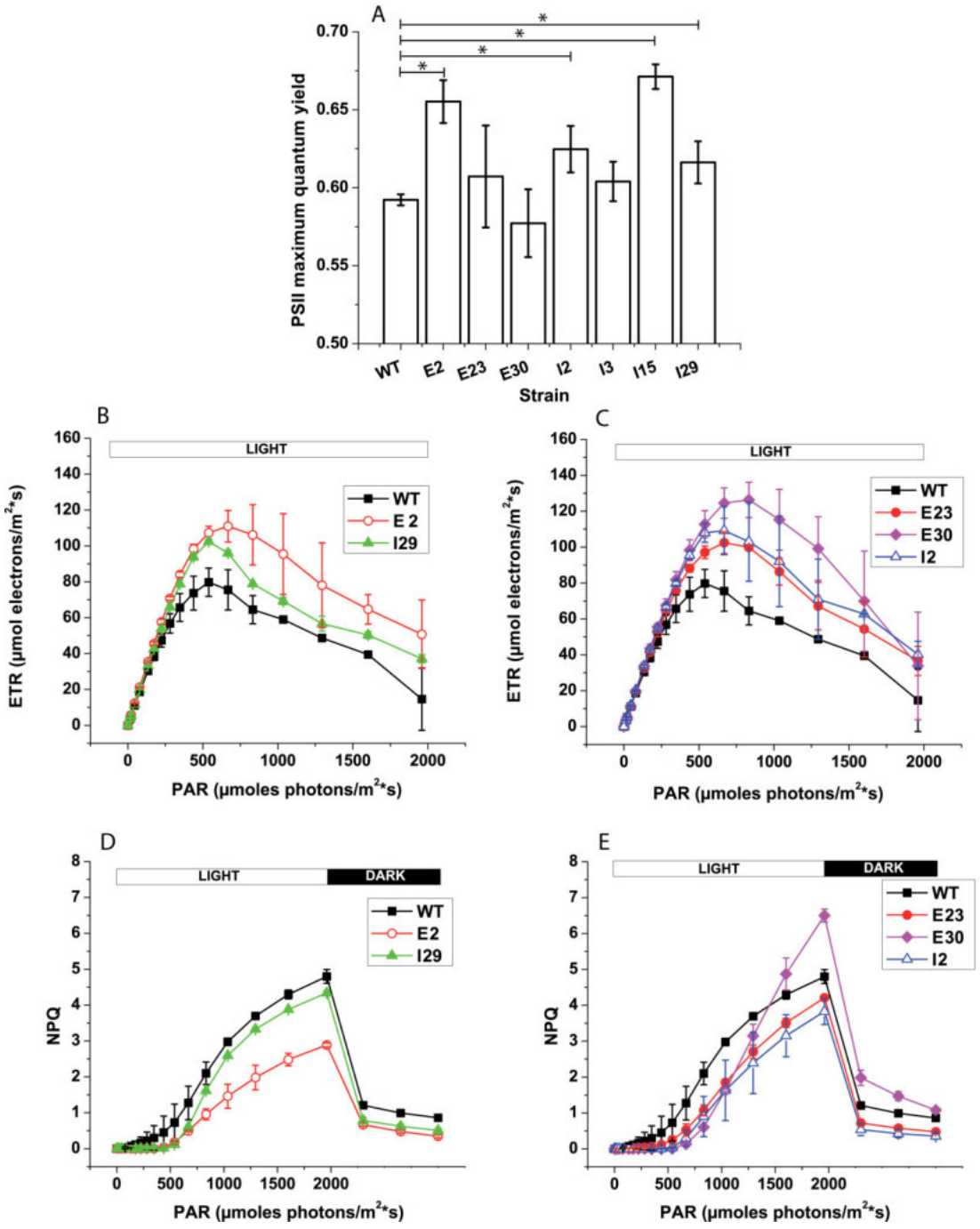

Figure 6. Measurements of photosynthetic activity in strains with reduced Chl contents. Photosynthetic activity in liquid cultures was monitoring using *in vivo* Chl fluorescence (see methods for details) at the end of exponential phase (4th day of growth). A) PSII maximum quantum yield); B-C) Photosynthetic electron transport rate (ETR); D-E) NPQ activation in cells exposed to increasing intensities of actinic light followed by 3 minutes of recovery in the dark. Only those mutant strains that significantly differed from WT are shown. The data are expressed as the mean ± SD, n = 4; values that significantly differed from wild-type are marked with an asterisk (ANOVA, p-value < 0.05).

For the mutant strain showing the largest increase in ETR photosynthetic efficiency (E2), we also measured the Photosynthesis-Irradiance (PI) curves to evaluate the dependence of the oxygen evolution rate on light intensity (see methods section for details). Similar to our observations of ETR measures, mutant strains E2 exhibited greater photosynthetic activity, with maximal activity that was (P_{max}) 44 % greater than the wild type strain (Figure 7A).

E2 strain productivity was also tested in fed-batch cultures, in conditions optimized for biomass productivity by providing excess CO_2 and enriching the media for nitrogen, phosphorus and iron (see methods for details). The light intensity was set to 400 µmol photons m^{-2} s^{-1} to reach light saturation in WT cells exposed to direct illumination and leave the cells deeper within the culture light-limited. The pH of the fed-batch culture was set to 8.0 and fresh media was added every other day to restore the initial cell biomass concentration to 1 gr/L to reproduce the high cell density conditions in industrial photobioreactors. As shown in Figure 7B, the E2 strain exhibited a 21 % increase of biomass productivity with respect to the WT strain under these conditions. It is worth emphasizing that this strain is the one that exhibited a reduced PSII antenna size, confirming the hypothesis that a specific decrease in these pigment-binding complexes without altering the reaction center contents could indeed be beneficial [19]. Although they do not ensure increased productivity in industrial-scale PBRs, these results are proof of concept that the photosynthetic productivity of WT algae can indeed be improved by genetic modification in an industrially relevant species such as *Nannochloropsis gaditana*.

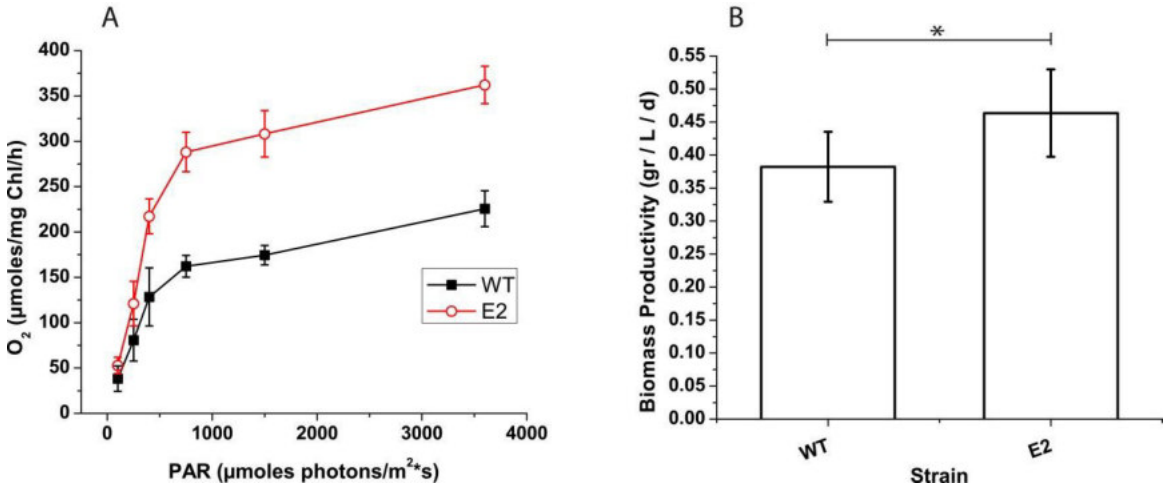

Figure 7. Photosynthesis-Irradiance (PI) and biomass productivity of a selected strain.

A) Photosynthesis-Irradiance (PI) curves of a selected strain (E2) showing increased photosynthetic activity; data are expressed as the mean ± SD, n = 4. B) Evaluation of the biomass productivity of strain E2 in lab-scale fed-batch cultures. Illumination was set to 400 µmol photons m^{-2} s^{-1} at pH 8.00. The starting culture concentrations were 150 * 10^6 cells/ml (corresponding to OD_{750} = 4.5, a 1 gr/L biomass concentration), and these concentrations were re-established every 2 days while the cells were still actively growing. Biomass productivity was calculated as reported in the methods section, and the presented values are the averages obtained from 4 weeks of culture; significant differences from WT are marked with an asterisk (ANOVA, p-value < 0.05).

CONCLUSIONS

Industrial cultivation of algae for biofuel production is highly promising, but will likely require the genetic optimization of these organisms. Here we described the generation and selection of a collection of *Nannochloropsis gaditana* strains with mutations affecting the photosynthetic apparatus, which is a valuable tool for achieving this objective.

Several mutant strains exhibiting reduced cellular chlorophyll contents were investigated in greater detail and they indeed exhibited improved photosynthetic activity, which in one case resulted in an improved biomass productivity. This work shows that the genetic approaches described are indeed capable of generating strains with potentially improved productivity in an obligatory phototroph such as *Nannochloropsis gaditana*. Moreover, it is worth emphasizing that the isolated mutant strains contain a pool of photosynthetic alterations that the entire scientific community can use to better understand photosynthesis regulation in such a new, promising, model organism.

COMPETING INTERESTS

The authors declare that they have no competing interests.

AUTHOR CONTRIBUTIONS

TM designed the research; GP, AB, and AS performed the mutagenesis screenings; GP, AB, and AM physiologically characterized the mutant strains; GP, AA, and TM wrote the manuscript. All authors read and approved the final manuscript.

ACKNOWLEDGEMENTS

This work was supported by the ERC starting grant BIOLEAP nr 309485 and PRIN 2012XSAWYM to TM. AB is grateful to the Centro studi di economia e tecnica dell'energia Giorgio Levi Cases of the University of Padova for support. We also thank Prof. Matthew Charles Posewitz of the Colorado School of Mines (USA) for sharing the transformation construct.

REFERENCES

1. Malcata FX: Microalgae and biofuels: a promising partnership? *Trends Biotechnol* 2011, 29:542–9.

2. Simionato D, Block MA, La Rocca N, Jouhet J, Maréchal E, Finazzi G, Morosinotto T: The response of Nannochloropsis gaditana to nitrogen starvation includes de novo biosynthesis of triacylglycerols, a decrease of chloroplast galactolipids, and reorganization of the photosynthetic apparatus. *Eukaryot Cell* 2013, 12:665–76.

3. Biondi N, Bassi N, Chini Zittelli G, De Faveri D, Giovannini A, Rodolfi L, Allevi C, Macrì C, Tredici MR: Nannochloropsis sp. F&M-M24: Oil production, effect of mixing on productivity and growth in an industrial wastewater. *Environ Prog Sustain Energy* 2013, 32:846–853.

4. Rodolfi L, Chini Zittelli G, Bassi N, Padovani G, Biondi N, Bonini G, Tredici MR: Microalgae for oil: strain selection, induction of lipid synthesis and outdoor mass cultivation in a low-cost photobioreactor. *Biotechnol Bioeng* 2009, 102:100–12.

5. Kirk J: Light and photosynthesis in aquatic ecosystems. 1994.

6. Simionato D, Basso S, Giacometti GM, Morosinotto T: Optimization of light use efficiency for biofuel production in algae. *Biophys Chem* 2013, 182:71–8.

7. Moody JW, McGinty CM, Quinn JC: Global evaluation of biofuel potential from microalgae. *Proc Natl Acad Sci U S A* 2014, 111:8691–6.

8. Sforza E, Cipriani R, Morosinotto T, Bertucco A, Giacometti GM: Excess CO2 supply inhibits mixotrophic growth of Chlorella protothecoides and Nannochloropsis salina. *Bioresour Technol* 2012, 104:523–9.

9. Zou N, Richmond A: Light-path length and population density in photoacclimation of Nannochloropsis sp. (Eustigmatophyceae). In *Journal of Applied Phycology*. *Volume 12*; 2000:349–354.

10. Carvalho AP, Silva SO, Baptista JM, Malcata FX: Light requirements in microalgal photobioreactors: an overview of biophotonic aspects. *Appl Microbiol Biotechnol* 2011, 89:1275–88.

11. Peers G, Truong TB, Ostendorf E, Busch A, Elrad D, Grossman AR, Hippler M, Niyogi KK: An ancient light-harvesting protein is critical for the regulation of algal photosynthesis. *Nature* 2009, 462:518–21.

12. Erickson E, Wakao S, Niyogi KK: Light stress and photoprotection in Chlamydomonas reinhardtii. *Plant J* 2015, 82:n/a–n/a.

13. Derks A, Schaven K, Bruce D: Diverse mechanisms for photoprotection in photosynthesis. Dynamic regulation of photosystem II excitation in response to rapid environmental change. *Biochim Biophys Acta - Bioenerg* 2015, 1847:468–485.

14. Tian W, Chen J, Deng L, Yao M, Yang H, Zheng Y, Cui R, Sha G: An irradiation density dependent energy relaxation in plant photosystem II antenna assembly. *Biochim Biophys Acta* 2015, 1847:286–93.

15. Melis A, Neidhardt J, Benemann JR: Dunaliella salina (Chlorophyta) with small chlorophyll antenna sizes exhibit higher photosynthetic productivities and photon use efficiencies than normally pigmented cells. *J Appl Phycol* 1998, 10:515–525.

16. Melis A: Solar energy conversion efficiencies in photosynthesis: Minimizing the chlorophyll antennae to maximize efficiency. *Plant Sci* 2009, 177:272–280.

17. Cuaresma M, Janssen M, Vílchez C, Wijffels RH: Productivity of Chlorella sorokiniana in a short light-path (SLP) panel photobioreactor under high irradiance. *Biotechnol Bioeng* 2009, 104:352–9.

18. Kirst H, Melis A: The chloroplast signal recognition particle (CpSRP) pathway as a tool to minimize chlorophyll antenna size and maximize photosynthetic productivity. *Biotechnol Adv* 2014, 32:66–72.

19. Formighieri C, Franck F, Bassi R: Regulation of the pigment optical density of an algal cell: filling the gap between photosynthetic productivity in the laboratory and in mass culture. *J Biotechnol* 2012, 162:115–23.

20. Wobbe L, Remacle C: Improving the sunlight-to-biomass conversion efficiency in microalgal biofactories. *J Biotechnol* 2014.

21. Melis A: Dynamics of photosynthetic membrane composition and function. *BBA - Bioenergetics* 1991:87–106.

22. Mussgnug JH, Wobbe L, Elles I, Claus C, Hamilton M, Fink A, Kahmann U, Kapazoglou A, Mullineaux CW, Hippler M, Nickelsen J, Nixon PJ, Kruse O: NAB1 is an RNA binding protein involved in the light-regulated differential expression of the light-harvesting antenna of Chlamydomonas reinhardtii. *Plant Cell* 2005, 17:3409–21.

23. Nakajima Y, Ueda R: The effect of reducing light-harvesting pigment on marine microalgal productivity. In *Journal of Applied Phycology*. *Volume 12*; 2000:285–290.

24. Bonente G, Formighieri C, Mantelli M, Catalanotti C, Giuliano G, Morosinotto T, Bassi R: Mutagenesis and phenotypic selection as a strategy toward domestication of Chlamydomonas reinhardtii strains for improved performance in photobioreactors. *Photosynth Res* 2011, 108:107–20.

25. Cazzaniga S, Dall'Osto L, Szaub J, Scibilia L, Ballottari M, Purton S, Bassi R: Domestication of the green alga Chlorella sorokiniana: reduction of antenna size improves light-use efficiency in a photobioreactor. *Biotechnol Biofuels* 2014, 7:157.

26. Polle JEW, Benemann JR, Tanaka A, Melis A: Photosynthetic apparatus organization and function in the wild type and a chlorophyll b-less mutant of Chlamydomonas reinhardtii. Dependence on carbon source. *Planta* 2000, 211:335–344.

27. Mussgnug JH, Thomas-Hall S, Rupprecht J, Foo A, Klassen V, McDowall A, Schenk PM, Kruse O, Hankamer B: Engineering photosynthetic light capture: impacts on improved solar energy to biomass conversion. *Plant Biotechnol J* 2007, 5:802–14.

28. Wobbe L, Blifernez O, Schwarz C, Mussgnug JH, Nickelsen J, Kruse O: Cysteine modification of a specific repressor protein controls the translational status of nucleus-encoded LHCII mRNAs in Chlamydomonas. *Proc Natl Acad Sci U S A* 2009, 106:13290–5.

29. Kirst H, García-Cerdán JG, Zurbriggen A, Melis A: Assembly of the light-harvesting chlorophyll antenna in the green alga Chlamydomonas reinhardtii requires expression of the TLA2-CpFTSY gene. *Plant Physiol* 2012, 158:930–45.

30. Elrad D: A Major Light-Harvesting Polypeptide of Photosystem II Functions in Thermal Dissipation. *PLANT CELL ONLINE* 2002, 14:1801–1816.

31. Horton P, Ruban A: Molecular design of the photosystem II light-harvesting antenna: photosynthesis and photoprotection. *J Exp Bot* 2005, 56:365–73.

32. De Mooij T, Janssen M, Cerezo-Chinarro O, Mussgnug JH, Kruse O, Ballottari M, Bassi R, Bujaldon S, Wollman F-A, Wijffels RH: Antenna size reduction as a strategy to increase biomass productivity: a great potential not yet realized. *J Appl Phycol* 2014.

33. Huesemann MH, Hausmann TS, Bartha R, Aksoy M, Weissman JC, Benemann JR: Biomass productivities in wild type and pigment mutant of Cyclotella sp. (Diatom). *Appl Biochem Biotechnol* 2009, 157:507–26.

34. Bonente G, Ballottari M, Truong TB, Morosinotto T, Ahn TK, Fleming GR, Niyogi KK, Bassi R: Analysis of LHcSR3, a protein essential for feedback de-excitation in the green alga Chlamydomonas reinhardtii. *PLoS Biol* 2011, 9:e1000577.

35. Radakovits R, Jinkerson RE, Fuerstenberg SI, Tae H, Settlage RE, Boore JL, Posewitz MC: Draft genome sequence and genetic transformation of the oleaginous alga Nannochloropis gaditana. *Nat Commun* 2012, 3:686.

36. Doan T, Obbard J: Enhanced intracellular lipid in< i> Nannochloropsis</i> sp. via random mutagenesis and flow cytometric cell sorting. *Algal Res* 2012.

37. Blaby IK, Blaby-Haas CE, Tourasse N, Hom EFY, Lopez D, Aksoy M, Grossman A, Umen J, Dutcher S, Porter M, King S, Witman GB, Stanke M, Harris EH, Goodstein D,

Grimwood J, Schmutz J, Vallon O, Merchant SS, Prochnik S: The Chlamydomonas genome project: a decade on. *Trends Plant Sci* 2014, 19:672–80.

38. Maxwell K, Johnson GN: Chlorophyll fluorescence - A practical guide. *Journal of Experimental Botany* 2000:659–668.

39. Simionato D, Sforza E, Corteggiani Carpinelli E, Bertucco A, Giacometti GM, Morosinotto T: Acclimation of Nannochloropsis gaditana to different illumination regimes: effects on lipids accumulation. *Bioresour Technol* 2011, 102:6026–32.

40. Vieler A, Wu G, Tsai C-HH, Bullard B, Cornish AJ, Harvey C, Reca I-BB, Thornburg C, Achawanantakun R, Buehl CJ, Campbell MS, Cavalier D, Childs KL, Clark TJ, Deshpande R, Erickson E, Armenia Ferguson A, Handee W, Kong Q, Li X, Liu B, Lundback S, Peng C, Roston RL, Sanjaya, Simpson JP, TerBush A, Warakanont J, Zäuner S, Farre EM, et al.: Genome, functional gene annotation, and nuclear transformation of the heterokont oleaginous alga Nannochloropsis oceanica CCMP1779. *PLoS Genet* 2012, 8:e1003064.

41. Basso S, Simionato D, Gerotto C, Segalla A, Giacometti GM, Morosinotto T: Characterization of the photosynthetic apparatus of the Eustigmatophycean Nannochloropsis gaditana: evidence of convergent evolution in the supramolecular organization of photosystem I. *Biochim Biophys Acta* 2014, 1837:306–14.

42. Niyogi KK, Truong TB: Evolution of flexible non-photochemical quenching mechanisms that regulate light harvesting in oxygenic photosynthesis. *Curr Opin Plant Biol* 2013, 16:307–14.

43. Wellburn AR: The spectral determination of chlorophylls a and b, as well as total carotenoids, using various solvents with spectrophotometers of different resolution. *J Plant Physiol* 1994, 144:307–313.

Additional File 1: Perin et al Supplementary material

SUPPLEMENTARY MATERIAL

Table S1. *In vivo* Chl fluorescence parameters used for screening mutant strains. The parameters reported below were employed to select strains with potential alterations in photosynthetic apparatus.

Fluorescence parameter	Phenotype
F_0/Area	Fluorescence intensity per area, indication of alteration in pigment contents
Φ_{PSII} in dark adapted cells	Alteration in cells photochemical ability
Φ_{PSII} in light adapted cells	Strong decrease / higher values in quantum yield indicate light sensitivity / improved photochemical ability.
NPQ in light adapted cells	Alteration in cell ability of heat dissipation

Figure S1. Verification of the successful integration of the *Sh-ble* gene in *N. gaditana* colonies. Colony PCR in *N. gaditana* insertional mutant strains confirming the presence of the transgene in six independent transformants (lanes 1-6), and its absence in a WT control (C-). Colony PCR templates were obtained with the Chelex-100 (BioRad) method (Cao et al., 2009) and were performed using the following primers: ZEO_FOR: ATGGCCAAGTTGACCAGTGC, ZEO_REV: TCAGTCCTGCTCCTCGGCC. C-, WT *N. gaditana* strain electroporated with water; C+, plasmid DNA (pPha-T1-UEP vector). (**Cao, M., Fu, Y., Guo, Y., and Pan, J.** (2009). Chlamydomonas (Chlorophyceae) colony PCR. Protoplasma **235**: 107–10.)

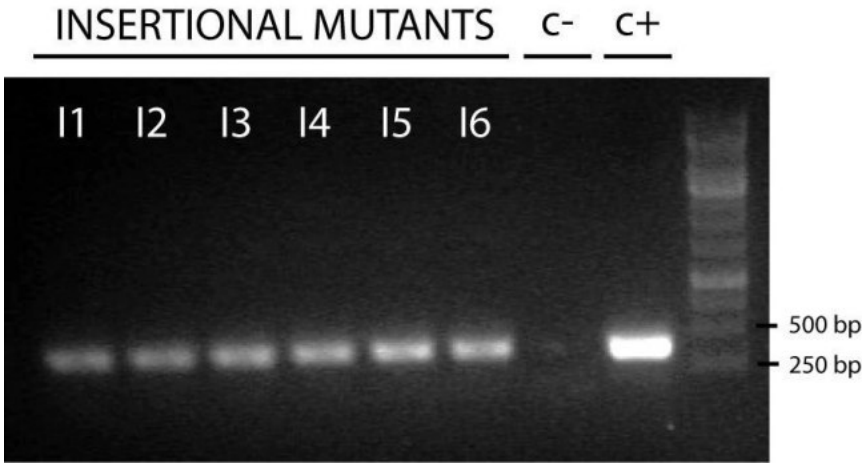

Figure S2. Example of fluorescence screening using homogenized inoculum. Fluorescence imaging (F_0) of F/2 agar plates in which all colonies were spotted homogenously, at equal cellular concentration (OD_{750} = 0.2). The first two lanes on the left show mutant strains coming from the chemical (E1-4) and the insertional mutagenesis (I1-4), respectively. The third lane shows 4 replicas of the WT strain.

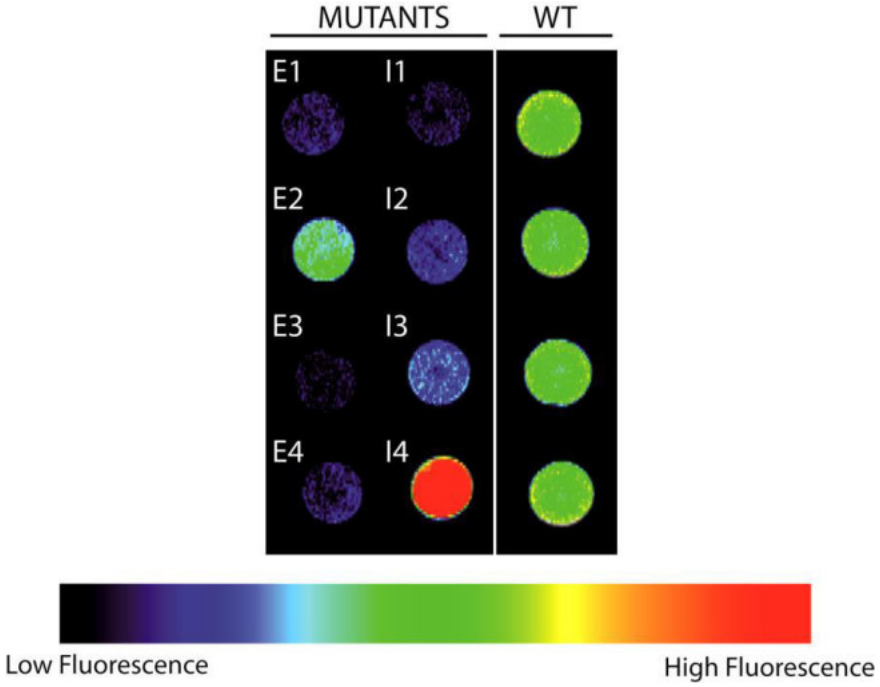

Figure S3. Outline of the three-step screening used to isolate *N. gaditana* photosynthetic mutant strains. In red is underlined the third round of screening after colonies inoculation at the same starting cellular concentration.

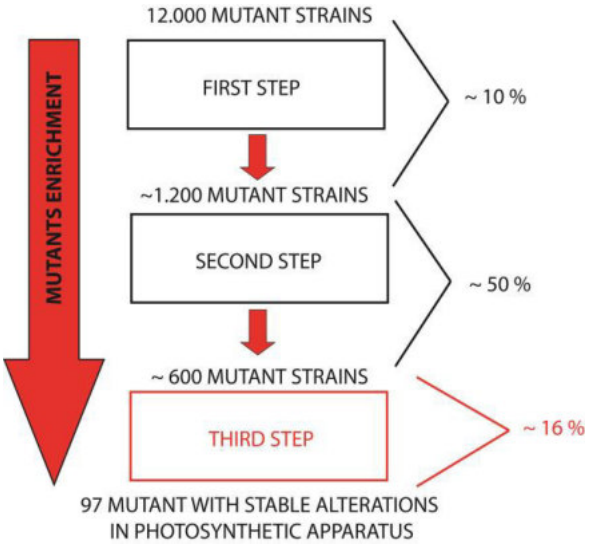

Figure S4. Growth rates and pigment contents of selected insertional mutant strains. Selected mutant strains produced by insertional mutagenesis were tested in liquid cultures and monitored for growth and cellular pigment content at the end of exponential phase (4th day of growth, see methods for details). Mutant strains with reduced cellular pigment content but unaffected growth compared to WT are circled with a continuous line. Mutant strains exhibiting both reduced pigment content and growth compared with WT colonies are circled with a dashed line. Strains with unaltered pigment content but with reduced growth are circled with a dotted line. WT (n = 7) is shown as red circle; mutant strains n = 2.

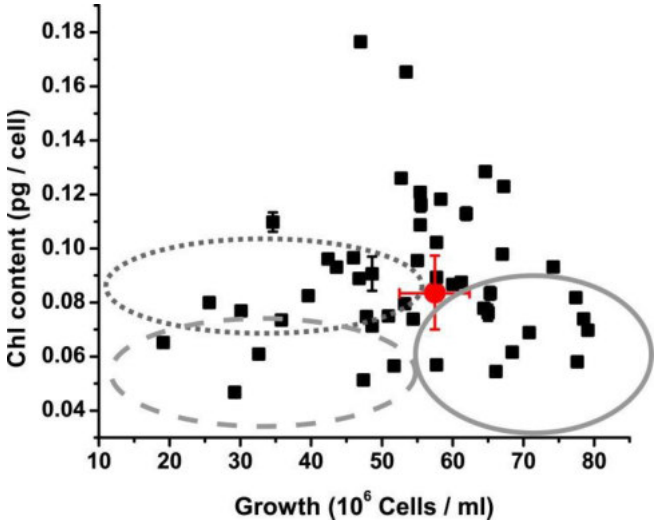

Figure S5. Western blot analysis of strains with reduced Chl contents that were selected from both screens. Western blot quantification of LHCf1 (A) and LHCX1 (B), two major antenna proteins of *Nannochloropsis gaditana* photosynthetic apparatus. As a control, the PSII core subunit D2 was also detected on the same membrane. Total cells extracts corresponding to the same total Chl content were loaded (0.4 µg for LHCf1 and 0.8 µg for LHCX1).

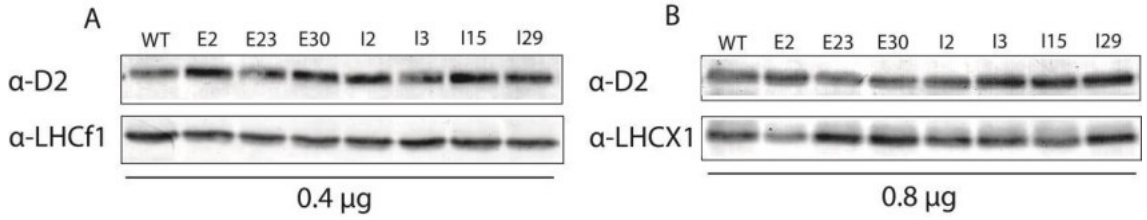

CHAPTER 3 :

Isolation and characterization of a *Nannochloropsis gaditana* low chlorophyll mutant for improved productivity in PBRs.

Authors name and affiliations

Alessandra Bellan[1], Giorgio Perin[2], and Tomas Morosinotto[1]

1-PAR-Lab_Padua Algae Research Laboratory, Department of Biology, University of Padova, Via U. Bassi 58/B, 35121 Padova, Italy.

2- Department of Life Sciences, Imperial College London, Sir Alexander Fleming Building, London, SW7 2AZ, UK.

CONTRIBUTION:

In this chapter AB performed all the experiments for the selection, the molecular characterization and the phenotypical evaluation in different light treatments. GP was in charge of the spectroscopic evaluation of the antenna size, during the preliminary growth curves.

ABSTRACT

In this chapter we presented the phenotypical and molecular characterization of *Nannochloropsis gaditana* insertional mutant strain I29 isolated, as described in chapter 2, because of a 20% decrease in chlorophyll (Chl) content with respect to the parental strain. A point mutation causes a frame shift and the early termination in a gene, which codifies for a key gene in the chlorophyll biosynthetic pathway and it was identified as the most likely responsible for the strain phenotype. Chl reduction in the cells leads to a global lower content in all components of photosynthetic apparatus whose relative composition is not significantly affected.

Cultivation of the strain in different conditions showed that I29 is able to remodel its photosynthetic apparatus in response to the light supply, maintaining its reduced chlorophyll content with respect to the wild type. The low chlorophyll phenotype of I29 is also maintained upon cultivation in lab scale PBR and this results in an improved productivity, most likely thanks to a better light penetration in the culture.

INTRODUCTION

As discussed in previous chapters, fossil fuel represents the largest fraction of global energy supply. Oil and other liquid fuels remain the largest source of energy for the transportation and industrial sector. The massive exploitation of fossil fuel leads to a release of large amount of carbon dioxide and other pollutants in the atmosphere. It is thus evident that there is a strong need of alternative, renewable and environmentally compatible sources of energy. Among all possible alternative solutions under development, microalgae are promising as sustainable source of biomass thanks to a high photosynthetic efficiency per area. Indeed cells are all photosynthetically active and their production can avoid seasonality (Matsumoto et al. 2017; Stephenson et al. 2011). In addition they do not compete with food production for arable land and they can couple biofuel production with wastewaters bioremediation, providing additional environmental benefits (Hannon et al. 2010; Palma et al. 2017). Despite these advantages microalgae biofuels production is still far from reality since costs are still not competitive with respect to the fossil fuel production. One of the main causes for this lack of competitiveness is the insufficient productivity obtained cultivating microalgae in an

industrial system. This low biomass accumulation is mainly due to the reduced photosynthetic efficiency experienced by microalgae in the industrial cultivation system, such as photobioreactors (PBR). In natural environment microalgae experience often a limiting light condition and to improve their competitiveness in their habitat, they evolved various class of antenna proteins to increase their ability to harvest light. While this property is advantageous in a natural environment, in an industrial system it leads to a strong optical density of the culture. Most of the available light is absorbed by the external layer, leaving the largest fraction of the cells in limiting light conditions (Mussgnug et al. 2007).

Chlorophyll is the main pigment responsible of light harvesting and it was suggested that the isolation of mutant strains with a reduced content could enhance the productivity by improving light penetration in the culture (Stephenson et al. 2011).

In this work we focused the attention on *N.gaditan*a which is a marine microalga that has been identified as a promising candidate for biofuel production thanks to its ability to accumulate lipids, especially in nitrogen starvation condition (Simionato et al. 2013). Its metabolism is photoautotrophic, so its photosynthetic efficiency is strictly correlated with biomass accumulation. As described in chapter 2 we isolated a collection of *N.gaditana* random mutant strains altered in the photosynthetic apparatus with alterations in the pigment content or in regulatory mechanisms of photosynthesis. In this chapter we focused our attention on one of the most promising among all the selected, I29, that showed a reduction in the chlorophyll content respect to the WT. The results of its molecular and a physiological characterization are reported, also testing its productivity in lab scale PBRs.

MATERIAL AND METHODS

Microalgae growth

Nannochloropsis gaditana (strain 849/5) from the Culture Collection of Algae and Protozoa (CCAP) is the WT strain. Cells were cultured in sterile F/2 media with sea salts (32 g/l, Sigma Aldrich), 40 mM Tris–HCl (pH 8) and Guillard's (F/2) marine water enrichment solution (Sigma Aldrich) in Erlenmeyer flasks with 100 μmol photons m^{-2} s^{-1} illumination and 100 rpm agitation at 22 ± 1 °C in a growth chamber.

Using a Multicultivator MC 1000-OD system (Photon Systems Instruments, Czech Republic) different light regimes were tested. The temperature was maintained at 21° C

and illumination was provided over a 16-h photoperiod (16-h light, 8-h dark) at intensities of 10, 100, and 1000 µmol of photons m^{-2} s^{-1} using an array of white LEDs. In this case, experiments were performed using a F/2 medium enriched with added nitrogen, phosphate and iron sources (0.75 g/l $NaNO_3$, 0.05 g/l NaH_2PO_4 and 0.0063 g/l $FeCl_3 \cdot 6 H_2O$ final concentrations). The suspension culture was constantly mixed and aerated through air bubbling.

A fed batch system was exploited for productivity evaluation. Algae were grown in 5 cm diameter Drechsel's bottles with a 250 ml working volume. Air enriched with 5 % CO_2 (v/v) was bubbled constantly. Illumination at 400 µmol of photons m^{-2} s^{-1} was given by a Neon Light Source. The pH of the fed-batch cultures was set to 8.00 and fresh media added every other day to restore the starting cell biomass concentration of 1 g/l or 1.7 g/l. Algal growth was measured by cells counting using a cell counter (Cellometer Auto X4, Nexcelom Bioscience). The biomass concentration was measured as a dry weight (DW) by filtering 5 ml of culture using 0.45 µm pore size cellulose acetate filters. The samples had been diluted 1:10 to dissolve salts. The filters were then dried at 70 °C for at least 24h and the dry weights were measured in grams per liter. Biomass productivity was then calculated as

$$([C_f] - [C_i])/(t_f - t_i)$$

where C is the final or initial biomass concentration of the culture and t is the day number.

Pigment content analysis

Chlorophyll a and total carotenoids were extracted using a 1:1 biomass to solvent ratio of 100 % N,N dimethylformamide (Sigma Aldrich). Cells were collected after 4 or 9 days of growth at the end of exponential phase. Pigments were extracted at 4 °C in the dark for at least 24h. Absorption spectra between 350 and 750 nm using a Cary 100 spectrophotometer (Agilent Technologies) were used to determine pigment concentrations using specific extinction coefficients. Absorption values at 664 and 480 nm were used to calculate the concentrations of chlorophyll a and total carotenoids, respectively.

Fluorescence measurements

Photosynthesis evaluation was done by measuring in vivo Chl fluorescence using a PAM 100 fluorimeter (Heinz-Walz, Effeltrich, Germany). PSII functionality was expressed as PSII maximum quantum yield (Fv/Fm), according to (Maxwell and Johnson 2000). Samples were exposed to increasing light intensity up to 2000 µmoles photons m^{-2} s^{-1}, and then light was switched off to evaluate NPQ relaxation kinetic. NPQ values were calculated as previously described (Maxwell and Johnson 2000).

PSII antenna sizes were determined in active growth conditions, using a JTS-10 spectrophotometer (Biologic, France). Samples (200 x 10^6 cells/ml final concentration) were dark-adapted for 20 minutes and incubated with 80 µM 3-(3,4-dichlorophenyl)-1,1-dimethylurea (DCMU) for 10 minutes. An excitation with 320 µmoles photons m^{-2} s^{-1} of actinic light at 630 nm was used to evaluate the fluorescence induction kinetics. The $t_{2/3}$ values obtained from the fluorescence induction curves were used to calculate the size of the PSII functional antenna (Bonente et al. 2011; Perin et al. 2015).

The P700 and the total electron flow (TEF) spectroscopic quantifications were performed measuring P700 (the primary electron donor to PSI) absorption at 705 nm in intact cells. Analyses were conducted exposing the samples (300 x 10^6 cells/ml final concentration) to saturating actinic light (2050 µmol of photons m^{-2} s^{-1}, at 630 nm) for 15 seconds to maximize P700 oxidation (P700) and reach a steady state. Then the light was switched off to follow the P700 re-reduction kinetic in the dark for 5 seconds. The total electron flow (TEF) was calculated from the monitoring of the P700 re-reduction rates after illumination in untreated cells. The electron transport rate was calculated assuming a single exponential decay of P700.

In this way the rate constant of P700 reduction was calculated as $1/\tau$. By multiplying the rate constant with the fraction of oxidized P700, and considering this value as 1 in DCMU- and DBMIB-treated cells we could evaluate the number of electrons transferred per unit of time per PSI unit (Simionato et al. 2013). The PSI content was evaluated from the maximum change in the absorption of P700 in cells treated with DCMU (80 µM) and DBMIB (dibromothymoquinone, 300 µM) at a saturating actinic light (2050 µmol of photons m^{-2} s^{-1}, at 630 nm) (Meneghesso et al. 2016).

DNA extraction, TAIL-PCR and whole genome re-sequencing.

N. gaditana strains genomic DNA was extracted from cultures in the exponential phase, grown in Erlenmeyer flasks using F/2 liquid media. Cells were lysed using a Mini Bead Beater (Biospec Products) at 3500 RPM for 20 s in the presence of glass beads (150–212 μm diameter). Genomic DNA was then purified using the EUROGOLD^{TM} Plant DNA Mini Kit (Euroclone), applying minor modifications. DNA concentration and purity was determined by 100 UV–VIS spectrophotometer (Cary Series, Agilent Technologies).

Thermal asymmetric interlaced (TAIL)-PCR utilizes nested-specific primers in successive reactions together with a shorter arbitrary degenerate primer. The relative amplification efficiencies of specific and non-specific products can be thermally controlled (Dent et al. 2005; Liu, Y G, Norihiro Mitsukawa, Teruko Oosumi 1995). The nested-specific primers used in the present study are reported in table 1. They were designed to be specific for the 3'-end of the gene conferring resistance to zeocine (Perin et al. 2015). The short degenerate oligonucleotides are called RMD227 and RMD228 and they were already successfully used by (Dent et al. 2005). Details of the PCR reaction mix and thermal cycles have been described in (Dent et al. 2005)

Table 1: In the table were reported the name of the primer and its sequence (5' – 3').

Primer I	**GAGATCGGCGAGCAGCCGTG**
Primer II	**GCCCTGCGCGACCCGGCCGG**
Primer III	**GTGGCCGAGGAGCAGGACTG**
RMD227	**NTCGWGWTSCNAGC**
RMD228	**WGNTCWGNCANGCG**

The whole genome re-sequencing for mutant strain I29 was performed by IGA Technologies Services (Udine, Italy), with the Illumina MiSeq platform, using 100 bp pair-end sequences leading to a 70-fold genome coverage. The *N. gaditana* B-31 genome published in (Corteggiani et al. 2014), was used as reference. Genetic variants annotation and their prediction effects was carried out using the SnpEff software.

Total RNA extraction and cDNA preparation.

Total RNA was extracted from the *N. gaditana* batch cultures after 4 days of growth in in Erlenmeyer flasks with F/2 media. Cells were lysed using liquid nitrogen and a Mini Bead Beater (Biospec Products) at 3500 RPM for 20 s in the presence of glass beads (150–212 μm diameter). Total RNA was thus purified using the TRI Reagent™ (Sigma Aldrich), applying minor modifications to the manufacturer's instruction. Total RNA concentration and purity was determined by 100 UV–VIS spectrophotometer (Cary Series, Agilent Technologies).

The cDNA was prepared from 1 μg of total RNA-template with the RevertAid Reverse Transcriptase cDNA kit (Thermo Fisher Scientific, Epson, UK). The cDNA was previously treated with the DNAse I kit (Sigma Aldrich).

RT-PCR

The cDNA was used as template for the RT-PCR reactions, in order to amplify the second exon of the founded gene from the WT and I29 strains templates. KAPA HIFI high-fidelity DNA polymerase (KAPA Biosystems) was used for this purpose.

Real time PCR

Quantitative PCR was performed using FluoCycle kit (Euroclone) in a 7500 Real-Time PCR System instrument (Applied Biosystems). Primers used are listed in table 3 and they were designed on the genes tRNA methyltransferase *(Naga_100165g15)*, short chain dehydrogenase reductase *(Naga_100165g16)* and S-adenosyl methionine synthetase (*Naga_100084g4*) (Rosic et al. 2011) as housekeeping gene. Primers design and amplification protocol were previously described in (Nolan, Hands, and Bustin 2006), only minor adjustment were applied.

Table 2: Primers sequences used in the Real Time PCR experiment.

Metil_RT_for	**TGCACTACACGCTCCAGGAT**
Metil_RT_rev	**GTACCCGGCGTTGATGAG**
Dei_RT_for	**GTGCGTGTGACTAACGTGCT**
Dei _RT_rev	**CATGATTTCGAGCGCATTTAC**
Sam_RT_for	**CACCCTTTGTCGGTCTTTGT**
Sam_RT_rev	**GGGCCGTTTCAAATTCAGGT**

Southern Blot

Different restriction enzyme where tested to digest the genomic DNA, like EcoRI and ApoI(NEB). The probe was prepared by DIG DNA labeling and Detection kit (Roche) using as template the resistance cassette or the ubiquitin promoter, that is the endogenous promoter present in the resistance cassette of the mutant strains. The digested DNA was transferred to a Hybond-N membrane (GE Healthcare, Little Chanfont, UK) by capillary transfer and hybridized with the labeled DNA probe overnight. The immunological detection was done by using an alkaline phosphatase conjugated secondary antibody.

RESULTS

Molecular identification of gene mutation responsible of the phenotype.

I29 is one of the insertional mutants selected for its altered photosynthetic apparatus (Perin et al. 2015), as described in chapter 2. The phenotype identified during the screening procedure was first confirmed in batch flask cultures with minimum medium and continuous light where I29 showed a ≈ 20% reduction in the chlorophyll content respect to the WT strain grown in the same conditions (fig 1-A). The PSII antenna size, evaluated using fluorescence kinetics, was instead not altered (fig 1-B). The photosynthetic electron transport rate (ETR), estimated from *in vivo* fluorescence, is higher respect to the wild type (fig 1-C), a feature that makes this mutant potentially interesting for improved biomass productivity. In flasks cultures, however, this improved

ETR did not correlate with improved growth, but this was expected since in these conditions algae are strongly limited by CO_2 availability (Meneghesso et al. 2016) .

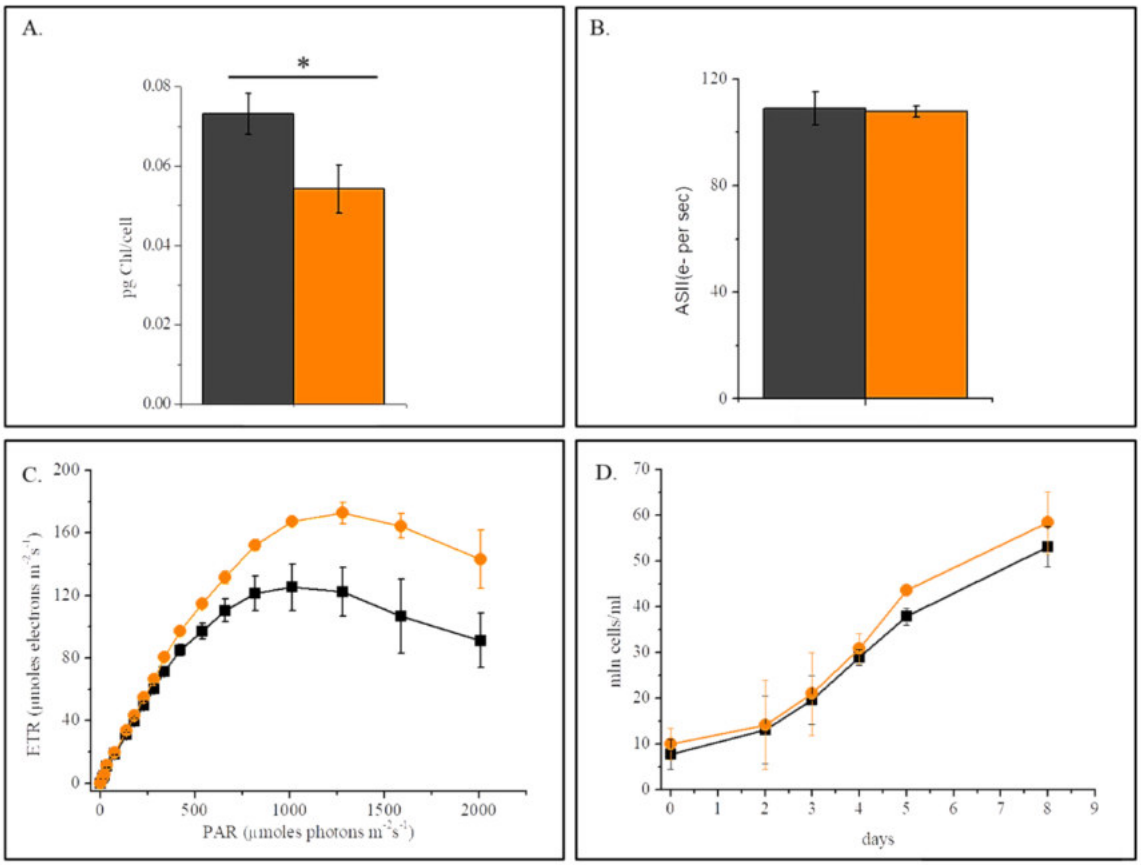

Figure 1: In A is reported the pg of chlorophyll per cell. In B is shown PSII antenna size evaluation, in C is reported the ETR saturation at increasing light intensities, and in D is shown the growth curve of the WT and the I29 in flask with F/2 medium. All the photosynthetic measurements were done after 4 days of culture (n=4), in all the panel dark gray stands for WT and orange stands for I29. Statistically significant differences between WT and strain I29 are marked with an asterisk (one-way ANOVA, p-value < 0.05).

I29 is an insertional mutant that should facilitate the identification of the genomic alteration responsible of the phenotype. To this aim we first investigated the number of insertions by Southern blot. We used the sequence of the zeocine resistance gene and of the endogenous promoter UEP as probes with the latter giving the best results in terms of signal intensity. With UEP the expectation was that a signal for the endogenous promoter will be present in the WT while the number of additional bands will be indicative of the number of insertions in the mutant. As is shown is fig 2-B in the case of I29 only two bands with similar intensity are detectable suggesting a single insertional event, the most desirable case to facilitate the potential identification of the insertion site.

TAIL PCR (fig 2-C) allowed amplifying the genomic region of the insertion site, that was identified to have occurred in a regulatory region between a tRNA methyltransferase *(Naga_100165g15)* and a short chain dehydrogenase reductase *(Naga_100165g16)* (fig 2-A). In order to confirm the insertion locus this region was amplified and in I29 the amplification product was about 1300 bp larger than in the wild type, consistent with the insertion of the resistance cassette (fig 2-D).

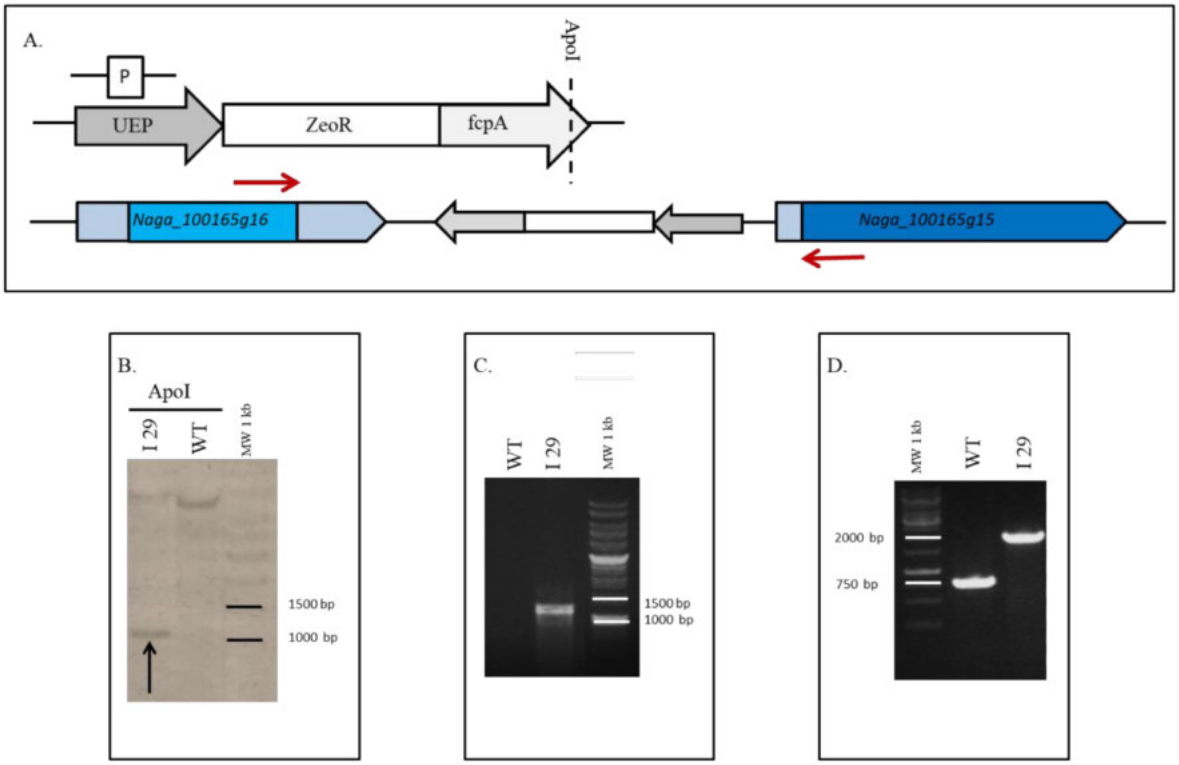

Figure 2: In A top is reported a schematic representation of the resistance cassette, P stands for probe that is given by the endogenous promoter UEP and the dashed line stands for the restriction site used for the Southern Blot. On the bottom there is the schematic representation of the insertional locus with in red the primers used to verify the insertion. In B is shown the Southern blot result using alkaline phosphatase reaction to reveal the bands, the arrow highlight the single insertion in I29. In C is presented TAIL PCR result, there is an amplification only in I29 because of the specific primers are designed on the exogenous fcpA terminator. In D is shown the amplification on the insertional locus identified by TAIL PCR, red arrow in A shows the amplification site.

Transcription of both genes closer to the insertion site were assessed by Real Time PCR that surprisingly revealed that the insertion did not affect significantly their expression levels suggesting the insertion of the resistance cassette has only minor effects on expression of the closer genes (fig 3).

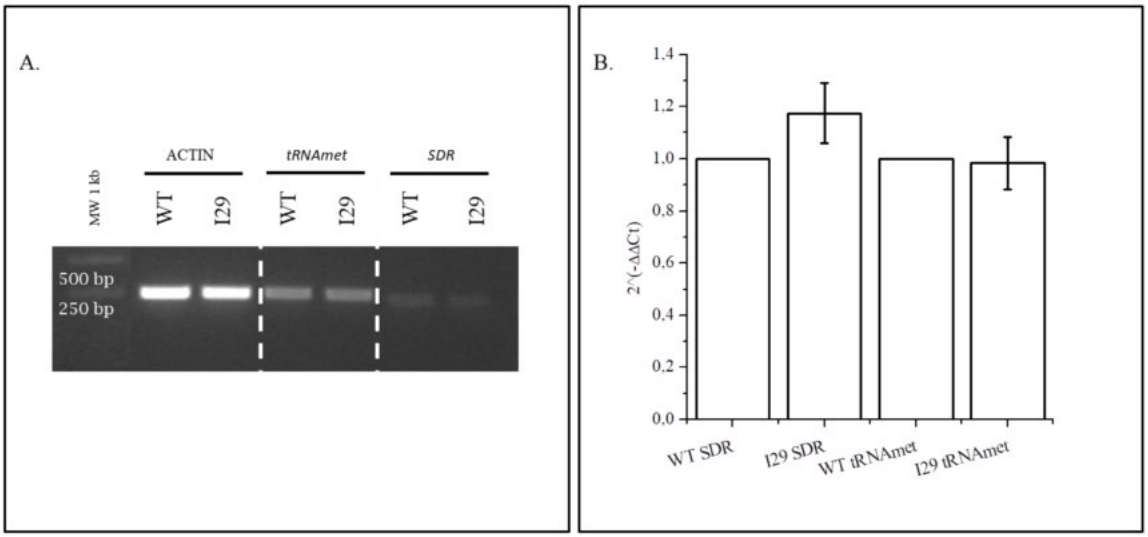

Figure 3: In A is reported the RT PCR results on the genes close to the insertion site, actin is used as reference gene. In B are shown Real time PCR results, that are represented as the relative transcription of interesting genes between WT and I29 (n=3). SDR marks the short chain dehydrogenase reductase and tRNAmet marks the tRNA methyltransferase. The data analysis was done using 2^(ΔΔCt) methods. The results shown used as reference gene SAM, but a similar result was obtained using as reference gene actin (data not shown).

In order to identify the molecular event causing the phenotype, I29 genome was completely re-sequenced and aligned with the reference *N.gaditana* genome (Corteggiani et al. 2014). The genome resequencing confirmed the individual insertion of the resistance cassette but it also revealed 42 additional point mutations that can be attributed to differences in the strain, to mutations appearing due to the electroporation or to the use of zeocine as selective marker. 39 of these point mutations affect non-coding regions or they are silent because they do not change the protein sequence. Although it cannot be excluded that mutations on non-coding regions can cause a phenotype, the most likely candidates were considered the 3 point mutations affecting protein sequences. The three altered genes are annotated as a predicted protein *(Naga_100087g18)*, a lipase containing protein *(Naga_100011g88)* and a promising gene with a signal peptide to the chloroplast. This gene codify for a key protein [1]of the tetrapyrroles biosynthetic pathway (fig 4).

[1] The name of the gene and the references are not mentioned because it will be proposed for a patent.

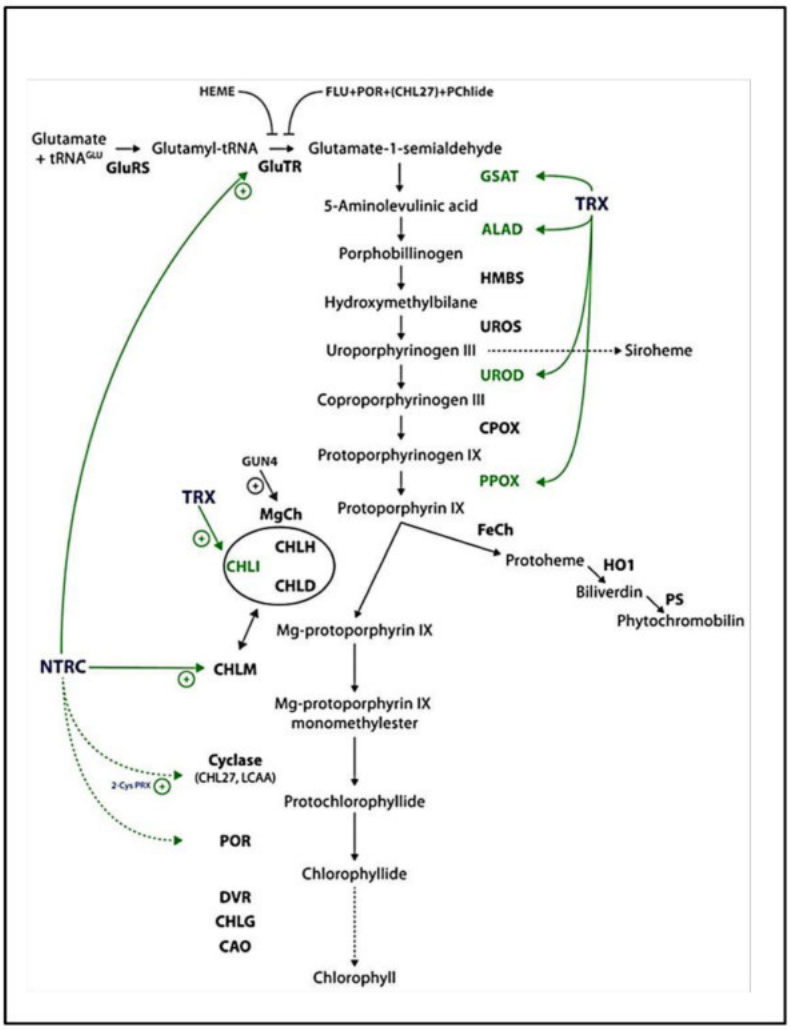

Figure 4: Tetrapyrroles biosynthetic pathway schematic representation adapted from (Richter and Grimm 2013).

This class of proteins is well conserved not only in photosynthetic organism but also in mammals since the same biosynthetic pathway leads to the production of cofactors like EME. For photosynthetic organisms tetrapyrroles biosynthetic pathway is crucial to produce chlorophyll, the fundamental pigment involved in the light harvesting, without with photosynthesis is not possible. Indeed plants and algae normally possess at least two copies of these genes and two genes encoding for it are also present in *N.gaditana* genome.

A mutation in one of the two genes reducing Chl biosynthesis efficiency is thus well consistent with I29 phenotype. Further analysis showed that in I29 there is an insertion of a cytosine in the first exon of the gene, generating a frame shift in the translation and an early termination at the beginning of the second exon (fig 5-C). We tried to amplify the

second exon transcript, as is reported in figure 5-A, but in I29 we could not found any amplified mRNA. An hypothesis is that a premature termination of the protein is thus likely causing a feedback inhibition of the transcription or mRNA stability, resulting in the loss of this protein in the mutant. Clearly other experiments will be necessary to validate this hypothesis.

The homologous is instead expressed in I29 as in the WT, as expected since a double mutation would be lethal (fig 5-B).

This alteration in the expression of one of these genes is thus a highly likely candidate as responsible for the low chlorophyll content of the strain and this will be verified by complementing the mutant strain with a WT gene.

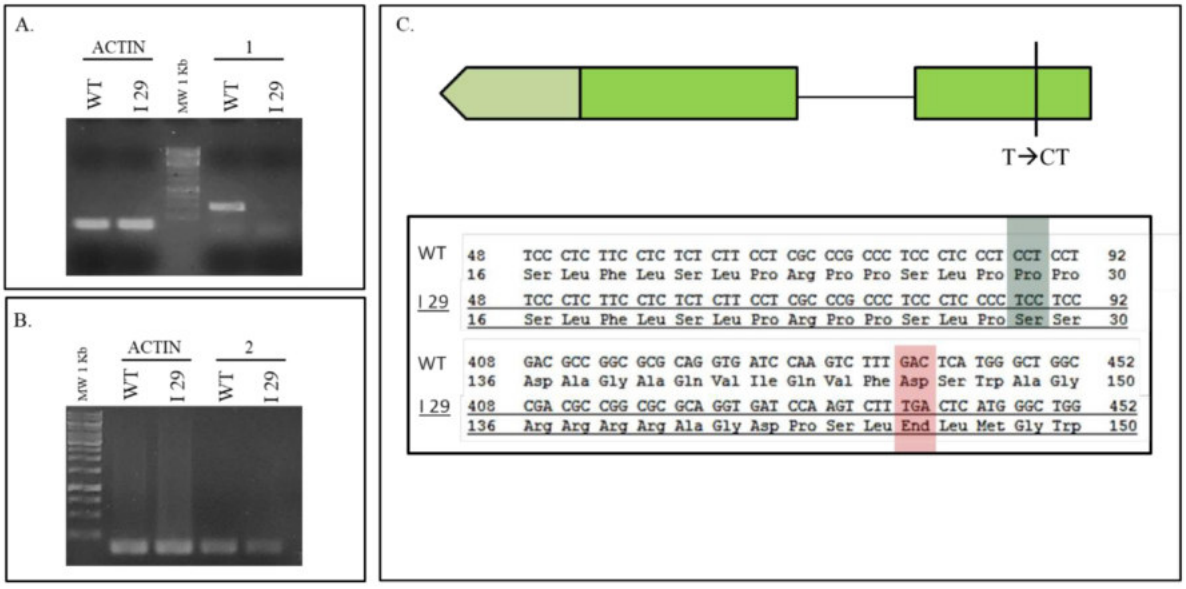

Figure 5: In A there is the RT PCR that confirm the premature termination of the transcript called 1 for the described key protein involved in Chl synthesis in I29, actin is used as control. In B is shown the amplification from cDNA of the second gene, which codify for the same protein (2) in WT and I29. In C is reported a schematic representation of the mutated gene structure and the site of the point mutation. Under the gene representation is shown the alignment of the WT sequence respect to the mutated one, in green is highlighted the point mutation occurred and in red the stop codon in the second exon caused by the frame shift induced by the mutation.

Response of I29 to cultivation in different light conditions

Photosynthetic organisms respond to growth conditions by modulating the composition and function of their photosynthetic apparatus in a process called acclimation. Regulation of Chl content is one of main component of acclimation, common in all photosynthetic

organisms. For this reason it was important to assess if the mutation also affected the I29 ability to remodel the chlorophyll content under different light regimes. Indeed we verified that this acclimation response has a major impact on productivity in PBR cultures (Perin et al. 2017, Appendix 1). To this aim I29 and WT were cultivated under different light intensity using three light regimes: HL (high light 1000 µmol photons $m^{-2}s^{-1}$), ML (medium light 100 µmol photons $m^{-2}s^{-1}$), LL (low light 10 µmol photons $m^{-2}s^{-1}$). The experiment was performed in a Multicultivator system where CO_2 was provided by air bubbling.

Evaluation of growth curve (fig 6-A) showed that I29 duplication rate was similar to WT in all light regimes, including HL. Photosynthetic efficiency of the culture was also evaluated monitoring Fv/Fm (fig 6-B) by *in vivo* fluorescence analysis. As shown in fig 6-B I29 had the same photosynthetic efficiency of the WT also in HL cultures, without any increase in photosensitivity. This is particularly significant because instead plant mutants lacking one of this kind of genes showed a high light sensitivity. For Nannochloropsis this is not the case and I29 showed instead no apparent increase in sensitivity to excess illumination.

As it is described in (Meneghesso et al. 2016) changes in *Nannochloropsis* photosynthetic apparatus composition are the response to different light conditions, which induces a remodeling of its Chl content. For example as it is shown in figure 6-C Chl content decreases with the exposition to more intense light in order to reduce the excess light absorption. I29 was able to remodel cellular pigments content in response to different light intensities as the WT (fig 6-C). In all conditions however, I29 total chlorophyll content remained lower than the WT, despite the activation of an acclimation response.

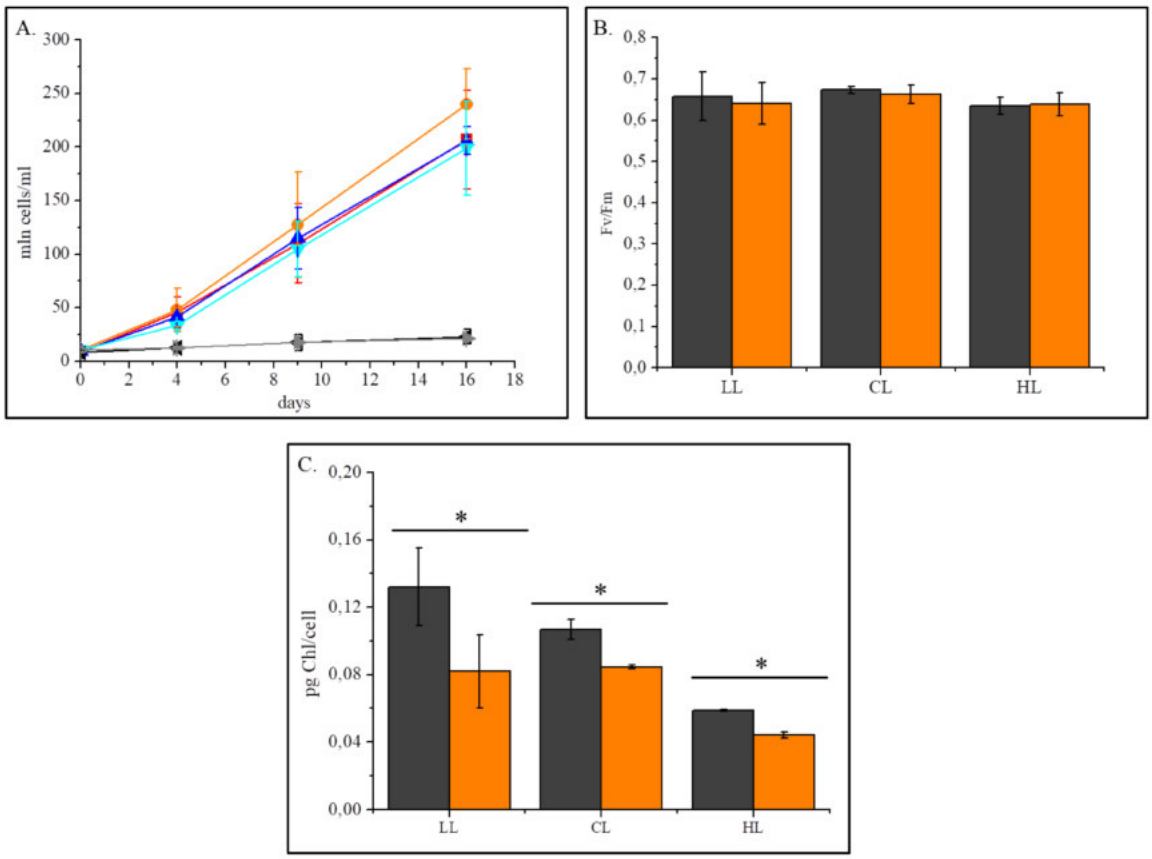

Figure 6: In A are reported the growth curves (n=3) at different light intensity, in red WT HL, orange I29 HL, blue WT CL, light blue I29 CL, dark WT LL and grey I29 LL. In B and C are shown respectively the PSII quantum yield (Fv/Fm) and the Chl content of the WT (dark gray) and I29 (orange) after 9 days of culture. Statistically significant differences between WT and strain I29 are marked with an asterisk (one-way ANOVA, p-value < 0.05).

Evaluation of biomass productivity in lab scale PBR

Cultures presented above are batch dilute cultures in a condition in which CO_2 is limiting. They are not indicative of a productivity in industrially relevant conditions where cells concentration is much higher and nutrients and CO_2 are normally provided (see Appendix 1). In the last part of the work we thus assessed I29 productivity in industrially relevant conditions to evaluate its effect on biomass production. In order to simulate industrial conditions we used lab scale photobioreactors run in a fed batch system, in which every two days the culture was diluted to the initial concentration. This was maintained high to have inhomogeneous light distribution, as expected in a large scale culture (see Appendix 1 for a more extensive description of the conditions).

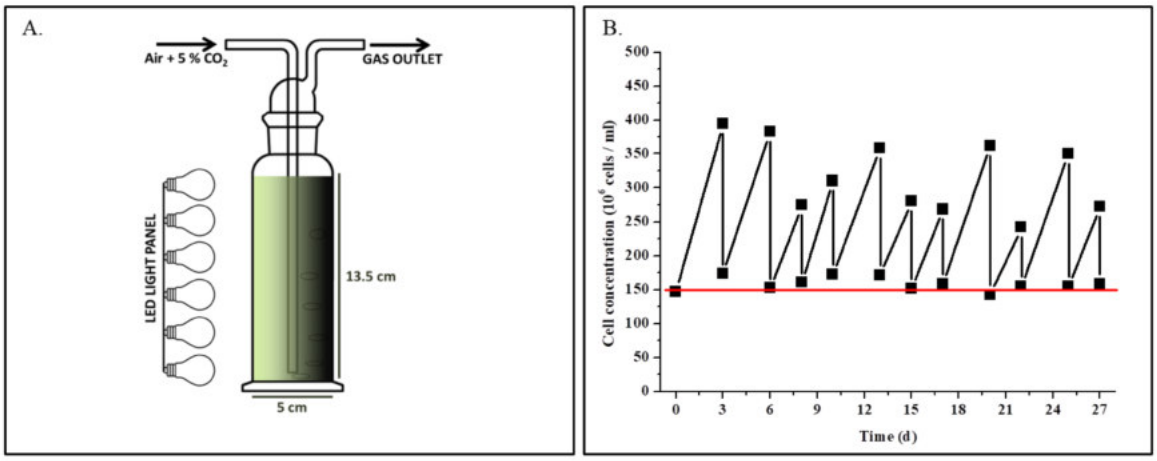

Figure 7: In A was shown a schematic representation of the fed batch system, which consists in a Drechsel's bottle with 5 cm of diameter, an air inlet of air +5% CO_2 and a set of led light coming from one side. Culture mixing is ensured by air bubbling. In B is reported an example of a semi-continuous culture run. In this case is shown the starting concentration of 150x10^6cells/ml, at which the sample is bring back every two days.

As discussed in more detail in Appendix 1 cultivation parameters can have a major influence on a strain performances. So as done in Appendix 1, we tested different conditions to assess where I29 has more advantages respect to the wild type. In particular we used:

1- 150 x 10^6 cells/ml as starting concentration and light intensity 400 µmol photons $m^{-2}s^{-1}$ (150_400);
2- 250 x 10^6 cells/ml as starting concentration and light intensity 400 µmol photons $m^{-2}s^{-1}$, (250_400);
3- 250 x 10^6 cells/ml as starting concentration and light intensity 1200 µmol photons $m^{-2}s^{-1}$, (250_1200);

I29 showed a higher productivity respect to the WT in 150_400, when it had a gain in biomass accumulation of 14% while the productivities were not distinguishable in the other conditions.

Table 4: In the table is reported the productivity in terms of grams of biomass per liter per day (g/l/d). In bold type and with the asterisks is marked the statistically significant differences between WT and strain I29 (one-way ANOVA, p-value < 0.05).

Dry weight (g/l/d)			
	150_400	**250_400**	**250_1200**
WT (n=37)	0,33 ± 0,05	0,37 ± 0,07	0,48± 0,11
I29 (n=10)	**0,39 ± 0,05****	0,34 ± 0,08	0,47 ± 0,12

In the PBR cultures I29 Chl content was reduced in 150_400 (43%) and 250_400 (27%), whereas in 250_1200 there was no difference between the WT and I29 (fig 8). Chl content found in this experiment are different respect to the batch experiment because in fed batch the cultures reached higher concentrations and they were in a condition of enriched media and not limiting CO_2. So different growth conditions lead to different acclimation responses.

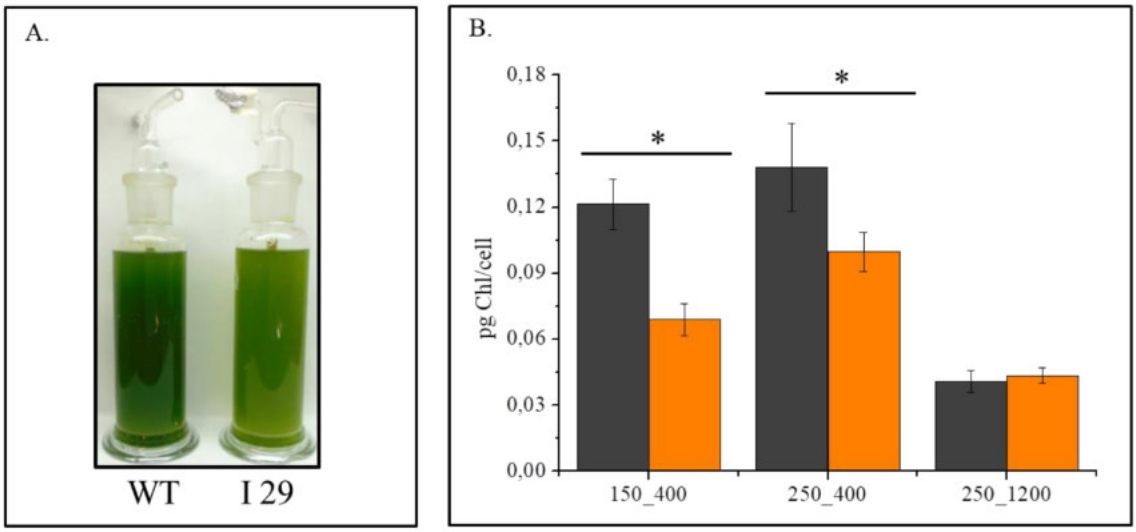

Figure 8: In A is shown how I29 and WT looks in 150_400 condition, it is evident the pale color of the mutant. In B is shown how the Chl content was changed in response to the different light regimes for the WT (dark gray) and I29 (orange)(n=6). Statistically significant differences between WT and strain I29 are marked with an asterisk (one-way ANOVA, p-value < 0.05).

The conditions with the largest chlorophyll reduction respect to the WT also showed the maximal ETR with respect to the WT (fig 9). A higher electron transport rate means that the photosynthetic chain is saturated at higher light intensity. Increased ETR was observed to correlate with reduction of Chl content and productivity also in other mutants (Perin et al 2017, Appendix 1).

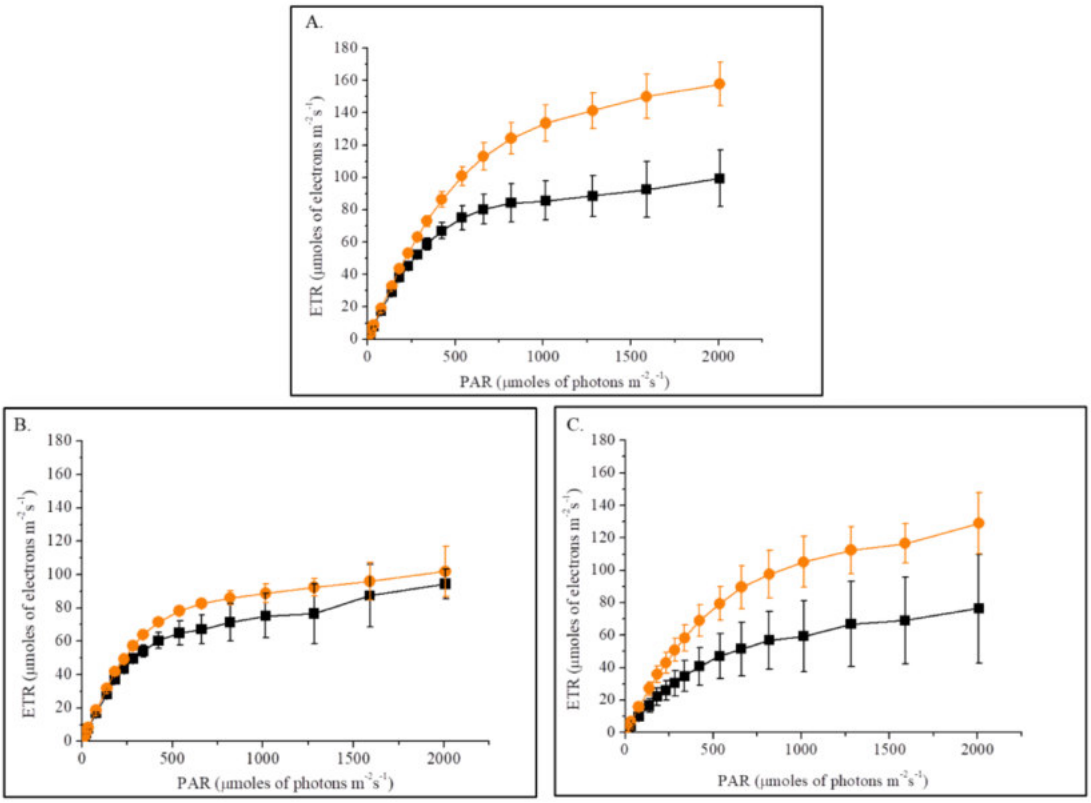

Figure 9: ETR evaluation was performed using a light curve protocol in which light intensity increases from 6 to 2000 µmol photons $m^{-2}s^{-1}$. In vivo fluorescence of Chl variation during light exposure was used to calculate this parameter. Data were reported using dark squares for WT and orange circles for I29. In A is shown the condition 150_400, in B 250_400 and in C 250_1200 (n=6).

P700 analysis highlighted a reduction in I29 P700 content per cell of about 27% in the most productive condition. Despite this when we looked to the PSII/PSI ratio we saw that it was not altered. This result suggests that Chl reduction does not affect photosynthetic apparatus composition, but it rather induces a general decrease in photosystems content. This result is in agreement with observation from batch analysis. P700 measurements evaluated also total electrons flow (TEF). The data showed in 150_400 a TEF increase of 37% for I29 respect to the WT, consistently with the higher ETR showed in fig 9 and with the different biomass productivity observed in this condition. Instead at 250_400 I29 and

WT had the same TEF, whereas in 250_1200 the situation was inverted so we found I29 with a lower TEF respect to the WT of about 28%.

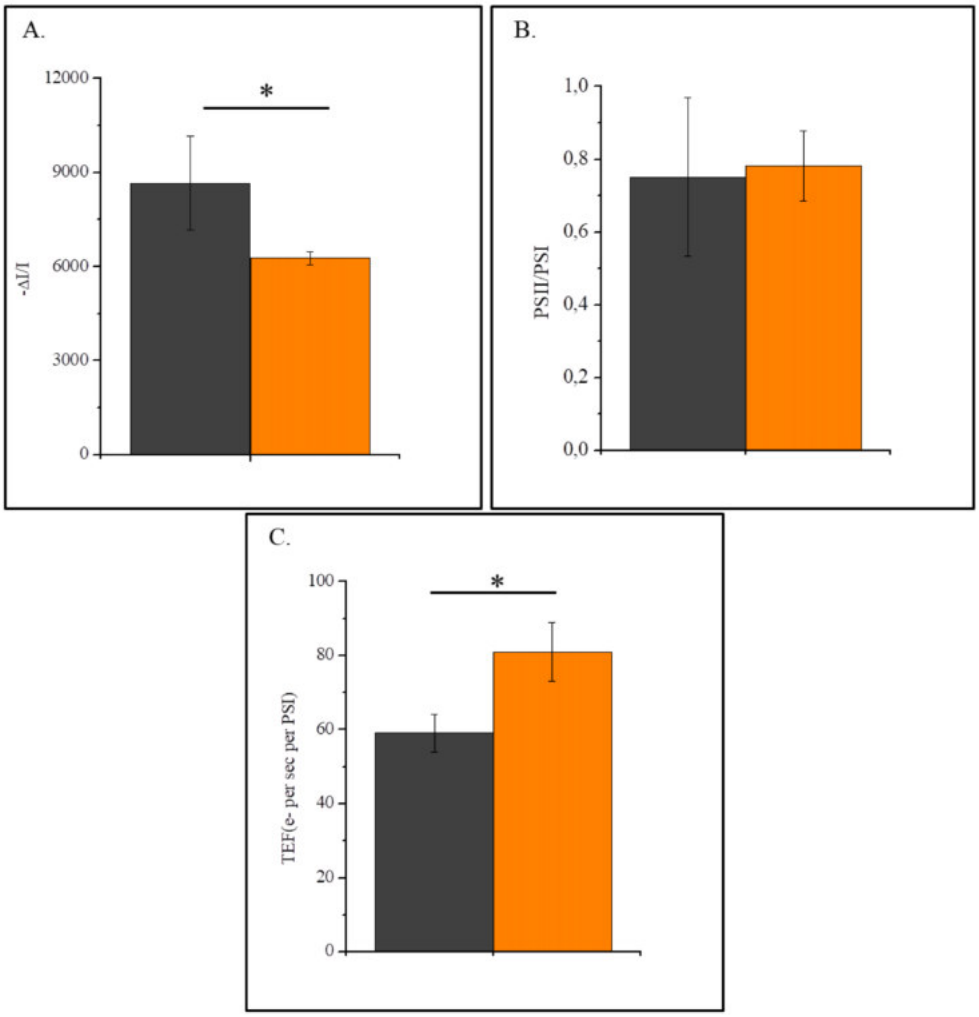

Figure 10: Data shown are obtained by spectroscopic quantifications performed measuring P700 (the primary electron donor to PSI) absorption at 705 nm in intact cells and by electron chromic shift (ECS) evaluation. In dark gray is represented the WT in orange I29 (n=6). In A is reported the maximum absorption at 705 nm of oxidized P700, which was used to evaluate PSI content in 150_400. In B is reported PSII/PSI ratio measured by ECS in 150_400. In C is shown TEF evaluation in 150_400. It was determined from the kinetics of P700 re-reduction after light was switched off. Data are normalized to PSI content using single flash. Statistically significant differences between WT and strain I29 are marked with an asterisk (one-way ANOVA, p-value < 0.05).

DISCUSSION

Nannochloropsis gaditana genetic engineering: a powerful tool but with some issues.

I29 molecular characterization revealed a single insertion event, which is the ideal situation to correlate phenotype with genotype. The insertion locus was identified by TAIL PCR in a non-coding region between two genes encoding for a short chain dehydrogenase reductase and a tRNA methyltransferase. The insertion however did not impair the transcription of any of the genes that was unaffected in I29. Genome resequencing evidenced the presence of a large number of point mutations, likely due to electroporation high voltage (Sosnowski et al. 1997; Stacey et al. 2003) or to the use of zeocine as selection (Chankova et al. 2007), that can induce double strand breaks of the DNA. Such a large number of point mutations is a significant issue during the molecular characterization, because it makes laborious the identification of the mutation responsible for the phenotype. This issue would have to be addressed, even if till now electroporation is the only transformation protocol demonstrated to be effective for *Nannochloropsis*. *N.gaditana* cell wall is composed of a layer of algaenans which makes the digestion not possible at present.

A promising candidate for a low chlorophyll content phenotype

Genome resequencing allowed identifying a candidate point mutation that is the most likely responsible for I29 phenotype. It is located in a gene encoding for a gene involved in the biosynthesis of the Chl and it resulted in the absence of the corresponding mRNA in I29. This mutation in I29 is not lethal because Chl biosynthesis can be partially sustained by the second copy of this gene, which transcription is not impaired in the mutant respect to the WT. Full demonstration of this conclusion is still missing since it will require complementation with a WT gene to confirm that other mutations don't influence the phenotype. Until now all the complementation experiments have been unsuccessful. I29 showed recalcitrance to transformation with very low yields. We made a similar observation with WT strains kept in the lab for a long time. In the case of WT this was solved restarting from frozen stocks. For this reason we are pursuing an alternative strategy by RNAi and CRISPR approach.

In I29 the mutation decreased the efficiency of chlorophyll biosynthesis resulting in a decreased pigments content per cell. Only in stable conditions with excess illumination (250_1200 in semi continuous see Appendix 1) the Chl biosynthesis appeared to not be limited even in the mutant.

The mutation in other plants was shown to cause leaf necrosis due to the accumulation of intermediate biosynthetic compounds, which are phototoxic in high light treatments. I29 instead did not show any increased photosensitivity with respect to WT nor in batch nor in semi-continuous cultures. Indeed I29 was able to grow and to perform photosynthesis with the same efficiency of the WT, and even higher, in all the light conditions tested. I29 also maintained the ability to acclimation to different light intensity by modulating its photosynthetic apparatus, a useful trait to employ I29 in an industrial cultivation system.

I29 productivity evaluation in a fed batch system

The last part of the work demonstrated that I29 exploitation can result in a higher biomass productivity respect to the WT. It was interesting to notice that the best improvement of productivity was correlated with ETR and TEF increase and with the reduction in the Chl content of about 43% in 150_400. This result confirmed as highlighted in Appendix 1 that the productivity strictly correlates with photosynthetic apparatus functionality. P700 measurement showed at 150_400 a reduction in I29 P700 per cell, but PSII/PSI ratio was the same respect to the WT, so there was a reduction in the content both of PSII and PSI. A 43% Chl reduction led to a higher light penetration. An hypothesis can be that this reduction in I29 photosystems content can be due to the acclimation of the higher light perceived by the mutant cells respect to the WT.

In 250_400 I29 is similar to the WT both in growth and in photosynthetic performance. A reduction of 27% was not sufficient to result in a gain in biomass productivity because it was not sufficient to lead to a higher electron transport. Indeed comparing results from all mutants (see Appendix 1) there is a strong correlation between reduced Chl content per cell, increased TEF and productivity. The latter in particular appears to be a good predictor of productivity in these conditions.

REFERENCES

Bonente, Giulia et al. 2011. “Analysis of LHcSR3, a Protein Essential for Feedback de-Excitation in the Green Alga Chlamydomonas Reinhardtii.” *PLoS Biology* 9(1):1-17.

Chankova, S.G., et al. 2007. "Induction of DNA double-strand breaks by zeocin in Chlamydomonas reinhardtii and the role of increased DNA double-strand breaks rejoining in the formation of an adaptive response". *Radiat Environ Biophys* 46(4): 409-416

Corteggiani, Elisa et al. 2014. “Chromosome Scale Genome Assembly and Transcriptome Profiling of Nannochloropsis Gaditana in Nitrogen Depletion.” *Molecular Plant* 7(2): 323–35.

Dent, Rachel M et al. 2005. “Functional Genomics of Eukaryotic Photosynthesis Using Insertional Mutagenesis of Chlamydomonas Reinhardtii.” *Plant physiology* 137(2): 545–56.

Faarber, Andreas, and Peter Jahns. 1998. “The Xanthophyll Cycle of Higher Plants: Influence of Antenna Size and Membrane Organization.” *Biochimica et Biophysica Acta - Bioenergetics* 1363(1): 47–58.

Hannon, Michael et al. 2010. “Biofuels from Algae: Challenges and Potential.” *Biofuels* 1(5): 763–84.

Hu, Gongshe, Nasser Yalpani, Steven P Briggs, and Gurmukh S Johal. 1998. “A Porphyrin Pathway Impairment Is Responsible for the Phenotype of a Dominant Disease Lesion Mimic Mutant of Maize.” *Plant ce*ll 10: 1095–1105.

Liu, Y G, Norihiro Mitsukawa, Teruko Oosumi, Robert F Whittier. 1995. “Efficient isolation and mapping of Arabidopsis thaliana T-DNA insert junctions by thermal asymmetric interlaced PCR" *The plant journal* 8(3):457-463.

Matsumoto, Mitsufumi et al. 2017. “Outdoor Cultivation of Marine Diatoms for Year-Round Production of Biofuels.” *Marine Drugs* 15(4): 8–10.

Maxwell, K, and G N Johnson. 2000. “Chlorophyll Fluorescence--a Practical Guide.” *Journal of experimental botany* 51(345): 659–68.

Meneghesso, Andrea et al. 2016. “Photoacclimation of Photosynthesis in the Eustigmatophycean Nannochloropsis Gaditana.” *Photosynthesis Research* 129(3): 291–305.

Mussgnug, Jan H et al. 2007. “Engineering Photosynthetic Light Capture: Impacts on Improved Solar Energy to Biomass Conversion.” *Plant biotechnology journal* 5(6): 802–14.

Nolan, Tania, Rebecca E Hands, and Stephen a Bustin. 2006. “Quantification of mRNA Using Real-Time RT-PCR.” *Nature protocols* 1(3): 1559–82.

Palma, H. et al. 2017. “Assessment of Microalga Biofilms for Simultaneous Remediation and Biofuel Generation in Mine Tailings Water.” *Bioresource Technology* 234: 327–35.

Perin, Giorgio et al. 2015. “Generation of Random Mutants to Improve Light-Use Efficiency of Nannochloropsis Gaditana Cultures for Biofuel Production.” *Biotechnology for biofuels* 8: 161-174.

Richter, Andreas S, and Bernhard Grimm. 2013. “Thiol-Based Redox Control of Enzymes Involved in the Tetrapyrrole Biosynthesis Pathway in Plants.” *Frontiers in Plant Scienc*e 4(September): 1–11.

Rosic, Nedeljka N., Mathieu Pernice, Mauricio Rodriguez-Lanetty, and Ove Hoegh-Guldberg. 2011. “Validation of Housekeeping Genes for Gene Expression Studies in Symbiodinium Exposed to Thermal and Light Stress.” *Marine Biotechnology* 13(3): 355–65.

Simionato, Diana et al. 2013. “The Response of Nannochloropsis Gaditana to Nitrogen Starvation Includes de Novo Biosynthesis of Triacylglycerols, a Decrease of Chloroplast Galactolipids, and Reorganization of the Photosynthetic Apparatus.” *Eukaryotic Cell* 12(5): 665–76.

Sosnowski, Ronald G. et al. 1997. “Rapid determination of single base mismatch mutations in DNA hybrids by direct electric field control.” *Proc. Natl. Acad. Sci.* 94: 1119–1123

Stacey Michael et al. 2003. “Differential effects in cells exposed to ultra-short, high intensity electric fields: cell survival, DNA damage, and cell cycle analysis” *Mutation Research* 542: 65–75.

Stephenson, Patrick G et al. 2011. “Improving Photosynthesis for Algal Biofuels: Toward a Green Revolution.” *Trends in biotechnology* 29(12): 615–23.

CHAPTER 4 :

Isolation and characterization of a *Nannochloropsis gaditana* low NPQ mutant.

Authors name and affiliations

Alessandra Bellan[1], Giorgio Perin[1], and Tomas Morosinotto[1]

1-PAR-Lab_Padua Algae Research Laboratory, Department of Biology, University of Padova, Via U. Bassi 58/B, 35121 Padova, Italy.

2- Department of Life Sciences, Imperial College London, Sir Alexander Fleming Building, London, SW7 2AZ, UK.

CONTRIBUTION:

In this chapter AB performed all the experiments described for the strain selection, phenotypical and molecular characterization. GP was in charge of productivity evaluation where AB provided a contribution in DW and PAM analysis.

ABSTRACT

In natural environment light intensity is continuously changing. In conditions in which absorbed light exceeds the capacity of photosynthetic apparatus to exploit energy to fuel photochemical processes, both algae and plants experience an over-excitation of photosynthetic chain. This can lead to the production of harmful reactive oxygen species, finally causing oxidative stress and cell damage. Plants and algae evolved photoprotective mechanisms to avoid the damage from light excess. Non photochemical quenching (NPQ) contributes to this protection by dissipating excess light energy as heat and it has an important role in response of photosynthetic organisms to dynamic growing conditions. In this chapter we analyzed I48, another *Nannochloropsis gaditana* mutant isolated from the collection described in chapter 2, which has a severe reduction in NPQ. Molecular characterization leads to the identification of a point mutation in the gene LHCX1 which results in the loss of this protein. LHCX1 is an antenna protein, homologous of LHCSR proteins, known to be involved in the NPQ response in green algae. For this reason we used this mutant to analyze how the loss of LHCX1 can influence the response to variable light conditions and the impact that such an alteration in photosynthesis regulation can have upon cultivation in industrial cultivation conditions.

INTRODUCTION

Physiology and metabolism of photosynthetic organisms are highly influenced by external factors as light, temperature and nutrient availability. The reaction to environmental dynamics and the activation of appropriate responses has a fundamental influence on photosynthetic performances (Taddei et al. 2016). In particular high light exposure can be harmful because the reactions of oxygenic photosynthesis involve the formation of excited and highly reactive intermediates in the thylakoid membranes of chloroplasts (Baroli and Niyogi 2000). Indeed chlorophyll, the essential pigment for light harvesting to photochemical energy conversion, can act in its triplet excited state as a potent photosensitizer in the generation of singlet oxygen, a highly reactive species (Rinalducci, Pedersen, and Zolla 2008). The undesired result is an oxidative stress leading to damage of the photosynthetic apparatus (photoinhibition) and eventually cell death

(Lepetit et al. 2017). Plants and microalgae evolved different mechanisms to prevent photo-oxidative damage. One of them is the so called non-photochemical quenching (NPQ), which dissipates excess light energy as heat. Different components have been identified in NPQ: a fast component (called high energy quenching, qE) due to the proteins LHCSRs in algae (Maruyama, Tokutsu, and Minagawa 2014) or PsbS in plants (Alboresi et al. 2010), a slower one due to zeaxanthin accumulation (qZ) and the slowest associated to photo-inhibitory quenching (qI) (Muller, Li, and Niyogi 2001; Nilkens et al. 2010). When absorbed sunlight exceeds a plant capacity for CO_2 fixation this results in a buildup of the thylakoid ΔpH generated by photosynthetic electron transport. The decrease in pH within the thylakoid lumen is an immediate signal of excessive light that triggers the feedback regulation of light harvesting and activates NPQ (Muller, Li, and Niyogi 2001). The rapid qE component cooperates in a synergic way with the slower qZ to reduce the photodamage (Nilkens et al. 2010).

Proteins encoded by a gene family called *lhcsr*, in green algae and *lhcx* in diatoms are responsible for qE. They are antenna proteins constitutively involved in light energy dissipation, which are absent from higher plants (Niyogi and Truong 2013). In higher plants NPQ is instead mediated by the protein PsbS. This protein is active in NPQ thanks to interactions with different LHCII complexes that still remain not completely clear (Gerotto et al. 2015).

The slower qZ is due to activation of xanthophyll cycle, which consists in the accumulation of zeaxanthin from violaxanthin by two successive de-epoxidations (Arnoux et al. 2009; Goss and Jakob 2010).

NPQ is present in all photosynthetic eukaryotes but the comparison between land plants and algae unraveled distinct molecular machineries. The study of the LHC-dependent light energy dissipation in algal species may provide insight into an evolutionary turning point of high light stress acclimation in the green plant lineage (Alboresi et al. 2010).

In chapter 2 we described the generation and selection of a collection of *Nannochloropsis gaditana* random mutant strains, altered in the photosynthetic apparatus. Among them we isolated I48 with a severe reduction in the NPQ activation. This chapter presents its molecular and physiological characterization to investigate how this mechanism influences photosynthetic efficiency in different light conditions.

MATERIAL AND METHODS

Microalgae growth

Nannochloropsis gaditana (strain 849/5) from the Culture Collection of Algae and Protozoa (CCAP) were used as the WT strain. Cells were cultivated in sterile F/2 media with sea salts(32 g/l, Sigma Aldrich), 40 mM Tris–HCl (pH 8) and Guillard's (F/2) marine water enrichment solution (Sigma Aldrich) in Erlenmeyer flasks with 100 µmol photons m^{-2} s^{-1} illumination and 100 rpm agitation at 22 ± 1 °C in a growth chamber.
The comparison between different light regimes using a Multicultivator MC 1000-OD system (Photon Systems Instruments, Czech Republic) and the fed-batch experiment were performed as already described in chapter 3.

Pigment content analysis

Chlorophyll a and total carotenoids were extracted from cells at the end of the exponential phase of growth using a 1:1 biomass to solvent ratio of 100 % N,N dimethylformamide (Sigma Aldrich) at 4 °C in the dark for at least 24 h. Absorption spectra were determined between 350 and 750 nm using a Cary 100 spectrophotometer (Agilent Technologies) as described in chapter 3.

Fluorescence measurements

Photosynthesis evaluation was performed by measuring in vivo Chl fluorescence using a PAM 100 fluorimeter (Heinz-Walz, Effeltrich, Germany). PSII functionality was defined as PSII maximum quantum yield (Fv/Fm), according to (Maxwell and Johnson 2000). Samples were exposed to increasing light intensity up to 2000 µmoles photons m^{-2} s^{-1}, and then light was switched off to evaluate NPQ relaxation kinetic. NPQ values were calculated as previously described (Maxwell and Johnson 2000).
PSII antenna sizes were determined using a JTS-10 spectrophotometer (Biologic, France). Samples (200 x 10^6 cells/ml final concentration) were dark-adapted for 20 minutes and incubated with 80 µM 3-(3,4-dichlorophenyl)-1,1-dimethylurea (DCMU) for 10 minutes. Fluorescence induction kinetics were then monitored upon excitation with 320 µmoles photons m^{-2} s^{-1} of actinic light at 630 nm. The $t_{2/3}$ values obtained from the fluorescence induction curves were exploited to calculate the size of the PSII functional antenna (Bonente et al. 2011; Perin et al. 2015).

The P700 and the total electron flow (TEF) spectroscopic quantifications were done measuring P700 (the primary electron donor to PSI) absorption at 705 nm in intact cells. Analyses were conducted exposing the samples (300 x 10^6 cells/ml final concentration) to saturating actinic light (2050 μmol of photons m^{-2} s^{-1}, at 630 nm) for 15 seconds to maximize P700 oxidation (P700) and reach a steady state. Then the light was switched off to follow the P700 re-reduction kinetic in the dark for 5 seconds. The total electron flow (TEF) was derived from the monitoring of the P700 re-reduction rates after illumination in untreated cells. The electron transport rate was calculated assuming a single exponential decay of P700.

In this way the rate constant of P700 reduction was calculated as $1/\tau$. By multiplying the rate constant with the fraction of oxidized P700, and considering this value as 1 in DCMU- and DBMIB-treated cells we could evaluate the number of electrons transferred per unit of time per PSI unit (Simionato et al. 2013)

The PSI content was evaluated from the maximum change in the absorption of P700 in cells treated with DCMU (80 μM) and DBMIB (dibromothymoquinone, 300 μM) at a saturating actinic light (2050 μmol of photons m^{-2} s^{-1}, at 630 nm). Under these conditions, re-reduction of P700 through photosynthetic electron flow is largely slowed down, al lowing to evaluate the full extent of photooxidizable P700 (Meneghesso et al. 2016)

DNA extraction, TAIL-PCR and whole genome re-sequencing.

N. gaditana strains genomic DNA was extracted as described in chapter 3 from 4-day-old cultures, performed in Erlenmeyer flasks using F/2 liquid media. Thermal asymmetric interlaced (TAIL)-PCR was performed utilizing the same nested-specific primers exploited in chapter 3.

They were used in successive reactions together with a shorter arbitrary degenerate primer (Dent et al. 2005; Liu, Y G, Norihiro Mitsukawa, Teruko Oosumi 1995). Details of the PCR reaction mix and thermal cycles have been described in (Dent et al. 2005).

The whole genome re-sequencing for mutant strain I48 was performed by IGA Technologies Services (Udine, Italy), with the Illumina MiSeq platform, using 100 bp pair-end sequences leading to a 70-fold genome coverage. The *N. gaditana* B-31 genome published in (Corteggiani et al. 2014), was used as reference. Genetic variants annotation and their prediction effects was carried out using the SnpEff software.

Total RNA extraction and cDNA preparation.

Total RNA was extracted from the *N. gaditana* batch cultures. Cells were lysed using a Mini Bead Beater (Biospec Products) at 3500 RPM for 20 s in the presence of glass beads (150–212 μm diameter). Total RNA was thus purified using the TRI Reagent™ (Sigma Aldrich), applying minor modifications to the manufacturer's instruction. Total RNA concentration and purity was determined by 100 UV–VIS spectrophotometer (Cary Series, Agilent Technologies). cDNA was prepared from 1 μg of total RNA-template with the RevertAid Reverse Transcriptase cDNA kit (Thermo Fisher Scientific, Epson, UK). The cDNA was previously treated with the DNAse I kit (Sigma Aldrich).

RT-PCR.

The cDNA was used as template for the RT-PCR reactions, in order to amplify the LHCX1 (*Naga_100173g12*) gene from the WT and I48 strains templates. The primer sequences reported in table 1 and KAPA HIFI high-fidelity DNA polymerase (KAPA Biosystems) were used for this purpose.

Table 1: Primers sequences used to amply LHCX1

LHCX1_FOR
CATCATCACCACCATCACCGTGTACTCTCTTTCCTTGCTATTA
LHCX1_REV
GTGGCGGCCGCTCTATTATTAGAAGAAGAAGTTGTAGACGTCC

Southern Blot

The probe was prepared by DIG DNA labeling and Detection kit (Roche) using as template the ubiquitin promoter, that is the endogenous promoter present in the resistance cassette of the mutant strains. The digested DNA was transferred to a Hybond-N membrane (GE Healthcare, Little Chanfont, UK) by capillary transfer and hybridized with the labeled DNA probe overnight. The immunological detection was done by using alkaline phosphatase conjugated secondary antibody.

SDS-page and western blot.

A 12% SDS–page analysis for protein extracts was performed using a TRIS–glycine buffer system. The samples were solubilized for 20 minutes at RT in 10% glycerol, 45 mM TRIS (pH 6.8), 0.03 M dithiothreitol and 3% SDS. Western blot analyses were performed after transferring the proteins to nitrocellulose (Bio Trace, Pall Corporation), using alkaline phosphatase conjugated secondary antibodies. The antibody against D2 [UniProt: P06005 for D2] was generated by immunizing New Zealand rabbits with the spinach protein, whereas the recombinant proteins were used for the antibodies against VCP and LHCX1, which were obtained by cloning the two cDNA into pETite N-HIS (Lucigen-Expresso T7 Cloning and Expression System), expressing the proteins in Escherichia coli BL21 (DE3, Invitrogen), and purifying as inclusion bodies [UniProt: W7T4V5 for LHCf1, and Uniprot: K8YWB4 for LHCX1].

RESULTS

Molecular characterization of a NPQ depleted mutant.

I48 was selected among the strains isolated in previous chapter as particularly interesting to clarify molecular bases of NPQ mechanism in *N.gaditana*. In lab scale flask cultures I48 showed a growth (fig 1-A) and a pigment content indistinguishable from the wild type (fig 1-B) but confirmed the severe non photochemical quenching reduction with a complete depletion of the fast component qE (fig 1-C). Also in control light conditions maximum quantum yield of PSII (Fv/Fm) was reduced (fig1-D), even if it has not effect on growth kinetics.

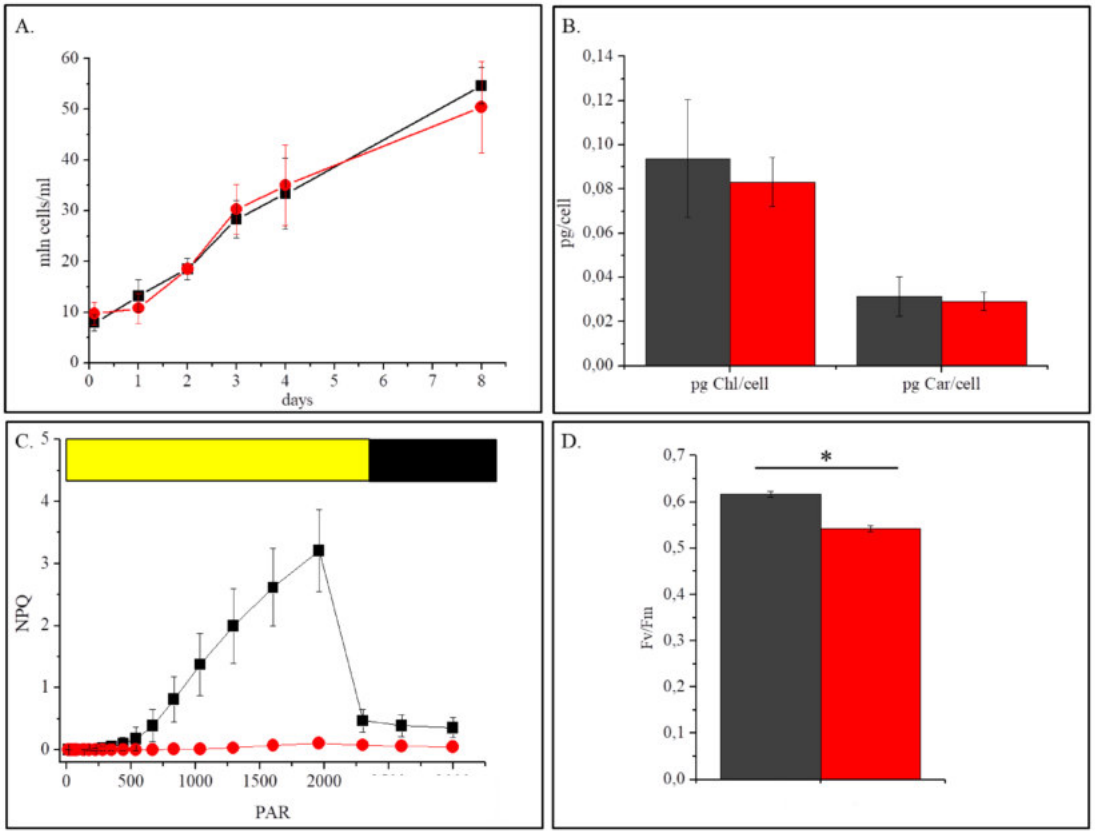

Figure 1: In A is shown the growth curve in terms of cells number per ml of culture, in dark is marked the WT and in red the mutant I48 (n=4). B-D all these measurements were done after 4 days of culture (n=4), in all the panels dark gray stands for WT and red stands for I48. In B is reported the pg of chlorophyll and carotenoids per cell. In C is reported the NPQ activation at increasing light intensities, in D is shown the evaluation of the photosynthetic efficiency of PSII, measured as Fv/Fm. Statistically significant differences between WT and strain I48 are marked with an asterisk (one-way ANOVA, p-value < 0.05).

I48 was generated by a random insertional mutagenesis and a Southern blot experiment was performed to identify the number of insertions. We tried different probes, using as template both the resistance gene and the endogenous promoter (UEP), which is present also in the resistance cassette (fig 2-A). The results were completely comparable so in fig 2-B we showed only UEP probe that returned the stronger signals.

The result for I48 was a marked signal at 1300 bp, that was also similarly present in other strains of the same collection (figure 2-B). Considering that we used as restriction enzyme ApoI that cuts in the exogenous terminator, a fragment of this size corresponds to the resistance cassette.

The southern blot signal for I48 was much stronger than for other strains (ex. No 6 in figure 2-B), and it was absent in I29, the mutant described in chapter 3 that we confirmed to have a single insertion. All results can be justified by the presence of tandem insertions

that will explain why a digestion with ApoI, which cuts in the exogenous terminator, cause the generation of multiple copies of a fragment with the same size (fig 2-A). ApoI isolates each single insertion. Indeed two or more cassettes can be retained in the same genomic fragment if the digestion is randomly outside the insertions. To confirm this hypothesis we set up a PCR using primers designed in order to produce an amplification only if at least two resistance cassettes are inserted in tandem in the genome (see fig 1-A). As it is shown in fig 2-D we used as controls the WT strain and also I29. As shown in figure 2-C in I48 there is an amplification product, confirming the presence of at least a multiple insertion event in this strain.

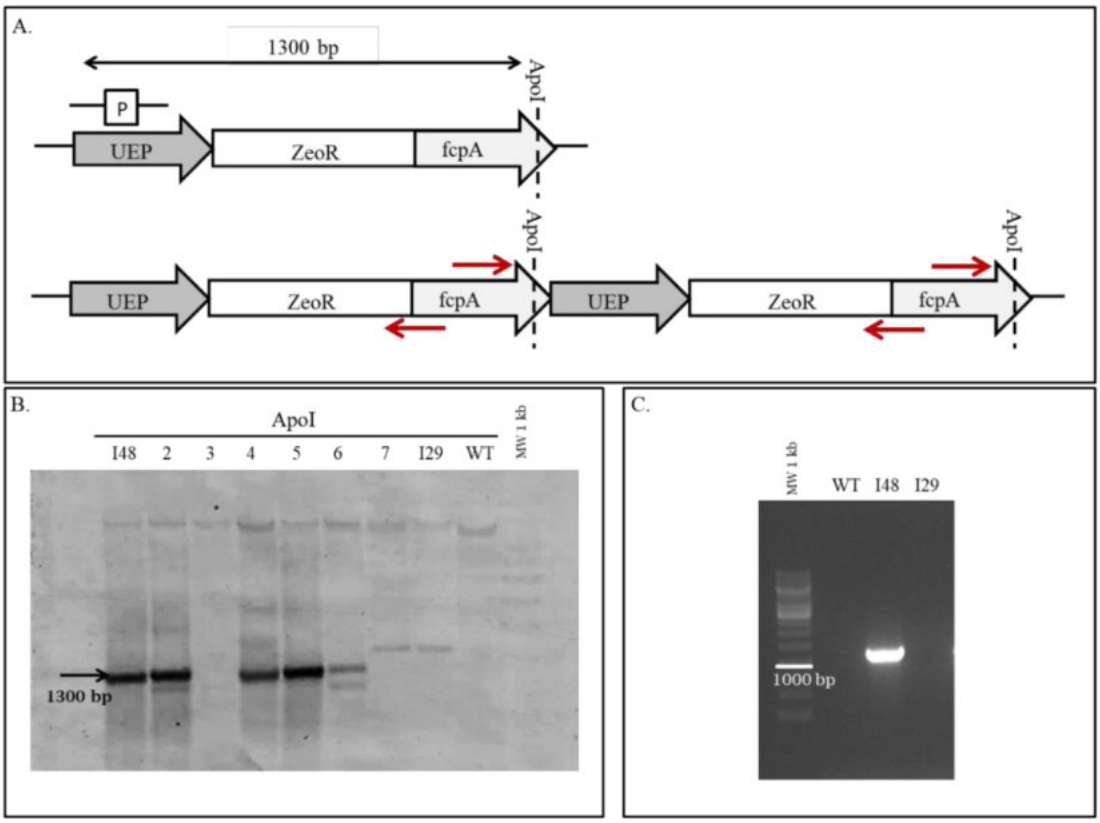

Figure 2: In A is shown on the top a model of the resistance cassette in which the restriction site is highlighted by a dashed line and the site of probe synthesis is marked as P. On the bottom is represent the possible conformation of the tandem insertion and with the red arrow are marked the primers used to confirm the event. In B is reported southern blot results with the endogenous promoter as probe template. There is a common band in all the sample, also in the WT given by the endogenous promoter, and then there is a number of signal proportional to the insertions number, for example in I29 the mutant described in chapter 3 there is only a signal, given by the single insertion present in this mutant. By the arrow is marked the strong signal at 1300 bp that can be symptomatic of a tandem event. In C is shown the result of the PCR performed with the primers represented by the red arrows in A. In the WT and in I29 there is not any amplification because in the first there isn't the resistance gene and in the second there is only one insertion, instead in I48 we found amplification due to the presence of at least two terminators in tandem.

The presence of tandem insertions also explains why the attempts to identify the insertion site by TAIL PCR were unsuccessful. Since TAIL PCR protocol amplified the region nearby the exogenous terminator we only obtained UEP promoter as the flanking sequence. The mutant strain was therefore subjected to the whole genome re-sequencing for the systematic identification of the mutations to identify the one(s) responsible for its photosynthetic phenotype. The latter was performed on an Illumina MiSeq to obtain a theoretical 70-fold genome coverage. The software SnpEff was then run to annotate the genetic variants identified in strain I48 on the *N. gaditana* reference genome, identifying 80 point mutations in total. The list of potentially affected genes included a gene (*Naga_100173g12*) encoding for LHCX1. This is a light-harvesting complex (LHC) protein belonging to the sub-clade of LHCX, which are known to be required for NPQ in diatoms (Bailleul et al. 2010). This is also the most abundant LHCX isoform in *N.gaditana* according to transcriptomic and proteomic analysis (Alboresi et al. 2016) and thus the mutation in this gene clearly was the most likely responsible for I48 NPQ phenotype and it was thus analyzed in more detail.

The genetic variant was located in position 1510841 bp of chromosome 01, falling in the genomic locus occupied by LHCX1 gene. The identified point mutation involves a deletion of a thymine, that is not part of the coding sequence but it is part of the first two nucleotides of the 5'-donor splicing site of the 4^{th} intron (GT). It was observed that all intron sequences in eukaryotes (both plants and animals) contain two highly conserved di-nucleotides, a GT at 5'-end and an AG at the 3'-end, which are responsible for the efficient binding of the spliceosome. Therefore, the identified deletion of the thymine of the donor splicing site could have a major effect on the splicing efficiency, leading to the possible retention of the intron in the mature mRNA (fig 3-A). In order to confirm this hypothesis we performed a RT PCR that showed an amplification product of 700bp for the WT and about 1000bp for the mutant (fig 3-C). The sequencing of both the amplification products of WT and I48 confirmed that the increase in the LHCX1 mRNA length in I48 is due to the retention of the fourth intron.

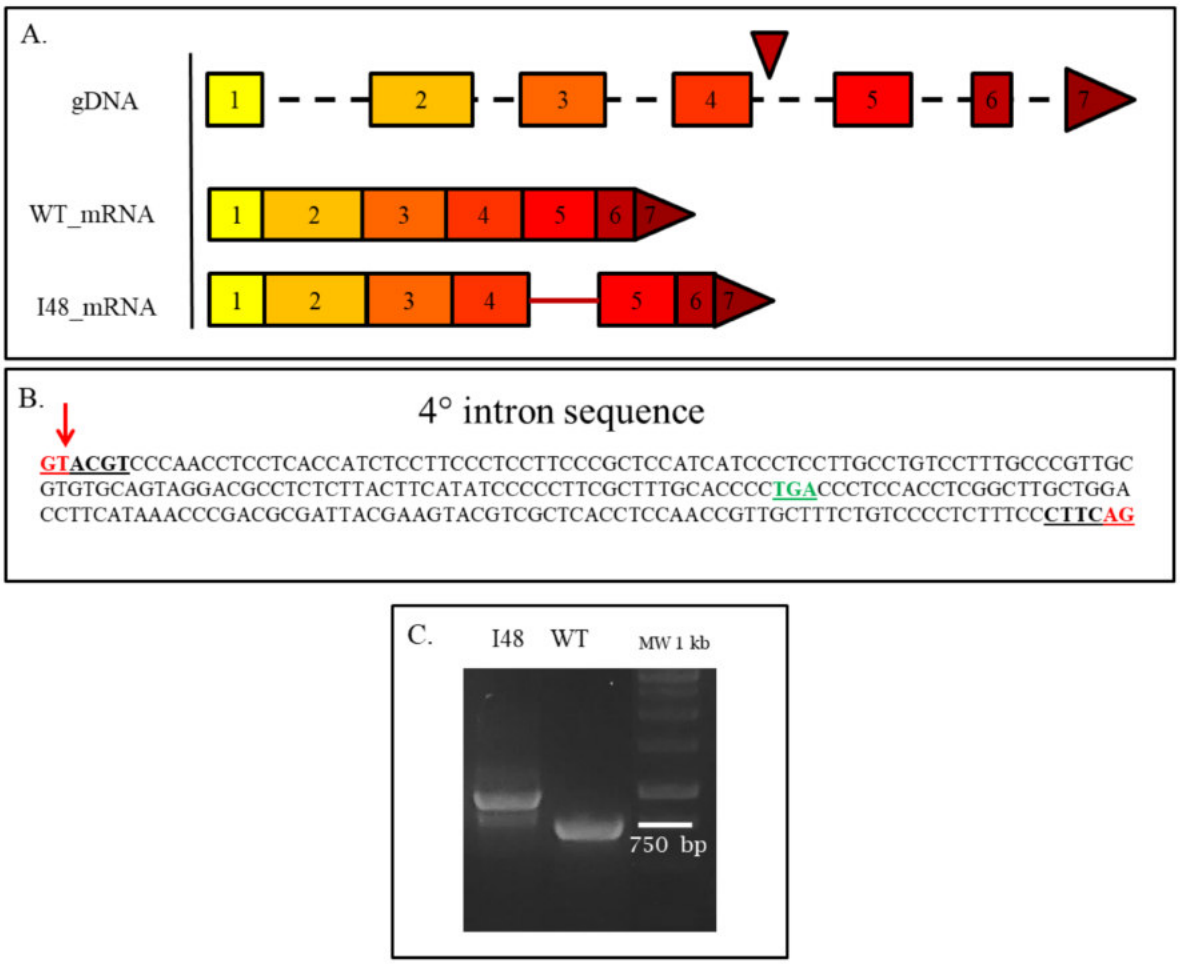

Figure 3: In A is reported the schematic representation of LHCX1 gene, in which dashed lines marked the introns and the colored squares the exons. On the top is shown the genomic DNA and the red arrow marked the point mutation site. In the middle is reported the WT mRNA with the correct splicing of introns, and on the bottom it is shown I48 mRNA, in which with the red line is marked the intron retained because of the point mutation. In B is shown the sequence of the 4th intron retained in I48, the red triangle marked the point mutation and in green is highlighted the stop codon which is inserted because of the intron retention. In C is reported the amplification of LHCX1 on cDNA for I48 and the WT.

The retention of an intron clearly causes a drastic change in the protein sequence. The LHCX1 protein in I48 mutated is identical to the WT for the first 150 aa while they differ starting from the amino acid 151 as a consequence of the retained intron. The mutation also introduces a premature stop codon in the retained intron sequence (fig 3-B) thus leading to a truncated protein of 193 aa, instead of 231 aa as the WT. Because of this stop

codon the protein sequence misses the third transmembrane helix, a conserved feature of LHC complexes and known to be fundamental for protein stability (fig 4-A).

Protein stability was assessed using a Western blot experiment with specific antibodies produced against *Nannochloropsis* LHCX1 isolated after overexpression in *E.coli*. LHCX1 protein was undetectable in the I48 total extract, also at low molecular weight respect to the WT. While the control protein PSII core subunit D2 protein was unaffected (fig 4-B) .

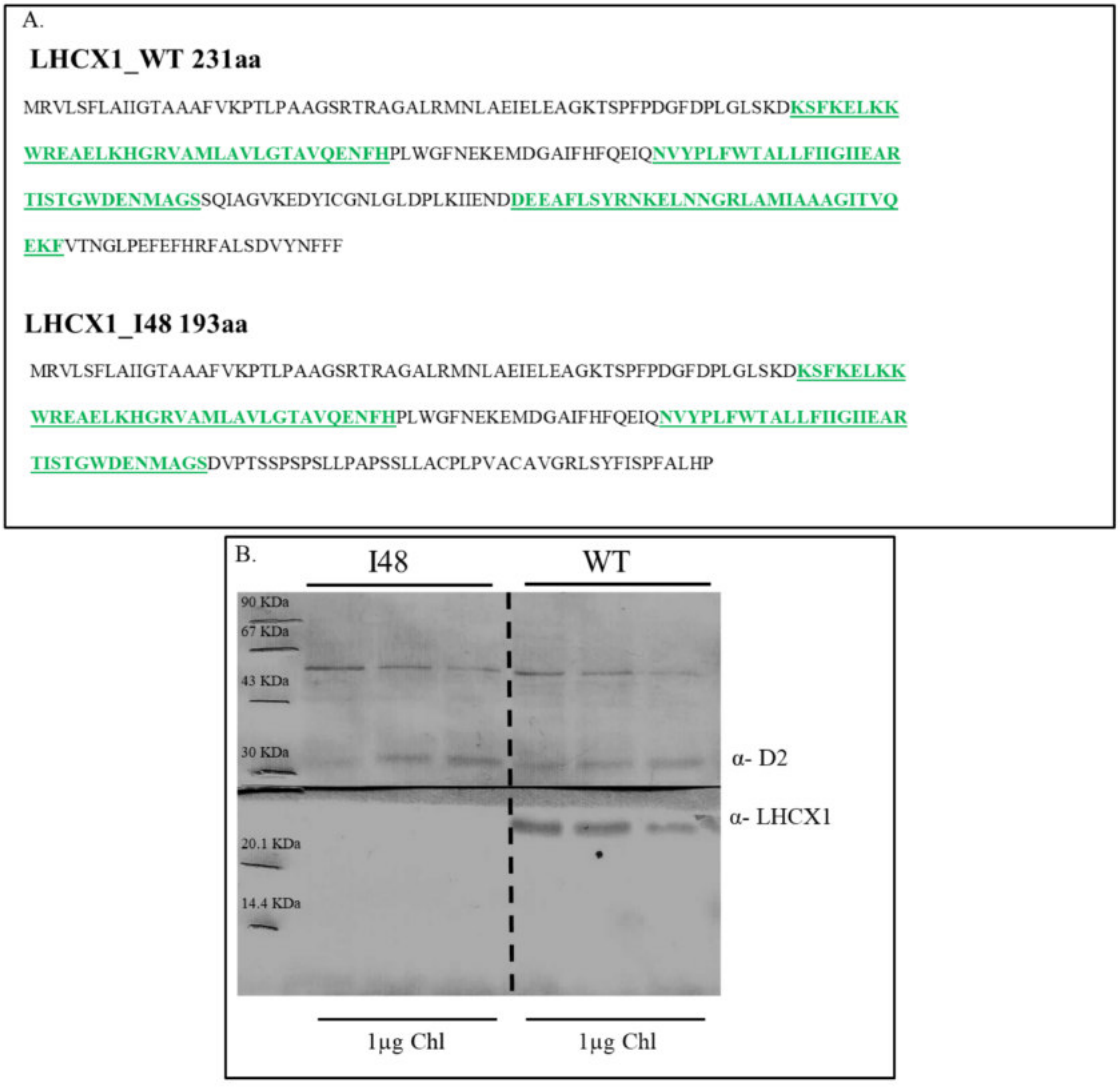

Figure 4: In A top is reported the sequence of LHCX1 protein WT and in the bottom the prediction for LHCX1 protein product of I48. In green are marked the putative residues involved in transmembrane helixes formation. In B is reported the western blot result, in which 1 µg of chlorophyll was loaded for each sample.

Biological role of NPQ in response to different light intensities

Previous results strongly suggest that LHCX1 is responsible for non-photochemical quenching activation in *Nannochloropsis*. This is consistent with mutants with an alteration in NPQ, both of microalgae and mosses even if a definitive demonstration will require the complementation of the strain. In order to assess the biological role of NPQ in this organism we investigated I48 response to different light regimes. We grew in a Multicultivator system WT and I48 with three different light intensities:

- LL: low light 10 μmol of photons m^{-2} s^{-1};
- ML: medium light 100 μmol of photons m^{-2} s^{-1};
- HL: high light 1000 μmol of photons m^{-2} s^{-1}.

I48 showed a growth (fig 5-A) comparable with the WT in all the conditions tested and in ML it is even higher respect to the WT. In this Multicultivator experiment respect to the preliminary flask cultures, the samples reached higher density, due to the rich media exploited. So it seems that the low NPQ phenotype can be advantageous when the optical density of the culture is increased. Moreover in ML conditions I48 showed also a small reduction both in the Chl and Car content respect to the WT (fig 5-B) even though the Chl/Car is maintained. This pigment content reduction can increase light penetration and so I48 growth. Instead the pigment content is similar to the WT in LL and HL condition.
The maximum quantum yield of PSII (Fv/Fm) is similar to the WT in LL and ML, but it is significantly reduced in HL condition with respect to WT. This is a clear indication that the lack of the fast component of NPQ caused a stronger photoinhibition respect to the WT, when the HL exposition is prolonged. In any case this photoinhibition does not affect the growth in a significant way and so it seems that other NPQ mechanisms like xanthophyll cycle are sufficient to avoid cell death.

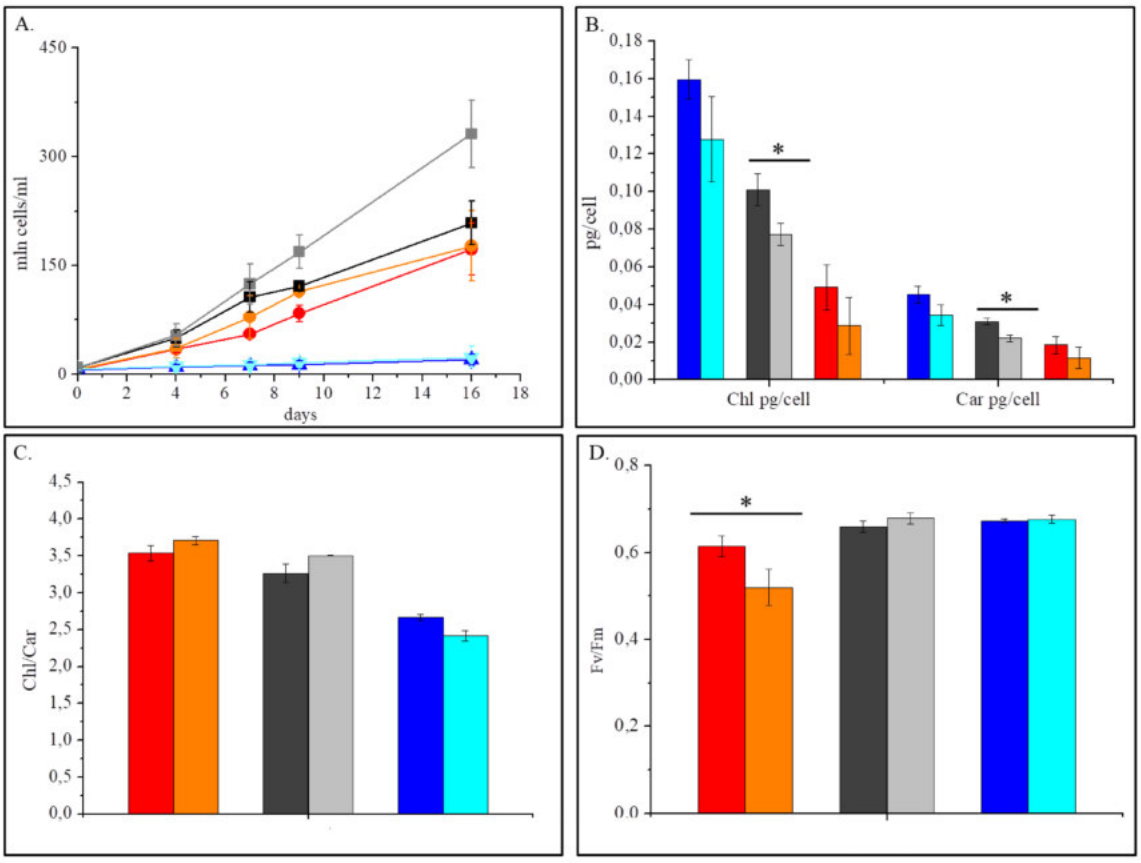

Figure 5: In A is shown the growth curves expressed as millions of cells/ml in the different light treatments: red- WT HL, orange- I48 HL, black- WT CL, gray- I48 CL, blue- WT LL, light-blue I48 LL (n=3). In B is reported the Chl and Car content per cell. In C is shown the maximum quantum yield of PSII expressed as Fv/Fm. Statistically significant differences between WT and strain I48 are marked with an asterisk (one-way ANOVA, p-value < 0.05)

Evaluation of NPQ impact on biomass productivity

NPQ has also been suggested as a possible target for improving biomass accumulation (Berteotti, Ballottari, and Bassi 2016) since NPQ activation reduces light use efficiency dissipating up to 80% of absorbed energy as heat (Simionato, Basso, et al. 2013). A reduction in NPQ activation could be potentially beneficial leaving more energy for photochemistry especially in the internal layers of a photobioreactor. In order to verify this hypothesis in the last part of this work we evaluated the productivity of I48 in the same semi-continuous system previously described in chapter 3. Also in this case we tested the same three different conditions tested in Appendix 1, with variable light supplies to the cell:

4- 150 x 10^6 cells/ml as starting concentration and light intensity 400 µmol photons $m^{-2}s^{-1}$, (150_400);
5- 250 x 10^6 cells/ml as starting concentration and light intensity 400 µmol photons $m^{-2}s^{1}$, (250_400);
6- 250 x 10^6 cells/ml as starting concentration and light intensity 1200 µmol photons $m^{-2}s^{-1}$, (250_1200).

First of all we quantified the productivity by dry weight measurement, in terms of grams of biomass produced per liter per day. As is shown in table 2 I48 had a significantly higher productivity respect to the WT in the first two conditions where light was limiting. Instead in the last one in which the exposure light had a higher intensity there was no statistically significant difference, suggesting that absence of NPQ does not cause reduction of growth under intense illumination.

In 150_400 I48 had a 20% increased productivity with respect to the WT, which became even higher when the starting cell density was increased, reaching the 24%. This thus suggests that a reduction in NPQ is advantageous in conditions mimicking industrial system. The advantage is larger in 250_400 where the culture is denser and thus light is less homogeneously distributed.

Table 2: In the table is reported the productivity in terms of grams of biomass per liter per day (g/l/d). In bold type and with the asterisks is marked the statistically significant differences between WT and strain I48 (one-way ANOVA, p-value < 0.05).

Dry weight (g/l/d)			
	150_400	**250_400**	**250_1200**
WT (n=37)	0.33 ± 0.05	0.37 ± 0,07	0.48± 0,11
I48 (n=23)	**0.40 ± 0,05****	**0.47 ± 0,04****	0.56 ± 0,05

In all the conditions tested I48 maintained its NPQ phenotype as is shown in fig 6-A. The higher productivity in 150_400 and 250_400 was coupled with a higher TEF respect to the WT (fig 6-B) that was correlated with biomass productivity in these conditions.

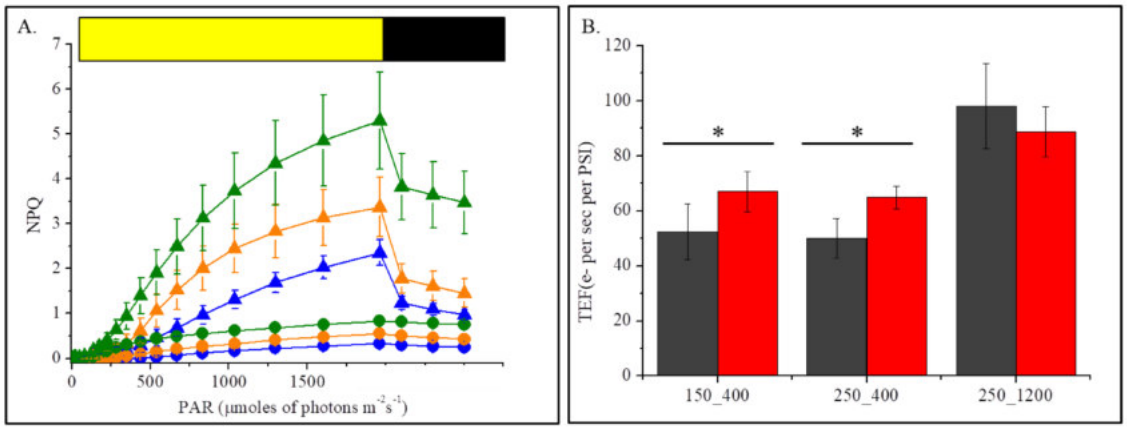

Figure 6: In A is shown the NPQ profile of the WT (triangle) and the I48 (circle) in the three treatment: green 250_1200, orange 250_400, blue 150_400. In B is reported the total electron low estimation as electrons per second per PSI. The asterisk marks the statistically significant differences between WT and strain I48 (one-way ANOVA, p-value < 0.05).

Pigment content analysis also revealed a small decrease in pigments content between the WT and I48 (fig 7-A/B), even if Chl/Car ratio is the same (fig 7-C) in 150_400. In 250_400 the difference was no more statistically significant and in 250_1200 I48 and WT showed the same pigments content (fig 7).

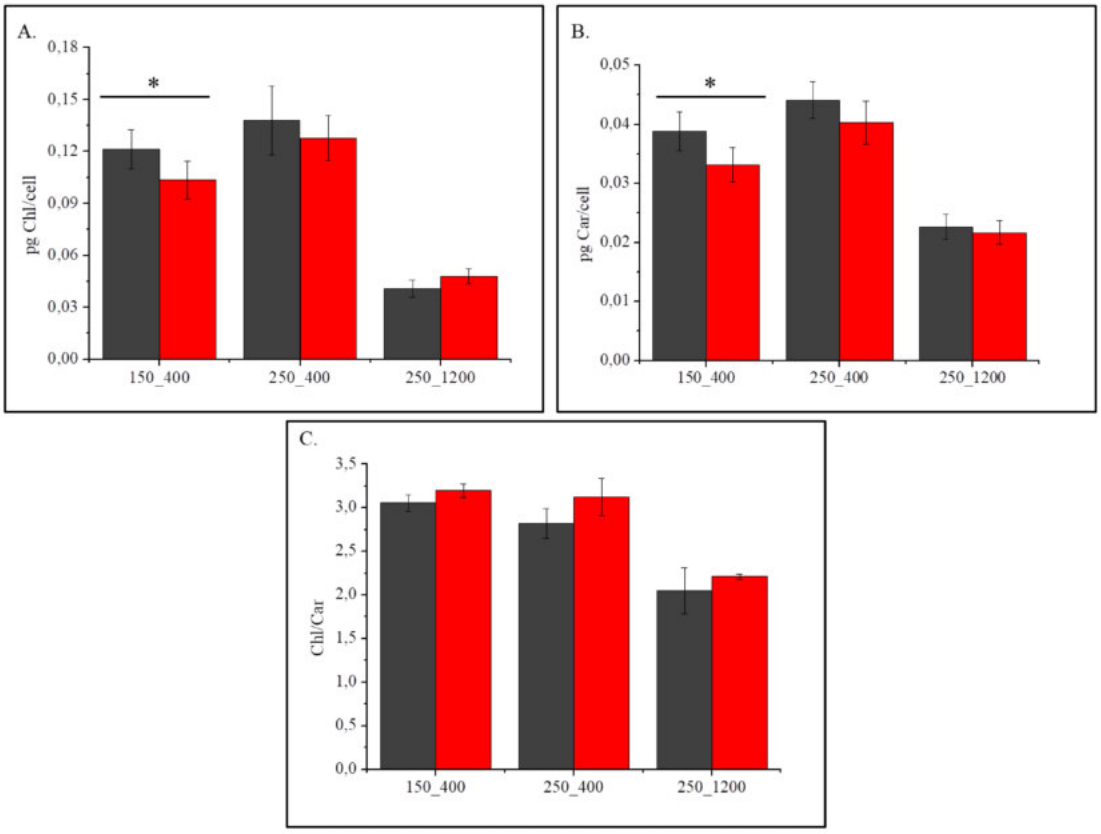

Figure 7: In A is reported the Chl content as pg of Chl/cell. In B is shown the Car content as pg of Car/cell. In C is reported the ratio between I48 and the WT (n=6). In each panel dark grey stands for WT and red stands for I48. The asterisk marks the statistically significant differences between WT and strain I48 (one-way ANOVA, p-value < 0.05).

DISCUSSION

Strategies for random mutagenesis in Nannochloropsis gaditana

The issues identified with transformation procedure and selection protocol has been already described in chapter 3. Results presented here exacerbate the issues as evidenced by the presence of tandem insertions in I48, a feature shared with several other strains isolated. The tendency of this species of integrating multiple copies of the exogenous DNA suggests that the insertional strategy to generate mutants is not suitable since in most cases it causes a loss of the main advantage of this approach, the possibility of quickly identifying the insertion site. In I48 the tandem event is particularly problematic becouse the strong signal given by the high number of resistance cassettes did not allow to find the insertion locus even after genome resequencing. Indeed the genome sequencing highlight only the presence of microsatellite regions localized in the telomeres

(like TAACCC) near to the resistance cassette, without any possibility to find any other genomic position.

This, combined with the development of sequencing technologies that allow fast and cheap resequencing of isolated mutants, suggests that chemical strategies are likely more suitable for generation of random mutants collections. Once the mutation of interest is identified a modified strain can be produced by using genome editing approaches, avoiding the main limitation of chemical mutagenesis, the accumulation of multiple mutations.

Biological role NPQ in Nannochloropsis gaditana

The isolation of I48 showing a severe qE reduction is a seminal tool to clarify the molecular mechanisms for NPQ activation in *N.gaditana* and the biological role of this regulatory mechanism in this organism. Genome sequencing combined with the transcriptomic data, leads to the identification of a mutation which likely correlates with the phenotype. LHCX1 is already been studied in other species like *Phaeodactylum tricornutum*, in which it was clearly established a correlation with the fast component of NPQ. RT PCR confirmed the effect of the point mutation, which avoids the splicing of the fourth intron. This retention inserts an early stop codon which results in a truncated protein. The prediction of the LHCX1 protein 3D structure suggests the loss of the third membrane-spanning alpha helix in the mutated version of the protein. All LHC proteins share the presence of three transmembrane helixes. The absence of one of them would strongly impact on the mutated protein structure causing a misfolding .

By Western Blot we confirmed the loss of LHCX1 protein in I48, which can lead to the recorded sever reduction in qE. Obviously as already described in I29 we could not completely exclude that the other unidentified mutations also affect the phenotype and this should be verified by complementation. Unfortunately also for I48 attempts in this direction have been unsuccessful until now and as for I29 we are pursuing an alternative strategy demonstrating LHCX1 role in NPQ by RNAi and CRISPR/Cas9 approach.

Independently from this uncertainty the biological role of NPQ in response to excess of light was evaluated assessing I48 response to different light treatments. In batch cultures in HL I48 showed a decrease in PSII yield, a suggestion of increased photoinhibition. This however do not impact on the growth negatively since other mechanisms like the xanthophyll cycle, can be sufficient to protect the cells in order to avoid major

photodamage. Indeed zeaxanthin leads to enhanced dissipation of excess excitation energy in the photosystem II (PSII) antenna system. It forms a radical pair with Chl a upon excitation of the light-harvesting complex, thereby providing a route for energy dissipation. Multicultivator experiment, when the culture reached higher density respect to flask, revealed also that in ML, I48 seems to grow better than the WT. This suggests a possible advantage in a condition of high density culture as the industrial one.

NPQ impact on productivity

Productivity evaluation confirmed the positive effect of NPQ reduction on biomass accumulation. We saw that the gain in biomass of I48 respect to the WT can reach the 24% in 250_400 when light is more limiting with respect to the other conditions tested.

In a photobioreactor the culture is stratified with an external layer exposed to saturating light and an internal one in a condition of limiting light, which are continuously mixed. HL experiments showed that NPQ reduction has not great impact on the growth also in saturating light condition. Instead NPQ activation reduces light use efficiency and it remains active for minutes also after cell switch in the internal layer. A reduction in NPQ activation could avoid undesired energy dissipation in the internal layer. This saved energy can be used for photochemistry especially in the internal parts of a photobioreactor, with a gain in biomass growth.

It should be noted that in I48 there was also a reduction of pigments content per cell, justified by the fact that LHCX most likely also binds pigments (Bonente et al. 2011). Indeed a low pigment content also leads to a decrease in light harvesting, which avoid the oversaturation of the photosynthetic apparatus. The final result is that even if cells in the external layer experienced a reduction in photosynthetic efficiency, the internal ones has a gain in energy utilization efficiency which is higher respect to loss of the external one. This condition leads to a general advantage of the industrial system with NPQ defective strains.

REFERENCES

Alboresi, Alessandro et al. 2010. "Physcomitrella Patens Mutants Affected on Heat Dissipation Clarify the Evolution of Photoprotection Mechanisms upon Land Colonization." *Proceedings of the National Academy of Sciences of the United States of America* 107(24): 11128–33.

Alboresi, Alessandro et al. 2016. "Light Remodels Lipid Biosynthesis in Nannochloropsis Gaditana by Modulating Carbon Partitioning between Organelles." *Plant Physiology* 171(August): 2468–82.

Arnoux, Pascal et al. 2009. "A Structural Basis for the pH-Dependent Xanthophyll Cycle in Arabidopsis Thaliana." *Plant cell* 21(July): 2036–44.

Bailleul, Benjamin et al. 2010. "An Atypical Member of the Light-Harvesting Complex Stress-Related Protein Family Modulates Diatom Responses to Light." *Proceedings of the National Academy of Sciences of the United States of America* 107(42): 18214–18219

Baroli, I, and K K Niyogi. 2000. "Molecular Genetics of Xanthophyll-Dependent Photoprotection in Green Algae and Plants." *Philosophical transactions of the Royal Society of London. Series B, Biological sciences* 355(1402): 1385–94.

Berteotti, Silvia, Matteo Ballottari, and Roberto Bassi. 2016. "Increased Biomass Productivity in Green Algae by Tuning Non-Photochemical Quenching." *Scientific Reports* 6(1): 21339.

Bonente, Giulia et al. 2011. "Analysis of LHcSR3, a Protein Essential for Feedback de-Excitation in the Green Alga Chlamydomonas Reinhardtii." *PLoS Biology* 9(1).

Corteggiani, Elisa et al. 2014. "Chromosome Scale Genome Assembly and Transcriptome Profiling of Nannochloropsis Gaditana in Nitrogen Depletion." *Molecular Plant* 7(2): 323–35.

Dent, Rachel M et al. 2005. "Functional Genomics of Eukaryotic Photosynthesis Using Insertional Mutagenesis of Chlamydomonas Reinhardtii." *Plant physiology* 137(2): 545–56.

Gerotto, Caterina, Cinzia Franchin, Giorgio Arrigoni, and Tomas Morosinotto. 2015. “In Vivo Identi Fi Cation of Photosystem II Light Harvesting Complexes Interacting with PHOTOSYSTEM II.” *Plant physiology* 168(August): 1747–61.

Goss, Reimund, and Torsten Jakob. 2010. “Regulation and Function of Xanthophyll Cycle-Dependent Photoprotection in Algae.” *Photosynthesis research* 106(1-2): 103–22.

Lepetit, Bernard et al. 2017. “The Diatom Phaeodactylum Tricornutum Adjusts Nonphotochemical Fluorescence Quenching Capacity in Response to Dynamic Light via Fine-Tuned Lhcx and Xanthophyll Cycle Pigment Synthesis.” *New Phytologist* 214(1): 205–18.

Liu, Y G, Norihiro Mitsukawa, Teruko Oosumi, Robert F Whittier. 1995. “Thermal asymmetric interlaced PCR: automatable amplification and sequencing of insert end fragments from P1 and YAC clones for chromosome walking." *Genomics* 25(3):674-81

Maruyama, Shinichiro, Ryutaro Tokutsu, and Jun Minagawa. 2014. “Transcriptional Regulation of the Stress-Responsive Light Harvesting Complex Genes in Chlamydomonas Reinhardtii." *Plant &cell physiology*.” 81(0): 1304–10.

Maxwell, K, and G N Johnson. 2000. “Chlorophyll Fluorescence--a Practical Guide.” *Journal of experimental botany* 51(345): 659–68.

Meneghesso, Andrea et al. 2016. “Photoacclimation of Photosynthesis in the Eustigmatophycean Nannochloropsis Gaditana.” *Photosynthesis Research* 129(3): 291–305.

Muller, Patricia, Xiao-ping Li, and Krishna K Niyogi. 2001. “Non-Photochemical Quenching. A Response to Excess Light Energy 1.” *Update on Photosynthesis* 125(April): 1558–66.

Nilkens, Manuela et al. 2010. “Identification of a Slowly Inducible Zeaxanthin-Dependent Component of Non-Photochemical Quenching of Chlorophyll Fluorescence Generated under Steady-State Conditions in Arabidopsis.” *Biochimica et Biophysica Acta - Bioenergetics* 1797(4): 466–75.

Niyogi, Krishna K., and Thuy B. Truong. 2013. “Evolution of Flexible Non-Photochemical Quenching Mechanisms That Regulate Light Harvesting in Oxygenic Photosynthesis.” *Current Opinion in Plant Biology* 16(3): 307–14.

Perin, Giorgio et al. 2015. “Generation of Random Mutants to Improve Light-Use Efficiency of Nannochloropsis Gaditana Cultures for Biofuel Production.” *Biotechnology for biofuels* 8: 161-174.

Rinalducci, Sara, Jens Z Pedersen, and Lello Zolla. 2008. “Generation of Reactive Oxygen Species upon Strong Visible Light Irradiation of Isolated Phycobilisomes from Synechocystis PCC 6803.” *Biochimica et Biophysica Acta* 1777: 417–24.

Simionato, Diana , et al. 2013. “The Response of Nannochloropsis Gaditana to Nitrogen Starvation Includes de Novo Biosynthesis of Triacylglycerols, a Decrease of Chloroplast Galactolipids, and Reorganization of the Photosynthetic Apparatus.” *Eukaryotic Cell* 12(5): 665–76.

Simionato, Diana, Stefania Basso, Giorgio M. Giacometti, and Tomas Morosinotto. 2013. “Optimization of Light Use Efficiency for Biofuel Production in Algae.” *Biophysical Chemistry* 182(July): 71–78.

Taddei, Lucilla et al. 2016. “Multisignal Control of Expression of the LHCX Protein Family in the Marine Diatom Phaeodactylum Tricornutum.” *Journal of Experimental Botany* 67(13): 3939–51.

CHAPTER 5 :

Fluctuating light response in *Nannochloropsis gaditana*.

Authors name and affiliations

Alessandra Bellan[1] and Tomas Morosinotto[1]

1-PAR-Lab_Padua Algae Research Laboratory, Department of Biology, University of Padova, Via U. Bassi 58/B, 35121 Padova, Italy.

CONTRIBUTION:

AB performed all experimental work and most of the writing.

ABSTRACT

Photosynthetic organisms are exposed to highly dynamic conditions in natural environment that include frequent changes in light availability. Microalgae evolved different mechanisms to modulate their photosynthetic machinery allowing for the colonization of diverse habitats. Two major mechanisms have been suggested to be involved in response to fluctuating light: non photochemical quenching of the energy excess and regulation of auxiliary electron transports. The aim of this work is to clarify the role of those mechanisms in response to fluctuating light in the Heterokont *Nannochloropsis gaditana*. Fluctuating light is shown to have a major negative impact on *N.gaditana* growth. Deeper photosynthetic analysis revealed that fluctuating light does not affect PSII photosynthetic efficiency but instead drastically reduces the number of active PSI per cell, leading to an overall reduction in the total electron transport capacity. PSI damage seems to be due to the lack of the key alternative electron transport components in this microalga.

INTRODUCTION

In natural environment photosynthetic organisms, both plants and algae, are exposed to continuous fluctuations in light intensity. Sun position, clouds movements, wind, waves and phytoplankton migration are all phenomena that cause changes in incident light (Allahverdiyeva et al. 2015). In such a dynamic environment an optimal performance of photosynthesis requires a continuous tuning between light harvesting and metabolic reactions involved in the energy conversion (Peltier, Tolleter, and Billon 2010).

While the basic photochemical reactions are highly conserved, different mechanisms for regulation of photosynthetic apparatus have been identified in various group of organisms. Investigation of the diversity of photosynthetic organisms and how they deal with dynamic light conditions can thus be highly informative to understand the principles for this regulation. In this context algae with their large biodiversity and complex evolutionary history can be particularly informative.

One of the major mechanisms for response to light variations is Non Photochemical Quenching (NPQ). NPQ has a key role in avoiding over excitation of the photosynthetic apparatus under excess illumination that can lead to the generation of reactive oxygen species (ROS) (Goss and Lepetit 2015). NPQ in plants have been shown to be seminal for plants fitness upon growth in natural dynamic conditions (Kulheim, Agren, and Jansson 2002).

In algae this mechanism depends from light harvesting stress related protein (LHCSR or LHCX proteins) identified both in green algae and diatoms (Maruyama, Tokutsu, and Minagawa 2014; Taddei et al. 2016). NPQ has been suggested to be involved in the algae response to FL even if there are opposing opinions about its role and regulation in this response. (Grouneva et al. 2016) showed that the diatom *Thalassiosira pseudonana* under fluctuating light experiences a remodeling of the LHC and LHC-like protein abundance. In particular they found a down-regulation of LHCX6, an antenna protein involved in photoprotection, which suggests reduced need of photoprotection in FL condition. On the contrary in (Lepetit et al. 2017) in *Phaeodactylum tricornutum* the acclimation strategy to FL was suggested to be enhancing NPQ activation thanks to a transcriptional and post transcriptional regulation of LHCXs antenna proteins involved in non-photochemical quenching mechanism (in particular LHCX2 and LHCX3).

Another major regulatory mechanism for photosynthesis is the modulation of electron transport reactions that avoids the over-reduction of the photosynthetic apparatus in stressful light condition, that is particularly damaging for PSI. Forward and reverse genetic approaches allowed identifying auxiliary electron transports that modulates NADPH/ATP ratio (Peltier, Tolleter, and Billon 2010) such as proton gradient regulator 5 (PGR5), proton gradient regulator like 1 (PGRL1), NAD(P)H dehydrogenase type 2 (Ndh-2), plastid terminal oxidase (PTOX) and flavodiiron proteins (FLV). These are the molecular components involved in these auxiliary electron transport pathways and interestingly these components are differently distributed in different organisms (Peltier, Tolleter, and Billon 2010; Shikanai 2016).

Among all these components, FLV emerged as one of the auxiliary electron transport pathway more involved in fluctuating light response (Allahverdiyeva et al. 2015; Gerotto et al. 2016; Shikanai 2016). They work as a dimer and they catalyze NAD(P)H-mediated O_2 reduction to water. FLV proteins maintain the redox balance of the electron transfer chain in condition of over-excitation providing photoprotection for PSI.

The aim of this work is to clarify what is the mechanism adopted by *Nannochloropsis gaditana* to deal with fluctuating light. *N.gaditana* was chosen because from an evolutionary point of view it holds a peculiar position since it originated from a secondary endosymbiotic event and it has a peculiar photosynthetic apparatus, in which only chlorophyll a is present and violaxanthin is the main carotenoid in the antenna proteins (Basso et al. 2014). Its investigation can contribute to the exploration of response to FL in marine organisms.

MATERIAL AND METHODS

Microalgae growth

Nannochloropsis gaditana (strain 849/5) from the Culture Collection of Algae and Protozoa (CCAP) were exploited for this experiment. Cells were cultivated in sterile F/2 media with sea salts (32 g/l, Sigma Aldrich), 40 mM Tris–HCl (pH 8) and Guillard's (F/2) marine water enrichment solution (Sigma Aldrich) in Erlenmeyer flasks with 100 µmol photons m^{-2} s^{-1} illumination and 100 rpm agitation at 22 ± 1 °C in a growth chamber.

The comparison between different light regimes were done using a Multicultivator MC 1000-OD system (Photon Systems Instruments, Czech Republic), in which the temperature was maintained at 21° C and illumination was provided with a photoperiod of 16-h light, 8-h dark at an averaged intensities of 150 µmol of photons m^{-2} s^{-1} using an array of white LEDs. Control sample were exposed to a continuous light intensity, the fluctuating ones were exposed to:

- FL1: 10 min of 1000 µmol of photons m^{-2} s^{-1} every 60 min of 10 µmol of photons m^{-2} s^{-1}
- FL2: 1 min of 1000 µmol of photons m^{-2} s^{-1} every 6 min of 10 µmol of photons m^{-2} s^{-1} ;
- FL3: 10 sec of 1000 µmol of photons m^{-2} s^{-1} every 60 sec of 10 µmol of photons m^{-2} s^{-1}

In Multicultivator system experiments were performed using a F/2 medium enriched as already described in chapter 3. The suspension culture was constantly mixed and aerated

through air bubbling. Algal growth was measured by cells counting using a cell counter (Cellometer Auto X4, Nexcelom Bioscience).

Pigment content analysis

Chlorophyll a and total carotenoid extraction from entire cells was done after 9 days of growth using a 1:1 biomass to solvent ratio of 100 % N,N dimethylformamide (Sigma Aldrich). Pigments were extracted at 4 °C in the dark for at least 24 h. Absorption spectra were performed between 350 nm and 750 nm using a Cary 100 spectrophotometer (Agilent Technologies) to spectrophotometrically determine pigment concentrations using specific extinction coefficients. Absorption values at 664 and 480 nm were used to calculate the concentrations of chlorophyll a and total carotenoids, respectively.

Photosynthetic analysis

In vivo Chl fluorescence was measured using a PAM 100 fluorimeter (Heinz-Walz, Effeltrich, Germany). PSII functionality was expressed as PSII maximum quantum yield (Fv/Fm), as described by (Maxwell and Johnson 2000). The light treatment exposed the samples to increasing light intensity up to 2000 µmoles photons m^{-2} s^{-1}, and then light was switched off to evaluate NPQ relaxation kinetic. NPQ was evaluated in accord with (Maxwell and Johnson 2000).

PSII antenna sizes were determined using a JTS-10 spectrophotometer (Biologic, France). Samples of 200 x 10^6 cells/ml final concentration were dark-adapted for 20 minutes and incubated with 80 µM 3-(3,4-dichlorophenyl)-1,1-dimethylurea (DCMU) for 10 minutes. Fluorescence induction was measured after an excitation with 320 µmoles photons m^{-2} s^{-1} of actinic light at 630 nm. The t2/3 values were calculated from the fluorescence induction curves and then the size of the PSII functional antenna was calculated as described in (Perin et al. 2015).

Electron chromic shift (ECS) measurements were done on 200 x 10^6 cells/ml (intact cells). Data were analyzed as the difference between the signals at 520 and 498 nm (which represent the positive and negative peaks of the ECS signal in *Nannochloropsis*, respectively) to deconvolute this signal from other spectral changes not related to the building of the transmembrane potential (Simionato et al. 2013).

The P700 and the total electron flow (TEF) spectroscopic quantifications were performed measuring P700 (the primary electron donor to PSI) absorption at 705 nm in intact cells. Samples of 300 x 10^6 cells/ml final concentration were exposed to 2050 µmoles photons m^{-2} s^{-1}, at 630 nm for 15 seconds to maximize P700 oxidation and reach a steady state. Then P700 re-reduction kinetic in the dark for 5 seconds was followed. The total electron flow (TEF) was evaluated from P700 re-reduction rates after illumination in untreated cells. Assuming a single exponential decay of P700 the rate constant of P700 reduction was calculated as $1/\tau$. By multiplying the rate constant with the fraction of oxidized P700, and considering this value as 1 in DCMU- and DBMIB-treated, the number of electrons transferred per unit of time per PSI unit was calculated (Simionato et al. 2013).
The PSI content was estimated from the maximum change in the absorption of P700 in cells treated with DCMU (80 µM) and DBMIB (dibromothymoquinone, 300 µM) at 2050 µmoles photons m^{-2} s^{-1}at 630 nm (Simionato et al. 2013).

Bioinformatic analysis

In order to investigate if *N.gaditana* has one or more of the proteins recognized as to be involved in the alternative electron transports, a BLAST alignment was done in the genome browser of *N.gaditana* (http://www.nannochloropsis.org/). An e-value cut-off from e^{-12} to e^{-3} was tested to align the protein sequences reported in table 1.

Table 1: In the table are reported the ID of the protein sequences that have been aligned on *N.gaditana* genome browser. We used sequences from *A.thaliana, P. patens*, *M. polymorpha* and *C. reinhardtii.*

	Protein ID used in the analysis
PGR5	XP_001769396-XP_001755090-XP_001700905
PGRL1	NP_567672-XP_001772047-XP_001692513
PTOX	XP_001692600- XP_001703466
NDH-2	XP_001691969- XP_001691969
FLVA	XP_001759251-AMJ52189
FLVB	XP_001756079-AMJ52190

RESULTS

Impact of fluctuating light on N. gaditana growth

N.gaditana response to fluctuating light (FL) was investigated by comparing a culture exposed to continuous light (CL) at the intensity of 150 µmol of photons m^{-2} s^{-1} with three different fluctuating lights, as described in figure 1:

- FL1: 10 min 1000 µmol of photons m^{-2} s^{-1} - 60 min 10 µmol of photons m^{-2} s^{-1}, average light intensity =150 µmol of photons m^{-2} s^{-1};
- FL2: 1 min 1000 µmol of photons m^{-2} s^{-1} - 6 min 10 µmol of photons m^{-2} s^{-1}, average light intensity =150 µmol of photons m^{-2} s^{-1};
- FL3: 10 sec 1000 µmol of photons m^{-2} s^{-1}- 60 sec 10 µmol of photons m^{-2} s^{-1}, average light intensity =150 µmol of photons m^{-2} s^{-1};

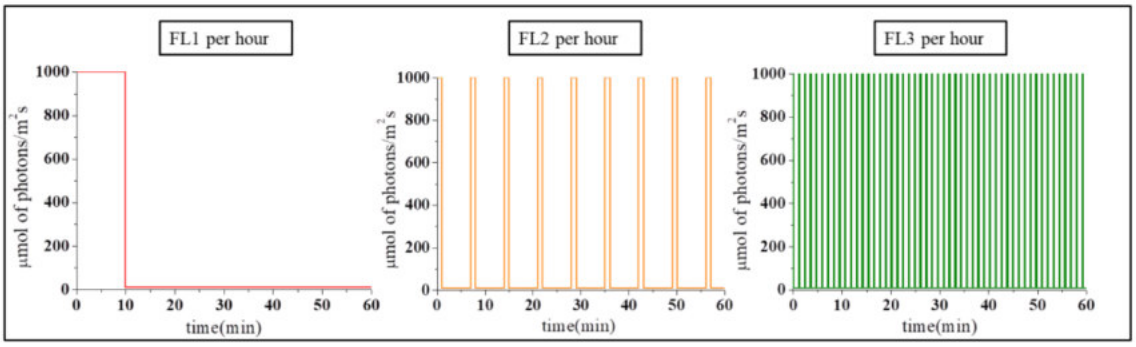

Figure 1: Schematic representation of light treatment per hour in FL1 (red), FL2 (orange), and FL3 (green).

It is worth underlining that in all cases in FL there is an alternation between two light intensities, 1000 and 10 µmol of photons m^{-2} s^{-1} that are respectively saturating and limiting for *Nannochloropsis* (Sforza et al. 2012). At the same time the total amount of photons provided is the same for all conditions and it corresponds to the optimal illumination of ≈ 150 µmol of photons m^{-2} s^{-1} (Sforza et al. 2012). This experimental design ensures that all eventual effects observed are due to the light dynamics and not to the total amount of light provided.

FL treatments resulted in a considerable growth reduction with respect to control conditions (fig 2-A), showing that light fluctuations have an important impact. The growth reduction became particularly severe with the increase of flashes frequency from FL1 to FL3.

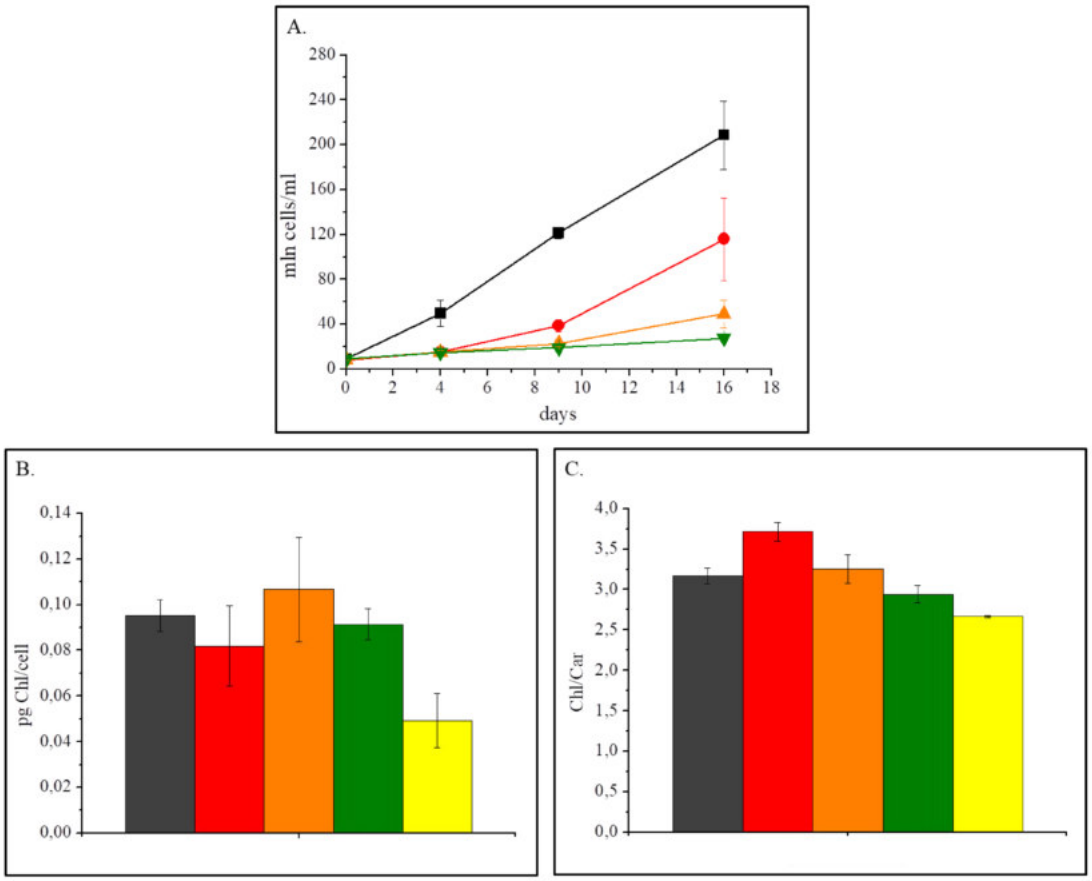

Figure 2: The data show the CL treatment in black/dark grey, FL 1 in red, FL 2 in orange, FL 3 in green and HL treatment in yellow. In A were reported the growth curves. In B is shown chlorophyll content and in C the ratio between Chl and Car content. All the parameters are measured the 9th day of the culture (n=4).

It is interesting to notice that pigments content in all FL conditions is similar to the CL (fig 2-B), suggesting that FL does not induce any specific acclimation response. This is highly unusual since stressful conditions such as strong irradiation or nutrients deficiency have a major impact on pigments content and induce an acclimation response (Meneghesso et al. 2016; Simionato et al. 2013). Fig 2-B and C report the comparison with a culture cultivated with HL treatment at 1000 µmol of photons m^{-2} s^{-1}, showing a major impact on chlorophyll content per cell due to the activation of acclimation mechanisms, which are not observed in response to FL. In FL cultures also the carotenoid content is not affected, again another response normally observed in stressing conditions.

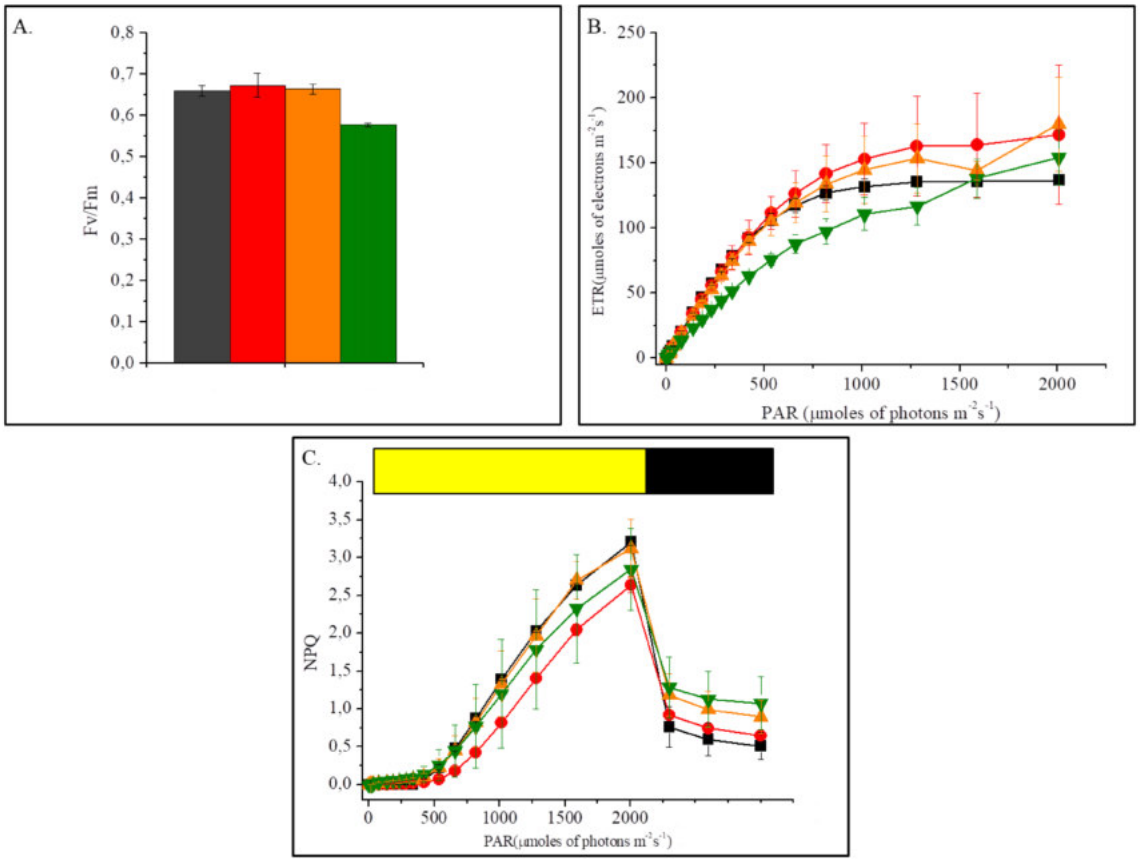

Figure 3: The data show the CL treatment in black/dark grey, FL 1 in red, FL 2 in orange and FL 3 in green. In A were reported the maximum quantum yield of PSII, in B is shown the electron transport rate (ETR). All the parameters are evaluated the 9th day of the culture (n=4). In C is reported NPQ kinetics at increasing light intensity for 17 min, with 3 min of dark recovery in the end.

Photosystem II efficiency was evaluated by measuring PSII maximum quantum yield (Fv/Fm) (fig 3-A), electron transport rate (ETR) (fig 3-B) and NPQ (fig 3-B). Surprising there are no large effects due to FL treatments with only FL3 showing a slight decrease in Fv/Fm. This is not at all consistent with the drastic effect on growth and suggests that FL phenotype is likely not due to PSII photoinhibition.

ECS measurement highlighted a major reduction of PSI/PSII ratio that is reduced by ≈50 % respect to CL (fig 4-A). PSI content per cell, quantified from P700+ absorption signal demonstrated that such a reduction in PSI/PSII is due to strong decrease in the number of active PSI per cell (fig 4-B).

When we measured the total electron flow (TEF) per PSI per sec, it was not affected in the cultures, not even in FL3 cells the ones with the largest growth effect. This is because TEF measurement considers the electron transport per each active PSI (fig 4-C). So in

FL3 there is not a reduction in the electrons transport per each active PSI, but there is a general reduction in the total amount of electrons transported per cell, because the active PSI are an half respect to the CL. This reduction in active PSI per cell and so in the overall electron transport can correlates with the strong growth reduction on FL3 condition. It is interesting to notice also that there is also no significant activation of alternative electron flow respect to the CL (fig 4-C).

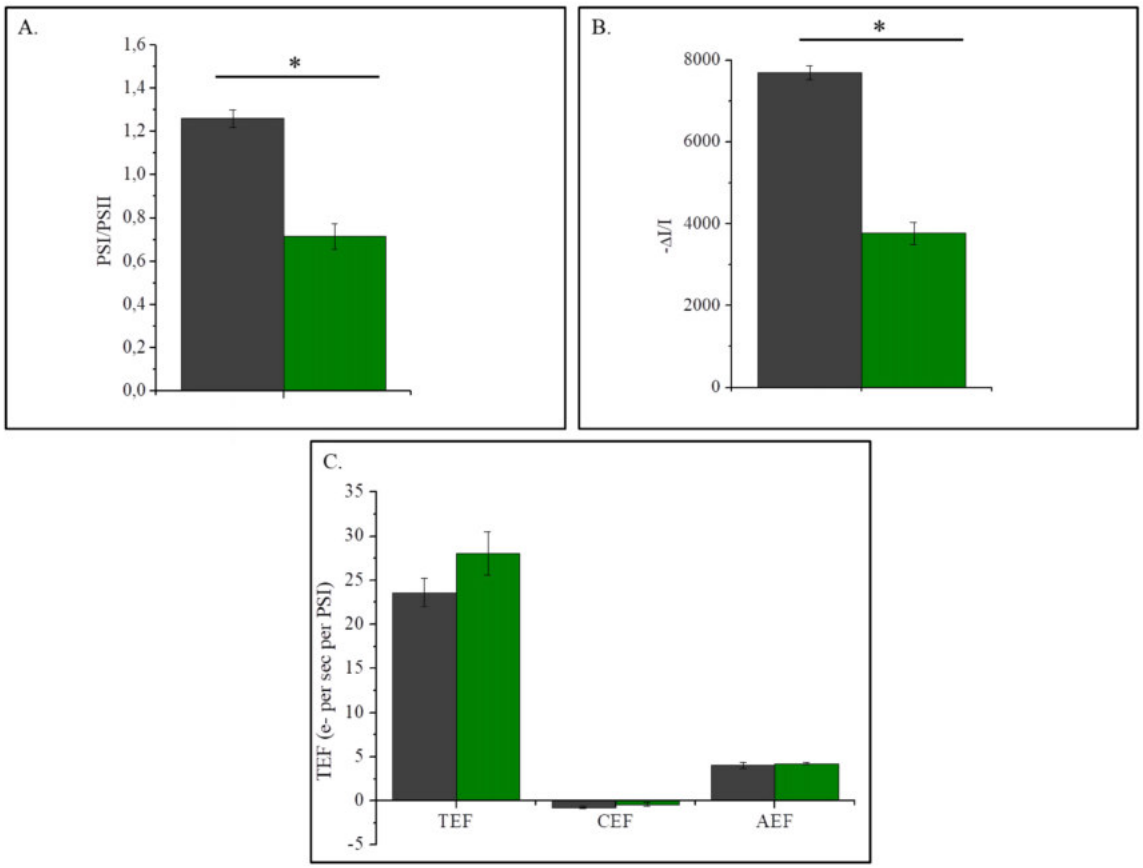

Figure 4: In A is shown the PSI/PSII ratio, obtained by ECS measurement (n=3). In B is reported P700 maximum oxidation level reached at the steady state during the light treatment in cells acclimated to different light conditions. These values represent an indicator of the PSI content (n=3). In C is shown the determination of the total, the cyclic and the alternative photosynthetic electron flow. The electron flow was determined from the kinetics of P700+ re-reduction after light was switched off (n=3). Data are normalized to the PSI content using single flash, so it is expressed as TEF per PSI per sec. Statistically significant differences between CL in black and FL3 in green are marked with asterisks (one-way ANOVA, p-value < 0.05).

Role of NPQ activation in response to fluctuating light

NPQ has been suggested to play a major role in response to fluctuating light intensities in plants (Kulheim, Agren, and Jansson 2002) as well as in algae.

In order to assess NPQ activation upon treatment with FL, control cells were exposed for 45 minutes to the FLs treatments described above monitoring effect on Chl fluorescence. We observed that NPQ requires several minutes of continuous illumination to be activated and especially in FL3 this response is very slowly activated (fig 5).

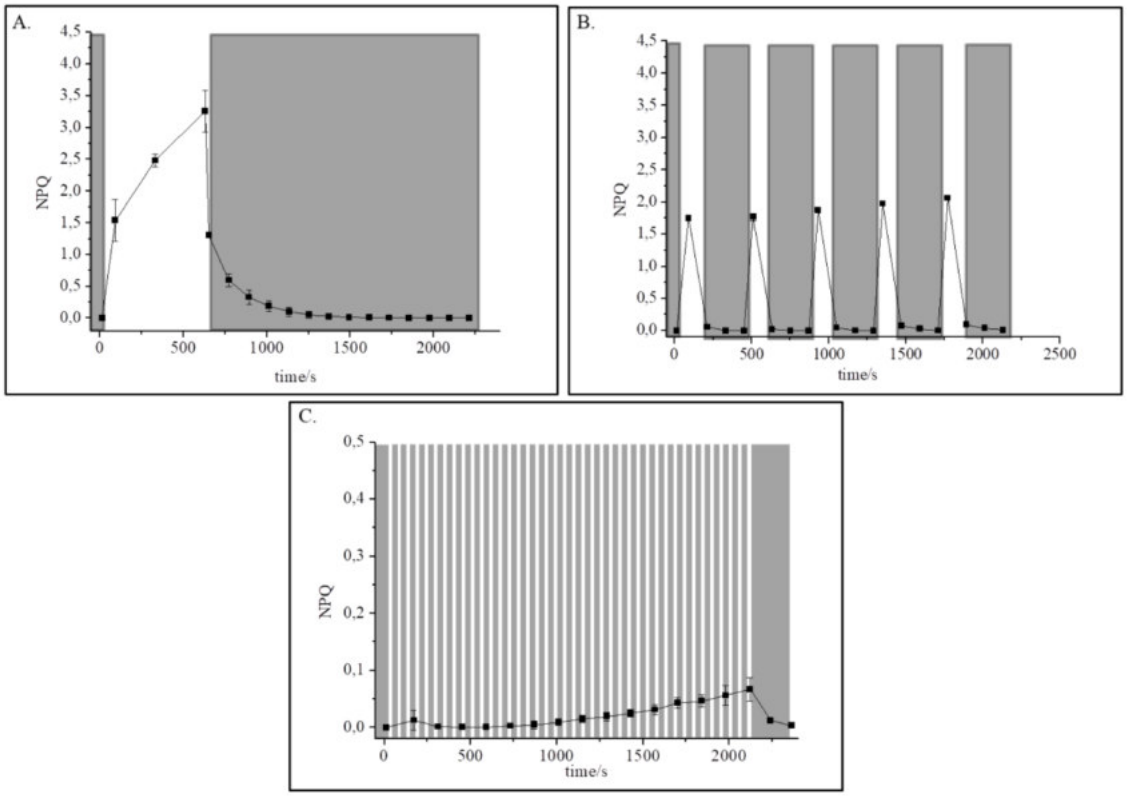

Figure 5: NPQ analysis with a light treatment that mimic A-FL3, B-FL2 and C-FL1. Grey squares represent low light period during the kinetics (n=3).

This delay in NPQ activation however cannot explain the growth reduction observed above since i) a drastic growth reduction was present in all conditions even in FL1 where NPQ was activated; ii) cultures are exposed to FL continuously, thus a slower activation should have smaller effect on the long term.

In order to properly evidence the influence of NPQ in FL response in *N.gaditana*, we tested the mutant I48 described in chapter 4 in the same fluctuating light conditions. This mutant has a severe NPQ reduction, and thus it allows evidencing directly the influence

of this response in FL. As it is shown in fig 6 in all the FL treatments I48 growth is highly similar to the WT. Also Fv/Fm measurement confirmed that the lack of NPQ activation has no impact on PSII efficiency in FL treatments. These data suggest that NPQ does not have a major influence on *Nannochloropsis* response to FL.

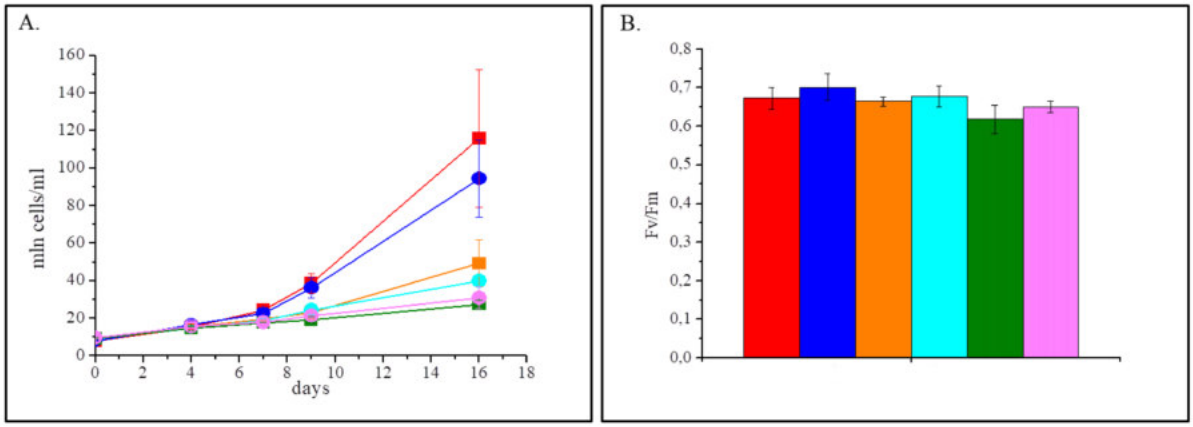

Figure 6: In A is shown the growth curve of WT (square) and I48 (circle) treated with the 3 FL described above: in red WT FL1, in blue I48 FL1, in orange WT FL2, in light blue I48 FL2, in dark green WT FL3 and in pink I48 FL3 (n=3). With the same colors in B is reported the Fv/Fm evaluation in WT and I48, for all the FL treatment.

DISCUSSION

Light fluctuations have a major influence on photosynthetic organisms metabolism. From one side light excess is a dangerous source of excess energy, on the other they must keep light use efficiency high during the low light parts. Different groups of organisms have differentiated responses to these conditions and this chapter presents a first analysis of *N.gaditana* response to fluctuating light with a high light illumination of 10 sec, 1 min or 10 min. Cultures showed a major effect of the light dynamic even if they were provided with the same total amount of photons and high light flashes had the same intensity. The effects observed can be specifically attributed to the light variations with the highest flash frequency showing the largest effect. Indeed higher is the flash frequency higher is the growth impairment experienced by the culture. This result is in apparent contrast with previous ones in (Sforza et al. 2012) where FL did not have harmful effects. In this case

however the duration of the light treatments was much faster (from 30ms to 100ms) and not sufficient to oversaturate electron transport chain.

Pigment content analysis showed that also there is no activation of any acclimation response. This is highly unusual since all photosynthetic organisms modulate the composition of their photosynthetic apparatus in response to different illumination. Indeed as reported in (Meneghesso et al. 2016) *N.gaditana* is not different, it remodels its photosynthetic apparatus in response to different light treatments. As it is shown in fig 2 B and C HL leads to a reduction of in the Chl content, in order to reduce the absorption and to avoid the over saturation of the photosynthetic apparatus in a condition of excess of light. In FL treatment instead the pigment content is similar to the CL even if the culture is exposed to HL flashes. This suggests that in these conditions the signals activation acclimation are not activated.

Spectroscopic analysis revealed that FL light treatments employed here have a limited effect on PSII that is normally the major target for photoinhibition upon strong illumination. Indeed there is no reduction of Fv/Fm except in FL3, but the small reduction recorded is not sufficient to justify the growth impairment observed. On the other hand we observed a major inactivation of PSI, whose content per cell is reduced by 50%. Fluctuating light has been shown to have negative effects on PSI in other organisms because of an over-reduction of PSI (Kono, Noguchi, and Terashima 2014; Shikanai 2016)

In these conditions PSI is limited by the acceptor side and excess electrons are damaging PSI. Remarkably it has been observed that PSI does not have an efficient repair system in place and thus any damage has a major impact on growth.

While an impact on PSI stability by FL on PSI has been already observed it has to be mentioned that this is the case only for mutants affected in cyclic or alternative electron transport mechanisms. In plants and green algae WT instead does not easily show damage to PSI. It thus appears that such mechanisms active in protecting PSI from excess radiation are not present in *N. gaditana*.

BLAST research on *N.gaditana* genome with sequences derived from *A.thaliana*, *P.patens*, *M.polymorpha* and *C.reinhardtii* showed that this microalga does not present homologous to fundamental proteins involved in auxiliary electron transports. There isn't any protein homologous to Flvs and PGRL1. Ndh-2 and PTOX showed homologous sequences but the putative proteins are predicted to be located in the mitochondrion, so their role is uncertain. PGR5 is the only protein that seems to be present also in

N.gaditana (table 2). In this case however the functionality is far from sure since in plants PGR5 needs PGRL1 to be active in cyclic electron transport. This situation is really similar to those one described for diatoms (Grouneva et al. 2016; Peltier, Tolleter, and Billon 2010). Indeed also in diatoms FLV and NDH proteins are missed. It seems to be present an homologous of PTOX but its function has still to be clarified. PGR5 and PGRL1 are the only detectable proteins found. (Grouneva et al. 2016; Lepetit et al. 2017) suggested that alternative electron flows do not play any significant role in photosynthesis regulation in diatoms. Instead regulation of NPQ, in particular LHCXs expression, seems to be one of the key responses in FL conditions, even if there are variable responses in different diatoms species.

Table 2: Summary of the BLAST research on *N.gaditana* genome for the protein involved in cyclic and alternative electron transport. ? marked the proteins that gives a result but the proteins highlighted seem to have a target peptide to the mitochondria.

PROTEIN	BLAST on N.gaditana genome
PGR5	FOUND (Naga_100940g3)
PGRL1	NOT FOUND
PTOX	?
NDH-2	?
FLVs	NOT FOUND

This is not the case for *N.gaditana* as confirmed by I48 growth in FL in *N.gaditana* NPQ has no a significant effect in FL responses. So these data suggest that *Nannochloropsis* is particularly sensitive to FL because of the absence of many molecular players in cyclic electron transport.

REFERENCES

Allahverdiyeva, Yagut, Marjaana Suorsa, Mikko Tikkanen, and Eva-mari Aro. 2015. "Photoprotection of Photosystems in Fluctuating Light Intensities." *Journal of Experimental Botany* 66(9): 2427–36.

Basso, Stefania et al. 2014. "Characterization of the Photosynthetic Apparatus of the Eustigmatophycean Nannochloropsis Gaditana: Evidence of Convergent Evolution in the Supramolecular Organization of Photosystem I." *Biochimica et biophysica acta* 1837(2): 306–14.

Gerotto, Caterina et al. 2016. "Flavodiiron Proteins Act as Safety Valve for Electrons in *Physcomitrella Patens*." *Proceedings of the National Academy of Sciences* 113(43): 12322–27.

Goss, Reimund, and Bernard Lepetit. 2015. "Biodiversity of NPQ." *Journal of Plant Physiology* 172: 13–32.

Grouneva, Irina, Dorota Muth-pawlak, Natalia Battchikova, and Eva-mari Aro. 2016. "Changes in Relative Thylakoid Protein Abundance Induced by Fluctuating Light in the Diatom Thalassiosira Pseudonana." *Journal of proteome* 15: 1649–58.

Kono, Masaru, Ko Noguchi, and Ichiro Terashima. 2014. "Roles of the Cyclic Electron Flow Around PSI (CEF-PSI) and O 2 -Dependent Alternative Pathways in Regulation of the Photosynthetic Electron Flow in Short-Term Fluctuating Light in Arabidopsis Thaliana." *Plant and Cell Physiology* 55(5): 990–1004.

Kulheim, Carsten, Jon Agren, and Stefan Jansson. 2002. "Rapid Regulation of Light Harvesting and Plant Fitness in the Field." *Science* 297(July): 91–94.

Lepetit, Bernard et al. 2017. "The Diatom Phaeodactylum Tricornutum Adjusts Nonphotochemical Fluorescence Quenching Capacity in Response to Dynamic Light via Fine-Tuned Lhcx and Xanthophyll Cycle Pigment Synthesis." *New Phytologist* : 205–18.

Maruyama, Shinichiro, Ryutaro Tokutsu, and Jun Minagawa. 2014. "Transcriptional Regulation of the Stress-Responsive Light Harvesting Complex Genes in Chlamydomonas Reinhardtii Special Focus Issue – Regular Paper." *Plant and Cell Physiology* 81(0): 1304–10.

Maxwell, K, and G N Johnson. 2000. “Chlorophyll Fluorescence--a Practical Guide.” *Journal of experimental botany* 51(345): 659–68.

Meneghesso, Andrea et al. 2016. “Photoacclimation of Photosynthesis in the Eustigmatophycean Nannochloropsis Gaditana.” *Photosynthesis Research* 129(3): 291–305.

Peltier, Gilles, Dimitri Tolleter, and Emmanuelle Billon. 2010. “Auxiliary Electron Transport Pathways in Chloroplasts of Microalgae.” *Photosynthesis research* 106: 19–31.

Perin, Giorgio et al. 2015. “Generation of Random Mutants to Improve Light-Use Efficiency of Nannochloropsis Gaditana Cultures for Biofuel Production.” *Biotechnology for biofuels* 8: 161-174.

Sforza, Eleonora et al. 2012. “Adjusted Light and Dark Cycles Can Optimize Photosynthetic Efficiency in Algae Growing in Photobioreactors.” *PloS one* 7(6).

Shikanai, Toshiharu. 2016. “Regulatory Network of Proton Motive Force : Contribution of Cyclic Electron Transport around Photosystem I.” *Photosynthesis Research*.

Simionato, Diana et al. 2013. “The Response of Nannochloropsis Gaditana to Nitrogen Starvation Includes de Novo Biosynthesis of Triacylglycerols, a Decrease of Chloroplast Galactolipids, and Reorganization of the Photosynthetic Apparatus.” *Eukaryotic Cell* 12(5): 665–76.

Taddei, Lucilla et al. 2016. “Multisignal Control of Expression of the LHCX Protein Family in the Marine Diatom Phaeodactylum Tricornutum.” *Journal of Experimental Botany* 67(13): 3939–51.

CHAPTER 6:

Evaluation of the potential of a low chlorophyll content mutant of *Scenedesmus obliquus* in a continuous system.

Authors name and affiliations

Alessandra Bellan[1], Giorgio Perin[2], Diana Simionato[1] and Tomas Morosinotto[1]

1-PAR-Lab_Padua Algae Research Laboratory, Department of Biology, University of Padova, Via U. Bassi 58/B, 35121 Padova, Italy

2- Department of Life Sciences, Imperial College London, Sir Alexander Fleming Building, London, SW7 2AZ, UK.

CONTRIBUTION:

In this chapter AB performed all the experiments described for the continuous system evaluation. GP performed the mutagenesis and the strain selection. DS was involved in the preliminary growth curves evaluation.

ABSTRACT

In this chapter was evaluated the potential of a low chlorophyll content mutant of *Scenedesmus obliquus*, a green microalga already recognized as a promising feedstock not only for biofuel but also for proteins and edible oil production. The mutant strain was screened from a collection of chemically induced mutants because of a lower pigment content, also to verify the applicability of the methods developed for *Nannochloropsis* to other species. The selected strain showed indeed a ≈50 % reduction of total chlorophyll content with respect to the wild type. The strain performances in industrially significant conditions were assessed using a flat panel photobioreactor run in continuous mode, also allowing a comparison with analogous experiments with semi-continuous cultures. Three different residence times were evaluated and at least in one of them the mutant showed a higher productivity respect to the wild type.

INTRODUCTION

Scenedesmus obliquus is a green microalga that has been suggested as a candidates species for biofuels feedstock, thanks to the ability to accumulate TAG up to 30%-45% dry weight. It also has the advantage of a constant biomass composition being less dependent from nutrients supply than other species (Gris et al. 2014). Total fatty acids (TFA) composition is enriched in saturated and monounsaturated fatty acids that are suitable for biodiesel production. *S.obliquus* has also potential as source of protein and edible oils and various works highlighted the possibility to combine its cultivation with wastewaters bioremediation (Chaudhary, Dikshit, and Tong 2017).

As discussed extensively in previous chapters, algae potential is still not fulfilled at the industrial scale. We already discussed in chapter 1 and in chapter 3 how genetic engineering can be an instrument to achieve this objective by improving productivity for the industrial cultivation of algae in photobioreactors. In this work we tested the possibility of applying the mutagenesis approach developed for *Nannochloropsis* in (Perin et al. 2015) to another species of industrial interest. To this aim we generated a collection of random mutants by ethyl methane sulfonate (EMS) treatment and selected

the ones with a reduced pigment content. The most promising strain (SOB17) was assessed in flat panel photobioreactors run in continuous mode. The advantage of a continuous system is that there is a constant supply of fresh media and a consequent constant biomass collection and they can yield higher productivities and culture stability on a large scale (Sforza, Gris, and Farias 2014). When a continuous system after a transitory phase reaches a so called stationary state, the culture has always the same concentration and also the same physiological-chemical characteristics (Bertucco, Beraldi, and Sforza 2014; Sforza, Enzo, and Bertucco 2013). For this reason continuous cultivation is especially suitable for large-scale industrial plants, becouse it can result in a stable and continuous biomass production.

In the present work we also assessed how the strain performances are influenced by operating variables as residence time and biomass concentration also analyzing the alterations in cells properties such as pigment content or biochemical composition in different stable conditions.

MATERIAL AND METHODS

Algal strain and culture media

S. obliquus 276.7 was obtained from SAG-Goettingen, Germany. It was maintained in sterile BG11 medium, with 1.5 g /l $NaNO_3$ (247 mg/l N) and 30.5 mg/l K_2HPO_4 (5.4 mg/l P), buffered with 10 mM HEPES pH 8. In continuous experiments, BG11 was further modified in order to guarantee non limiting nutrient concentrations with 494 mg/l of N and 89 mg/l P.

Mutagenesis and mutant selection

Mutant collection was generated setting mutagenesis condition to induce 90% cell mortality to ensure a high mutation frequency. Microalgae suspensions (OD_{750}= 0.5) in the late exponential growth phase were mutagenized using 200 mM EMS (Sigma Aldrich) for 1 h in darkness at room temperature with mild agitation. Then cells were centrifuged at 5000g for 8 min. To remove the excess of EMS cells were washed four

times with sterile BG11 media and plated on BG11 agar dishes. Plates were disposed at 22 ± 1 °C with 20 µmol photons m^{-2} s^{-1} illumination until algae colonies appeared.

Photobioreactor set up and experimental condition

Microalgae were cultivated in an aseptic flat panel made with polycarbonate (PBR) with a working volume of 190 ml. The irradiated surface was 100 cm^2 and the depth 1.3 cm. Light was continuously given at 150 µmol of photons $m^{-2}s^{-1}$. The temperature was kept constant at 23 ± 1 °C in a refrigerated incubator. CO_2–air mixture was provided from the bottom of the reactor, ensuring culture mixing, which was also aided by a stirring magnet. A peristaltic pump (Sci-Q 400, Watson Marlow, USA) ensured a fresh medium supply at a determine inlet flow-rate. An overflow tube in the upper part of the panel kept the reactor volume constant and it permitted the biomass collection at a fixed flow rate. The residence time of the culture inside the PBR was regulated by the pump, and calculated according to:

$$\tau = V_R/Q$$

where V_R stands for reactor volume and Q for the volumetric flow rate.

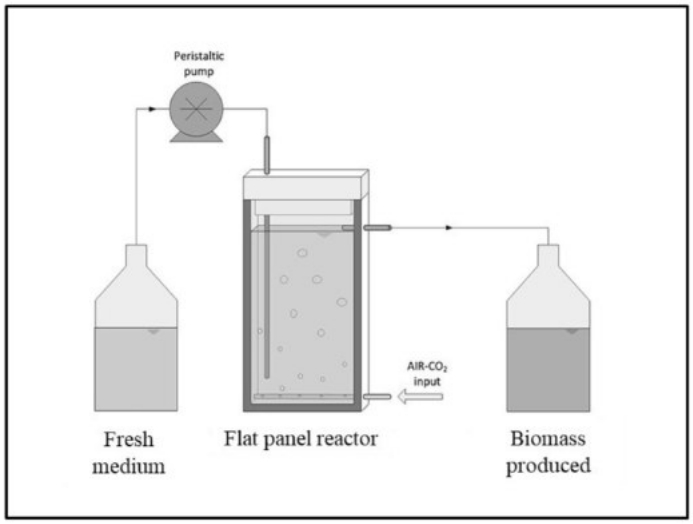

Figure 1: Schematic representation of the flat panel continuous system adapted from (Sforza et al. 2012).

Biomass production estimation

Algal growth was measured by cells counting using a cell counter (Cellometer Auto X4, Nexcelom Bioscience) and by optical density evaluation at 750nm (OD_{750}) with a Cary 100 spectrophotometer (Agilent Technologies). The biomass concentration was measured gravimetrically as a dry weight (DW) by filtering 8 ml using 0,45 µm pore size cellulose acetate filters. The filters were then dried at 70 °C for at least 24 h and the dry weights were measured in grams per liter.

Pigment extraction and quantification

Chlorophyll a and total carotenoids were extracted by adding 1:2 volume of dimethyl sulfoxide (DMSO) (Sigma Aldrich) after mechanical lysis in a Mini Bead Beater (Biospec Products) with the help of glass beads (150–212 µm in diameter). The samples were warmed at 65 degree for 8 minutes and then centrifuged. Absorption spectra were determined between 350 and 750 nm using a Cary 100 spectrophotometer (Agilent Technologies) to spectrophotometrically evaluate pigment concentrations using specific extinction coefficients. Absorption values at 664, 649 and 480 nm were used to calculate the concentrations of chlorophyll a, chlorophyll b and total carotenoids, respectively.

Antenna size measurement

PSII antenna sizes were determined in active growth conditions, using a JTS-10 spectrophotometer (Biologic, France). Samples (30 x 10^6 cells/ml final concentration) were dark-adapted for 10 minutes and incubated with 20 µM 3-(3,4-dichlorophenyl)-1,1-dimethylurea (DCMU) for 2 minutes. Fluorescence induction kinetics were then monitored upon excitation with 320 µmoles photons m^{-2} s^{-1} of actinic light at 630 nm. The $t_{2/3}$ values obtained from the fluorescence induction curves were used to calculate the size of the PSII functional antenna (Bonente et al. 2011; Perin et al. 2015).

RESULTS

At the beginning of this work a culture of *S. obliquus* in the late exponential growth phase was treated with ethyl methane sulfonate (EMS). As already described in chapter 2, EMS is an alkylating agent that induces a high frequency of nucleotide substitutions and has been largely exploited to induce random point mutations in various organisms. Chemical mutagenesis generates mutants that are not considered as genetically modified organisms (GMOs). This approach allows obtaining strains that are potentially readily applicable to large-scale systems. Low pigments strains were selected as in (Perin et al. 2015), retaining only the pale mutants, generating a collection of 23 strains.

For those strains the reduction in Chl content was confirmed by growth curves in flasks. Among all strains isolated, SOB17 was particularly promising because of a strong reduction in total Chl content per cell (44% less than WT) as shown in fig 2-A. Chl a/b ratio was also increased, suggesting a selective reduction in Chl b (fig 2 A-B). Since in green algae Chl b is specifically bound to antenna complexes, this reduction suggests a specific depletion in these proteins, a property that should provide advantages in terms of productivity (De Mooij et al. 2014). In flasks SOB17 also showed a slightly reduced growth with respect to the WT, which instead is a negative property (fig 2-C).

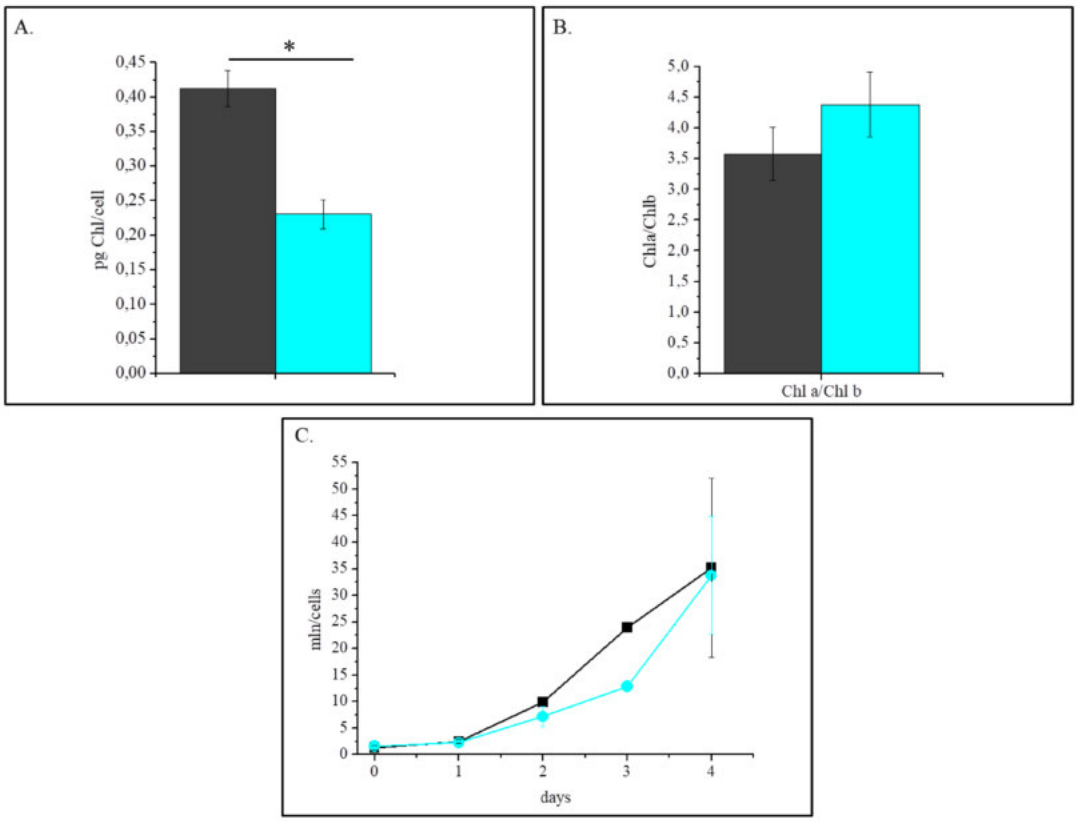

Figure 2: In A is reported the Chl in batch culture after 4 days of growth. In B is shown the Chl a/Chl b ratio. In C are reported the growth curves in batch system. In all the panels dark grey stands for WT and light blue for the mutant SOB17 (n=3). Statistically significant differences between WT and strain SOB17 are marked with an asterisk (one-way ANOVA, p-value < 0.05).

In order to evaluate the productivity potential of this strain and assess the impact of the genetic modification SOB17 was compared with WT in industrially relevant conditions. In particular we chose a flat panel photobioreactor with a 1.3 cm thickness. This system ensures a more homogeneous light distribution in the cultures. Indeed a high surface area to volume ratio has been recognized as a way to improve light distribution (Carvalho et al. 2011; Singh and Sharma 2012). This geometry has also an experimental advantage since it allows monitoring with higher precision the light passing through the culture.

This system was run in continuous mode, as described in fig 3 to obtain a stable culture conditions. In a continuous system the culture reaches a stationary state where biomass concentration is stable indefinitely and it has always the same characteristics for example in term of lipids and pigment composition.

Continuous cultures are constantly diluted with a fresh medium. Residence time is determined by the rate of this dilution, which defined the time that each cell stays in the photobioreactor before to be collected.

These residence times were selected taking in count the maximum growth rate reached in the same flat panel system run in batch. Indeed $1/\tau$ determines the growth rate necessary to sustain the continuous at the chosen residence time without the washout of the culture from the system. In batch experiment we determined that WT growth rate was 0.89 d^{-1} which means that the washout threshold is 1.12 days as residence time. SOB17 instead in batch has a growth rate of 0.79 d^{-1}, which leads to a washout threshold of 1.26 d.

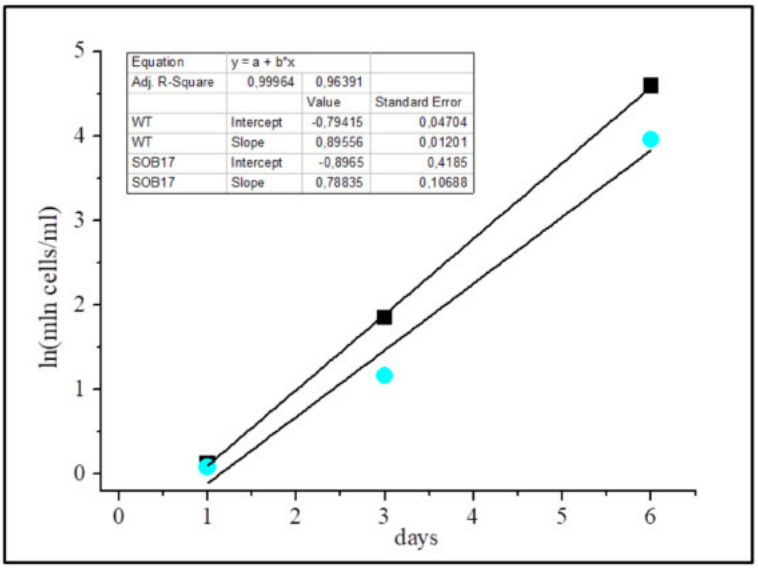

Figure 3: In this figure is reported the growth rate of WT(black) and SOB17(cyan) in the flat panel run in batch before to start the continuous. The growth rate is evaluated as the slope of line due to the natural logarithm of the cell concentration on days.

Considering strains growth, three different residence times (τ) were chosen to assess the effect of different biomass concentrations and light availability on productivity:

- 1.3 days;
- 2.6 days;
- 3.7 days;

One time was close to the washout limits (1.3 d) while the other were higher to obtain different biomass concentrations in the system. Cultivation experiments were run in total for more than 30 weeks using the same culture showing how in these conditions algae

culture can be extremely stable and it maintains a constant growth for a long time without interruption. The only drawback was that the mixing was not optimal and there was a small and undesired sedimentation of biomass in the angles of the reactors. This however did not affect the stability of the culture nor had a measurable impact on productivity.

In a continuous system each time that a residence time is set, the culture experienced a transitory phase of adaptation to the altered dilution rate with fresh medium. The duration of this transition was variable but at the end the culture reached a stationary state where growth corresponded to dilution rate and thus the biomass concentration was stable. In this phase the concentration of the biomass was stable indefinitely as shown in fig 4, in which is reported the OD_{750} measurement during transitory and stationary phase (blue square). In continuous cultures cells are always actively growing but at the same time they are exposed to stable environmental conditions and thus their properties like pigment content and photosynthetic efficiency remain stable during the time.

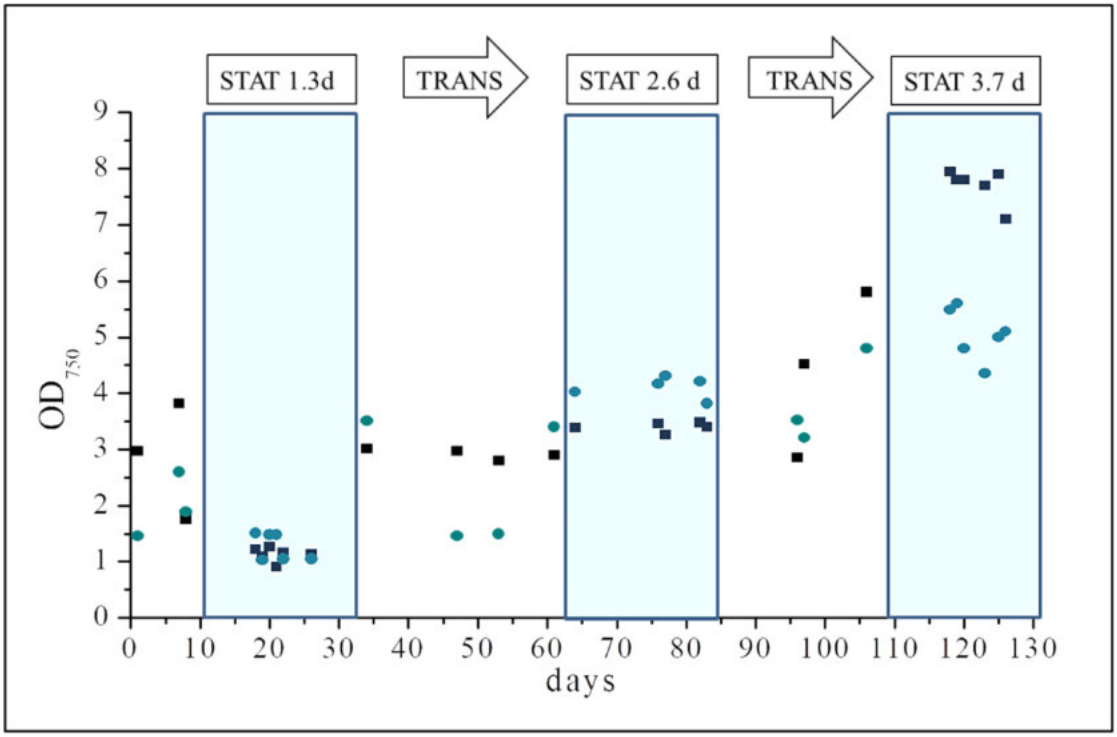

Figure 4: Experiment with continuous cultures. OD_{750} monitoring for the WT (dark squares) and SOB17 (light blue circles). STAT and the blue square marked the stationary phase at each residence time tested, instead TRANS marked the transitory phase from a residence time to another. For each stationary state are shown 6 points but we evaluated 10 points for each stationary state.

Each time that a stationary phase was reached we evaluated also the dry weight of the biomass by sampling for several days (10 days). At 1.3 d SOB17 biomass productivity

was equivalent to WT while at 3.7 d productivity was lower. At intermediate residence time 2.6 d SOB17 productivity was instead 20% higher with respect to the WT (fig 5).

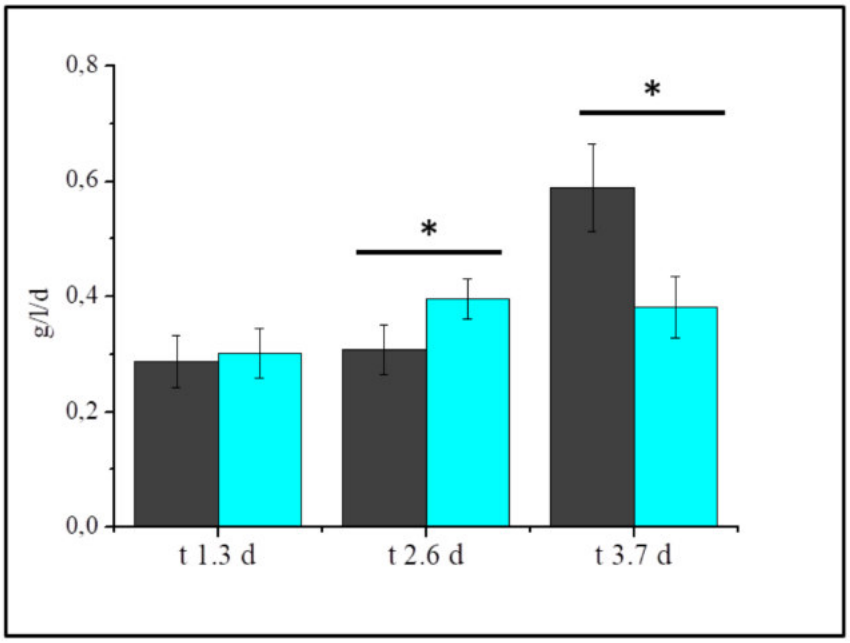

Figure 5: It is shown the productivity in terms of grams per liter per day. Dark grey stands for WT and light blue for the mutant SOB17 (n=10). Statistically significant differences between WT and strain SOB17 are marked with an asterisk (one-way ANOVA, p-value <0.05).

These results show that growing conditions have major impact on productivity and strain performances, consistently with what was discussed in Appendix 1. Considering this strong impact on productivity we investigated in more detail the acclimation response of WT and SOB17 to different growing conditions. In cultures 2.6 d and 1.3 d SOB17 showed a reduction in Chl content respect to the WT (fig 6-A). In 2.6 d this Chl reduction is accompanied also with a reduction in the ASII of the mutant that instead is not detectable in 1.3 d (fig 6-B).

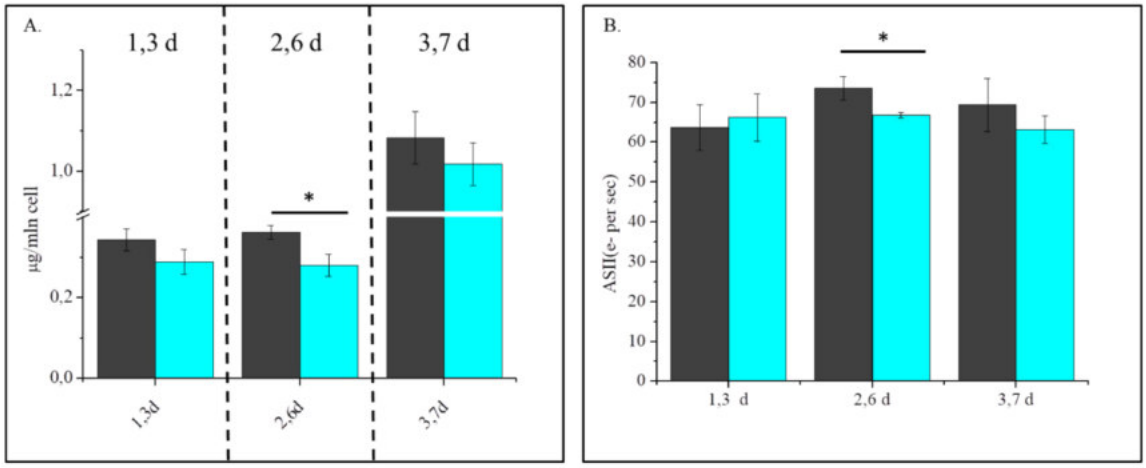

Figure 6: In A is shown the Chl content in the different residence time tested. In B is reported the ASII evaluation. In dark grey is marked the WT and in light blue the mutant SOB17 (n=4). Statistically significant differences between WT and strain SOB17 are marked with an asterisk (one-way ANOVA, p-value < 0.05).

DISCUSSION

SOB17 isolation was performed with the same approach described in (Perin et al. 2015), confirming the possibility of its application to different algae species. Among the strains isolated SOB17 was the most promising showing a particularly low Chl content. At the same time this strain also show a negative feature with a slightly impaired growth. This was clearly undesirable, it is indicative of the disadvantages of this approach, the accumulation of multiple mutations that can, in some cases, have negative effects.

The productivity performances of this strain were assessed in a continuous culture. This condition is particularly interesting because it reproduces an intensive culture system, which is emerging as promising cultivation mode applicable on a large scale production (Sforza, Gris, and Farias 2014). So a lab scale system like this can provide productivity estimations translatable on an industrial scale. Indeed these experiments provided excellent results in terms of stability since the culture was maintained for more than 30 weeks without interruption. Such a stability clearly would be an extremely valuable advantage for industrial cultivation, which needs to obtain a stable production.

The continuous experiment was conducted in a flat panel with 1.3 cm width. This geometry was chosen to have a good and homogeneous light penetration even at a higher concentrations. On the other hand this geometry caused some limitations in mixing efficiency that was provided by air bubbling and a magnetic stirrer. Despite this

combination mixing was not sufficient to maintain completely in suspension the culture because of *Scenedesmus* tendency to sediment. Clearly this is not an optimal condition since this biomass can influence productivity evaluations by for instance subtracting nutrients. In the future experiments thicker panels could possibly address this issue.

Despite these problems different residence time evaluations highlighted that also in this case as already described in Appendix 1 the acclimation response has a major effect on algae properties and productivity. With the higher residence time (3.7 d) cell concentration was higher and cells were light limited because of the shading effect. In this condition cells responded by increasing the Chl content per cell, both in WT and in SOB17. This increase had the final effect of canceling the mutant low Chl content phenotype, losing any advantage in light distribution. Since SOB17 had also a slower growth rate in these conditions the overall productivity in SOB17 was even lower than the WT. In 1.3 d cultures cell concentration was lower and SOB17 maintained the low Chl content but the advantage in light distribution and the growth impairment appeared to be balanced, yielding no net advantage or disadvantage. In fact in these conditions cells duplication rate is maximal to keep pace with the dilution rate, which is close to the washout threshold.

Instead at 2.6 d the advantage due the reduction in Chl content compensate the growth impairment of the mutant and it leaded also to an overall higher productivity for the mutant. This work with a completely different mutant and algal species confirms results reported in Appendix 1, suggesting that the operational conditions have a fundamental influence on performances of a mutant strain with a possible promising phenotype not only in *N.gaditana*. Moreover the use of a powerful tool like a flat panel continuous system to evaluate productivity results successful even if it is still possible to improve the geometry in order to enhance an efficient mixing.

REFERENCES

Bertucco, Alberto, Mariaelena Beraldi, and Eleonora Sforza. 2014. "Continuous Microalgal Cultivation in a Laboratory-Scale Photobioreactor under Seasonal Day – Night Irradiation : Experiments and Simulation." *Bioprocess and Biosystems Engineering* 37: 1535–42.

Bonente, Giulia et al. 2011. "Analysis of LHcSR3, a Protein Essential for Feedback de-Excitation in the Green Alga Chlamydomonas Reinhardtii." *PLoS Biology* 9(1):1-17.

Carvalho, Ana P, Susana O Silva, José M Baptista, and F Xavier Malcata. 2011. "Light Requirements in Microalgal Photobioreactors: An Overview of Biophotonic Aspects." *Applied microbiology and biotechnology* 89(5): 1275–88.

Chaudhary, Ramjee, Anil Kumar Dikshit, and Yen Wah Tong. 2017. "Carbon-Dioxide Biofixation and Phycoremediation of Municipal Wastewater Using Chlorella Vulgaris and Scenedesmus Obliquus." *Environmental Science and Pollution research*.

Gris, Barbara et al. 2014. "Cultivation of Scenedesmus Obliquus in Photobioreactors: Effects of Light Intensities and Light-Dark Cycles on Growth, Productivity, and Biochemical Composition." *Applied Biochemistry and Biotechnology* 172(5): 2377–89.

De Mooij, Tim et al. 2014. "Antenna Size Reduction as a Strategy to Increase Biomass Productivity : A Great Potential Not yet Realized." *Journal of Applied Phycology*.

Perin, Giorgio et al. 2015. "Generation of Random Mutants to Improve Light-Use Efficiency of Nannochloropsis Gaditana Cultures for Biofuel Production." *Biotechnology for biofuels* 8: 161-173.

Sforza, Eleonora et al. 2012. "Adjusted Light and Dark Cycles Can Optimize Photosynthetic Efficiency in Algae Growing in Photobioreactors." *PloS one* 7(6).

Sforza, Eleonora, Mattia Enzo, and Alberto Bertucco. 2013. "Chemical Engineering Research and Design Design of Microalgal Biomass Production in a Continuous Photobioreactor : An Integrated Experimental and Modeling Approach." *Chemical Engineering Research and Design* 92(6): 1153–62.

Sforza, Eleonora, Barbara Gris, and Carlos E De Farias. 2014. “Effects of Light on Cultivation of Scenedesmus Obliquus in Batch and Continuous Flat Plate Photobioreactor.” *Chemical Engineering Transactions* 38: 211–16.

Singh, R.N., and Shaishav Sharma. 2012. “Development of Suitable Photobioreactor for Algae Production – A Review.” *Renewable and Sustainable Energy Reviews* 16(4): 2347–53.

APPENDIX I :

Cultivation in industrially relevant conditions has a strong influence on biological properties and performances of *Nannochloropsis gaditana* genetically modified strains.

Authors name and affiliations

Giorgio Perin[2], Diana Simionato[1], Alessandra Bellan[1], Michele Carone [1,4], Massimo Emilio Maffei [3,4], Tomas Morosinotto[1]

1-PAR-Lab_Padua Algae Research Laboratory, Department of Biology, University of Padova, Via U. Bassi 58/B, 35121 Padova, Italy.

2- Department of Life Sciences, Imperial College London, Sir Alexander Fleming Building, London, SW7 2AZ, UK

3-Biosfered S.r.l., Innovation Centre, Academic Spin-Off of the University of Turin, Via Quarello 15/A, Turin 10135, Italy

4-Department of Life Sciences and Systems Biology, Innovation Centre, University of Turin, Via Quarello 15/A, Turin 10135, Italy

THIS CHAPTER WAS PUBLISHED IN ALGAL RESEARCH JOURNAL (2017)

The format is different from the main chapters because it is that one required by the journal.

CONTRIBUTION:

AB provided a contribution in DW and PAM analysis.

ABSTRACT

Microalgae are promising feedstocks for the production of biofuels thanks to their high biomass yield and the lack of competition with food crops for arable land. Algal industrial exploitation, however, still needs to address several technological challenges to reach energetic and economic sustainability. Genetic improvement of microalgae strains is seminal to fully exploit the potential of these organisms.

In this work, we investigated how key environmental parameters affected productivity of a promising genetically modified algal strain cultivated in industrially relevant conditions. We observed that intensive growth conditions strongly influenced algae biology, as evidenced by molecular and functional analyses. We also showed that specific operational conditions significantly affected performances, enhancing or reducing the advantages of the strains genetic modification, such as the chlorophyll content per cell and the abundance of photosynthetic apparatus components.

This work demonstrates the presence of a strong influence of cultivation environment on the phenotype of improved strains, suggesting that operational parameters have a seminal influence on algae performances and must be taken into full account during strains development efforts.

KEYWORDS

Photosynthesis; biomass productivity; *Nannochloropsis*; microalgae; genetic engineering; photobioreactor.

LIST OF ABBREVIATIONS

Abbreviations used are: AEF, alternative electron flow; AS, antenna size; Car, Carotenoids; CEF, cyclic electron flow; Chl, Chlorophyll; DBMIB, dibromothymoquinone; DCMU, 3-(3,4-dichlorophenyl)-1,1-dimethylurea; ECS, electrochromic shift; EMS, Ethyl Methane Sulfonate; ETR, Electron Transport Rate; GC-FID, gas-chromatography coupled to a flame ionization detector; GC-MS, gas-chromatography coupled to mass spectrometry; HA, hydroxylamine; Lab, laboratory; FA, fatty acid; FAME, fatty acid methyl esters; LHC, Light Harvesting Complex; MV, methyl

viologen; NPQ, Non-Photochemical Quenching; PE, photosynthetic efficiency; PBR, Photobioreactor; PS, Photosystem; RT, room temperature; ROS, Reactive Oxygen Species; TAG, triacylglycerol; TEF, total electron flow; WT, Wild Type.

INTRODUCTION

The current global economy strongly relies on fossil fuels that are responsible for a massive release of greenhouse gases in the atmosphere with detrimental effects on the climate and environment [1–3]. The development of renewable and clean energy sources to mitigate the effects of the intensive exploitation of fossil fuels is thus an unavoidable challenge for our society. The exploitation of microalgae biomass as a source of energy and materials could provide a valuable contribution [3,4] thanks to these organisms high efficiency in the fixation of carbon dioxide *via* photosynthesis [5]. Some species of algae are indeed able to accumulate high amounts of triacylglycerols (TAGs), which are convertible into biofuels [6–9]. Algae cultivation can also be combined with wastewater treatment [10] or with the sustainable production of valuable molecules (e.g. pigments, food additives [11–13]) that, coupled with the energy production, could enhance overall environmental benefits and the economic balance.

Despite these advantages, the industrial potential of algae is far from being fulfilled. One of the major limitations is that the potential of these organisms is not fully exploitable using wild type (WT) strains isolated in nature that do not reach their maximal productivity in artificial cultivation systems [14]. The industrial exploitation of algae biomass thus requires efforts in strains improvement or domestication as well in the selection of specific genetic features that are advantageous for the cultivation in intensive conditions [15–17].

One of the main factors influencing algae productivity is the sunlight fueling photosynthetic metabolism. Despite being highly abundant, in fact, sunlight is distributed on large surfaces and algae growth is often limited by the available irradiance [18]. The improvement of light energy to biomass conversion efficiency is therefore seminal to increase the productivity of algae industrial cultivation and make it economically and energetically sustainable [19]. As example, light-use efficiency of algae in photobioreactors (PBRs) is strongly influenced by the inhomogeneous distribution of light in the culture due to cells self-shading. In these conditions, cells exposed to full

sunlight easily experience saturating irradiation while the rest of the culture is under limiting illumination conditions, reducing overall light-use efficiency [19].

One possibility to improve light-use efficiency for algae in PBRs is to tune their photosynthetic properties and optimize them to cultivation in intensive growth conditions. Microalgae evolved in a natural environment that was often limited by light availability and their ability to absorb photons is increased by pigment binding proteins called antennas, that enhanced their competitiveness with other organisms [18]. In a PBR culture, however, such a competition for light is instead detrimental for overall productivity and the reduction of cells antenna content has been suggested as a strategy to improve algae growth performances [14,20]. In the past few years, several efforts have been made to alter composition and/or regulation of the photosynthetic apparatus [21,22], and succeeded in isolating strains with a higher maximum photosynthetic rate in lab scale evaluations. This work was mostly performed in the model genus *Chlamydomonas reinhardtii* [23–28] but also in a few other species of industrial interest [17,29–31].

Despite promising achievements at the lab scale, improved strains produced contrasting results when tested in larger scale PBRs [31,32]. A clear understanding of how the artificial environment of cultivation affects algae productivity is indeed still missing, affecting the ability to predict which phenotypes isolated in the lab can lead to higher productivities in PBRs. In order to address this limitation, we used a *Nannochloropsis gaditana* strain altered in specific photosynthetic properties (strain E2) and showing improved productivity [17], to assess the impact of operational parameters in intensive growth conditions. We observed that intensive operational conditions have an extensive biological effect on algae and strongly influence E2 strain performances, by either enhancing or masking the advantages of the genetic modification. Our results demonstrate that the intensive environment of cultivation has a strong influence on improved strains phenotype, suggesting the need to take the former into full account during strain development and evaluation.

MATERIAL AND METHODS

Culture conditions and growth determination.

Strains used in this work. Nannochloropsis gaditana, strain 849/5, from the Culture Collection of Algae and Protozoa (CCAP) were used as the WT strain. A random mutagenesis was performed as previously described [17], and the E2 strain tested here was isolated among a pool of ethyl methane sulfonate (EMS) treated mutants, consequently selected for altered photosynthetic performances. In brief, *Nannochloropsis gaditana* strain CCAP 849/5 was mutagenized with EMS. 5000 colonies were collected and screened with a FluorCam FC 800 imaging apparatus (Photons Systems Instruments, PSI, Brno, Czech Republic) to identify strains showing alterations in photosynthetic apparatus. Among them, strain E2 was selected for a 45% reduction in Chl / cell content upon cultivation in flasks.

Cultivation conditions.

Algae were maintained in F/2 solid media, with 32 g/L sea salts (Sigma Aldrich), 40 mM Tris-HCl (pH 8), Guillard's (F/2) marine water enrichment solution (Sigma Aldrich), 1 % agar (Duchefa Biochemie). Cells were pre-cultured in sterile F/2 liquid media in Erlenmeyer flasks irradiated with 100 µmoles photons m^{-2} s^{-1} (illumination rate was determined using the LI-250A photometer (Heinz-Walz, Effeltrich, Germany)) and 100 rpm agitation at 22 ± 1 °C in a growth chamber. In this work, we refer to this condition of cultivation as the flask condition.

Semi-continuous cultures starting from high biomass concentrations (> 1 g/L) were performed in 5 cm diameter Drechsel bottles, illuminated from one side, with a 250 ml working volume and bubbled using air enriched with 5 % CO_2 (v/v), at a total flow rate of 1 L/h (for bubbling apparatus set-up see [33]) (Figure 1A and supplementary figure S1).

In this case, F/2 growth media was enriched with added nitrogen, phosphate and iron sources (0.75 g/L $NaNO_3$, 0.05 g/L NaH_2PO_4 and 0.0063 g/L $FeCl_3$•6 H_2O final concentrations). In this work we refer to these growth conditions as intensive cultivation conditions, simulating what happens in industrial PBRs. Constant illumination was provided by a white LED light source SL 3500 (Photons Systems Instruments, PSI, Brno, Czech Republic). The pH of the semi-continuous cultures was set to 8.00 and fresh media was added every other day to restore the starting cell concentration (Figure 1B and C).

The light transmitted by the cultures was measured using LI-250A photometer (Heinz-Walz, Effeltrich, Germany) with a circular probe thus detecting also scattering. Transmitted light was sampled in 9 different points to obtain an average value.

Analytical procedures and energy balance.

Algal growth was monitored using a cell counter (Cellometer Auto X4, Nexcelom Bioscience) and by evaluation of biomass concentration (dry weight), measured gravimetrically as previously reported in [17]. The specific growth rate was calculated by the slope of logarithmic phase for the number of cells. Biomass productivity was calculated as $([C_f] - [C_i]) / (t_f - t_i)$, where C is the final or initial dried biomass concentration of the culture and t is the number of days.

The photosynthetic efficiency (PE) of semi-continuous cultures (expressed as percentage of the Photosynthetic Active Radiation (PAR)), which represents the fraction of received light energy converted into biomass, was calculated according to the following equation:

$$PE = \frac{P_x \cdot V_{PBR} \cdot LHV}{PFD_{abs} \cdot E_p \cdot A_{PBR}}$$

where P_x is the biomass productivity of the algae strains used in this work (g L^{-1} d^{-1}), V_{PBR} is the volume of the culture (L), LHV is the lower heating value of the dry microalgae (assumed equal to 22.2 kJ/g, [34]), PFD_{abs} is the PAR photon flux density absorbed by the culture (μmoles photons/ m^{-2} s^{-1}), E_p is the energy of photons (kJ/μmoles photons) and A_{PBR} is the irradiated surface of the reactor (m^2). In addition, the specific light supply rate per unit mass of cell r_{Ex} (mmoles photons g^{-1} d^{-1}) in the growth conditions of this work was calculated, according to [34], as:

$$r_{Ex} = \frac{PFD_{abs} \cdot A_{PBR}}{C_x \cdot V_{PBR}}$$

where C_x is the starting biomass concentration inside the culture (g L^{-1}) and all the other mentioned parameters were described above.

Pigments extraction

Pigments were extracted from cells grown in semi-continuous conditions, during active growth. Chlorophyll a and total carotenoids were extracted from intact cells, using a 1:1 biomass to solvent ratio of 100 % N,N-dimethylformamide (Sigma Aldrich) [35], at 4 °C in the dark, for at least 24 h. Absorption spectra were registered between 350 and 750 nm using a Cary 100 spectrophotometer (Agilent Technologies) to determine pigment concentrations, using specific extinction coefficients [36,37].

High-pressure liquid chromatography (HPLC) analyses were carried out to determine the individual carotenoids content of the cells. Pigments were extracted from cells lysed using a Mini Bead Beater (Biospec Products) at 3500 RPM for 20 s in the presence of glass beads (150 – 212 μm diameter, Sigma Aldrich) and 80 % acetone. HPLC analyses were performed using a Beckman System Gold instrument equipped with a UV-VIS detector and a C-18 column (25 cm by 4.6 mm; Zorbax octyldecyl silane). Runs were performed using 86.7 % acetonitrile, 9.6 % methanol and 3.6 % Tris-HCl, pH 7.8 and then 80 % methanol and 20 % hexane as elution solvent. The peaks of each sample were identified through the retention time and absorption spectrum [38] and quantified as described previously [39]. The vaucheriaxanthin retention factor was estimated by correcting that of violaxanthin for their different absorption at 440 nm.

Thylakoids isolation

Intact thylakoids from *N. gaditana* cells were extracted according to the protocol previously described in [40], performing all the steps at 4 °C and at dim light. The thylakoids in the appropriate buffer were immediately frozen in liquid nitrogen and stored at −80 °C until further use. Total pigments were extracted using 80 % acetone, and the chlorophyll concentration of the samples was determined spectrophotometrically as described above.

Fluorescence measurements

Photosynthetic performances estimation. Photosynthesis monitoring was performed by measuring *in vivo* Chl fluorescence using a PAM 100 fluorimeter (Heinz-Walz, Effeltrich, Germany). PSII functionality was expressed as PSII maximum quantum yield (ϕ_{PSII}), according to [41].

PSII functional antenna size evaluation. PSII antenna sizes were determined for semi-continuous cultures in active growth conditions, using a JTS-10 spectrophotometer (Biologic, France). Samples (200 x 10^6 cells/ml final concentration) were dark-adapted for 20 minutes and incubated with 80 µM 3-(3,4-dichlorophenyl)-1,1-dimethylurea (DCMU) for 10 minutes. Fluorescence induction kinetics were then monitored upon excitation with 320 µmoles photons m^{-2} s^{-1} of actinic light at 630 nm. The $t_{2/3}$ values obtained from the fluorescence induction curves were used to calculate the size of the PSII functional antenna [17,42].

Spectroscopic analysis

All the following spectroscopic analyses were performed using a JTS-10 spectrophotometer (Biologic, France).

Electrons flows estimation. The spectroscopic quantification of the electrons which flow through the photosynthetic electron transport chain was performed measuring P_{700} (the primary electron donor to PSI) absorption at 705 nm in intact cells. Analyses were conducted exposing the samples (300 x 10^6 cells/ml final concentration) to saturating actinic light (2050 µmoles photons m^{-2} s^{-1}, at 630 nm) for 15 seconds to maximize P_{700} oxidation (P_{700}^+) and reach a steady state. Then the light was switched off to follow the P_{700}^+ re-reduction kinetic in the dark for 5 seconds.

The total electron flow (TEF), namely the sum of all the electron transport processes through PSI, was calculated from the monitoring of the P_{700}^+ re-reduction rates after illumination in untreated cells. The electron transport rate was calculated assuming a single exponential decay of P_{700}^+. This allowed calculating the rate constant of P_{700}^+ reduction as $1/\tau$. By multiplying the rate constant with the fraction of oxidized P_{700} (comparing DCMU- and dibromothymoquinone (DBMIB)-poisoned cells, see below for concentrations details), and considering this value as 1 in DCMU- and DBMIB-treated cells (see below) we could evaluate the number of electrons transferred per unit of time per PSI unit [43].

The same procedure was followed to evaluate the contribution of cyclic electron flow (CEF), in samples treated with DCMU (80 µM), and to measure any possible residual electron injection into PSI, with DCMU in combination with DBMIB (300 µM).

PSI content. The total PSI content was evaluated from the maximum change in the absorption of P_{700}^+ in cells treated with DCMU (80 µM) and DBMIB (300 µM) at a

saturating actinic light (2050 µmoles photons m^{-2} s^{-1}, at 630 nm). Under these conditions, re-reduction of P_{700}^{+} through photosynthetic electron flow is largely slowed down, allowing to evaluate the full extent of photo-oxidizable P_{700} [43,44]. The treatment was previously assessed to completely oxidize P_{700} [45].

PSI antenna size evaluation. The PSI antenna size was assessed by measuring the rate constant of P_{700} oxidation kinetics at 705 nm in isolated dark-adapted thylakoids (40 µg of Chl) incubated with methyl viologen (MV) (375 µM) and ascorbate (2 mM) for 5 min. The photo-oxidation kinetics was measured upon excitation with 150 µmoles photons m^{-2} s^{-1} of actinic light at 630 nm [42,46].

Photosynthetic complexes amount evaluation. Changes in the amount of functional photosynthetic complexes were evaluated after measuring the electrochromic shift (ECS) spectral change in intact cells (200 x 10^6 cells/ml final concentration), representing a shift in the pigment absorption bands associated with changes in the membrane potential. Data were collected as the difference between the signals at 520 and 498 nm (which represent the positive and negative peaks of the ECS signal in *Nannochloropsis* cells, respectively) to deconvolute this signal from other spectral changes not related to the building of the transmembrane potential [47]. The PSII contribution to this shift was evaluated by poisoning the algae with DCMU (80 µM) and hydroxylamine (HA) (4 mM). PSI contribution was instead estimated as the fraction of the signal that was insensitive to these inhibitors.

<u>*Lipids analysis*</u>

Nile-Red staining. The neutral lipid content was determined by staining cells (2 x 10^6 cells in 1.9 ml final volume of deionized water) with Nile Red dye, 2.5 µg/mL final concentration, for 10 min at 37 °C. The fluorescence was measured using a spectrofluorimeter (OLIS DM45) with excitation wavelength at 488 nm and emission wavelength range between 500 and 700 nm. The relative fluorescence of Nile Red for the neutral lipids was obtained by subtracting the auto-fluorescence of the cells and Nile Red alone.

Fatty-acids profile. Total lipids were extracted from lyophilized samples, preserved in liquid nitrogen. Pellet were then broken with a pestle to facilitate lipids extraction and the transesterification reaction. The latter was performed in glass tubes. Samples (5-10 mg) were weighed with an analytical scale (Crystal 300 CAL, Gibertini) and 0.5 ml of boron

trifluoride (10 % w/v in methanol) (Fluka), 50 µg of nonadecanoic acid (C19:0) (1 mg/ml in hexane) (FA-FAME kit 14, Supelco, USA) were added as internal standards. Samples were mixed vigorously for 30 seconds and then extracted in an ultrasonic bath (Ultrasonic cleaner, VWR), for 15 min at room temperature (RT). Samples were then transferred to 80 °C for 1 h. Fatty acid methyl esters (FAME) were purified through liquid-liquid purification, adding 0.5 ml ultrapure water (Simplicity 185, Millipore) and 0.5 ml hexane (GC-grade VWR). Samples were mixed vigorously to induce FAME extraction in the hexane phase. This procedure was repeated twice. The non-polar fraction was further purified and dehydrated through an anhydrous $MgSO_4$ (Sigma-Aldrich) purification column. FAME identification was performed by gas-chromatography coupled to mass spectrometry (GC-MS) (5975T, Agilent Technologies, USA). FAME quantitative analyses were performed through by GC coupled to a flame ionization detector (GC-FID) (GC-2010 Plus, SHIMADZU, Japan). The GC carrier gas was helium with a constant flux of 1 ml/min, and separation was obtained with a non-polar capillary column ZB5-MS (30 m length, 250 µm diameter and stationary phase thickness of 0,25 µm, 5 % phenyl-arylene and 95% of poly-dimethyl siloxane stationary phase) (Phenomenex, USA). GC-FID FAME separation was performed in the same conditions, by using a similar column. Mass spectrometer parameters were: ionization energy of the ion source set to 70 eV and the acquisition mode set to 50-350 m/z. Separated molecules were identified through comparison of mass fragmentation spectra with reference spectra of the software NIST v2.0 and libraries NIST 98, by comparison of Kovats indexes and the internal standard injection (C17 – Sigma-Aldrich, C20:4, C20:5 - Supelco, USA). FAME quantification was realized by using nonadecanoic acid (C19) as internal standard. At least three biological replicates were run for each sample.

Statistical analysis

Descriptive statistical analysis with mean and standard deviation was applied for all the data reported in this work. Statistical significance was evaluated by one-way analysis of variance (One-way ANOVA), applied using the OriginPro 8 software (http://www.originlab.com/). Samples size was > 40 for all the measurements performed in this work.

RESULTS

Nannochloropsis gaditana lab-scale intensive cultures.

The performances of *Nannochloropsis gaditana* WT and E2, a strain altered in the photosynthetic apparatus [17], were evaluated in lab-scale PBRs. Cultures were operated in semi-continuous mode (Figure 1B) restoring the starting cell concentration every other day by substituting part of the culture with fresh media (Figure 1B and 1C, see Methods for details).

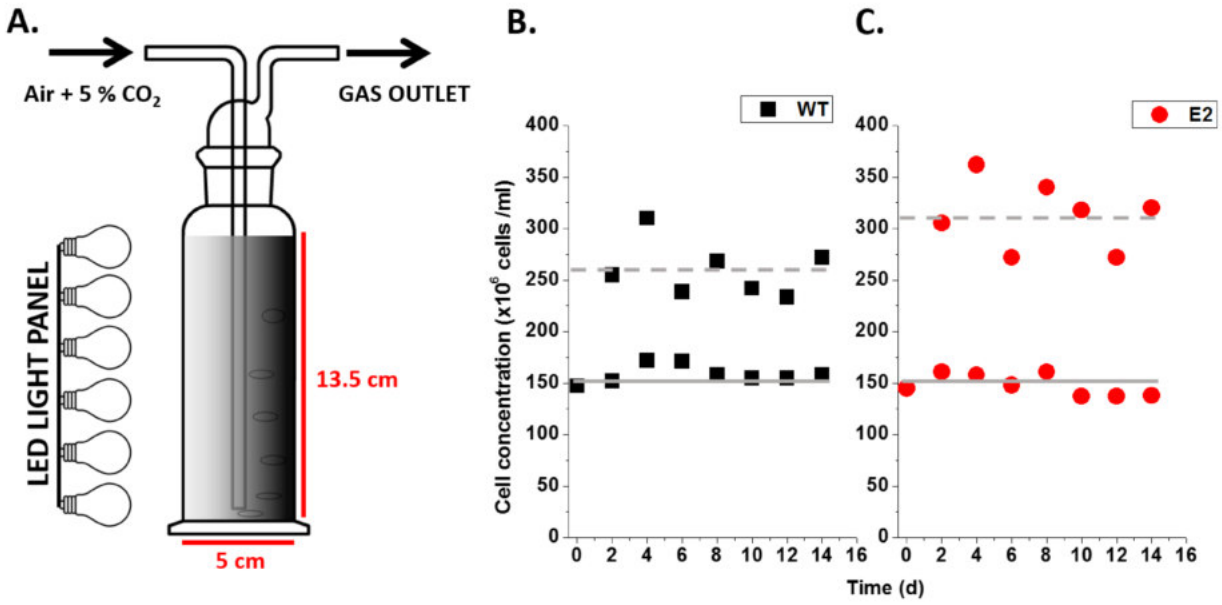

Figure 1. Growth evaluation of *Nannochloropsis gaditana* strains in lab-scale PBR. A) Scheme of lab-scale cultures exploited in this work. Lab-scale systems were chosen to simulate the geometry of a tubular PBR [48]. Cultures were continuously (24 h / 24 h) illuminated only from one side with 400 µmol photons m^{-2} s^{-1} to generate a light gradient, as expected in an outdoor system. Cultures were run in semi-continuous mode to maintain actively growing cells in a high-density culture. B-C). WT and E2 cultures started at equal cell concentration (in the example shown, 150 x 10^6 cells/ml - corresponding to approx. 1 g/L of biomass concentration, see also supplementary figure S1) and this value was restored every other day by diluting the culture with fresh media. The average values of cellular concentration determined before and after dilution are shown respectively as dashed and solid lines (8 points out of a total of 27 are shown).

We chose this cultivation method to maintain cells actively growing in stable environmental conditions, in order to reliably assess growth performances and biological properties of the strains. The fact that cells were maintained actively growing was demonstrated by monitoring cells growth rate either after 2 or 3 days of cultivation. As

shown in Supplementary Table S1 growth rate was undistinguishable suggesting that growth was not limited. A further advantage of this approach is that it allows working at high cell concentrations to simulate the growth conditions achieved in industrial cultivation systems [49], with the consequent inhomogeneous light distribution in the culture (Figure 1A). Nutrients (nitrogen, phosphate and iron particularly) were provided in excess, as well as the CO_2 (Figure 1A), to ensure that the biomass productivity depended mainly from strains light-use efficiency.

The effect of a different light availability on *N. gaditana* cultures productivity was assessed by changing the illumination intensity and cell concentration. The light transmitted through the culture in both WT and E2 strains was also measured (see 2.1.2 for details and Supplementary Figure S2), allowing for the calculation of the light supply rate per unit mass of cell (r_{Ex}) in different conditions [34]. Three conditions with increasing light supply rates of respectively 500, 700 and 1500 mmoles photons (g biomass)$^{-1}$ d^{-1} (hereafter named CI, CII and CIII), were chosen for a deeper analysis.

Biomass productivity and fatty acids content in lab-scale intensive cultures

WT and E2 were maintained in semi-continuous cultivation described above for ≈ 9 months (approximately 3 months for each of the 3 growth conditions here tested), repeating the cultivation cycle twice for both strains, starting from a pre-inoculum in flask. Results obtained from the two cycles showed no distinguishable differences and all data for each growth condition were eventually pooled together.

The parental WT strain showed a similar biomass productivity when cultivated in the two lower light supplies (CI and CII, 500 and 700 mmoles photons (g biomass)$^{-1}$ d^{-1}, respectively). Biomass productivity was instead higher when light supply rate was increased further in CIII (Figure 2A, one-way ANOVA, p-value < 0.05).

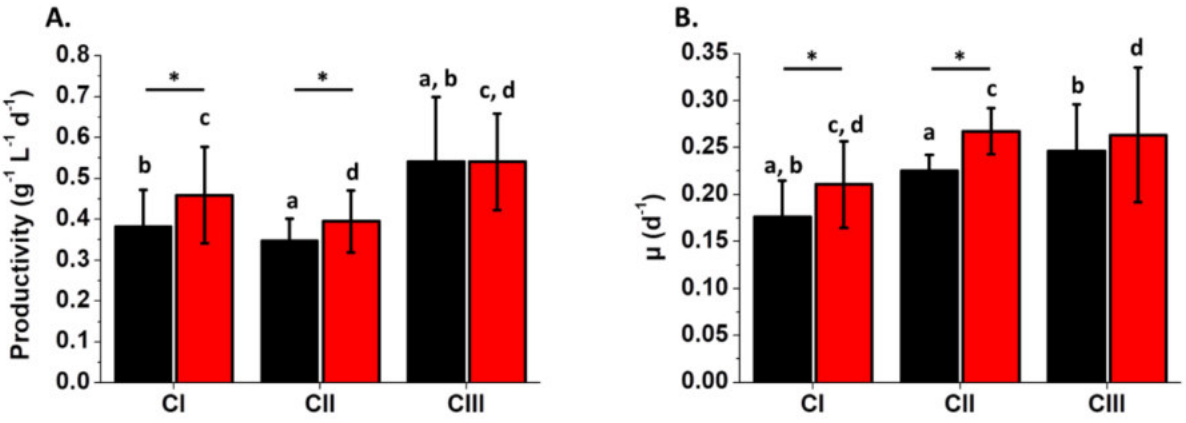

Figure 2. Biomass productivity and specific growth rates (μ) for *Nannochloropsis gaditana* WT and E2 strains cultivated in lab-scale PBR. Biomass productivity (g L^{-1} d^{-1}) obtained from semi-continuous cultures exposed to increasing light supply rates (CI < CII < CIII) is presented in A. The specific growth rate (μ) (d^{-1}) calculated for strains in the same growth conditions is shown in B. Data are expressed as the average ± SD (n > 40). Statistically significant differences between WT (black) and strain E2 (red) are marked with an asterisk, while the same alphabet letter indicates statistically significant differences for the same strain in different growth conditions (one-way ANOVA, p-value < 0.05).

Mutant strain E2 showed a similar trend of biomass productivity between the different conditions, with the highest observed in CIII. Strain E2 showed an improvement in biomass productivity of 22 and a 14 % (achieving an overall dry weight gain of 0.08 and 0.05 g L^{-1} d^{-1}, respectively) in CI and CII when compared to the WT cultivated in the same conditions (Figure 2A). This was also confirmed by calculating its specific growth rate (μ), which in CI and CII showed respectively an increase of 20 and a 18 % with respect to the WT (Figure 2B). With the highest light supply rate tested, instead, strain E2 did not show any increase in biomass productivity (Figure 2A) nor in specific growth rate with respect to the parental strain (Figure 2B). These data thus demonstrate that the selected strain is indeed able to increase the biomass productivity of *N. gaditana* cultures in multiple intensive cultivation conditions, but also that this advantage is strongly influences by the growth environment.

The biomass productivity values were also exploited to calculate the photosynthetic efficiency (PE) of the cultures (Table 1), expressed as percentage of the light energy absorbed that is converted into biomass. The highest PE was observed in CI and CII for both strains while in CIII we observed the lowest values. This is expected considering that the observed ≈ 50 % increase in biomass productivity (increasing the overall biomass yield of 0.16 g L^{-1} d^{-1}, Figure 2A) was obtained with a 2.5 times stronger illumination. In

both CI and CII strain E2 showed a higher PE than the WT (Table 1) while this was the same in CIII

Table 1. Photosynthetic efficiency (PE) of *Nannochloropsis gaditana* WT and E2 strains.
The calculated PE (ratio between energy stored as biomass produced and light absorbed by the culture) is expressed as percentage of the photosynthetic active radiation (PAR). Data are expressed as the average ± SD (n > 40). Statistically significant differences between WT and strain E2 are marked with an asterisk, while the same alphabet letter indicates statistically significant differences for the same strain in different growth conditions (one-way ANOVA, p-value < 0.05).

	CI		CII		CIII	
	WT	E2	WT	E2	WT	E2
PE (% PAR)	4.42 ± 0.85^{*,a}	5.41 ± 1.21^{*,c}	3.84 ± 0.59^{*,b}	4.38 ± 0.84^{*,d}	2.01 ± 0.59^{a,b}	2.01 ± 0.44^{c,d}

In order to rationalize the differences in biomass productivity and PE so far observed, we estimated a simplified distribution of light in the cultures for both strains, measuring the light transmitted by the culture (Supplementary figure S2) and assuming the light absorption followed the Lambert- Beer law [50] (Figure 3). In the case of WT, *Nannochloropsis* cells have the highest biomass productivity when exposed to over 50 µmoles photons m^{-2} s^{-1} [51]. Area exposed to this illumination is the largest in CIII (Figure 3C), thus explaining its high biomass yield. In CIII a large fraction of the culture is also exposed to saturating light (> 150 µmol photons m^{-2} s^{-1}), explaining its lower photosynthetic efficiency.

Light distribution in the culture allowed also explaining the observed different performances between the two strains since in both CI and CII E2 has a lower fraction of the culture exposed to light intensity below the compensation point, 5 µmoles photons m^{-2} s^{-1}, where photosynthesis is slower that respiration and the culture is not productive (Figure 3).

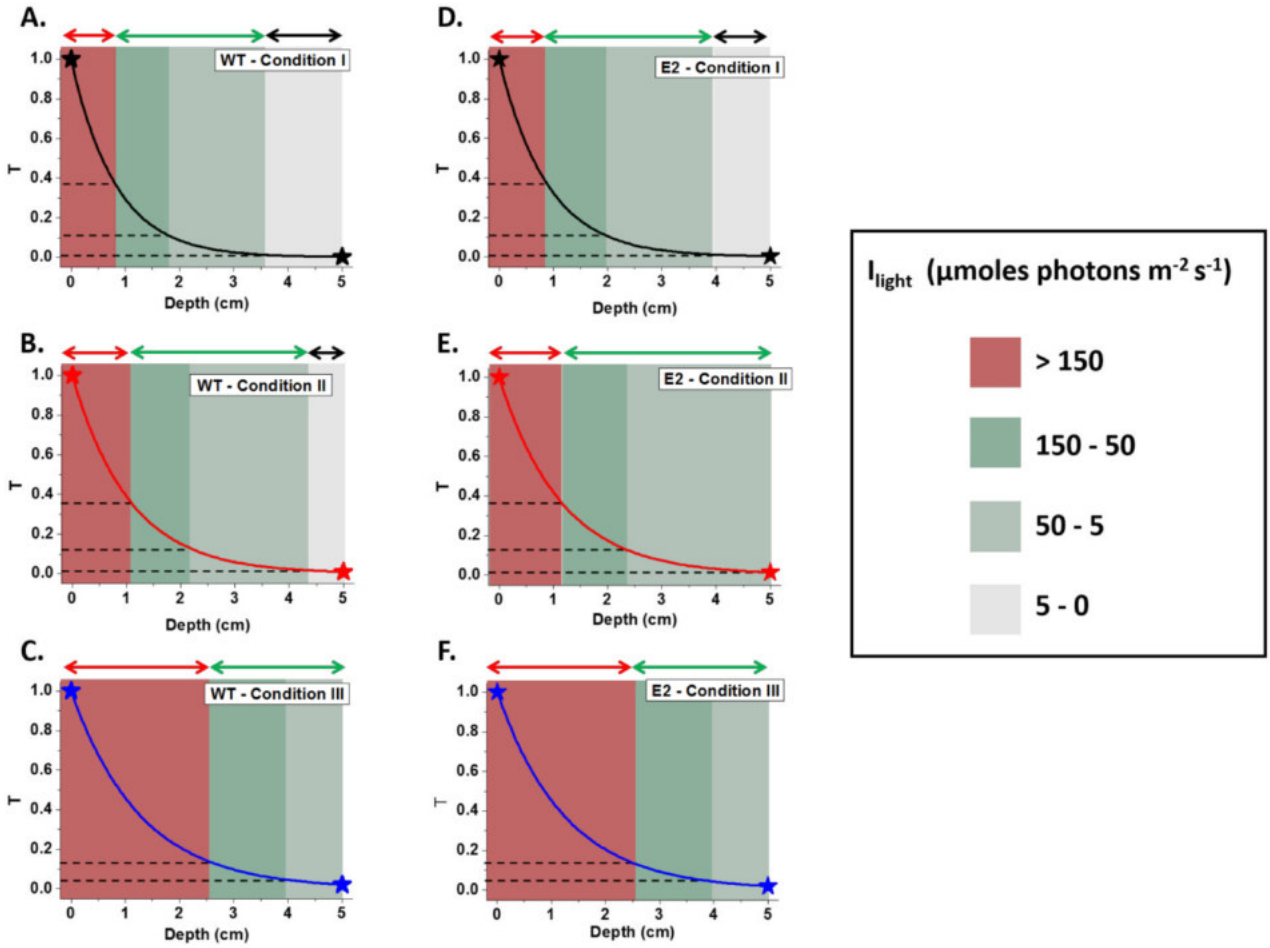

Figure 3. Light attenuation profile for *Nannochloropsis gaditana* WT and strain E2 cultivated in intensive conditions. The light intensity attenuation profile (expressed as transmittance (T), the ratio between transmitted/incident light intensities), according to the culture depth (expressed in centimeters, cm) for the WT (A, B and C) and the E2 strain (D, E and F), cultivated in intensive conditions with increasing light supply rates (CI in A) and D), CII in B) and E) and CIII in C) and F)), is here shown. Light attenuation profile inside the culture was estimated using the Lambert-Beer law and it was calculated from the values of transmitted light intensity measured after 5 cm of culture (values are reported in supplementary figures S2). Graphs are divided in areas of different colors, according to the light intensity reaching cells populating specific culture layers. Red, regions at high biomass productivity and low PE; Dark green, regions at high biomass productivity and high PE; Light green, regions at low biomass productivity and high PE; grey, regions at biomass consumption and negative productivity. Double arrows above the graphs indicate culture regions at low (red and black) or high light-use efficiency (green).

Lipids productivity was also evaluated in the same cultures along with biomass. WT strain showed a 17 % total fatty acids content (w/w biomass) in CI and CII (Figure 4A).

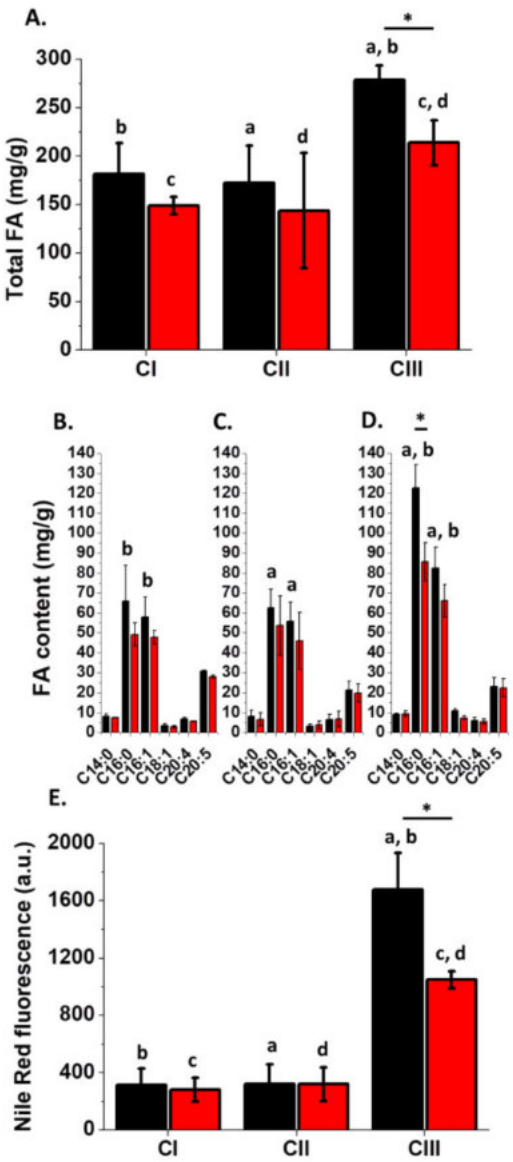

Figure 4. Effect of the growth conditions on lipids content of *Nannochloropsis gaditana* WT and E2 strains. A) Total fatty acids (FA) content, expressed as mg/g of biomass, for WT (black) and E2 (red) strains in CI, CII, CIII. B-D) Fatty acids composition of the cells in the three growth conditions. Only the most abundant FAs are shown here but the complete datasets are shown in supplementary Table S2. CI, CII and CIII are shown in B, C and D respectively. E) Neutral lipids accumulation quantified from the fluorescence of Nile Red-stained cells, normalized to the same cell number (a.u., arbitrary units, see methods for details). Data are expressed as average ± SD (n = 12). Statistically significant differences between WT and strain E2 are marked with an asterisk, while the same alphabet letter indicates significant differences for the same strain in different growth conditions (one-way ANOVA, p-value < 0.05).

This value increased up to the 27 % (w/w biomass) with the highest light supply (CIII, Figure 4A), suggesting stronger illumination stimulates lipids accumulation [52]. E2 showed the same total fatty acids content than the WT strain in CI and CII (Figure 4A),

suggesting lipids biosynthesis is not affected by its genetic modification. Lipids content was however lower in CIII (Figure 4A), suggesting in this strain light excess had a smaller effect in inducing lipids biosynthesis. It should be mentioned that the difference in lipid content between the strains in CIII has an influence on the energy content of the cells (in this work assumed equal to 22.2 kJ/g, [34]) and thus also influences PE estimations presented in table 1.

The analysis of the fatty acid methyl esters (FAME) profile of the cultures showed no significant differences between the two strains, with C16:0 representing the main fatty acid (FA) followed by C16:1, C20:5 and C14:0, respectively (see figure 4B and 4C and supplementary Table S2). A decrease in C16:0 content was observed in E2, but only in CIII, explaining the total FA reduction previously observed (Figure 4D and supplementary Table S2). Since in *N. gaditana* cells C16:0 and C16:1 are the major constituents of TAGs [52–54], this observation suggested a reduction in reserve lipids in CIII. This was confirmed by quantifying the neutral lipids fraction from the fluorescence of Nile Red-stained cells, which showed that E2 indeed had a reduction in neutral lipids content with respect to the WT in CIII (Figure 4E).

Photosynthetic apparatus composition is modulated by intensive growth conditions

Results presented above suggest that cultures productivity is largely determined by how the intensive environment influence algae light-use efficiency, thus we decided to investigate the molecular bases of these results by evaluating the properties of photosynthetic machinery of the different cultures.

Table 2. Chlorophyll content of *Nannochloropsis gaditana* WT and E2 strains in different growth conditions. **Chlorophyll a values (picograms per cell – pg/cell) for *N. gaditana* WT and E2 are reported for the different growth conditions tested in this work. Data are compared to cultures in flask conditions collected during the screening [17]. Data are reported as average ± SD (n = 24). Statistically significant differences between WT and E2 are marked with asterisks, while the same alphabet letter indicates significant differences for the same strain in different growth conditions (one-way ANOVA, p-value < 0.05).**

	Flask		Lab scale PBR					
			CI		CII		CIII	
	WT	E2	WT	E2	WT	E2	WT	E2
Chl content (pg/cell)	0.08 ± 0.01$^{*, a, b}$	0.04 ± 0.01$^{*, c}$	0.14 ± 0.01$^{*, a}$	0.12 ± 0.01$^{*, c, d}$	0.12 ± 0.01$^{*, b}$	0.10 ± 0.01$^{*, c, d}$	0.05 ± 0.01$^{a, b}$	0.05 ± 0.01^{d}

Pigments are major components of the photosynthetic apparatus and their content determines cells light harvesting ability. The WT strain cultivated at high cell concentration (CI) showed a strong increase in Chl content per cell with respect to flask cultures (Table 2). The increase of light supply rate in CII and CIII stimulated a significant reduction in pigments content, which was particularly strong in CIII, as typical of a culture exposed to excess light.

Strain E2 responded with the same trend in the different conditions, showing that the mutation did not affect its ability to activate an acclimation response. During the acclimation to CI and CII, the increase in Chl content was even higher than observed for the WT, reducing the difference with respect to the parental strain. In CIII this difference was completely lost (Table 2).

Carotenoids (Car) are also seminal pigments for photosynthetic apparatus, being involved in light harvesting but also in protection from light stress. In CI and CII, Chl /Car ratio was maintained in both strains (Table 3) while CIII showed a relative increase in Car content (Table 3), confirming the activation of a light excess response. Carotenoids composition was analyzed by HPLC in both strains and no differences in their relative content were observed between the flask cultures and CI and CII, with violaxanthin and vaucheriaxanthin being the most abundant carotenoids, as expected for *Nannochloropsis* cells [40]. On the contrary, CIII showed a reduction of violaxanthin with an increased accumulation of antheraxanthin, zeaxanthin and cantaxanthin, which is consistent with the photo-protective role of these carotenoids. Car composition had no significant differences between WT and E2, both showing a very similar response to cultivation conditions.

Table 3. Effect of growth conditions on carotenoids content of *Nannochloropsis gaditana* WT and E2 strains. Carotenoids content, expressed as Chl / Car ratio, was evaluated for *N. gaditana* WT and mutant strain E2. Individual carotenoids content, obtained from HPLC analysis, is expressed as mol/100 Chls. Data from WT cells cultivated in flasks are also reported as comparison. Data are expressed as average ± SD (n = 10). The same alphabet letter indicates significant differences for the same strain in different growth conditions (one-way ANOVA, p-value < 0.05). Violax, violaxanthin; Vaucheriax, vaucheriaxanthin; Anterax, anteraxanthin; Zeax, zeaxanthin; Cantax, cantaxanthin; β-car, β-carotene.

	Flask	Lab scale PBR					
		CI		CII		CIII	
	WT	WT	E2	WT	E2	WT	E2
Chl/Car	3.00 ± 0.44^{a}	2.94 ± 0.24^{b}	2.78 ± 0.23^{d}	2.99 ± 0.1^{c}	3 ± 0.08^{e}	2.23 ± 0.09^{a,b,c}	2.12 ± 0.09^{d,e}
Violax	20.52 ± 3.31^{a}	20.49 ± 1.27^{b}	21.82 ± 1.36^{d}	19.50 ± 0.93^{c}	18.27 ± 1.31^{e}	8.87 ± 1.04^{a,b,c}	10.06 ± 2.28^{d,e}
Vaucheriax	7.62 ± 1.89	7.84 ± 0.58	7.85 ± 0.68	7.23 ± 0.29	7.17 ± 0.15	8.65 ± 2.01	7.95 ± 2.48
Anterax	2.24 ± 0.45^{a,b}	1.17 ± 0.28^{a,c}	1.02 ± 0.53^{e}	0.81 ± 0.14^{b,d}	0.65 ± 0.12^{f}	2.63 ± 0.38^{c,d}	2.30 ± 0.63^{e,f}
Zeax	1.25 ± 0.63^{a,b}	0.77 ± 0.23^{a,c}	0.77 ± 0.27^{e}	0.53 ± 0.27^{b,d}	0.80 ± 0.57^{f}	3.87 ± 1.96^{c,d}	2.84 ± 1.26^{e,f}
Cantax	0.81 ± 0.18^{a,b}	2.42 ± 0.84^{a,c}	2.86 ± 0.56^{e}	1.18 ± 0.50^{b,d}	1.88 ± 0.64^{f}	9.12 ± 1.73^{c,d}	10.17 ± 2.74^{e,f}
β-Car	5.02 ± 0.18	3.01 ± 1.18	2.85 ± 0.66	3.43 ± 1.54	2.61 ± 0.64	6.85 ± 1.24	7.50 ± 2.50

The regulation of accumulation of photosynthetic machinery components in *N. gaditana* was investigated in more detail using spectroscopic methods. The photosystem I (PSI) content per cells was evaluated by quantifying the maximum signal of P_{700}^{+} absorption in samples illuminated with saturating light and in presence of DCMU and DBMIB to prevent P_{700} re-reduction (see supplementary figure S3 and methods for details). WT cells in CI and CII in the PBR strongly increased their PSI content per cell with respect to flask cultures (Figure 5A). However, when the available light was increased in CIII, P_{700} content was strongly reduced (Figure 5A).

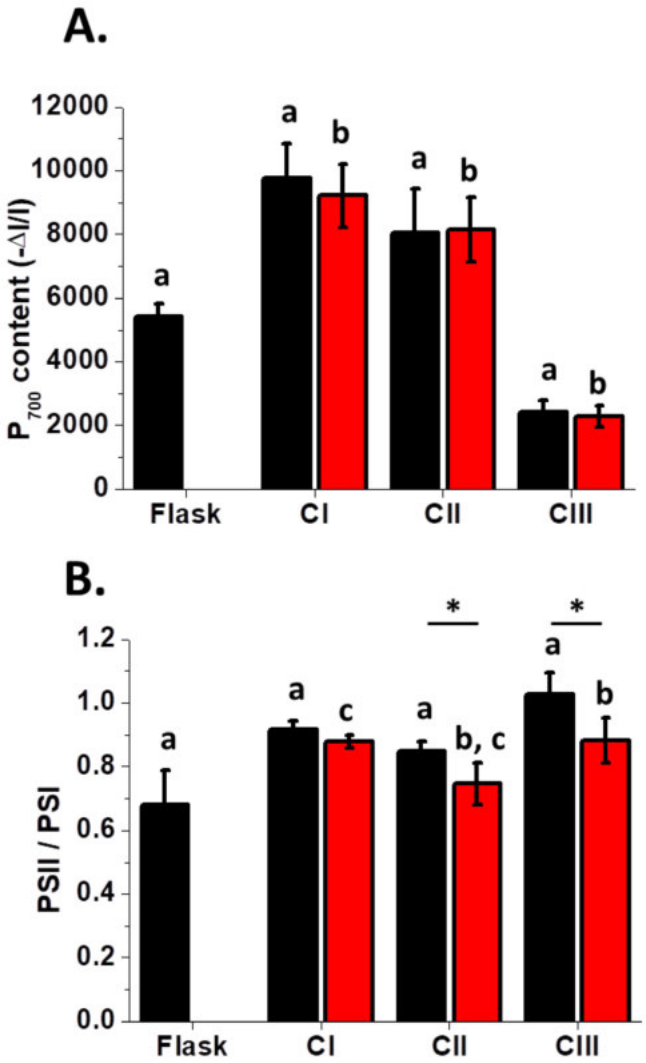

Figure 5. Dependence of photosystems content from growth conditions, in *Nannochloropsis gaditana* WT and E2 strains. PSI quantification for cells grown in an intensive environment and exposed to 3 light regimes (CI, CII, CIII) is shown in A). The maximum absorption at 705 nm of oxidized P_{700} was used to evaluate PSI content, according to the corresponding traces in supplementary figure S3. The PSII/PSI ratio obtained from the ECS signal for *N. gaditana* WT (black) and E2 (red) strain cells exposed to the same 3 light regimes is shown in B). The data are expressed as mean ± SD (n > 20). Both P_{700} and PSII/PSI data are compared to the values observed in flask conditions for the WT strain [45]. Statistically significant differences between WT and E2 are marked with asterisks, while the same alphabet letter indicates significant differences for the same strain in different growth conditions (one-way ANOVA, p-value < 0.05).

The PSII content was estimated by monitoring the PSII/PSI ratio using ECS measurements [47] and in WT strain it showed an increase in PBR cultures (Figure 5B), suggesting that PSII content increased even more than PSI. When light supply was altered, this affected PSII/PSI ratio but changes were limited (less than 20 %), suggesting

the balance between the two photosystems was maintained (Figure 5B). The strain E2 did not show any major alteration in PSI and PSII content with respect to the parental strain and also the different growth conditions had a very similar influence on both strains (Figure 5).

Photosystems are composed also by an antenna moiety, responsible of increasing their light harvesting ability, whose content can be modulated depending from growth conditions [55]. The functional antenna size (AS) of both PSI and PSII was evaluated by measuring respectively the P_{700} oxidation (Supplementary figure S4) and fluorescence induction kinetics [17,42,45]. WT cells cultivated in PBR showed a reduction in the PSI functional antenna size (Figure 6A) that was reduced further increasing the light supply (Figure 6A). Strain E2 showed the same PSI functional antenna size of the WT in all the tested conditions, suggesting its composition and regulation is not affected by the genetic modification (Figure 6A).

Cultivation in PBR led on the contrary to an increase of PSII functional antenna size (ASII) for the WT strain, with respect to the flask culture (Figure 6B). Different light supplies had a limited effect on ASII, although this should be taken with some caution for CIII, considering that photo-inhibition may cause over-estimation. Strain E2 showed a reduced ASII in flask with respect to the WT [17] but this difference was reduced upon cultivation in PBR (Figure 6B).

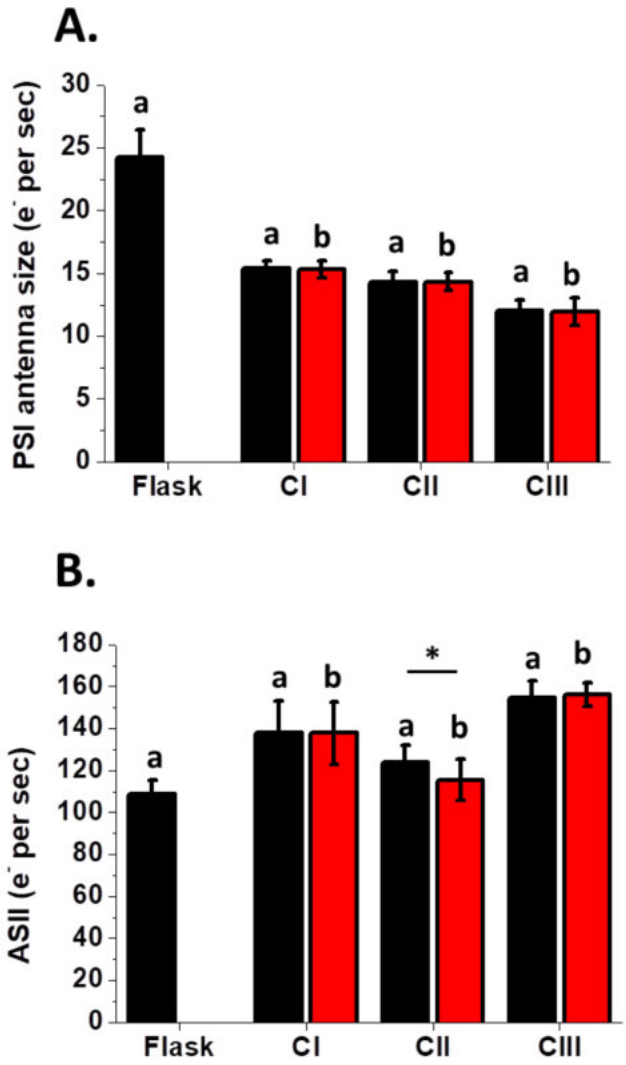

Figure 6. ***Nannochloropsis gaditana*** **modulation of the functional antenna size of both PSI and PSII. Averages values of the PSI functional antenna size (ASI) measured for** ***N. gaditana*** **WT (black) and E2 (red) cells are shown in A). The PSI antenna size values were calculated from the P_{700} oxidation kinetics in purified thylakoids incubated with methylviologen and ascorbate (corresponding traces are shown in supplementary figure S4). The functional PSII antenna size values were instead calculated from the fluorescence induction kinetics of DCMU-treated intact cells for cultures in the same growth conditions and are shown in B). All data are expressed as average ± SD (n > 20). Both ASI and ASII data are compared to the values observed in flask conditions for the WT strain [17,45]. Statistically significant differences between WT and E2 are marked with asterisks, while the same alphabet letter indicates significant differences for the same strain in different growth conditions (one-way ANOVA, p-value < 0.05).**

All data taken together highlighted that WT cultivated in PBR showed a substantial remodeling of the photosynthetic apparatus components with respect to flask cultures. Strain E2 showed instead a response to environmental stimuli very similar to the WT. Overall the acclimation response reduced the differences in photosynthetic apparatus

composition between the two strains with respect to previous comparisons in flask conditions [17] and in CIII, where cells experienced excess illumination, E2 become indistinguishable from WT.

Modulation of photosynthetic efficiency in PBR cultures.

The remodeling of the photosynthetic apparatus components observed in PBR cultures affected both PSI and PSII and it was thus expected to influence *N. gaditana* photosynthetic performances.

Table 4. PSII maximum quantum yield (Φ_{PSII}) of *Nannochloropsis gaditana* WT and E2 strain in lab-scale PBRs. Φ_{PSII} is as indicator of the PSII functionality, according to [41]. Data are expressed as average ± SD (n > 20). Data from flask cultures are reported as comparison [17]. Statistically significant differences between WT and E2 are marked with asterisks, while the same alphabet letter indicates significant differences for the same strain in different growth conditions (one-way ANOVA, p-value < 0.05).

	Flask	Lab scale PBR					
		CI		CII		CIII	
	WT	WT	E2	WT	E2	WT	E2
Φ_{PSII}	0.59 ± 0.01^{a}	0.61 ± 0.02$^{*, b}$	0.65 ± 0.03$^{*, d}$	0.63 ± 0.02$^{*, c}$	0.65 ± 0.02$^{*, e}$	0.48 ± 0.04$^{a, b, c}$	0.43 ± 0.03$^{d, e}$

Photosynthesis functionality in PBR cultures was first assessed exploiting *in vivo* Chl fluorescence measurements. PSII functionality, evaluated from its maximum quantum yield (Φ_{PSII}) [41] (Table 4), showed in CI and CII optimal values for WT *Nannochloropsis* cells. On the contrary, when the light supply rate increased further in CIII, we observed a decrease in its value, indication that a significant fraction of PSII units suffered from photoinhibition due to light excess (Table 4). Mutant strain E2 showed a slightly higher Φ_{PSII} with respect to the parental strain in both CI and CII (Table 4), suggesting a possible improvement in photosynthetic efficiency (Table 4). When the light supply rate increased in CIII, also in this case there was a significant decrease in Φ_{PSII}, reaching WT levels (Table 4).

Cells photosynthetic electron transport capacity can be evaluated from the PSI reduction kinetics after a treatment with saturating light (Figure 7 and supplementary figures S5).

The total electron flow (TEF) in the WT strain cultivated in PBR was more than double with respect to lab-scale cultures (Figure 7).

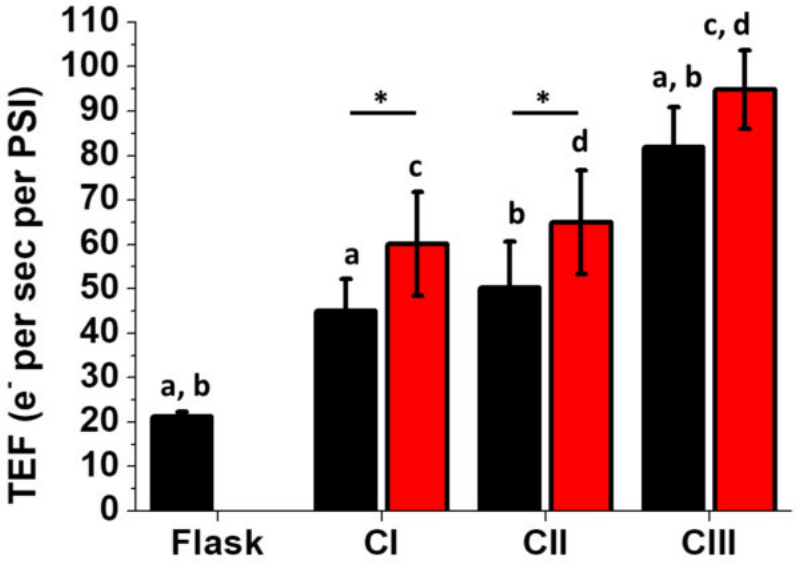

Figure 7. Photosynthetic electron transport rate per PSI for *Nannochloropsis gaditana* WT and E2 in lab-scale PBR. Total photosynthetic electron flow (TEF) was determined from the kinetics of P_{700}^{+} re-reduction after light was switched off (measurement traces are shown in supplementary figure S5). Data are expressed as average ± SD (n > 24). Data are normalized to the PSI content using single flash. Measurements for flask cultures are reported as comparison. Statistically significant differences between WT (black) and strain E2 (red) are marked with asterisks, while the same alphabet letter indicates significant differences for the same strain in different growth conditions (one-way ANOVA, p-value < 0.05).

In CI and CII, the WT strain showed comparable TEF values, with a further 60 % increase in CIII (Figure 7), suggesting that higher light availability induced higher photosynthetic capacity.

Strain E2 showed a similar response to different cultivation conditions (Figure 7 and supplementary figure S5). The most interesting observation is that E2 showed a higher total electron flow (TEF) with respect to the parental strain, both in CI and CII (Figure 7 - 34 and 30 % increase, respectively), consistently with the increased biomass productivity observed in these conditions. These conclusions were also confirmed by estimating photosynthetic electron transportation rate (ETR) with an independent approach, exploiting *in vivo* Chl fluorescence, that confirmed this increase in E2 with respect to the WT, both in CI and CII (Supplementary Figure S6). The enhanced electron transport

capacity is attributable to an increase in the linear transport from water to $NADP^+$ since cyclic/alternative electron flows [56] had a minor contribution in all tested conditions (Supplementary Figure S7). It is noteworthy that cyclic electron flow (CEF) remains minor (< 2 % of the whole TEF) also in the most stressful condition of this work (CIII_ Supplementary Figure S7B).

DISCUSSION

Algae acclimation response to intensive growth conditions strongly influences strains performances

N. gaditana WT and mutant strain E2, previously isolated for an altered photosynthetic apparatus [17], were tested in a lab-scale PBR working at high cells concentration to evaluate the impact of intensive cultivation environment on biomass productivity and strain properties [48]. The similarity between analyzed cultures and *Nannochloropsis* outdoor cultivations was confirmed by observations such as the PE values measured [48] and fatty acid content in CI and CII [49].

Analyzed cultures responded to different growth conditions tested by modulating the composition of their photosynthetic apparatus activating a response called acclimation. A typical indication of this process is the modulation of Chl content, that is a general response to different illumination intensities shared by all photosynthetic organisms [55]. Another typical response is the accumulation of carotenoids under stronger illumination as observed here in CIII, where we indeed observed an increase in antheraxanthin and zeaxanthin, involved in the xanthophyll cycle [57], and cantaxanthin, active in free radicals scavenging [58].

The characterization of cells in lab-scale PBR clearly showed significantly different properties than algae from flask cultures. The different light supply also played an influence and in CI and CII cells showed features typical of a light limited culture such as the increase in Chl content per cell. On the contrary, in CIII cells showed indications of a light excess such as the reduction of the Chl content per cell, the reduction of PSII quantum yield and the accumulation of carotenoids. It should also be noted that the response activated in PBR cultures is different from the one of *Nannochloropsis* cultures in flasks acclimated to different light intensities [45] such as a different modulation of PSII / PSI ratio and PSII antenna size that in flasks decreased with the stronger

illuminations but not in PBR cultures. PSI content and its functional antenna size were instead regulated similarly, increasing in light limitation [45,59]. Under strong illumination, the content of all photosynthetic components decreased with a strong reduction in P_{700} content in both WT and E2 and no induction of cyclic electron transport. This suggested that cells acclimation response does not depend only on light intensity but also that other environmental parameters (e.g. CO_2 supply) play a significant influence.

The most relevant observation obtained from the detailed characterization of photosynthetic properties of the different cultures was the strong increase in photosynthetic electron transport capacity observed in PBR cultures. This higher transport in conditions where the influence of other major parameters such as CO_2 and nutrients were minimized, correlated with a much higher biomass yield. Also when comparing different genotypes when E2 showed a higher photosynthetic capacity than WT it correlated with higher biomass productivity by 15 and 20% depending from the growth conditions. This observation suggest that the photosynthetic electron transport capacity can be a valuable proxy to predict biomass productivity of different cultures. Overall these results also suggest that acclimation response is influencing algae also in outdoor conditions and, by modulating the photosynthetic electron transport capacity, it plays a major influence on cultures performances.

The *N. gaditana* mutant strain E2 was selected after a screening of a large collection of random mutants for its specific photosynthetic features, reduced Chl content and ASII, that were potentially interesting in the perspective of an industrial cultivation [17]. In this work this strain was shown to be capable of acclimating to different growth conditions similarly to the WT, showing that the mutation does not affect its ability to activate this response. However, cell acclimation influenced E2 phenotype and the difference in Chl content was in general smaller in PBR cultures with respect to flask and negligible when cells were acclimated to the highest light supply rate, in CIII. This demonstrates that the PBR environment plays a major influence on multiple phenotypic features, and that the operational conditions can strongly influence the effects of a given genetic modification, enhancing or reducing its advantages.

Recent efforts for improving algae productivity led to some promising results at lab-scale [26,31,60] but strains potential was not always confirmed in larger scale conditions [32]. Results presented here provide a possible explanation by suggesting that different results are likely due to the influence of the specific environmental conditions that heavily influences strains performances also possibly masking potential benefits of the genetic

modifications. On the other hand, this conclusion also motivates the need for a deeper investigation of the impact that environment has on algae physiology and metabolic regulation during cultivation in industrially relevant conditions to drive more efficient genetic modifications efforts.

The genetic modification of selected strain is stable over a long-term cultivation

Algae cells undergo a huge number of duplication events during mass cultivation and thus phenomena like genetic drift are expected to occur in long term cultures. Genetic drift endangers the rationale of isolating genetically modified strains, since could affect the newly introduced features [61,62]. It is thus fundamental to assess if the effect of improved strains genetic modification is stable over generations going from the lab-scale isolation to large scale cultivation. This issue was poorly investigated in literature despite its seminal relevance for the successful industrial cultivation of improved strains. The present work indeed provides an indication on the stability of a selected genetic modification in an improved strain over thousands of generations upon cultivation in intensive conditions, simulating an industrial PBR

In our experiments, both WT and E2 were maintained in semi-continuous cultivation for a total of ≈ 9 months. The cultivation was however repeated twice and in one case the conditions were changed going from CI to CII and then CIII, while the other following the opposite direction. In both cases the results were indistinguishable and all data were eventually pooled together. This observation demonstrates that observed differences between WT and E2 were stable over many generations and are thus attributable to the selected genetic modification in strain E2. Differences observed in the three cultivation conditions were thus due to the acclimation of the culture and not to a genetic drift. These are seminal observations in the perspective of intensive algae cultivation, where any genetic feature newly introduced in a strain must be stably transmitted between generations, in order to be effective.

CONCLUSION

In this work, a genetically modified *N. gaditana* strain was exploited to assess how cultivation in industrially relevant conditions affected phenotype performances of improved strains. Operational conditions were indeed shown to influence the phenotype of this strain, enhancing or reducing the advantages of the selected genetic modification. A better understanding of the influence of the PBR environment on algae biology is thus seminal to drive further genetic engineering approaches to make strains development efforts more effective, and this work provides indeed a deep insight on it

Declarations

Conflicts of interests: none;

Funding

This work was supported by ERC starting grant BIOLEAP n° 309485 to TM

Authors' contributions:

TM Conception and design; GP, MC, DS, AB, MEM and AO Collection and assembly of data; GP Analysis and interpretation of data; GP and TM Drafting of the article. All authors Final approval of the article.

Acknowledgments

AB is thankful to "Centro studi di economia e tecnica dell'energia Giorgio Levi Cases" of the University of Padova for support. The authors would like to thank Davide Dal Bo for assistance in setting up lab-scale photobioreactors.

REFERENCES

[1] R.H. Moss, J.A. Edmonds, K.A. Hibbard, M.R. Manning, S.K. Rose, D.P. van Vuuren, T.R. Carter, S. Emori, M. Kainuma, T. Kram, G.A. Meehl, J.F.B. Mitchell, N. Nakicenovic, K. Riahi, S.J. Smith, R.J. Stouffer, A.M. Thomson, J.P. Weyant, T.J. Wilbanks, The next generation of scenarios for climate change research and assessment., Nature. 463 (2010) 747–56. doi:10.1038/nature08823.

[2] E.H. Allison, H.R. Bassett, Climate change in the oceans: Human impacts and responses, Science (80-.). 350 (2015) 778–782. doi:10.1126/science.aac8721.

[3] B.J. Walsh, F. Rydzak, A. Palazzo, F. Kraxner, M. Herrero, P.M. Schenk, P. Ciais, I.A. Janssens, J. Peñuelas, A. Niederl-Schmidinger, M. Obersteiner, New feed sources key to ambitious climate targets, Carbon Balance Manag. 10 (2015) 26. doi:10.1186/s13021-015-0040-7.

[4] E. Kazamia, A.G. Smith, Assessing the environmental sustainability of biofuels., Trends Plant Sci. 19 (2014) 615–8. doi:10.1016/j.tplants.2014.08.001.

[5] F.M. Salih, Microalgae Tolerance to High Concentrations of Carbon Dioxide: A Review, J. Environ. Prot. (Irvine,. Calif). 2 (2011) 648–654. doi:10.4236/jep.2011.25074.

[6] J.-Y. Park, M.S. Park, Y.-C. Lee, J.-W. Yang, Advances in direct transesterification of algal oils from wet biomass., Bioresour. Technol. 184 (2015) 267–75. doi:10.1016/j.biortech.2014.10.089.

[7] S.R. Medipally, F.M. Yusoff, S. Banerjee, M. Shariff, Microalgae as sustainable renewable energy feedstock for biofuel production., Biomed Res. Int. 2015 (2015) 519513. doi:10.1155/2015/519513.

[8] A. Teymouri, S. Kumar, E. Barbera, E. Sforza, A. Bertucco, T. Morosinotto, Integration of biofuels intermediates production and nutrients recycling in the processing of a marine algae, (2016). doi:10.1002/aic.15537.

[9] B. Kim, Y.K. Chang, J.W. Lee, Efficient solvothermal wet in situ transesterification of Nannochloropsis gaditana for biodiesel production, Bioprocess Biosyst. Eng. (2017). doi:10.1007/s00449-017-1738-6.

[10] E.A. Ramos Tercero, E. Sforza, M. Morandini, A. Bertucco, Cultivation of Chlorella protothecoides with urban wastewater in continuous photobioreactor: biomass productivity and nutrient removal., Appl. Biochem. Biotechnol. 172

(2014) 1470–85. doi:10.1007/s12010-013-0629-9.

[11] M.L. Kagan, D.W. Sullivan, S.C. Gad, C.M. Ballou, Safety assessment of EPA-rich polar lipid oil produced from the microalgae Nannochloropsis oculata., Int. J. Toxicol. 33 (2014) 459–74. doi:10.1177/1091581814553453.

[12] J.A. Gimpel, V. Henríquez, S.P. Mayfield, In Metabolic Engineering of Eukaryotic Microalgae: Potential and Challenges Come with Great Diversity., Front. Microbiol. 6 (2015) 1376. doi:10.3389/fmicb.2015.01376.

[13] H.-P. Tsai, L.-T. Chuang, C.-N.N. Chen, Production of long chain omega-3 fatty acids and carotenoids in tropical areas by a new heat-tolerant microalga Tetraselmis sp. DS3., Food Chem. 192 (2016) 682–90. doi:10.1016/j.foodchem.2015.07.071.

[14] C. Formighieri, F. Franck, R. Bassi, Regulation of the pigment optical density of an algal cell: filling the gap between photosynthetic productivity in the laboratory and in mass culture., J. Biotechnol. 162 (2012) 115–23. doi:10.1016/j.jbiotec.2012.02.021.

[15] R. Radakovits, R.E. Jinkerson, A. Darzins, M.C. Posewitz, Genetic engineering of algae for enhanced biofuel production., Eukaryot. Cell. 9 (2010) 486–501. doi:10.1128/EC.00364-09.

[16] L. de Jaeger, R.E. Verbeek, R.B. Draaisma, D.E. Martens, J. Springer, G. Eggink, R.H. Wijffels, Superior triacylglycerol (TAG) accumulation in starchless mutants of Scenedesmus obliquus: (I) mutant generation and characterization., Biotechnol. Biofuels. 7 (2014) 69. doi:10.1186/1754-6834-7-69.

[17] G. Perin, A. Bellan, A. Segalla, A. Meneghesso, A. Alboresi, T. Morosinotto, Generation of random mutants to improve light-use efficiency of Nannochloropsis gaditana cultures for biofuel production., Biotechnol. Biofuels. 8 (2015) 161. doi:10.1186/s13068-015-0337-5.

[18] J. Kirk, Light and photosynthesis in aquatic ecosystems, (1994). http://books.google.it/books?hl=it&lr=&id=It5GePwa2EIC&oi=fnd&pg=PR11&dq=kirk+jto&ots=JRshZRehFf&sig=aGCXWxh9YtclvH5V93en30wozEI (accessed January 28, 2015).

[19] D. Simionato, S. Basso, G.M. Giacometti, T. Morosinotto, Optimization of light use efficiency for biofuel production in algae., Biophys. Chem. 182 (2013) 71–8. doi:10.1016/j.bpc.2013.06.017.

[20] A. Melis, Dynamics of photosynthetic membrane composition and function,

Biochim. Biophys. Acta - Bioenerg. 1058 (1991) 87–106. doi:10.1016/S0005-2728(05)80225-7.

[21] L. Wobbe, C. Remacle, Improving the sunlight-to-biomass conversion efficiency in microalgal biofactories., J. Biotechnol. (2014). doi:10.1016/j.jbiotec.2014.08.021.

[22] L. Wobbe, R. Bassi, O. Kruse, Multi-Level Light Capture Control in Plants and Green Algae, Trends Plant Sci. 21 (2015) 55–68. doi:10.1016/j.tplants.2015.10.004.

[23] Y. Nakajima, R. Ueda, The effect of reducing light-harvesting pigment on marine microalgal productivity, in: J. Appl. Phycol., 2000: pp. 285–290. http://www.scopus.com/inward/record.url?eid=2-s2.0-0033727975&partnerID=tZOtx3y1.

[24] Y. Nakajima, M. Tsuzuki, R. Ueda, Improved productivity by reduction of the content of light-harvesting pigment in Chlamydomonas perigranulata, J. Appl. Phycol. 13 (2001) 95–101. doi:10.1023/A:1011192832502.

[25] L. Wobbe, O. Blifernez, C. Schwarz, J.H. Mussgnug, J. Nickelsen, O. Kruse, Cysteine modification of a specific repressor protein controls the translational status of nucleus-encoded LHCII mRNAs in Chlamydomonas., Proc. Natl. Acad. Sci. U. S. A. 106 (2009) 13290–5. doi:10.1073/pnas.0900670106.

[26] J. Beckmann, F. Lehr, G. Finazzi, B. Hankamer, C. Posten, L. Wobbe, O. Kruse, Improvement of light to biomass conversion by de-regulation of light-harvesting protein translation in Chlamydomonas reinhardtii., J. Biotechnol. 142 (2009) 70–7. doi:10.1016/j.jbiotec.2009.02.015.

[27] M.H. Huesemann, T.S. Hausmann, R. Bartha, M. Aksoy, J.C. Weissman, J.R. Benemann, Biomass productivities in wild type and pigment mutant of Cyclotella sp. (Diatom)., Appl. Biochem. Biotechnol. 157 (2009) 507–26. doi:10.1007/s12010-008-8298-9.

[28] G. Bonente, C. Formighieri, M. Mantelli, C. Catalanotti, G. Giuliano, T. Morosinotto, R. Bassi, Mutagenesis and phenotypic selection as a strategy toward domestication of Chlamydomonas reinhardtii strains for improved performance in photobioreactors., Photosynth. Res. 108 (2011) 107–20. doi:10.1007/s11120-011-9660-2.

[29] A. Melis, J. Neidhardt, J.R. Benemann, Dunaliella salina (Chlorophyta) with small chlorophyll antenna sizes exhibit higher photosynthetic productivities and photon

use efficiencies than normally pigmented cells, J. Appl. Phycol. 10 (1998) 515–525. doi:10.1023/A:1008076231267.

[30] D.J. Lea-Smith, P. Bombelli, J.S. Dennis, S.A. Scott, A.G. Smith, C.J. Howe, Phycobilisome-Deficient Strains of Synechocystis sp. PCC 6803 Have Reduced Size and Require Carbon-Limiting Conditions to Exhibit Enhanced Productivity., Plant Physiol. 165 (2014) 705–714. doi:10.1104/pp.114.237206.

[31] S. Cazzaniga, L. Dall'Osto, J. Szaub, L. Scibilia, M. Ballottari, S. Purton, R. Bassi, Domestication of the green alga Chlorella sorokiniana: reduction of antenna size improves light-use efficiency in a photobioreactor., Biotechnol. Biofuels. 7 (2014) 157. doi:10.1186/s13068-014-0157-z.

[32] T. de Mooij, M. Janssen, O. Cerezo-Chinarro, J.H. Mussgnug, O. Kruse, M. Ballottari, R. Bassi, S. Bujaldon, F.-A. Wollman, R.H. Wijffels, Antenna size reduction as a strategy to increase biomass productivity: a great potential not yet realized, J. Appl. Phycol. (2014). doi:10.1007/s10811-014-0427-y.

[33] E. Sforza, A. Bertucco, T. Morosinotto, G.M. Giacometti, Photobioreactors for microalgal growth and oil production with Nannochloropsis salina: From lab-scale experiments to large-scale design, Chem. Eng. Res. Des. 90 (2012) 1151–1158. doi:10.1016/j.cherd.2011.12.002.

[34] E. Sforza, C. Calvaruso, A. Meneghesso, T. Morosinotto, A. Bertucco, Effect of specific light supply rate on photosynthetic efficiency of Nannochloropsis salina in a continuous flat plate photobioreactor., Appl. Microbiol. Biotechnol. 99 (2015) 8309–18. doi:10.1007/s00253-015-6876-7.

[35] R. Moran, D. Porath, Chlorophyll determination in intact tissues using n,n-dimethylformamide., Plant Physiol. 65 (1980) 478–9. http://www.pubmedcentral.nih.gov/articlerender.fcgi?artid=440358&tool=pmcentrez&rendertype=abstract (accessed December 2, 2015).

[36] R.J. Porra, W.A. Thompson, P.E. Kriedemann, Determination of accurate extinction coefficients and simultaneous equations for assaying chlorophylls a and b extracted with four different solvents: verification of the concentration of chlorophyll standards by atomic absorption spectroscopy, Biochim. Biophys. Acta - Bioenerg. 975 (1989) 384–394. doi:10.1016/S0005-2728(89)80347-0.

[37] A.R. Wellburn, The spectral determination of chlorophylls a and b, as well as total carotenoids, using various solvents with spectrophotometers of different resolution, J. Plant Physiol. 144 (1994) 307–313.

http://www.scopus.com/inward/record.url?eid=2-s2.0-0028007844&partnerID=tZOtx3y1.

[38] S.W. Jeffrey, R.F.C. Mantoura, S.W. Wright, Phytoplankton pigments in oceanography: guidelines to modern methods, Monogr. Oceanogr. Methodol. (1997). http://www.marsnetwork.org/imis?module=ref&refid=26657&printversion=1&dropIMIStitle=1 (accessed December 31, 2015).

[39] A. Färber, P. Jahns, The xanthophyll cycle of higher plants: influence of antenna size and membrane organization, Biochim. Biophys. Acta - Bioenerg. 1363 (1998) 47–58. doi:10.1016/S0005-2728(97)00093-5.

[40] S. Basso, D. Simionato, C. Gerotto, A. Segalla, G.M. Giacometti, T. Morosinotto, Characterization of the photosynthetic apparatus of the Eustigmatophycean Nannochloropsis gaditana: evidence of convergent evolution in the supramolecular organization of photosystem I., Biochim. Biophys. Acta. 1837 (2014) 306–14. doi:10.1016/j.bbabio.2013.11.019.

[41] K. Maxwell, G.N. Johnson, Chlorophyll fluorescence - A practical guide, J. Exp. Bot. 51 (2000) 659–668. http://www.scopus.com/inward/record.url?eid=2-s2.0-0034063592&partnerID=tZOtx3y1.

[42] G. Bonente, S. Pippa, S. Castellano, R. Bassi, M. Ballottari, Acclimation of Chlamydomonas reinhardtii to different growth irradiances., J. Biol. Chem. 287 (2012) 5833–47. doi:10.1074/jbc.M111.304279.

[43] D. Simionato, M.A. Block, N. La Rocca, J. Jouhet, E. Maréchal, G. Finazzi, T. Morosinotto, The response of Nannochloropsis gaditana to nitrogen starvation includes de novo biosynthesis of triacylglycerols, a decrease of chloroplast galactolipids, and reorganization of the photosynthetic apparatus., Eukaryot. Cell. 12 (2013) 665–76. doi:10.1128/EC.00363-12.

[44] J. Alric, Cyclic electron flow around photosystem I in unicellular green algae, Photosynth. Res. 106 (2010) 47–56. http://www.scopus.com/inward/record.url?eid=2-s2.0-78650228974&partnerID=tZOtx3y1.

[45] A. Meneghesso, D. Simionato, C. Gerotto, N. La Rocca, G. Finazzi, T. Morosinotto, Photoacclimation of photosynthesis in the Eustigmatophycean Nannochloropsis gaditana, 129 (2016) 291–305. doi:10.1007/s11120-016-0297-z.

[46] W.D. Swingley, M. Iwai, Y. Chen, S. Ozawa, K. Takizawa, Y. Takahashi, J.

Minagawa, Characterization of photosystem I antenna proteins in the prasinophyte Ostreococcus tauri., Biochim. Biophys. Acta. 1797 (2010) 1458–64. doi:10.1016/j.bbabio.2010.04.017.

[47] B. Bailleul, P. Cardol, C. Breyton, G. Finazzi, Electrochromism: A useful probe to study algal photosynthesis, Photosynth. Res. 106 (2010) 179–189. doi:10.1007/s11120-011-9704-7.

[48] J.H. De Vree, R. Bosma, M. Janssen, M.J. Barbosa, R.H. Wijffels, Comparison of four outdoor pilot-scale photobioreactors, 8 (2015). doi:10.1186/s13068-015-0400-2.

[49] G. Benvenuti, R. Bosma, A.J. Klok, F. Ji, P.P. Lamers, M.J. Barbosa, R.H. Wijffels, Microalgal triacylglycerides production in outdoor batch-operated tubular PBRs., Biotechnol. Biofuels. 8 (2015) 100. doi:10.1186/s13068-015-0283-2.

[50] F.G.A. Fernández, F.G. Camacho, J.A.S. Pérez, J.M.F. Sevilla, E.M. Grima, A model for light distribution and average solar irradiance inside outdoor tubular photobioreactors for the microalgal mass culture, Biotechnol. Bioeng. 55 (1997) 701–714. doi:10.1002/(SICI)1097-0290(19970905)55:5<701::AID-BIT1>3.0.CO;2-F.

[51] E. Sforza, D. Simionato, G.M. Giacometti, A. Bertucco, T. Morosinotto, Adjusted light and dark cycles can optimize photosynthetic efficiency in algae growing in photobioreactors., PLoS One. 7 (2012) e38975. doi:10.1371/journal.pone.0038975.

[52] A. Alboresi, G. Perin, N. Vitulo, G. Diretto, M.A. Block, J. Jouhet, A. Meneghesso, G. Valle, G. Giuliano, E. Maréchal, T. Morosinotto, Light Remodels Lipid Biosynthesis in Nannochloropsis gaditana by Modulating Carbon Partitioning Between Organelles., Plant Physiol. (2016). doi:10.1104/pp.16.00599.

[53] J. Li, D. Han, D. Wang, K. Ning, J. Jia, L. Wei, X. Jing, S. Huang, J. Chen, Y. Li, Q. Hu, J. Xu, Choreography of Transcriptomes and Lipidomes of Nannochloropsis Reveals the Mechanisms of Oil Synthesis in Microalgae., Plant Cell. 26 (2014) 1645–1665. doi:10.1105/tpc.113.121418.

[54] D. Wang, K. Ning, J. Li, J. Hu, D. Han, H. Wang, X. Zeng, X. Jing, Q. Zhou, X. Su, X. Chang, A. Wang, W. Wang, J. Jia, L. Wei, Y. Xin, Y. Qiao, R. Huang, J. Chen, B. Han, K. Yoon, R.T. Hill, Y. Zohar, F. Chen, Q. Hu, J. Xu, Nannochloropsis Genomes Reveal Evolution of Microalgal Oleaginous Traits, PLoS Genet. 10 (2014). doi:10.1371/journal.pgen.1004094.

[55] P.G. Falkowski, J. LaRoche, ACCLIMATION TO SPECTRAL IRRADIANCE IN

ALGAE, J. Phycol. 27 (1991) 8–14. doi:10.1111/j.0022-3646.1991.00008.x.

[56] F. Chaux, G. Peltier, X. Johnson, A security network in PSI photoprotection: regulation of photosynthetic control, NPQ and O2 photoreduction by cyclic electron flow., Front. Plant Sci. 6 (2015) 875. doi:10.3389/fpls.2015.00875.

[57] Z. Li, S. Wakao, B.B. Fischer, K.K. Niyogi, Sensing and responding to excess light., Annu. Rev. Plant Biol. 60 (2009) 239–60. doi:10.1146/annurev.arplant.58.032806.103844.

[58] T. Esatbeyoglu, G. Rimbach, Canthaxanthin: From molecule to function, Mol. Nutr. Food Res. (2016). doi:10.1002/mnfr.201600469.

[59] D. Bína, Z. Gardian, M. Herbstová, R. Litvín, Modular antenna of photosystem I in secondary plastids of red algal origin: a Nannochloropsis oceanica case study, Photosynth. Res. 131 (2017) 255–266. doi:10.1007/s11120-016-0315-1.

[60] M. Oey, I.L. Ross, E. Stephens, J. Steinbeck, J. Wolf, K.A. Radzun, J. Kügler, A.K. Ringsmuth, O. Kruse, B. Hankamer, RNAi knock-down of LHCBM1, 2 and 3 increases photosynthetic H2 production efficiency of the green alga Chlamydomonas reinhardtii., PLoS One. 8 (2013) e61375. doi:10.1371/journal.pone.0061375.

[61] J.C. Gwo, J.Y. Chiu, C.C. Chou, H.Y. Cheng, Cryopreservation of a marine microalga, Nannochloropsis oculata (Eustigmatophyceae), Cryobiology. 50 (2005) 338–343. doi:10.1016/j.cryobiol.2005.02.001.

[62] M. Hagedorn, V.L. Carter, H. Putnam, R. Gates, J. Acker, I. Baums, Seasonal Preservation Success of the Marine Dinoflagellate Coral Symbiont, Symbiodinium sp., PLoS One. 10 (2015) e0136358. doi:10.1371/journal.pone.0136358.

SUPPLEMENTARY MATERIAL

Supplementary Table S1. Specific growth rates (μ) for *Nannochloropsis gaditana* WT and E2 strains, restoring the starting biomass concentration value every 2 or 3 days.

Supplementary Table S2. Fatty acids composition of *Nannochloropsis gaditana* WT and E2 strains in intensive growth conditions.

Supplementary Figure S1. *Nannochloropsis gaditana* WT and E2 strains in lab scale PBR.

Supplementary Figure S2. Light penetration in *Nannochloropsis gaditana* WT and E2 strain cultures in lab scale PBR.

Supplementary Figure S3. Representative traces of PSI quantification.

Supplementary Figure S4. Representative traces of functional PSI antenna size quantification.

Supplementary Figure S5. Representative traces of oxidized P_{700} re-reduction kinetics.

Supplementary Figure S6. ETR measured at the PSII level for *Nannochloropsis gaditana* WT and E2 strains in lab-scale PBR.

Supplementary Figure S7. Cyclic/alternative electron transport efficiency in intensive cultures of *Nannochloropsis gaditana* WT and E2 strains.

SUPPLEMENTARY MATERIAL

Supplementary Tables.

	WT		**E2**	
	2 days	**3 days**	**2 days**	**3 days**
μ (d^{-1})	0.22 ± 0.02	0.22 ± 0.03	0.26 ± 0.02	0.25 ± 0.04

Supplementary Table S1. Specific growth rates (μ) for *Nannochloropsis gaditana* WT and E2 strains, restoring the starting biomass concentration value every 2 or 3 days. Data were collected for cells cultivated in CII of this work. Data are expressed as mean ± SD for 10 samples and were collected from 2 month of cultivation in both operational conditions. Data for the same strain were not statistically different (one-way ANOVA, p-value > 0.05).

	CI		CII		CIII	
	WT	E2	WT	E2	WT	E2
C8:0	0.22 ± 0.01	0.19 ± 0.01	0.27 ± 0.18	0.28 ± 0.21	0.14 ± 0.05	0.11 ± 0.01
C10:0	0.14 ± 0.01	0.13 ± 0.02	0.20 ± 0.09	0.22 ± 0.15	0.12 ± 0.05	0.09 ± 0.01
C12:0	0.67 ± 0.05	0.69 ± 0.01	0.71 ± 0.30	0.59 ± 0.32	0.64 ± 0.04	0.72 ± 0.07
C14:0	8.05 ± 1.27	7.52 ± 0.12	8.09 ± 3.00	6.64 ± 3.32	9.04 ± 0.70	9.50 ± 1.34
C15:0	0.42 ± 0.02	0.41 ± 0.06	0.43 ± 0.20	0.53 ± 0.32	0.12 ± 0.05	0.09 ± 0.04
C16:0	65.77 ± 17.92^{a}	49.14 ± 5.84^{c}	62.44 ± 9.44^{b}	53.57 ± 14.84^{d}	122.62 ± 11.70^{a,b,*}	85.64 ± 9.55^{c,d,*}
C16:1	57.82 ± 10.18^{a}	47.71 ± 3.40^{c}	55.85 ± 9.56^{b}	46.03 ± 14.26^{d}	82.47 ± 10.28^{a,b}	66.08 ± 8.19^{c,d}
C16:2	1.75 ± 0.02	1.61 ± 0.06	2.21 ± 1.46	2.25 ± 2.02	1.11 ± 0.09	1.20 ± 0.14
C18:0	0.87 ± 0.23^{a}	0.85 ± 0.10^{c}	1.45 ± 0.81^{b}	1.45 ± 0.89^{d}	5.05 ± 2.59^{a,b}	3.13 ± 1.01^{c,d}
C18:1	3.37 ± 1.07^{a}	2.78 ± 0.60^{c}	3.13 ± 0.95^{b}	3.85 ± 1.89^{d}	10.81 ± 1.04^{a,b}	7.29 ± 0.99^{c,d}
C18:2	1.16 ± 0.22	0.97 ± 0.01	1.52 ± 0.46	2.23 ± 1.37	1.96 ± 0.36	1.34 ± 0.21
C18:3	0.44 ± 0.07	0.37 ± 0.03	0.84 ± 0.60	0.79 ± 0.63	0.81 ± 0.39	0.57 ± 0.20
C18:4	0.66 ± 0.01	0.55 ± 0.01	0.85 ± 0.60	0.84 ± 0.75	0.18 ± 0.03	0.25 ± 0.04
C20:0	0.10 ± 0.03	0.08 ± 0.01	0.12 ± 0.12	0.14 ± 0.15	0.72 ± 0.62	0.31 ± 0.12
C20:3	0.55 ± 0.19	0.47 ± 0.01	0.63 ± 0.16	0.80 ± 0.44	0.58 ± 0.18	0.52 ± 0.13
C20:4	6.87 ± 0.81	5.69 ± 0.07	6.40 ± 2.83	6.73 ± 3.84	5.94 ± 1.51	5.57 ± 1.33
C20:5	30.89 ± 0.21^{a,b}	28.08 ± 0.73^{c,d}	21.35 ± 4.39^{a}	19.81 ± 4.55^{c}	23.08 ± 4.38^{b}	22.42 ± 4.49^{d}

Supplementary Table S2. Fatty acids composition of *Nannochloropsis gaditana* WT and E2 strains in intensive growth conditions. The data are expressed as mg of lipids per gram of dried biomass (mg/g). The data are expressed as mean ± Standard Deviation (SD), n = 12; statistically significant differences between the WT and the E2 strain are marked with an asterisk, while the same alphabet letter indicates differences between the same strain in different growth conditions (one-way ANOVA, p-value < 0.05).

Supplementary Figures.

Supplementary Figure S1. ***Nannochloropsis gaditana*** **WT and E2 strains in lab scale PBR.** The picture was taken when cultures were exposed to CII (700 mmoles photons (g biomass)$^{-1}$ d^{-1}), after the dilution with fresh media restored an equal cell concentration.

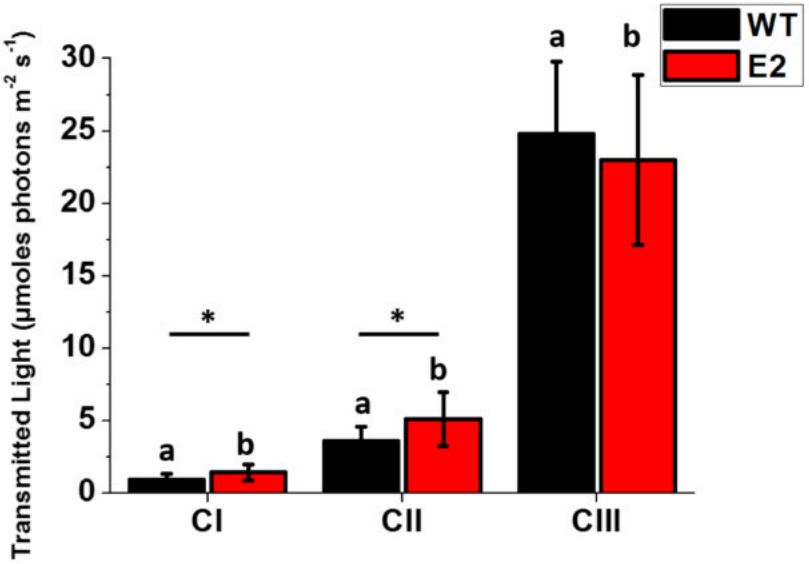

Supplementary Figure S2. Light penetration in *Nannochloropsis gaditana* WT and E2 strain cultures in lab scale PBR. Light transmitted through the cultures, exposed to increasing light supply rates (CI < CII < CIII), after the initial cell concentration value was restored by diluting the culture with fresh media. Data are expressed as the average values of at least 40 measurements for each growth condition ± SD. Each of these measurements came from the average of 9 measurements in different points. Statistically significant differences between WT and strain E2 are marked with an asterisk, while the same alphabet letter indicates significant differences for the same strain in different growth conditions (one-way ANOVA, p-value < 0.05).

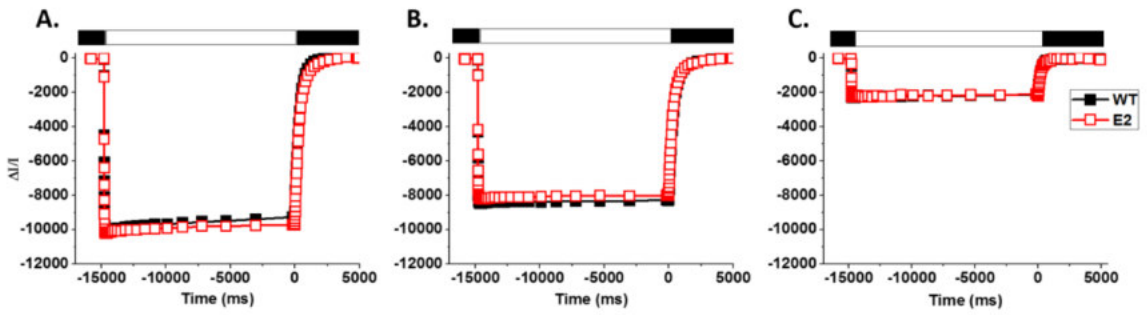

Supplementary Figure S3. Representative traces of PSI quantification. The PSI content in the 3 light supply regimes investigated in this work, CI in A), CII in B) and CIII in C), was evaluated from the maximum absorption of P_{700}^{+} at 705 nm, in the presence of DCMU and DBMIB and a saturating light of 2050 µmoles photons m^{-2} s^{-1} (see methods for the details); 300 x 10^6 cells/ml were employed for the measurement. White box, actinic light on; black box, actinic light off.

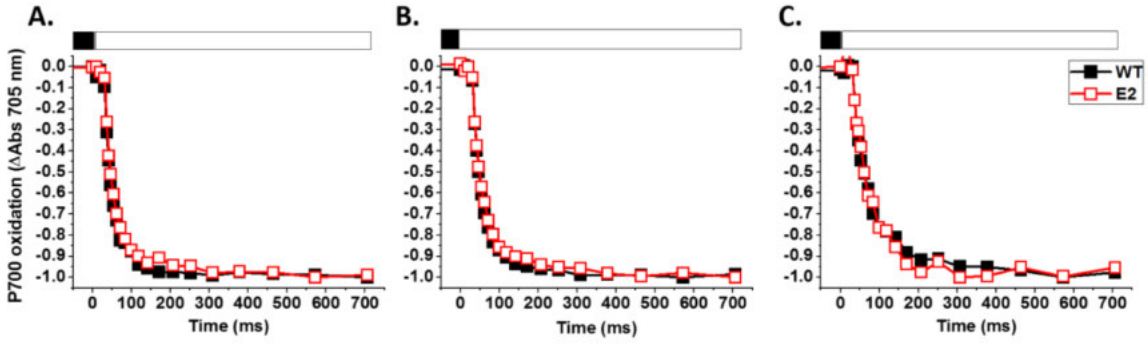

Supplementary Figure S4. Representative traces of functional PSI antenna size quantification. Representative P_{700} oxidation kinetics at 705 nm for thylakoids treated with methylviologen and ascorbate, extracted from cultures expose to 3 light regimens in intensive cultures (CI in A), CII in B) and CIII in C)). Measurements were performed with 150 µmoles photons m^{-2} s^{-1} of actinic light at 630 nm; see methods for the details. White box, actinic light on; black box, actinic light off.

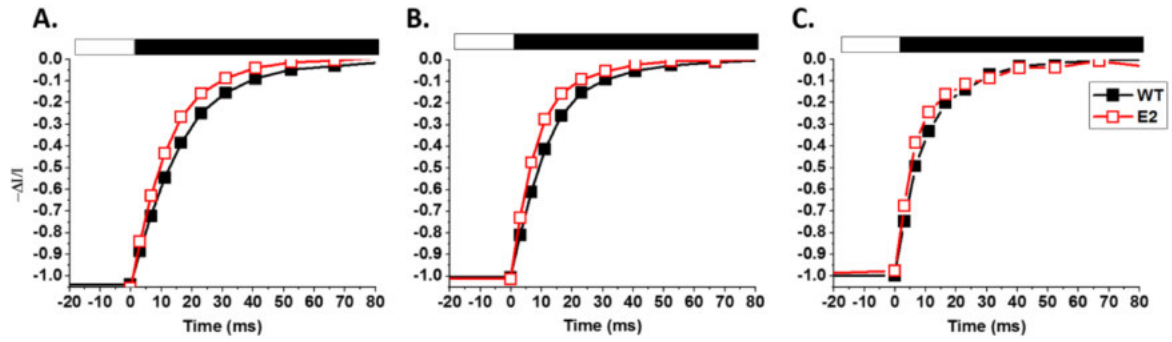

Supplementary Figure S5. Representative traces of oxidized P_{700} re-reduction kinetics. The kinetics were used for the total electron transport (TEF) quantification (see methods for details) for cultures exposed to increasing light regimes (CI in A), CII in B) and CIII in C)), in intensive growth conditions. Cells were exposed to a saturating light intensity (2050 µmoles photons m^{-2} s^{-1}) before evaluating the recovery kinetics in the dark, here reported. White box, actinic light on; black box, actinic light off.

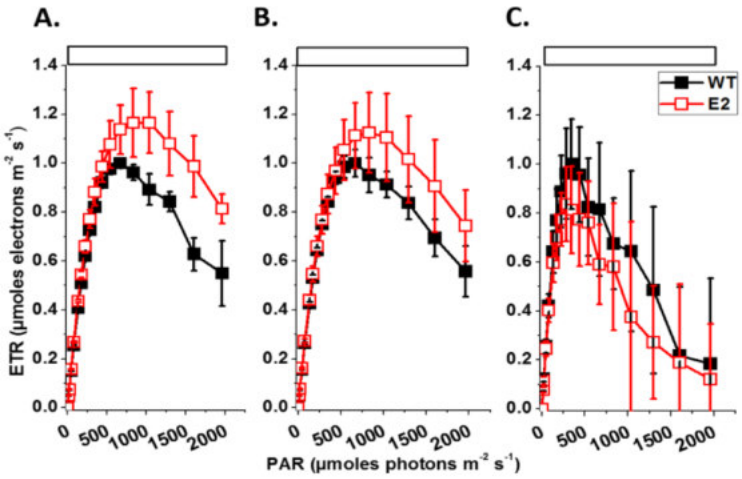

Supplementary Figure S6. ETR measured at the PSII level for *Nannochloropsis gaditana* WT and E2 strains in lab-scale PBR. The photosynthetic electron transport efficiency at the PSII level (electrons transport rate, ETR) for cells grown in CI (A), CII (B) and CIII (C) is here shown. ETR was monitored by measuring *in vivo* Chl fluorescence (see methods for details) of samples treated with increasing light intensity up to 2000 µmoles photons m^{-2} s^{-1}. ETR values were calculated as previously described [1,2]. The data are expressed as mean ± SD (n = 24). Data were normalized to the maximum value of ETR for the WT strain in each condition. White boxes, actinic light on.

[1] K. Maxwell, G.N. Johnson, Chlorophyll fluorescence - A practical guide, J. Exp. Bot. 51 (2000) 659–668. http://www.scopus.com/inward/record.url?eid=2-s2.0-0034063592&partnerID=tZOtx3y1.

[2] B. Demmig-Adams, W.W. Adams, K. Winter, A. Meyer, U. Schreiber, J.S. Pereira, A. Krüger, F.C. Czygan, O.L. Lange, Photochemical efficiency of photosystem II, photon yield of O2 evolution, photosynthetic capacity, and carotenoid composition during the midday depression of net CO2 uptake in Arbutus unedo growing in Portugal., Planta. 177 (1989) 377–87. doi:10.1007/BF00403596.

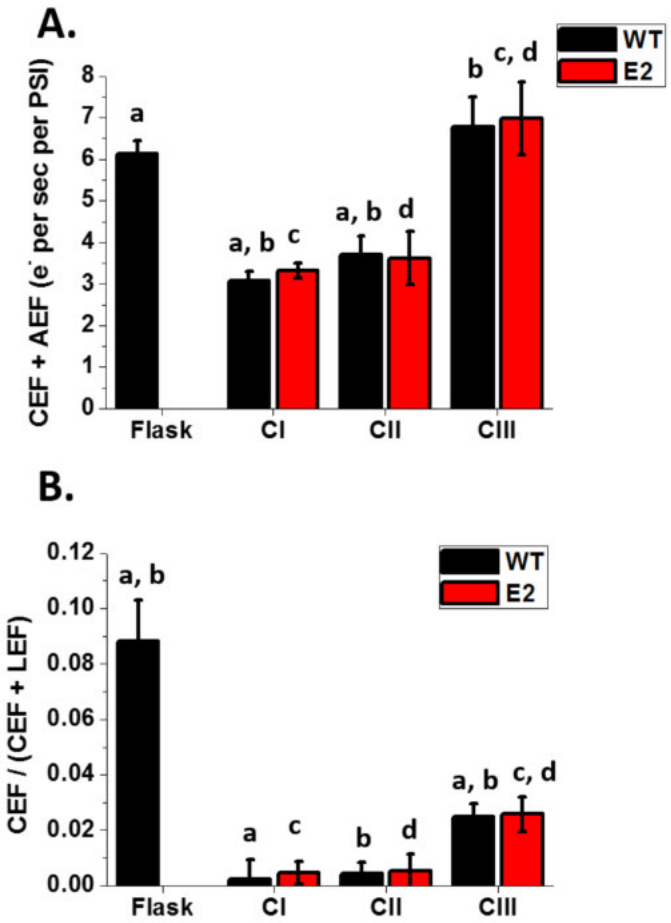

Supplementary Figure S7. Cyclic/alternative electron transport efficiency in intensive cultures of *Nannochloropsis gaditana* WT and E2 strains. The values were calculated from P_{700} re-reduction kinetics, after exposing cells to a saturating light intensity (2050 µmoles photons m^{-2} s^{-1}). The data reported in A) represent electron transport rates for DCMU (cyclic and alternative electron flows, CEF + AEF) treated cells. The rate of cyclic electron flow (CEF), compared with the sum of cyclic and linear (CEF + LEF), is instead reported in B). The values were calculated for cells cultivated at the 3 light regimes investigated in the intensive conditions of this work (CI < CII < CIII). The data are expressed as average ± SD (n > 24). Data are compared to the values measured in flask conditions (mean ± SD of 4 data points). The same alphabet letter indicates significant differences for the same strain in different growth conditions (one-way ANOVA, p-value < 0.05).

APPENDIX II :

A mathematical model to guide Genetic Engineering of Photosynthetic Metabolism.

Authors name and affiliations

Giorgio Perin[2], Andrea Bernardi[3], Alessandra Bellan[1], Fabrizio Bezzo[3] and Tomas Morosinotto[1]

1-PAR-Lab_Padua Algae Research Laboratory, Department of Biology, University of Padova, Via U. Bassi 58/B, 35121 Padova, Italy.

2- Department of Life Sciences, Imperial College London, Sir Alexander Fleming Building, London, SW7 2AZ, UK

3- CAPE-Lab (Computer-Aided Process Engineering Laboratory) and PAR-Lab (Padua Algae Research Laboratory), Department of Industrial Engineering, University of Padova, via Marzolo 9, 35131 Padova, Italy

THIS CHAPTER WAS PUBLISHED IN METABOLIC ENGINEERING JOURNAL (2017)

The format is different from the main chapters because it is that one required by the journal.

CONTRIBUTION:

AB provided a contribution in the photosynthesis measurements and growth monitoring in PBR.

ABSTRACT

The optimization of algae biomass productivity in industrial cultivation systems requires genetic improvement of WT strains isolated from nature. One of the main factors affecting algae productivity is their efficiency in converting light into chemical energy and this has been a major target of recent genetic efforts. However, photosynthetic productivity in algae cultures depends on many environmental parameters, making the identification of advantageous genotypes complex and the achievement of concrete improvements slower than expected. In this work, we developed a mathematical model to describe the key factors influencing algae biomass productivity in PBR, using experimental measurements of photosynthesis for the wild type strain of *Nannochloropsis gaditana*. The model was then exploited to predict the effect of potential genetic modifications on algae performances in an industrial context, showing the ability to predict the productivity of mutants with specific photosynthetic phenotypes. These results show that such a quantitative model can be exploited to predict the genetic modifications with the highest effect on productivity taking into full account the complex influence of environmental conditions, efficiently guiding genetic engineering efforts.

KEYWORDS
Modeling, biomass productivity, photobioreactor, *Nannochloropsis*, genetic engineering

ABBREVIATIONS[2]

[2] ASII, antenna size of photosystem II; chl, chlorophyll; DCMU, 3-(3,4-dichlorophenyl)-1,1-dimethylurea; NPQ, non-photochemical quenching; P, oxygen evolution rate; PBR, photobioreactor; PI, photosynthesis-irradiance; PSII, photosystem II; ROS, reactive oxygen species; TAGs, triacylglycerols; WT, wild type.

INTRODUCTION

Global demand for products derived from biomass such as food, feed or fuels is continuously expanding and not satisfactorily fulfilled. New technologies to improve the current biomass production are thus strongly needed to meet this increasing demand and also to improve sustainability. One major strategy to increase biomass production is to develop technologies to exploit new biomass sources to complement plant crops. Microalgae are highly promising for this purpose since they are diverse, unicellular, eukaryotic photosynthetic organisms that use sunlight to produce biomass and oxygen from carbon dioxide (CO_2), water, and nutrients. They can be cultivated in marginal or saline water on unproductive land and thus do not compete with agriculture for arable soils and freshwater, making them a promising resource for a highly sustainable production of biomass (Gangl et al., 2015; Leu and Boussiba, 2014). Microalgae advantages are largely recognized and several promising applications have been suggested (e.g. bio-plastics, human diet supplements, feed and biofuels) and developed, but the potential of these organisms still remains largely untapped. Significant improvement in strains performances and cultivation technologies is in fact strongly required to reduce the currently high production costs of algal biomass, which is limiting their exploitation to the only production of high-value bio-products. Efforts in this direction are thus seminal to expand the possible applications of algae biotechnology to commodities with a lower market value.

Algae large scale cultures are often limited by available irradiation and a main target of optimization efforts aims to improve their efficiency in converting light energy into reduced carbon. Wild type (WT) algae adapted during evolution to a natural environment where conditions are largely different from those found during industrial cultivation in a photobioreactor (PBR) and thus genetic modifications are expected to have a seminal impact to reach the maximal potential productivity. As example, in nature algae often deal with limiting light conditions and accumulate a large number of chlorophylls to compete with other organisms for energy capture. This ability is instead detrimental in intensive cultivation systems where algae normally reach high cellular densities, with external layers absorbing most of the energy and leaving the rest of the culture in strong light limitation. On the other hand, algae also evolved mechanisms (non-photochemical quenching, NPQ) to deal with excess irradiation, to avoid over-excitation and the generation of reactive oxygen species (ROS) that compromise photosynthesis

functionality. These mechanisms are especially activated by external cells more exposed to illumination, which thus activate NPQ with a reduction of their light use efficiency (Simionato et al., 2013), dissipating up to 80 % of absorbed energy as heat (Peers et al., 2009).

Algae thus need to be domesticated to optimize their productivity upon cultivation in industrial conditions. Several modifications of the photosynthetic apparatus were proposed in recent years to improve light homogeneity inside the culture and consequently productivity (Formighieri et al., 2012; Wobbe et al., 2015). Among them, one often suggested strategy is the generation of strains with a reduced chlorophyll (Chl) content. Out of the ~300 chlorophyll molecules bound to both photosystems, in fact, only about one third are associated to the core complexes and thus involved in fundamental reactions of the photosynthesis, while the others are in principle dispensable (Melis, 1991). It is thus theoretically possible to reduce the pigment content of a cell by 2/3 leading to more transparent mass cultures where light is more homogenously distributed and increases overall productivity. Another often suggested strategy is to reduce the number of antenna complexes, the chlorophyll (Chl) binding proteins bound to the two photosystems, that are responsible for most of the light harvesting (Dall'Osto et al., 2015; Polle et al., 2002). In a mass culture context a reduction in antenna content should reduce cells light harvesting ability but also prevent over-excitation in excess light conditions, increasing the amount of light energy exploitable at high efficiency (Mitra et al., 2012; Simionato et al., 2013; Wobbe and Remacle, 2014). A third strategy concerns the reduction of NPQ, which, channeling more energy into photochemistry rather than wasting it through heat dissipation, could lead to increase the efficiency of light energy conversion in biomass (Erickson et al., 2015).

Genetic modifications of algae photosynthetic properties have been shown to be beneficial for productivity in lab scale conditions by several groups, including ours (Berteotti et al., 2016; Kirst et al., 2012; Perin et al., 2015). These advantages however still need to be validated on a larger cultivation scale and first attempts were successful in some cases but not others (Cazzaniga et al., 2014; de Mooij et al., 2014). One major explanation for the different results is that environmental conditions experienced in large scale cultivation are significantly different from lab scale and have a major unexpected impact on performances of genetically improved strains (Perin et al., submitted). Algae cultivated in a PBR / pond are in fact exposed to a complex environment, where many

different parameters influence productivity, impairing the possibility of extrapolating the impact of a genetic modification on productivity from simple lab scale evaluations.
On the other hand, productivity evaluations on a large scale are highly time consuming, expensive and thus discourage a trial and error approach, supporting the need for a more rational approach. One strategy to tackle this issue is to develop mathematical models capable of describing quantitatively the influence of major cultivation parameters on algae performances. The metabolism of light-energy conversion spans numerous time-scales ranging from milliseconds to days and it is thus particularly intricate. We presently have developed a model capable of reliably describing photosynthetic light conversion, accounting for processes like photoproduction, photoinhibition and photo-regulation (Bernardi et al., 2016; Nikolaou et al., 2015). In this work, this model was further implemented to account for the light distribution in a PBR, achieving a reliable description of algae photosynthetic productivity in an industrially relevant environment. This model was exploited to predict the effect of genetic modifications of the photosynthetic apparatus and to assess their impact on biomass productivity during large scale cultivation. These predictions were shown to be consistent with experimental data, proving that modelling approaches represent powerful tools for productivity improvement and can be exploited for predicting the effect of a given genetic modification, making the identification of the ones providing the largest advantages much more effective.

MATERIALS AND METHODS

Nannochloropsis gaditana was selected for this work because it is widely recognized as model organism for algae industrial applications, because of its ability to accumulate triacylglycerols (TAGs) (Bondioli et al., 2012; Rodolfi et al., 2009; Simionato et al., 2013).

Culture conditions and growth determination

Nannochloropsis gaditana, strain 849/5, from the Culture Collection of Algae and Protozoa (CCAP) was used as the WT strain. Mutants with altered photosynthetic apparatus were isolated using random mutagenesis approaches, as previously described in (Perin et al., 2015). The three most promising strains (E2, I48 and I29) were employed in this work.

Cultivation conditions

All strains were maintained in F/2 solid media, with sea salts (32 g/L, Sigma Aldrich), 40 mM Tris-HCl (pH 8), Guillard's (F/2) marine water enrichment solution (Sigma Aldrich), 1 % agar (Duchefa Biochemie). Cells were pre-cultured in sterile F/2 liquid media in Erlenmeyer flasks with 100 μmoles photons m^{-2} s^{-1} illumination and 100 rpm agitation at 22 ± 1 °C in a growth chamber. Growth tests in PBR simulating industrial cultivation were performed with semi-continuous cultures in 5 cm diameter Drechsel bottles with a 250 ml working volume. Bottles were illuminated from one side (illumination rate was determined using the LI-250A photometer (Heinz-Walz, Effeltrich, Germany)) and bubbled using air enriched with 5 % CO_2 (v/v), at a total flow rate of 1 L/h, as detailed in (Sforza et al., 2012). In this case, F/2 growth media was enriched with added nitrogen, phosphate and iron sources (0.75 g/L $NaNO_3$, 0.05 g/L NaH_2PO_4 and 0.0063 g/L $FeCl_3$•6 H_2O final concentrations). Constant illumination at 400 μmoles photons m^{-2} s^{-1} was provided by a white LED light source SL 3500 (Photons Systems Instruments, PSI, Brno, Czech Republic). The pH of the semi-continuous cultures was set to 8.00 and fresh media was added every other day to restore the starting cell concentration to values between 150 and 250 x 10^6 cells/ml (corresponding to biomass concentration values between 1.0 and 1.8 g/L).

Analytical procedures and energy balance.

Algal growth was monitored using a cell counter (Cellometer Auto X4, Nexcelom Bioscience) and evaluating biomass concentration. The specific growth rate was calculated by the slope of logarithmic phase for the biomass concentration (dry weight) measured gravimetrically as previously reported in (Perin et al., 2015). Biomass productivity was calculated as ($[C_f]$ - $[C_i]$) / (t_f - t_i), where C is the final (f) (before dilution) or initial (i) (after dilution) biomass concentration of the culture and t is the growth time interval, expressed as number of days. The specific light supply rate per unit mass of cell, r_{Ex} (mmoles photons g^{-1} d^{-1}), in the growth conditions of this work was calculated according to (Sforza et al., 2015) as:

$$r_{Ex} = \frac{PFD_{abs} \cdot A_{PBR}}{C_x \cdot V_{PBR}} \qquad (1)$$

where PFD_{abs} is the PAR photon flux density absorbed by the culture (µmoles photons m^{-2} s^{-1}), A_{PBR} is the irradiated surface of the reactor (m^2), C_x is the microalgae concentration inside the PBR (g/L) and V_{PBR} is the volume of the culture.

Pigments extraction

Pigments were extracted from cells grown in semi-continuous conditions, during active growth. Chlorophyll a was extracted from intact cells, using a 1:1 biomass to solvent ratio of 100 % N,N-dimethylformamide (Sigma Aldrich) (Moran and Porath, 1980), at 4 °C in the dark, for at least 24 h. Absorption spectra were registered between 350 and 750 nm using a Cary 100 spectrophotometer (Agilent Technologies) to spectrophotometrically determine pigment concentrations, using specific extinction coefficients (Porra et al., 1989; Wellburn, 1994). Absorption values at 664 were used to calculate the concentrations of Chlorophyll a.

Photosynthetic performances.

Photosynthesis monitoring was performed by measuring *in vivo* Chl fluorescence using a PAM 100 fluorimeter (Heinz-Walz, Effeltrich, Germany). Samples were treated with increasing light intensity up to 2000 µmoles photons m^{-2} s^{-1} and then light was switched off to evaluate NPQ relaxation kinetic. NPQ was calculated as in (Demmig-Adams et al., 1989; Maxwell and Johnson, 2000).

PSII functional antenna size evaluation

PSII antenna sizes were determined for semi-continuous cultures in active growth conditions, using a JTS-10 spectrophotometer (Biologic, France). Samples (200 x 10^6 cells/ml final concentration) were dark-adapted for 20 minutes and incubated with 80 µM 3-(3,4-dichlorophenyl)-1,1-dimethylurea (DCMU) for 10 minutes. Fluorescence induction kinetics were then monitored upon excitation with 320 µmoles photons m^{-2} s^{-1} of actinic light at 630 nm. The $t_{2/3}$ values obtained from the fluorescence induction curves were used to calculate the size of the PSII functional antenna (Perin et al., 2015).

Mathematical modelling.

Simulations of the growth model were conducted in the modelling environment gPROMS (Process System Enterprise, gPROMS v 4.1, www.psenterprise.com/gproms, 1997-2016). Model parameters for the wild type strain were obtained in (Bernardi et al., 2016) using maximum likelihood optimisation criterion.

Statistical analysis.

We applied descriptive statistical analysis with mean and standard deviation for all the experimental data reported in this work. Statistical significance was evaluated by one-way analysis of variance (One-way ANOVA), using the OriginPro 8 software (http://www.originlab.com/). Samples size was > 40 for all the measurements performed in this work.

THEORY AND CALCULATION

Model for microalgae photosynthetic productivity.

The photosynthetic productivity of Nannochloropsis gaditana WT strain, as function of the incident irradiation, was described according to a previously developed model (Bernardi et al., 2016; Nikolaou et al., 2015), whose overall set of equations is provided below:

$$F = S_F \sigma \phi_f \tag{2}$$

$$\phi_f = \frac{1}{\frac{A}{\phi_f^A} + \frac{B}{\phi_f^B} + \frac{C}{\phi_f^C}} \tag{3}$$

$$\dot{A} = -I\sigma_{PS2}A + \frac{1}{\tau}B \tag{4}$$

$$\dot{B} = I\sigma_{PS2}A - \frac{1}{\tau}B + k_r C - k_d \sigma_{PSII} I B \tag{5}$$

$$1 = A + B + C \tag{6}$$

$$\sigma_{PS2} = \frac{\sigma}{N_v}\phi_P^A \tag{7}$$

$$\phi_P^A = \eta_P \phi_f^A \tag{8}$$

$$\phi_f^A = \frac{1}{1 + \eta_P + \eta_D + \eta_{qE}} \quad (9)$$

$$\phi_f^B = \frac{1}{1 + \eta_D + \eta_{qE}} \quad (10)$$

$$\phi_f^C = \frac{1}{1 + \eta_I + \eta_D + \eta_{qE}} \quad (11)$$

$$\dot{\alpha}_F = \xi_F (\alpha_{SS} - \alpha_F) \quad (12)$$

$$\dot{\alpha}_S = \xi_S (\alpha_{SS} - \alpha_S) \quad (13)$$

$$\alpha_{SS} = \frac{I^n}{I_{qE}^n + I^n} \quad (14)$$

$$\eta_{qE} = \alpha_F \left(\bar{\eta}_{qE}^F + \alpha_S \bar{\eta}_{qE}^C\right) + \alpha_S \bar{\eta}_{qE}^S \quad (15)$$

Equation 2 defines the fluorescence flux, F (V), as a function of the total cross-section, σ (m^2 g^{-1}_{chl}), the fluorescence quantum yield, ϕ_f (−), and a parameter depending on the characteristics of the pulse amplitude modulation (PAM) fluorometer and the chlorophyll content of the sample, S_F ($V g_{Chl} m^{-2}$). The fluorescence quantum yield given in equation 3 is the harmonic mean of the fluorescence quantum yields of open (A), closed (B) and damaged (C) reaction centers of photosystem II (RCII). The dynamics of A, B and C are described according to the Han model (Han et al., 2000) in equations 4-6, according to the parameters: the effective cross-section of the PSII, σ_{PS2} (m^2 μE^{-1}), the turnover rate, τ (s^{-1}), the damage rate constant, k_d (−), and the repair rate constant k_r (s^{-1}). Equation 7 relates the effective cross-section, σ_{PS2} of the Han model with σ, linking the state of the RCII with the fluorescence flux. It is worth noting that while σ_{PS2} is a constant in the Han model, here it becomes a function of the photoregulation activity (equation 15), via the quantum yield of photosynthesis of an open RCII (equations 8 and 9). The parameter N represents the chlorophyll specific number of photosynthetic units ($\mu moles_{O2}$ g^{-1}chl), and υ is a stoichiometric factor reflecting the minimum theoretical value of 4 electrons for each dissociated water molecule, according to the water dissociation reaction ($2H_2O + 4e^- \rightarrow O_2 + 4H^+$).

Equation 10 defines the quantum yield of photosynthesis of an open RCII. Equations 11-13 define the quantum yield of fluorescence of the open, closed and inhibited photosynthetic units (PSUs), with the parameters η_P, η_D and η_I representing the rates of photoproduction, basal thermal decay in dark-adapted state and qI-quenching, respectively. Parameter η_{qE} represents the combined quenching effect of light harvesting

complex (LHC) proteins involved in photoprotection (LHCX in Nannochloropsis species (Alboresi et al., 2016; Vieler et al., 2012)) and zeaxanthin, and it is calculated from equation 15, where the parameters $\bar{\eta}_{qE}^{F}$ and $\bar{\eta}_{qE}^{S}$ represent the rates of the fast (LHCX-related) and slow (zeaxanthin-related) components of the non-photochemical-quenching (NPQ) process, both relative to the rate of fluorescence; the parameter $\bar{\eta}_{qE}^{C}$represents the enhancing effect of zeaxanthin in the quenching capability of the LHCX proteins. The activities of the fast and slow NPQ components are described by the conceptual variables α_F and α_S, both modelled as first-order processes. Moreover, the reference α_{SS} is the same in equations 12 and 13 since LHCX- and zeaxanthin-related quenching are both triggered by low lumenal pH (Pinnola et al., 2013), yet with different time constants ξ_F and ξ_S. This reference is modelled by a sigmoid (Hill) function in equation 14, in agreement with experimental measurements of the NPQ index as function of I, according to (Kramer et al., 2004), with I_{qE} and n representing the irradiance level at which half of the maximal NPQ activity is triggered (α_{SS} = 0.5) and the sharpness of the switch-like transition, respectively.

Finally, the maximum and minimum fluorescence fluxes, F'_m and F'_0, can be calculated from equations 2 and 3, by varying A and B. Specifically F'_m is obtained by imposing A = 0 and B = 1 − C, whereas F'_0 by imposing A = 1 − C and B = 0. Moreover, the distinction between dark- and light-adapted fluxes depends on the value of the variables α_F and α_S, assuming $\alpha_F = \alpha_S = 0$ for the dark-adapted state.

Conversion of photosynthetic productivity in growth rate.

The model described in 3.1 expresses microalgae photosynthetic productivity as oxygen evolution rate, P [$g_{O2}/g_{chl}h$]. In order to predict microalgae biomass growth, we thus needed to convert the oxygen productivity into the growth rate constant, μ [d^{-1}], according to the product of four terms:

A conversion factor of 0.76 grams of biomass ($g_{biomass}$) per gram of O_2 (g_{O2}) produced (Béchet et al., 2015);

The [Chl]/ cell, which is $1.2 \cdot 10^{-13}$ g for the microalgae cultivated in the intensive growth conditions of this work;

The inverse of the cell weight, which corresponds to $1.5 \cdot 10^{11}$ g^{-1};

A factor of 24 to have the growth rate constant in d^{-1}.

Modelling of light attenuation in algal culture and model validation

In order to reliably describe the light attenuation profile inside the PBR the Lambert-Beer law is the simplest model available. This model assumes that the light intensity, I (z), decreases exponentially with the culture depth, z, according to equation 16:

$$I(z) = I(0)\exp(-K_{LB}z) \qquad (16)$$

where K_{LB} is the light attenuation coefficient, assumed to be linearly related with the biomass concentration of the sample. Since this is not the case in highly concentrated samples (> 1 g/L), we moved on the model by Yun et al. (Yun and Park, 2001) that overcomes this limitation and includes both absorption and scattering phenomena. This empirical model assumes a hyperbolic form to describe the variation of K_{LB} with the biomass:

$$K_{LB}(x_{biom}) = K_{LB}^{max}\frac{x_{biom}}{x_{biom} + k_B} \qquad (17)$$

where K_{LB}^{max} is the maximum absorption coefficient and k_B is a constant. According to this model, at low biomass concentrations, the attenuation change is linear with (x_{biom}), while at high biomass concentration it shows an asymptotic tendency towards a maximum.

Model calibration was performed by assessing the light absorbed by microalgae samples at different cell concentrations, using a 1-cm-path-length cuvette, irradiated from a fixed distance with increasing light intensities (Supplementary Table S1) with a halogen lamp (KL1500, Schott, Germany). For each sample, $K_{LB}(x_{biom})$ was calculated as:

$$K_{LB}(x_{biom}) = \frac{1}{h}\ln\left(\frac{I^w(h)}{I(h, x_{biom})}\right) \qquad (18)$$

where h is the path length, $I^w(h)$ is the light measured using a cuvette filled with water (blank) and I (h, x_{biom}) is the light measured when the cuvette is filled with the microalgae sample.

3.3.1 Light attenuation profile for photosynthetic mutants. The effects of hypothetical alterations of photosynthetic apparatus in mutants on light attenuation profile inside the PBR were described by modifying the light attenuation coefficient as:

$$K_{LB}^{mut} = K_{LB}^{WT} \frac{chl_{mut}\sigma_{mut}}{chl_{WT}\sigma_{WT}} \quad (19)$$

where K_{LB}^{mut} and K_{LB}^{WT} are the light attenuation coefficients for the mutants and the wild type, respectively, chl_{mut} and chl_{WT} represent the chlorophyll contents of mutants and the wild type, respectively and σ_{mut} and σ_{WT} are the chlorophyll specific total cross sections of the photosystems in mutants and wild type, respectively.

Modelling microalgae growth in PBR

In order to predict the growth of Nannochloropsis gaditana WT strain in PBR, we combined the model developed in (Bernardi et al., 2016) and here implemented to convert photosynthetic productivity in specific growth rate as function of the incident irradiation (see 3.2 for details), with the model describing the light attenuation profile in PBR developed in this work and presented in 3.3.

In order to account for the inhomogeneous light distribution in the mass culture:

- The photobioreactor was divided in ten discrete sub-regions, based on the distance from the half-circumference illuminated by the light source (see Supplementary Figure S1 for the scheme). In each region, a constant light intensity equal to the value predicted from the light attenuation model at the median point of the corresponding area was assumed. Therefore, as the biomass concentration increases during growth, light attenuation is expected to increase as a function of time.
- The model predictions of the growth rate constant in each region of the PBR were used to calculate the biomass concentration variations, assuming that cultures remain in an exponential growth phase;

- The biomass concentration inside the photobioreactor was obtained as the volumetric mean of the biomass concentrations in the different regions;
- The average growth rate constant was calculated according to the following equation:

$$\mu(T) = \frac{1}{T}\log\left(\frac{x_{biom}(T)}{x_{biom}(0)}\right) \quad (20)$$

where T is the growth time interval, expressed in days (d).

Model implementation to predict the growth of photosynthetic mutants in PBR

In order to predict the effect on growth in PBR of mutants showing alterations on photosynthesis, we modified a subset of model parameters values, earlier developed to describe WT photosynthetic productivity (see 3.1, (Bernardi et al., 2016)). For instance, in order to simulate in silico a mutant with a reduced NPQ activation, it is sufficient to reduce the values of the parameters $\bar{\eta}_{qE}^{F}$, $\bar{\eta}_{qE}^{S}$ and $\bar{\eta}_{qE}^{C}$, which describe the different components of photo-regulation of microalgae cells, according to equation 15 of 3.1.

Modifications of photosystem II (PSII) functional antenna size (ASII) and cell chlorophyll content are instead expected to lead to a variation of the following model parameters: σ, τ and N, representing the chlorophyll specific total cross section of the photosystems, the turnover rate of the PSII and the inverse of the Emerson and Arnold number (a measurement of the chlorophyll molecules associated with each reaction center of PSII), respectively. In particular:

- The antenna size in the model is represented by the ratio between σ and N, therefore to represent a reduction of antenna size this ratio has to be modified accordingly;
- The variation of Chl might lead to an increase in σ due to the self-shading effect between chlorophyll molecules (Falkowski and Raven, 2013);
- The parameter τ can decrease if the chlorophyll reduction leads to a reduction of the number of reaction centers (Falkowski and Raven, 2013).

- According to these considerations, we set the parameter σ varying linearly as function of the chlorophyll content of the cells, according to the following equation:

$$\sigma = \sigma_{WT} + \sigma_{WT} \frac{chl_{WT} - chl}{chl_{WT}} \quad (21)$$

with and the relative σ variation being equal to the opposite of the relative Chl variation. This assumption was validated using Nannochloropsis gaditana photosynthetic mutants with altered Chl content (strains E2 and I48 of this work) observing that the ratio between σ_{mut} and σ_{WT} is always greater than one in high density cultures (cells concentration > 150 x 10^6 cells/ml, corresponding to > 1 g L^{-1}), indicating that σ indeed increases as chlorophyll content decreases (see supplementary figure S2).

Another parameter that can vary according to the variations of Chl and ASII is the maximum turnover rate, τ. If we consider that Chl ∝ $ASII_{XN}$, where X_N is the number of photosynthetic units, a reduction in the values of Chl content and ASII is consistent with a reduction in the number of reaction centres, which is also expected to lead to a reduction of the maximum turnover rate (Falkowski, 1993). Therefore, we set the maximum turnover rate, τ, varying as function of the both the chlorophyll content and the ASII of the cell, according to the following mathematical relation:

$$\tau = \tau_{WT} \left(0.1 + (1 - 0.1) * \frac{chl}{chl_{WT}} \frac{ASII_{WT}}{ASII}\right) \quad (22)$$

with the variation of τ being directly proportional to the variation of the ratio chl/ASII. In order to assure that the parameter τ is always greater than zero an intercept of 0.1 has been imposed. The proposed formulation assures that if Chl and ASII are equal to the WT values, then $\tau = \tau_{WT}$ and that τ can be reduced maximum by one order of magnitude, which is consistent with the data reported in (Falkowski and Raven, 2013).

RESULTS

Quantitative description of light attenuation in an algae culture in PBR.

In an algae culture in a PBR, light intensity reaching each cell is highly different because of shading and scattering effects, and different culture layers are thus expected to have a different contribution on biomass productivity. Several models for light attenuation have been proposed in literature to describe absorption and scattering phenomena (Cornet et al., 1995, 1992; Yokota et al., 1991) and can be exploited to describe quantitatively the light attenuation profile in the PBR. We selected the one by Yun et al. (see 3.3 for details on the equations), that was demonstrated to describe accurately the light profile in an algae mass culture (Yun and Park, 2001). The model by Yun et al. was calibrated using a series of experimental measurements of light absorbed by a microalgae sample in dependence from cell concentration and the incident light intensity (see 3.3 and Supplementary Table S1 for data). As shown in Figure 1, following this approach it was possible to obtain a satisfactory correspondence between experimental data and model estimations of the light attenuation coefficient (K_{LB}) inside a culture in PBR for *N. gaditana* wild type cells.

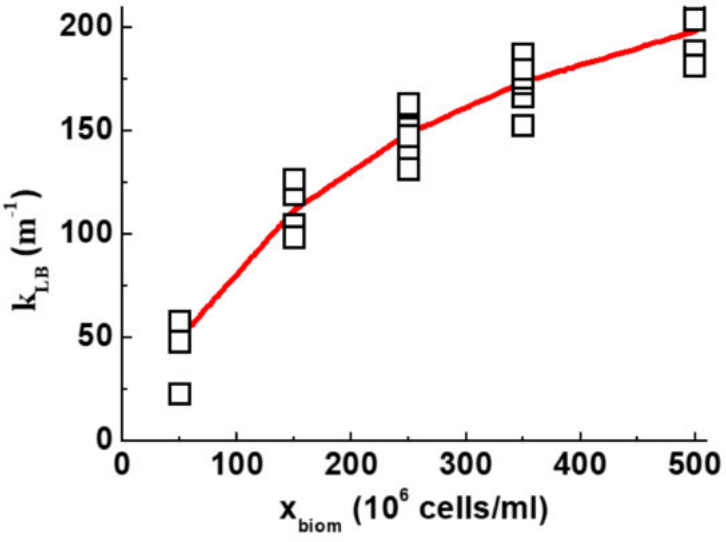

Figure 1. Light attenuation model in PBR. Measured (squares) and predicted (solid line) values of $K_{LB}(x_{biom})$ for *Nannochloropsis gaditana* wild type strain in a PBR. The values of the hyperbolic model parameters are K_{LB}^{max} = 296 and k_B = 248. (color, 1-column fitting image).

Modelling the growth of Nannochloropsis gaditana wild type strain in a PBR.

In order to describe quantitatively algae biomass productivity in intensive growth conditions, the mathematical description of the light attenuation profile inside a PBR (4.1) was combined with the model describing the dependence of algae photosynthetic productivity from incident irradiation (Bernardi et al., 2016) (see 3.1, 3.2 and 3.4 for details), including the photosynthetic performances of algal cells as a function of the available irradiation and considering different phenomena spanning different timescales, photoproduction, photoinhibition and photo-regulation.

The correspondence between model and experimental data were analysed using algae cultivated in lab-scale PBRs simulating industrial cultivation conditions (supplementary figure S1, (Benvenuti et al., 2016; De Vree et al., 2015), see 2.1.2 for details). Nutrients and CO_2 were provided in excess, in order to ensure that algae growth was mainly dependent from their light to biomass conversion efficiency. Incident light intensity I(0) was set at 400 μmoles photons $m^{-2}s^{-1}$ in order to achieve a light supply rate between 500 and 700 mmoles photons (g biomass-1) d-1, depending from the xbiom(0) value, which spanned between 1 and 1.8 g/L (see 2.1.3 and equation 1).

In order to predict cells growth in these conditions, the fluorescence model of (Bernardi et al., 2016) was calibrated using experimentally determined values of [chl]/cell (expressed in pg chl/cell), ASII (expressed as e^- per second), photosynthesis-irradiance (PI) curve and the fluorescence kinetic for the WT strains during cultivation in PBR. Figure 2 shows that the model is capable of representing accurately the experimental growth data of WT N. gaditana cultivated in the intensive conditions of a PBR. The model also correctly predicts that with the increase in biomass concentration ($x_{biom}(0)$) there is a progressive reduction in the specific growth rate constant (Figure 2A) but also a slight increase in biomass productivity (Figure 2B), as a consequence of the lower light intensity available per cell in more dense cultures.

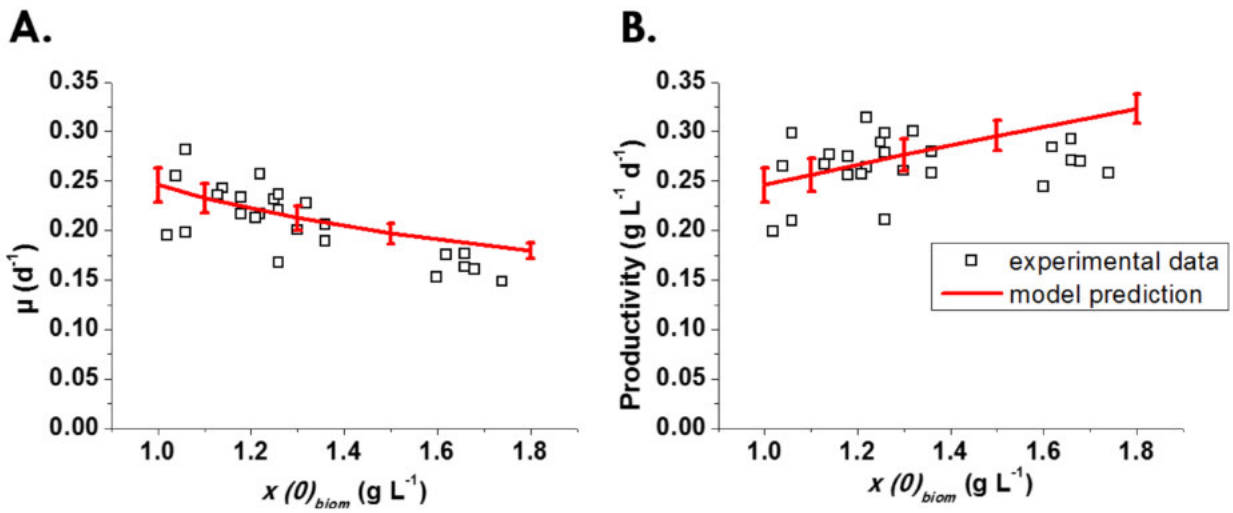

Figure 2. Growth of *Nannochloropsis gaditana* wild type strain in PBR. Squares represent the measured growth rate constants and biomass productivity values, respectively in A and in B. In both panels, the solid line represents the growth profile predicted by the model developed in this work. Error bars for the prediction of the model come from the uncertainty of both σ and τ parameters (see 3.4 and 3.5). The experimental growth data here reported were collected during WT cultivation in PBR operated in semicontinuous mode, as described in section 2.1.2. (color, 2-columns fitting image).

Prediction of the performances of hypothetical photosynthetic mutants in PBR.

Economic competitiveness of algae exploitation is expected to depend from the development of genetically improved strains (Simionato et al., 2013; Wobbe et al., 2015). Examples of modifications proposed to have potential benefits on productivity are the reduction of Chl content per cell, decrease of antenna size (AS) and NPQ (Formighieri et al., 2012). The model described above includes all these factors explicitly and it is thus possible to predict *in silico* the effect of such modifications on productivity by modifying the values of the corresponding photosynthetic parameters (see 3.1 and 3.5).

In order to simulate a reduction in the activation of NPQ is indeed sufficient to reduce the values of the parameters $\bar{\eta}_{qE}^{F}$, $\bar{\eta}_{qE}^{S}$ and $\bar{\eta}_{qE}^{C}$, which represent the contribution of the different components to this regulatory process, that are also activated with different timescales (see equation 15, see 3.1 and 3.5 for details). The antenna size of PSII (ASII) is instead expressed as the ratio between σ/N, which are the chlorophyll specific total cross section of the photosystems and the number of chlorophylls associated with each

reaction center, respectively. Therefore, in order to simulate a reduction of ASII, both σ and N have to be modified accordingly (see 3.1 and 3.5 for details).

Finally, given the parameter σ indeed depends on the self-shading between chlorophyll molecules, it is thus expected to be a decreasing function of the Chl content (see supplementary figure S2). Therefore, in order to simulate a reduction in the Chl content of the cells is sufficient to reduce the self-shading between chlorophylls and increase the value of σ (see 3.1 and 3.5 for details).

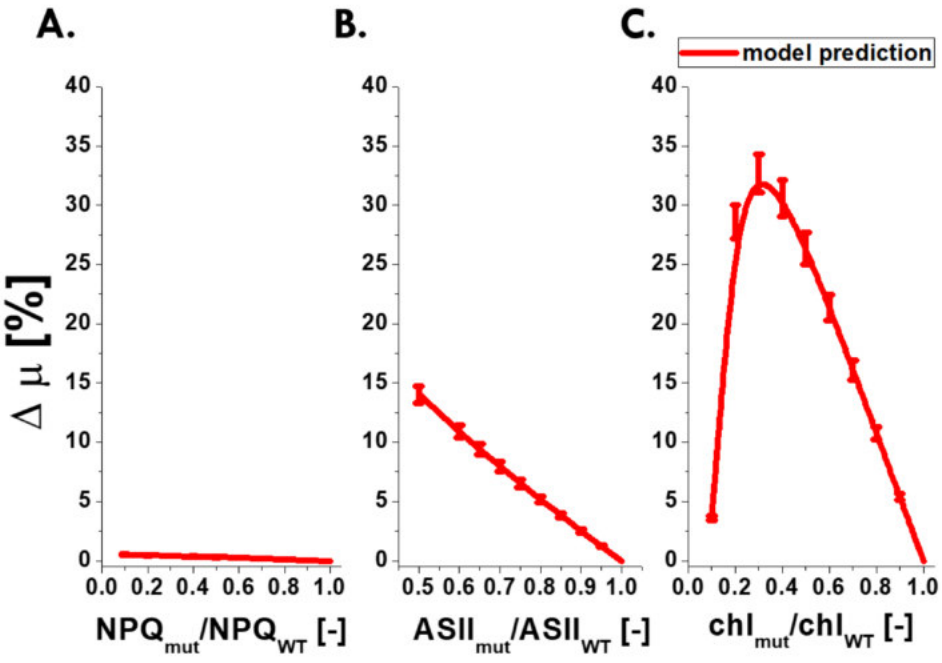

Figure 3. Growth prediction for *Nannochloropsis gaditana* photosynthetic mutants. The effect of modifications in the NPQ, ASII and Chl content on algae cultures productivity is shown in A, B and C, respectively. The increase in the specific growth rate of the hypothetical photosynthetic mutants (squares and solid lines) is here expressed as percentage with respect to the WT strain. Error bars for the predictions of the model come from the uncertainty of both σ and τ parameters (see 3.4 and 3.5). A maximal reduction of 50 % in the ASII was considered, since a significant fraction of the pigments are bound to the reaction centers and are thus not depletable (Melis, 1991). The predicted growth rate increase was calculated considering a starting biomass concentration ($x_{biom}(0)$) of 1.3 g L^{-1} for the WT strain, a median value of those concentrations considered in figure 2 (color, 1.5-column fitting image).

As shown in figure 3, according to the model predictions, all suggested modifications are expected to provide a benefit in the specific growth rate with respect to the WT. The impact is however largely different. For instance, the reduction in NPQ activation is predicted to have only a minimal effect (e.g. 0.5 % increase when $NPQ_{mut} / NPQ_{WT} = 0.1$, Figure 3A). This could be due to the fact that, at the considered growth conditions, the

model predicts a very modest activation of NPQ, with a 10 % of maximal activation in the more external layers (Figure 4) (in the model this activity is represented by the variables α_F and α_S, see 3.1 for details).

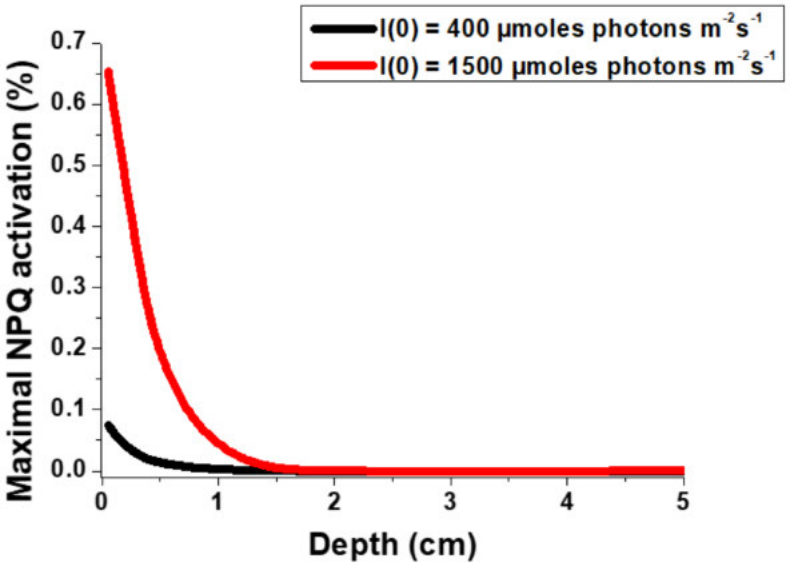

Figure 4. Model prediction of the maximal NPQ activation during *Nannochloropsis gaditana* cultivation in PBR. The prediction of NPQ activation is here expressed as percentage of its maximal activity for *Nannochloropsis gaditana* WT strain, as a function of the depth (in centimeters, cm) of the PBR. Two profiles of NPQ activation are here indicated, as a consequence of the light intensity reaching the culture, respectively 400 (black curve) or 1500 (red curve) µmoles photons $m^{-2}s^{-1}$. (color, 1-column fitting image).

However, *in silico* simulations suggest that even if a stronger illumination is adopted, for instance *I(0) = 1500* µmoles photons $m^{-2}s^{-1}$, inducing a stronger activation of NPQ (65 % of maximal activation in the more external layers, figure 4), the reduction of NPQ activation would however not lead to a greater gain in productivity. This can be explained because the reduction in this photo-protection mechanism indeed reduces energy dissipation in light limited cells but is also expected to reduce the ability of more external layers to withstand intense illumination. The latter cells are thus predicted to suffer higher light damage in the more external layers (Figure 5).

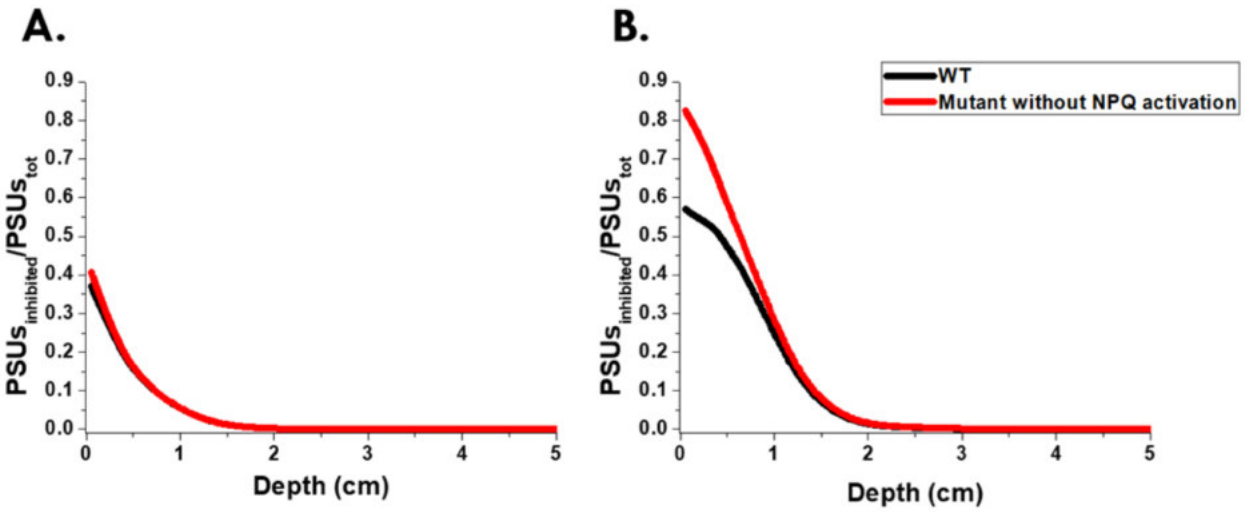

Figure 5. Model prediction of the inhibited photosynthetic units (PSUs) during *Nannochloropsis gaditana* cultivation in PBR. The prediction of the number of inhibited PSUs is here expressed as fraction of the total PSUs for *Nannochloropsis gaditana*, as a function of the depth (in centimeters, cm) of the PBR. The fraction of inhibited PSUs is here reported for cultures illuminated with 400 or 1500 µmoles photons $m^{-2}s^{-1}$, respectively in A and in B. Two profiles of fractions of inhibited PSUs are indicated in both panels, the black one refers to the WT, while the red one to an hypothetical mutant unable to activate NPQ. (color, 2-columns fitting image).

The reduction in the ASII shows a larger positive impact, with up to 14 % increase in the specific growth rate with a theoretical 50 % ASII reduction (Figure 3B). The modification with the largest potential impact is however the reduction in the Chl content that leads to more than a 30 % increase with respect to the WT with a ≈ 60 % reduction (Figure 3C). It is interesting to point out that the model also predicts that below this limit, the Chl reduction becomes actually detrimental, causing a decrease in the productivity advantage. This can be explained by the fact that algae culture transparency in this case is so large that a significant part of incident light is not absorbed (25 % according to the model prediction, see figure 6).

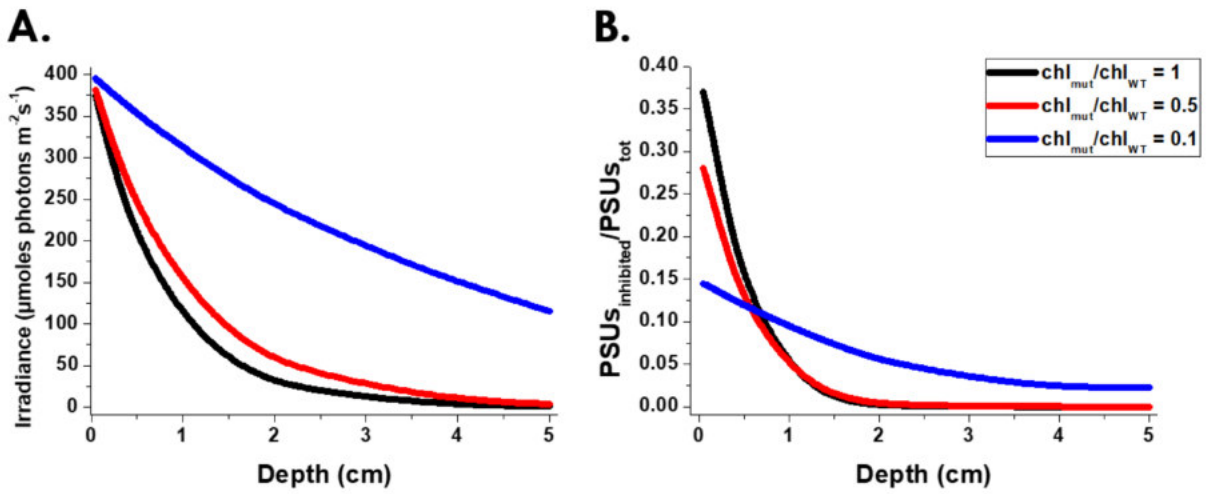

Figure 6. Model prediction of the light profile in the PBR as a function of the Chl content of the *Nannochloropsis gaditana* cells. The prediction of the irradiance reaching different culture layers and the fraction of the inhibited PSUs is expressed as a function of the depth (in centimeters, cm) of the PBR, respectively in A and B. Both panels show different profiles of irradiance or inhibited PSUs, according to the increasing reduction in the Chl content of mutant cells; chl_{mut}/chl_{WT} = 1 in black, chl_{mut}/chl_{WT} = 0.5 in red, chl_{mut}/chl_{WT} = 0.1 in blu. (color, 2-columns fitting image).

Validation of the model with experimental data of Nannochloropsis gaditana photosynthetic mutants.

The mathematical model previously described is expected to have a high potential in predicting the impact of different modifications of the photosynthetic apparatus on productivity and also in providing additional information on the status of the culture, such as the extent of the light induced damage (Figure 5A-B and 6B). We therefore assessed this hypothesis and the whole model prediction ability using three available *N. gaditana* photosynthetic mutants (Perin et al., 2015). As shown in Table 1, these mutants show variable alterations in the photosynthetic parameters here considered, since NPQ, ASII and Chl content are not completely independent and thus in real strains they show combined effects.

Strain	NPQ_{mut}/NPQ_{WT}	$ASII_{mut}/ASII_{WT}$	chl_{mut}/chl_{WT}	$Productivity_{mut}/Productivity_{WT}$	μ_{mut}/μ_{WT}
I48	0.05	0.95	0.85	1.13 ± 0.05	1.12 ± 0.04
E2	0.5	0.9	0.8	1.15 ± 0.06	1.18 ± 0.04
I29	1	0.75	0.57	1.17 ± 0.05	1.44 ± 0.05

Table 1. Photosynthetic properties and growth of selected *Nannochloropsis gaditana* mutant strains in PBR. The photosynthesis and growth data here reported were determined experimentally for microalgae cultivated in PBR operated in semicontinuous mode, as described in section 2.1.2. All data are here represented relatively to WT strain, while the whole panel of experimentally determined values is shown in supplementary figure S3. All these data indicate statistically significant differences between mutants and parental strain (One-way ANOVA, p-value < 0.05); n > 20 for photosynthetic data; n > 40 for growth data. (no color, 2-columns fitting table)

As shown in Table 1, I48 shows the largest reduction (95 %) in NPQ with respect to the WT strain and a smaller reduction, 5 and 15 %, in both ASII and Chl content, respectively. On the contrary, strain E2 shows a larger difference in ASII and Chl content and a more contained reduction in NPQ (50 %), as reported in Table 1. The third mutant, I29, shows instead an unaltered NPQ value than the parental strain and the largest reduction in both ASII and Chl content (Table 1). All three strains also showed an increased biomass productivity and specific growth rate with respect to the parental strain, during the cultivation in PBR (Table 1 and supplementary figure S3).

Experimental productivities were thus compared with model predictions for strains showing specific alterations in photosynthetic properties. As shown in figure 7, there is a very good fit for both E2 and I48 strains, while the increase in the specific growth rate for I29 exceeds the model prediction. Measured productivities also fully confirmed the model prediction, that alterations in NPQ activation have limited effects on *N. gaditana* productivity, at least for cells exposed to the growth conditions tested in this work (Figure 3A). On the other hand, the reduction in Chl content confirmed to have the largest impact on productivity in the tested conditions (Figure 7). I29 indeed showed the largest reduction in both ASII and Chl content with respect to the WT strain (Table 1) and also the best performances (Figure 7, Supplementary figure S4).

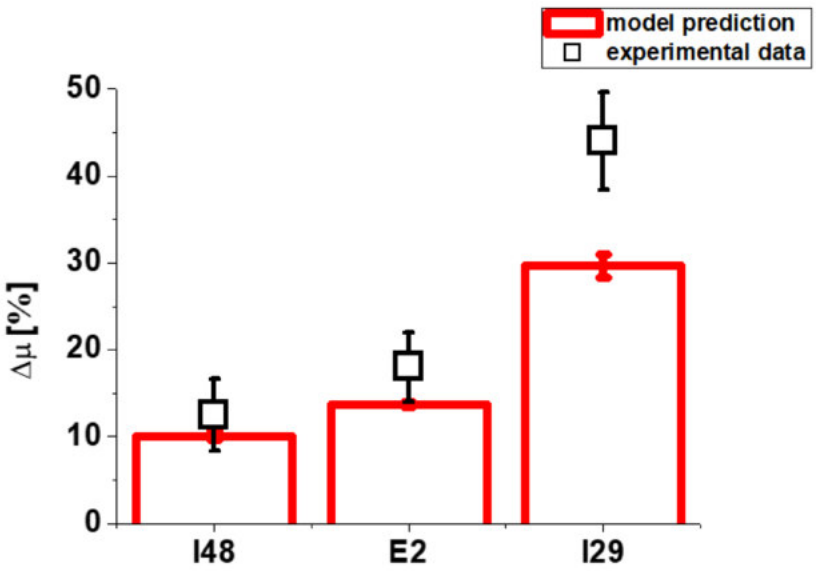

Figure 7. Model validation to drive genetic engineering of photosynthesis. The model prediction for the increase in the specific growth rate of selected *N. gaditana* photosynthetic mutants, expressed as percentage with respect to the WT, is here depicted by the histograms. Error bars for the predictions of the model come from the uncertainty of both σ and τ parameters (see 3.4 and 3.5). Solid squares instead represent the experimentally measured values of the specific growth rates for the three photosynthetic mutants available, when cultivated in PBR, according to the conditions chosen in this work (see 2.1.2 for details). Experimental measured data belong to a population with n > 40. The predicted growth rate increase was calculated considering as starting biomass concentration ($x_{biom}(0)$) for the WT strain, the average of the experimentally measured values (1.3 g/L). The whole model prediction profile is reported in supplementary figure S4) (color, 1-column fitting image)

The discrepancy between measured and predicted values in the case of I29 is likely due to an alteration in cells size in this strain with respect to the WT (50 % reduction). Even if culture biomass productivity does not directly depend form the cells size, this is a model parameter and thus if it is significantly altered in the mutant, it can affect the results. Moreover, we should point out that to predict the growth of I29 mutant we are using the model in extrapolation and a discrepancy between predicted and measured values is expected and acceptable.

It is worth noting that this model was calibrated only with photosynthetic data of the WT strain cultivated in PBR (e.g. Chl fluorescence, photosynthesis evaluation) and the growth predictions for the photosynthetic phenotypes here presented derive just from alterations of the WT parameters, performed *in silico*. Therefore, this model avoids the need to characterize the photosynthetic mutants experimentally, in order to predict the gain in growth achievable with their phenotypes, thus contributing to reduce the time and

experimental costs to achieve concrete improvements in the field of algae genetic engineering.

DISCUSSION

In this work, we developed a quantitative model to predict microalgae growth during intensive cultivation in a PBR, combining a model describing photosynthetic productivity as function of the available light (Bernardi et al., 2016) with the mathematical description of the light attenuation profile in a microalgae dense culture. The model was shown to be able to describe quantitatively microalgae growth in such environment and the influence of different light supply rates (Figure 2). It can be concluded that the presented model thus accounts for major parameters influencing microalgae growth in a PBR (see section 3 for details).

We thus decided to exploit the model developed in this work to simulate *in silico* alterations in key photosynthetic parameters, in order to evaluate whether their effect on light use efficiency could influence the growth in PBR. We assumed hypothetical reductions in ASII, Chl content and NPQ and observed that such alterations were predicted to have an overall positive effect on growth of microalgae cells (Figure 3). Model predictions suggested that different modifications had different impact on growth, with NPQ showing a negligible effect, while the Chl content was identified as the most promising target of genetic engineering (Figure 3). The reliability of the model predictions was tested with three photosynthetic mutants showing variable combinations of modifications of the photosynthetic apparatus, obtaining a satisfactory correspondence with experimental data (Figure 7). The developed model can thus be used to efficiently predict the effect of genetic modifications of the photosynthetic apparatus on algae productivity in PBR and it pushes genetic engineering towards the isolation of mutants with the greatest reduction in both ASII and Chl content parameters.

In the case of one mutant, I29, the difference between the model prediction and real data was larger, likely because the mutation also caused an alteration in cells size that was not included in the model. If a genetic modification indeed affects a feature which was not parametrized in the model, the latter would lose accuracy in its prediction capacity. This observation is useful as reminder that the model cannot predict phenomena that are not included and properly described. On the other hand, the satisfactory fit between

predictions and experimental data suggests that major phenomena affecting productivity are mathematically described and included.

This result suggests that the model can be exploited to predict reliably the performances of a modified strain without expensive larger scale validations. The presented model clearly suggests that the Chl content is the most impactful parameter and this, in combination with a reduction in antenna size, has the potential to provide a 43 % increase in biomass productivity (see supplementary figure S5). This model could thus make the whole process of isolation of improved strains much more efficient, reducing experimental time and costs. It is also worth underlining that once proved its applicability, such a model can be also applied to tailor the genetic modifications to reach the best productivities depending on the cultivation system used (e.g pond vs. PBR, semicontinuous vs continuous cultivation etc.) or on the environmental conditions at the installation site (e.g tropical or temperate areas). In the longer term, such model will be implemented to provide specific answers for each cultivation condition and will open the gates for the generation of strains tailored to a specific cultivation site.

It is also important to point out the limitations of the model, due to its construction. First of all, this model assumes that growth depends strictly from the available light, that is a correct assumption only when nutrients and CO_2 are provided in excess to the cultures as done here. Another limitation of the current model is that it describes algae growth in a stable cultivation environment where cells indeed show a unique photosynthetic acclimation state and it does not include the effects of a dynamic light environment.

Finally, the biological significance of model equations is general and do not depend from the species. However, the parameters were estimated using photosynthesis data of *Nannochloropsis gaditana* cells. The developed model could thus be applied to predict the growth in PBR of other algae species and consequently the effect on growth of modifications of their photosynthetic metabolism, after re-parametrization with new experimental data.

CONCLUSIONS

In this work, we developed an empirical light attenuation model to describe the light profile inside high density algae cultures. By combining this model with the mathematical description of algae photosynthetic productivity as function of available light, we predicted the growth of *Nannochloropsis gaditana* during cultivation in PBR. By changing the values of key photosynthetic parameters of the model is was possible to predict the growth of strains with altered photosynthetic phenotypes. Model predictions were validated with data from photosynthetic mutants, demonstrating that this tool can be exploited to direct genetic engineering *in silico* towards those photosynthetic targets showing the highest impact on biomass productivity.

ACKNOWLEDGMENTS

ABellan is grateful to the Interdepartmental Centre "Giorgio Levi Cases" for Energy Economics and Technology of the University of Padova for support.

AUTHORS' CONTRIBUTIONS

TM and FB designed the research; GP and ABellan performed the photosynthesis measurements and growth monitoring in PBR; ABernardi and FB built the mathematical models; GP and ABernardi analyzed data; GP and TM wrote the manuscript. All authors read and approved the final manuscript.

FUNDING

This work was supported by the ERC Starting Grant BioLEAP to TM [grant number: 309485].

COMPETING INTERESTS

The authors declare that they have no competing interests.

REFERENCES

Alboresi, A., Le Quiniou, C., Yadav, S.K.N., Scholz, M., Meneghesso, A., Gerotto, C., Simionato, D., Hippler, M., Boekema, E.J., Croce, R., Morosinotto, T., 2016. Conservation of core complex subunits shaped the structure and function of photosystem I in the secondary endosymbiont alga Nannochloropsis gaditana. doi:10.1111/nph.14156

Béchet, Q., Chambonnière, P., Shilton, A., Guizard, G., Guieysse, B., 2015. Algal productivity modeling: A step toward accurate assessments of full-scale algal cultivation. Biotechnol. Bioeng. 112, 987–996. doi:10.1002/bit.25517

Benvenuti, G., Lamers, P.P., Breuer, G., Bosma, R., Cerar, A., Wijffels, R.H., Barbosa, M.J., 2016. Microalgal TAG production strategies: why batch beats repeated-batch. Biotechnol. Biofuels 9, 64. doi:10.1186/s13068-016-0475-4

Bernardi, A., Nikolaou, A., Meneghesso, A., Morosinotto, T., Chachuat, B., Bezzo, F., 2016. High-fidelity modelling methodology of light-limited photosynthetic production in microalgae. PLoS One 11. doi:10.1371/journal.pone.0152387

Berteotti, S., Ballottari, M., Bassi, R., 2016. Increased biomass productivity in green algae by tuning non-photochemical quenching. Sci. Rep. 6, 21339. doi:10.1038/srep21339

Bondioli, P., Della Bella, L., Rivolta, G., Chini Zittelli, G., Bassi, N., Rodolfi, L., Casini, D., Prussi, M., Chiaramonti, D., Tredici, M.R., 2012. Oil production by the marine microalgae Nannochloropsis sp. F&M-M24 and Tetraselmis suecica F&M-M33. Bioresour. Technol. 114, 567–72. doi:10.1016/j.biortech.2012.02.123

Cazzaniga, S., Dall'Osto, L., Szaub, J., Scibilia, L., Ballottari, M., Purton, S., Bassi, R., 2014. Domestication of the green alga Chlorella sorokiniana: reduction of antenna size improves light-use efficiency in a photobioreactor. Biotechnol. Biofuels 7, 157. doi:10.1186/s13068-014-0157-z

Cornet, J.-F., Dussap, C.G., Gros, J.-B., Binois, C., Lasseur, C., 1995. A simplified monodimensional approach for modeling coupling between radiant light transfer and growth kinetics in photobioreactors. Chem. Eng. Sci. 50, 1489–1500. doi:10.1016/0009-2509(95)00022-W

Cornet, J.F., Dussap, C.G., Cluzel, P., Dubertret, G., 1992. A structured model for simulation of cultures of the cyanobacterium Spirulina platensis in photobioreactors:

II. Identification of kinetic parameters under light and mineral limitations. Biotechnol. Bioeng. 40, 826–34. doi:10.1002/bit.260400710

Dall'Osto, L., Bressan, M., Bassi, R., 2015. Biogenesis of light harvesting proteins. Biochim. Biophys. Acta 1847, 861–71. doi:10.1016/j.bbabio.2015.02.009

de Mooij, T., Janssen, M., Cerezo-Chinarro, O., Mussgnug, J.H., Kruse, O., Ballottari, M., Bassi, R., Bujaldon, S., Wollman, F.-A., Wijffels, R.H., 2014. Antenna size reduction as a strategy to increase biomass productivity: a great potential not yet realized. J. Appl. Phycol. doi:10.1007/s10811-014-0427-y

De Vree, J.H., Bosma, R., Janssen, M., Barbosa, M.J., Wijffels, R.H., 2015. Comparison of four outdoor pilot-scale photobioreactors 8. doi:10.1186/s13068-015-0400-2

Demmig-Adams, B., Adams, W.W., Winter, K., Meyer, A., Schreiber, U., Pereira, J.S., Krüger, A., Czygan, F.C., Lange, O.L., 1989. Photochemical efficiency of photosystem II, photon yield of O2 evolution, photosynthetic capacity, and carotenoid composition during the midday depression of net CO2 uptake in Arbutus unedo growing in Portugal. Planta 177, 377–87. doi:10.1007/BF00403596

Erickson, E., Wakao, S., Niyogi, K.K., 2015. Light stress and photoprotection in Chlamydomonas reinhardtii. Plant J. 82, 449–65. doi:10.1111/tpj.12825

Falkowski, P.G.. G.R.. K.Z., 1993. Light utilization and photoinhibition of photosynthesis in marine phytoplankton.

Falkowski, P.G., Raven, J.A., 2013. Aquatic Photosynthesis: (Second Edition).

Formighieri, C., Franck, F., Bassi, R., 2012. Regulation of the pigment optical density of an algal cell: filling the gap between photosynthetic productivity in the laboratory and in mass culture. J. Biotechnol. 162, 115–23. doi:10.1016/j.jbiotec.2012.02.021

Gangl, D., Zedler, J.A.Z., Rajakumar, P.D., Martinez, E.M.R., Riseley, A., Włodarczyk, A., Purton, S., Sakuragi, Y., Howe, C.J., Jensen, P.E., Robinson, C., 2015. Biotechnological exploitation of microalgae. J. Exp. Bot. doi:10.1093/jxb/erv426

Han, B.-P., Virtanen, M., Koponen, J., Stras ˇkraba, M., 2000. Effect of photoinhibition on algal photosynthesis: a dynamic model. J. Plankton Res. 22, 865–885.

Kirst, H., Garcia-Cerdan, J.G., Zurbriggen, A., Ruehle, T., Melis, A., 2012. Truncated photosystem chlorophyll antenna size in the green microalga Chlamydomonas reinhardtii upon deletion of the TLA3-CpSRP43 gene. Plant Physiol. 160, 2251–60. doi:10.1104/pp.112.206672

Kramer, D.M., Johnson, G., Kiirats, O., Edwards, G.E., 2004. New Fluorescence Parameters for the Determination of Q_A Redox State and Excitation Energy Fluxes.

Photosynth. Res. 79, 209–218. doi:10.1023/B:PRES.0000015391.99477.0d

Leu, S., Boussiba, S., 2014. Advances in the Production of High-Value Products by Microalgae. Ind. Biotechnol. 10, 169–183. doi:10.1089/ind.2013.0039

Maxwell, K., Johnson, G.N., 2000. Chlorophyll fluorescence - A practical guide. J. Exp. Bot.

Melis, A., 1991. Dynamics of photosynthetic membrane composition and function. Biochim. Biophys. Acta - Bioenerg. 1058, 87–106. doi:10.1016/S0005-2728(05)80225-7

Mitra, M., Kirst, H., Dewez, D., Melis, A., 2012. Modulation of the light-harvesting chlorophyll antenna size in Chlamydomonas reinhardtii by TLA1 gene over-expression and RNA interference. Philos. Trans. R. Soc. Lond. B. Biol. Sci. 367, 3430–43. doi:10.1098/rstb.2012.0229

Moran, R., Porath, D., 1980. Chlorophyll determination in intact tissues using n,n-dimethylformamide. Plant Physiol. 65, 478–9.

Nikolaou, A., Bernardi, A., Meneghesso, A., Bezzo, F., Morosinotto, T., Chachuat, B., 2015. A model of chlorophyll fluorescence in microalgae integrating photoproduction, photoinhibition and photoregulation. J. Biotechnol. 194. doi:10.1016/j.jbiotec.2014.12.001

Peers, G., Truong, T.B., Ostendorf, E., Busch, A., Elrad, D., Grossman, A.R., Hippler, M., Niyogi, K.K., 2009. An ancient light-harvesting protein is critical for the regulation of algal photosynthesis. Nature 462, 518–21. doi:10.1038/nature08587

Perin, G., Bellan, A., Segalla, A., Meneghesso, A., Alboresi, A., Morosinotto, T., 2015. Generation of random mutants to improve light-use efficiency of Nannochloropsis gaditana cultures for biofuel production. Biotechnol. Biofuels 8, 161. doi:10.1186/s13068-015-0337-5

Pinnola, A., Dall'Osto, L., Gerotto, C., Morosinotto, T., Bassi, R., Alboresi, A., 2013. Zeaxanthin binds to light-harvesting complex stress-related protein to enhance nonphotochemical quenching in Physcomitrella patens. Plant Cell 25, 3519–34. doi:10.1105/tpc.113.114538

Polle et al., 2002. Truncated chlorophyll antenna size of the photosystems?a practical method to improve microalgal productivity and hydrogen production in mass culture. Int. J. Hydrogen Energy 27, 1257–1264. doi:10.1016/S0360-3199(02)00116-7

Porra, R.J., Thompson, W.A., Kriedemann, P.E., 1989. Determination of accurate

extinction coefficients and simultaneous equations for assaying chlorophylls a and b extracted with four different solvents: verification of the concentration of chlorophyll standards by atomic absorption spectroscopy. Biochim. Biophys. Acta - Bioenerg. 975, 384–394. doi:10.1016/S0005-2728(89)80347-0

Rodolfi, L., Chini Zittelli, G., Bassi, N., Padovani, G., Biondi, N., Bonini, G., Tredici, M.R., 2009. Microalgae for oil: strain selection, induction of lipid synthesis and outdoor mass cultivation in a low-cost photobioreactor. Biotechnol. Bioeng. 102, 100–12. doi:10.1002/bit.22033

Sforza, E., Bertucco, A., Morosinotto, T., Giacometti, G.M., 2012. Photobioreactors for microalgal growth and oil production with Nannochloropsis salina: From lab-scale experiments to large-scale design. Chem. Eng. Res. Des. 90, 1151–1158. doi:10.1016/j.cherd.2011.12.002

Sforza, E., Calvaruso, C., Meneghesso, A., Morosinotto, T., Bertucco, A., 2015. Effect of specific light supply rate on photosynthetic efficiency of Nannochloropsis salina in a continuous flat plate photobioreactor. Appl. Microbiol. Biotechnol. 99, 8309–18. doi:10.1007/s00253-015-6876-7

Simionato, D., Basso, S., Giacometti, G.M., Morosinotto, T., 2013. Optimization of light use efficiency for biofuel production in algae. Biophys. Chem. 182, 71–8. doi:10.1016/j.bpc.2013.06.017

Vieler, A., Wu, G., Tsai, C.-H.H., Bullard, B., Cornish, A.J., Harvey, C., Reca, I.-B.B., Thornburg, C., Achawanantakun, R., Buehl, C.J., Campbell, M.S., Cavalier, D., Childs, K.L., Clark, T.J., Deshpande, R., Erickson, E., Armenia Ferguson, A., Handee, W., Kong, Q., Li, X., Liu, B., Lundback, S., Peng, C., Roston, R.L., Sanjaya, Simpson, J.P., TerBush, A., Warakanont, J., Zäuner, S., Farre, E.M., Hegg, E.L., Jiang, N., Kuo, M.-H.H., Lu, Y., Niyogi, K.K., Ohlrogge, J., Osteryoung, K.W., Shachar-Hill, Y., Sears, B.B., Sun, Y., Takahashi, H., Yandell, M., Shiu, S.-H.H., Benning, C., 2012. Genome, functional gene annotation, and nuclear transformation of the heterokont oleaginous alga Nannochloropsis oceanica CCMP1779. PLoS Genet. 8, e1003064. doi:10.1371/journal.pgen.1003064

Wellburn, A.R., 1994. The spectral determination of chlorophylls a and b, as well as total carotenoids, using various solvents with spectrophotometers of different resolution. J. Plant Physiol. 144, 307–313.

Wobbe, L., Bassi, R., Kruse, O., 2015. Multi-Level Light Capture Control in Plants and Green Algae. Trends Plant Sci. doi:10.1016/j.tplants.2015.10.004

Wobbe, L., Remacle, C., 2014. Improving the sunlight-to-biomass conversion efficiency in microalgal biofactories. J. Biotechnol. doi:10.1016/j.jbiotec.2014.08.021

Yokota, T., Yashima, K., Takigawa, T., Takahashi, K., 1991. A new random-walk model for assessment of light energy absorption by a photosynthetic microorganism. J. Chem. Eng. JAPAN 24, 558–562. doi:10.1252/jcej.24.558

Yun, Y.S., Park, J.M., 2001. Attenuation of monochromatic and polychromatic lights in Chlorella vulgaris suspensions. Appl. Microbiol. Biotechnol. 55, 765–70.

SUPPLEMENTARY MATERIAL

Supplementary Table S1. Values of $I^{w}(h)$ and $I^{WT}(h, x_{biom})$ for the *Nannochloropsis gaditana* WT and mutant strains I48 and E2.

Supplementary figure S1. Schematic representation of the lab-scale PBR used in this work.

Supplementary figure S2. Estimated ratio between σ in *Nannochloropsis gaditana* mutants showing a reduction in both Chl content and ASII in PBR and the value of the wild type strain.

Supplementary figure S3. Experimental data collected for all the *Nannochloropsis gaditana* strains exploited in this work.

Supplementary figure S4. Model validation.

Supplementary Figure S5. Model prediction of the greatest improvement in growth achievable in *Nannochloropsis gaditana*.

SUPPLEMENTARY MATERIAL

SUPPLEMENTARY TABLES.

Parameter/Variable	Description	Unit
ASII	Antenna size of photosystem II	e^- per sec per PSI
Chl	Chlorophyll content per cell	pg / cell
F	Fluorescence flux	V
$\mathbf{F'_m}$	Maximum fluorescence fluxe	V
$\mathbf{F'_0}$	Minimum fluorescence fluxe	V
$\mathbf{k_d}$	Damage rate constant	/
$\mathbf{k_r}$	Repair rate constant	s^{-1}
$\boldsymbol{K_{LB}}$	Light attenuation coefficient	m^{-1}
I	Light intensity	µmoles photons m^{-2} s^{-1}
M	Respiration factor	$g_{O2}/g_{chl}h$
N	Chlorophyll specific number of Photosynthetic units	$\mu moles_{O2}\ g^{-1}chl$
P	Oxygen evolution rate	$g_{O2}/g_{chl}h$
$\boldsymbol{S_F}$	Fluorescence instrument parameter	$Vg_{chl}\ m^{-2}$
z	Culture depth	m
$\boldsymbol{x_{biom}}$	Biomass concentration	$g\ L^{-1}$
$\boldsymbol{\alpha_F}$	Fast component of NPQ	/
$\boldsymbol{\alpha_S}$	Slow component of NPQ	/
σ	Chlorophyll specific total cross section of the photosystems	$m^2\ g^{-1}{}_{chl}$
τ	Turnover rate of the PSII	s^{-1}
$\boldsymbol{\phi_f}$	Fluorescence quantum yield	/
$\boldsymbol{\upsilon}$	Stoichiometric factor for water molecule dissociation	/
$\boldsymbol{\eta_P}$	Rate of photoproduction	/
$\boldsymbol{\eta_D}$	Rate of basal thermal decay in dark-adapted state	/
$\boldsymbol{\eta_I}$	Rate of qI-quenching	/
$\boldsymbol{\eta_{qE}}$	Quenching of LHC and zeaxanthin	/
$\boldsymbol{\overline{\eta}^F_{qE}}$	Rate of fast components of NPQ	/
$\boldsymbol{\overline{\eta}^S_{qE}}$	Rate of slow components of NPQ	/
$\boldsymbol{\overline{\eta}^C_{qE}}$	Enhancing effect of zeaxanthin in LHC quenching	/
$\boldsymbol{\xi_F}$	Fast quenching time constant	s^{-1}
$\boldsymbol{\xi_S}$	Slow quenching time constant	s^{-1}
µ	Growth rate constant	d^{-1}

Supplementary Table S1. Summary of all model variables and parameters including unit of measure.

$I(0)$	$I^w(h)$	x_{biom}	$I^{WT}(h, x_{biom})$	$I^{E2}(h, x_{biom})$	$I^{I48}(h, x_{biom})$
104	33	50	20.17	26.73	25
210	55.67	50	44.50	48.67	48.33
310	102	50	61.60	73.83	74.33
430	119	50	70.67	80.33	81.33
788	239	50	148.33	169.33	168
1300	414	50	233	283.67	274.67
104	33	150	11.67	12.67	12.87
210	55.67	150	20.83	19.67	23.67
310	102	150	30.33	34.33	34.33
430	119	150	36.33	41	41.33
788	239	150	72.67	88.67	80.00
1300	414	150	117.33	151.67	138
104	33	250	8.27	7.87	7.13
210	55.67	250	15	12.67	11.13
310	102	250	21.67	24.33	24.30
430	119	250	27.33	30	29
788	239	250	47.83	60	63
1300	414	250	81.33	99.33	93.33
104	33	350	6.27	6.43	6.33
210	55.67	350	12.13	9.97	9.83
310	102	350	18.17	21.33	19
430	119	350	20.67	23.87	22.2
788	239	350	36.90	47.67	42.67
1300	414	350	69	89	76.67
104	33	500	5.03	5.1	4.7
210	55.67	500	9.1	10.67	8.1
310	102	500	13.17	17	16
430	119	500	15.37	20.67	18.43
788	239	500	29.83	41.67	35.67
1300	414	500	54.03	73	66.67

Supplementary Table S2. Values of $I^w(h)$ and $I(h, x_{biom})$ measured for the *Nannochloropsis gaditana* WT and mutant strains I48 and E2. These strains were considered for calibrating the light attenuation model in a PBR and to validate the assumption that when the chl content of a mutant strain decreases, σ increases. All light intensity values are expressed in μmoles photons $m^{-2}s^{-1}$, while the biomass concentration (x_{biom}) is expressed as (x 10^6 cells/ml). h is the path length of the cuvette, $I(0)$ is the incident light intensity, $I^w(h)$ is the light measured using a cuvette filled with water (blank) and $I(h, x_{biom})$ is the light measured when the cuvette was filled with the microalgae sample.

	5 cm diameter PBR					
	The Netherlands		Italy		Gibraltar	
	WT	E2	WT	E2	WT	E2
	Productivity (g d^{-1})		Productivity (g d^{-1})		Productivity (g d^{-1})	
January	0 ± 0.02	0.01 ± 0.01	0.07 ± 0.02	0.11 ± 0.01	0.21 ± 0.03	0.28 ± 0.02
July	0.51 ± 0.1	0.64 ± 0.11	0.57 ± 0.1	0.72 ± 0.12	0.6 ± 0.1	0.75 ± 0.12

	10 cm diameter PBR					
	The Netherlands		Italy		Gibraltar	
	WT	E2	WT	E2	WT	E2
	Productivity (g d^{-1})		Productivity (g d^{-1})		Productivity (g d^{-1})	
January	0 ± 0.07	0 ± 0.05	0 ± 0.07	0 ± 0.05	0.1 ± 0.08	0.31 ± 0.06
July	0.68 ± 0.18	0.96 ± 0.19	0.78 ± 0.17	1.1 ± 0.19	0.86 ± 0.17	1.17 ± 0.2

Supplementary Table S3. Total biomass production predictions in PBRs with different depth. The average total biomass production (g d^{-1}) predictions during a day of outdoor cultivation of both *Nannochloropsis gaditana* WT strain and the photosynthetic improved strain E2 are here represented as a function of the cultivation site (The Netherlands; Italy (Padova) and Gibraltar) and season (January and July), in a cylindrical PBR with 5 or 10 cm diameter and 1 m length. Latitude: 52.4 (The Netherlands); 45.4 (Padova); 36.1 (Gibraltar).

SUPPLEMENTARY FIGURES.

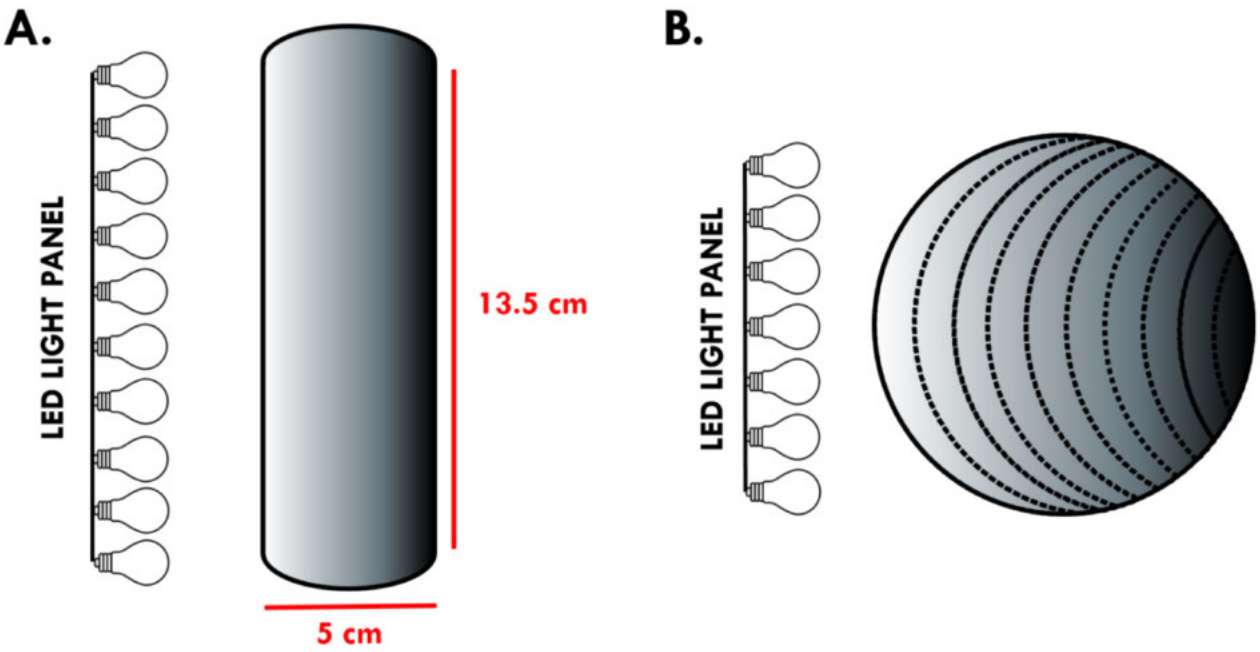

Supplementary figure S1. Schematic representation of the lab-scale PBR used in this work. A led light panel was used to irradiate the culture from one side. A side view of the PBR is represented in A., while a top view is represented in B., where the ten sub-regions in which the PBR was divided to develop the model predicting algae growth are delimited by iso-irradiance curves (dotted lines). Dimensions of the culture are indicated in centimeters (cm).

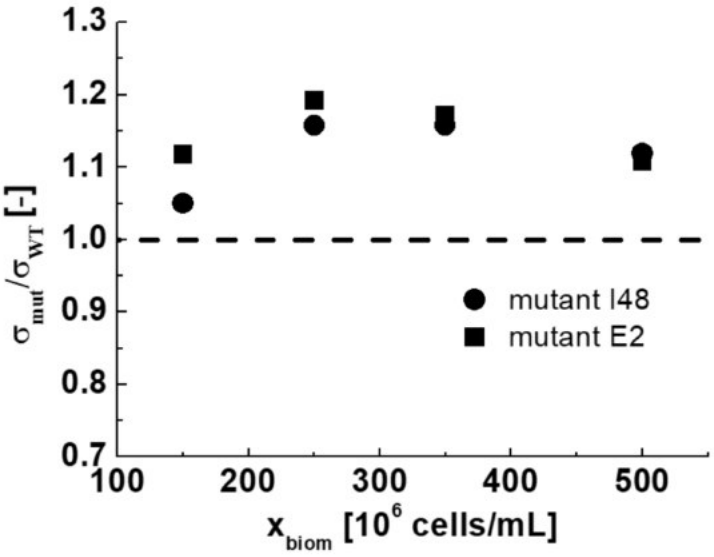

Supplementary figure S2. Estimated ratio between σ in *Nannochloropsis gaditana* mutants showing a reduction in both chl content and ASII in PBR and the value of the wild type strain. Mutants E2 and I48 were exploited to validate the light attenuation profile developed in this work. The dashed line indicates the corresponding value for the WT. The data come from the ratio between the measured absorption coefficient for both mutants and the predicted absorption coefficient, assuming a constant σ for the different cell concentrations here investigated. Only data for high density cultures (cell concentration > 150 x 10^6 cells /ml, corresponding to > 1 g L^{-1}) are here shown.

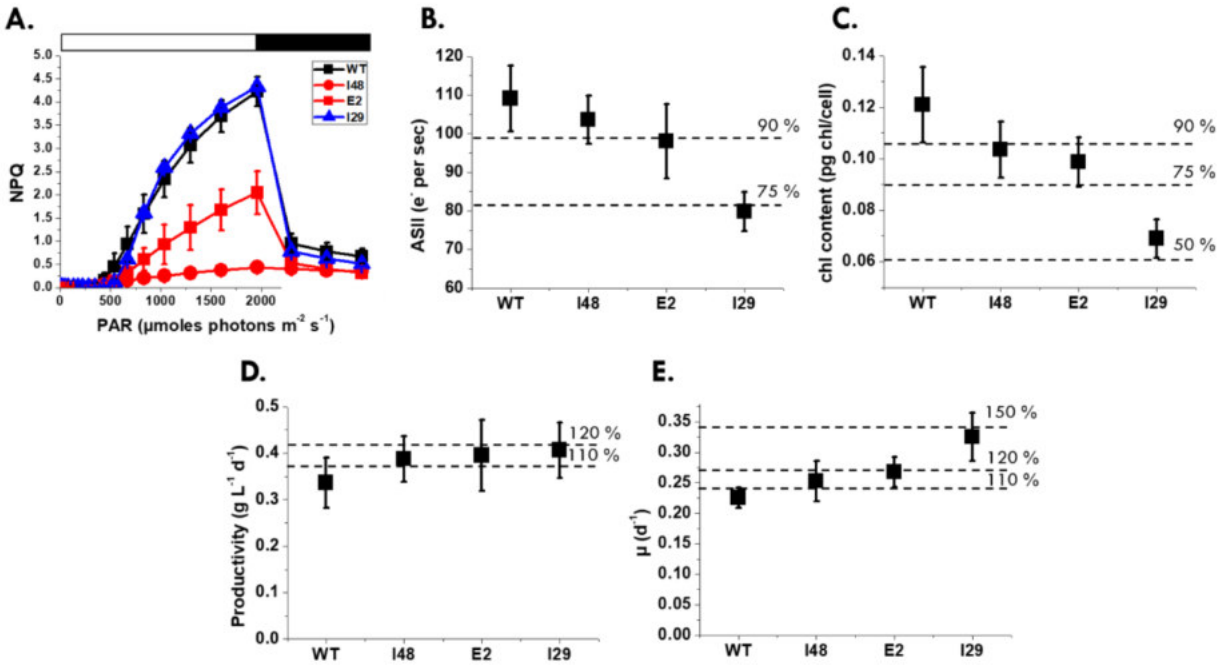

Supplementary figure S3. Experimental data collected for all the *Nannochloropsis gaditana* strains exploited in this work. Photosynthetic data are shown in A – C (NPQ, ASII and chl content respectively in A, B in C), while growth data are shown in D (biomass productivity) and in E (specific growth rate). Photosynthetic data are represented as mean ± SD with n > 20, while growth data are represented as mean ± SD with n > 40. All these data were collected during microalgae cultivation in PBR operated in semicontinous mode, as described in section 2.1 of methods. All the differences between mutants and parental strain shown in this figure are statistically significant (One-way ANOVA, p-value < 0.05).

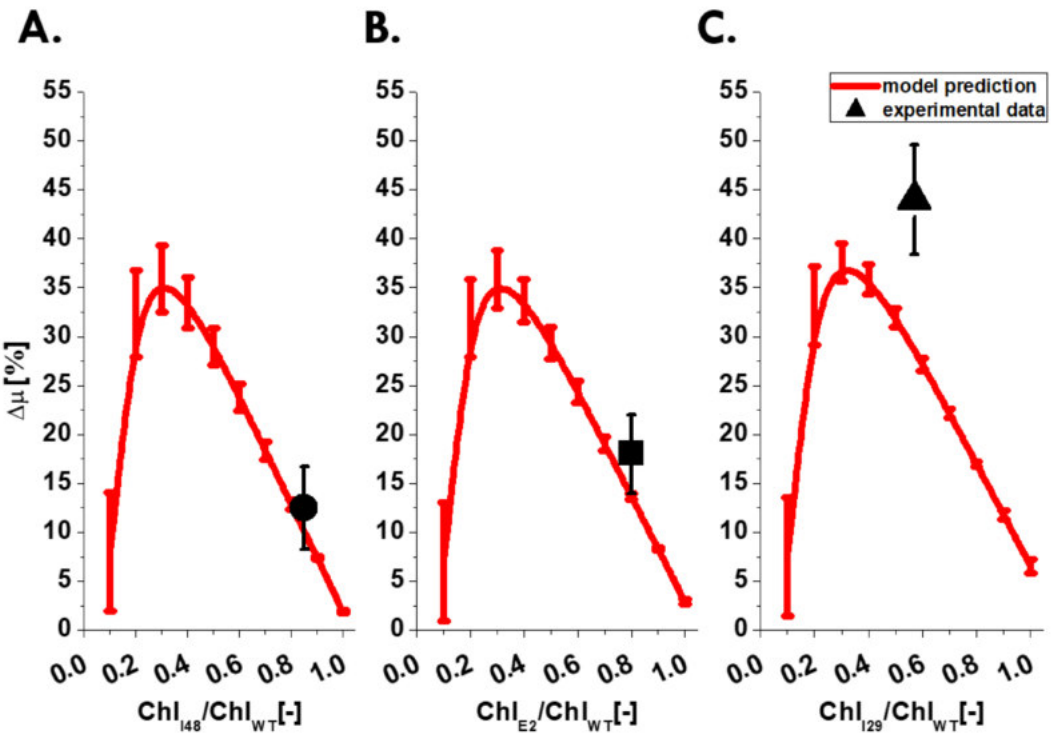

Supplementary figure S4. Model validation. The model prediction for the increase in the specific growth rate of selected *N. gaditana* photosynthetic mutants, expressed as percentage with respect to the WT, is here depicted by the red curves. The reliability of the model was validated by measuring the specific growth rates of *N. gaditana* mutant strains I48, E2 and I29 in PBR, here depicted respectively as black solid circle, square and triangle (see 2.1 for details on the cultivation conditions) in A, B and C, n > 40. The predicted growth rate increase was calculated considering as starting biomass concentration ($x_{biom}(0)$) for the WT strain, the average of the experimentally measured values (1.3 g/L).

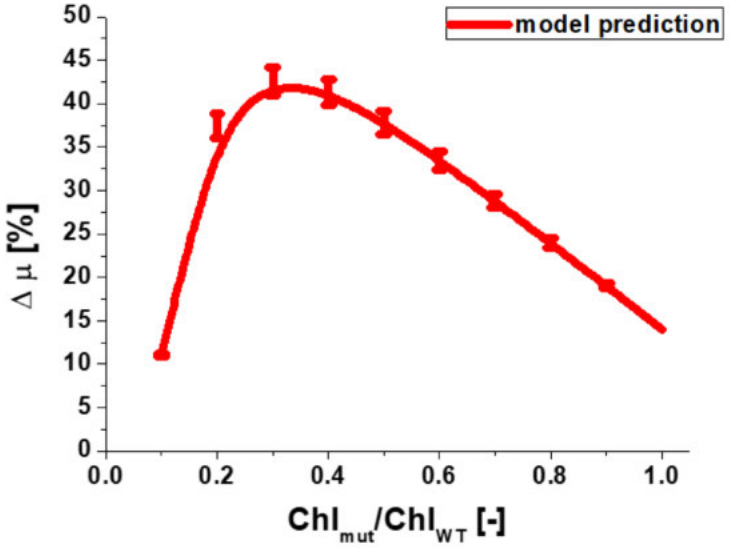

Supplementary Figure S5. Model prediction of the greatest improvement in growth achievable in *Nannochloropsis gaditana*. The increase in the specific growth rate for hypothetical photosynthetic mutants (solid line) is here expressed as percentage with respect to the WT strain as function of the reduction in the chl content of the cells, and assuming a 100 % and 50 % reduction in both NPQ and ASII, respectively. This graph represents the greatest theoretical improvement in growth achievable in *Nannochloropsis gaditana* in the growth conditions tested in this work, according to the model here developed.

APPENDIX III :

Identification of novel regulators of diatom photoacclimation and growth.

CONTRIBUTION:

The following data result from a collaboration with Prof. Angela Falciatore (Diatom Functional Genomics team, at the UPMC-Paris). This is a big project, but in this appendix will be presented only the part in which I was involved. A manuscript about the generation of the TF mutants and the screening procedure is in preparation.

INTRODUCTION

This work is integrated in a bigger project started by the team of Diatom Functional Genomics, at the UPMC-Paris. The basic idea was to generate the first collection of *Phaeodactylum tricornutum* transgenic lines genetically modified by the RNA interference approach (De Riso et al. 2009). Transcription Factors (TFs) are master regulators of cellular processes and have been shown to be excellent candidates both for fundamental research approaches (global understanding of biology) and for applied research (modification of complex traits) (Century et al. 2008; Rabara, Tripathi, and Rushton 2014). The expression of each of the 220 TF found in the diatom genome (Rayko et al. 2010) was modulated by RNAi. 10 transgenic lines potentially silenced for each TF (for a total of ~ 2200 strains) are currently generated, a number that, considering the high efficiency of the RNAi methodology (>30%) to perturb gene expression in diatoms (De Riso et al. 2009), is expected to be sufficient to generate a saturated collection. 1000 strains are already available and the entire collection will be completed by the end of 2017. In order to find new regulators of diatom photosynthesis the collection was analyzed by in vivo fluorescence as reported in (Perin et al. 2015). I was involved in this first large scale phenotyping of the TF-RNAi collection to isolate the best candidates to further detailed molecular and physiological characterization.

METHODS

Mutant selection and in vivo fluorescence-based high-throughput screening.

350 colonies have been screened using fluorescence imaging to identify alterations in growth or in photosynthetic apparatus, as in (Perin et al. 2015). To this aim Wild type (WT) and transformed strains were grown for 5 days on F/2 medium, adding 100µg/ml of zeocin in the case of RNAi lines. Strains resistant to zeocin (ZEO) after transformation with an empty vector were also included as controls in the analysis. All strains were analyzed by *in vivo* fluorescence using a FluorCam FC 800 video-imaging apparatus (Photon Systems Instruments, Brno, Czech Republic). Strains were retained for further analysis if they showed consistent differences from controls in three rounds of screening. In the 3rd round of selection all strains were inoculated from liquid cultures at the same OD_{750} to decrease experimental variability. In this final round the measurements were

done for plates grown in continuous light or photoperiod (16h light/8h dark) to verify the possible dependence of the phenotype from light/dark cycles.

RESULTS

In vivo chlorophyll fluorescence is widely used as a tool to evaluate the efficiency of the photosynthetic apparatus. Once a photon is adsorbed by a chlorophyll molecule the excitation energy can undergo three alternatives pathways: photosynthesis, heat dissipation, or fluorescence. These three pathways compete for the same excitation energy so it is possible to exploit variations in fluorescence to obtain indirect information on the others. In this work we used a video imaging apparatus to measure in vivo fluorescence in order to evaluate if the altered expression of transcriptional factors affected the strains fluorescence. Different parameters were measured: Fluorescence intensity per area (F0/area), PSII quantum yield in dark adapted cells (Qymax) and after 5 minutes of actinic light illumination (Qy'). The former parameter is indicative of the chlorophyll content per cell but is also affected by any genetic modification causing growth alteration also if independent from photosynthesis (see Figure 1). The latter two parameters are instead more specific and are able to evidence eventual major alterations in photosynthetic efficiency (fig 2 and 3).
Selection started from a pool of 350 strains and 37 of them were retained after the first 3 rounds of selection (table 1).

Table 1: Mutant strain selected after 3 round of screening

Transcription factor	Selected mutants	Phenotype
bHLH 1a-KD	4	Growth and Qy' reduction
bHLH 1b-KD	6	Growth alteration
bHLH 2-KD	5	Qymax reduction
bHLH 3-KD	3	Qy' reduction
bHLH 4-KD	4	Growth alteration
bHLH 5-KD	5	Growth alteration
bHLH 6-KD	4	Qy' reduction
bHLH domain KD	6	Altered response to light and dark cycle

The rationale used for the selection was to retain those mutants with clear differences with respect to the wild type considering the reproducibility of the data measured (Perin et al. 2015). We retained also at least a couple of mutants with the same trend of the selected but with a low difference respect to the wild type, in order to avoid the retention of only the extreme phenotypes.

Example of phenotypes selected in shown in fig 2 and 3 clearly shown alteration of parameters given by the altered accumulation of these transcription factor families. Obviously there is a variability in the severity of the phenotype, that probably correlates with the transcriptional level of the transcription factors on various knockdown strains.

The screening data have to be confirmed by growth curves and by transcripts quantification in order to establish if there is effectively a correlation between the severity of the phenotype and the modulation of the TFs transcription.

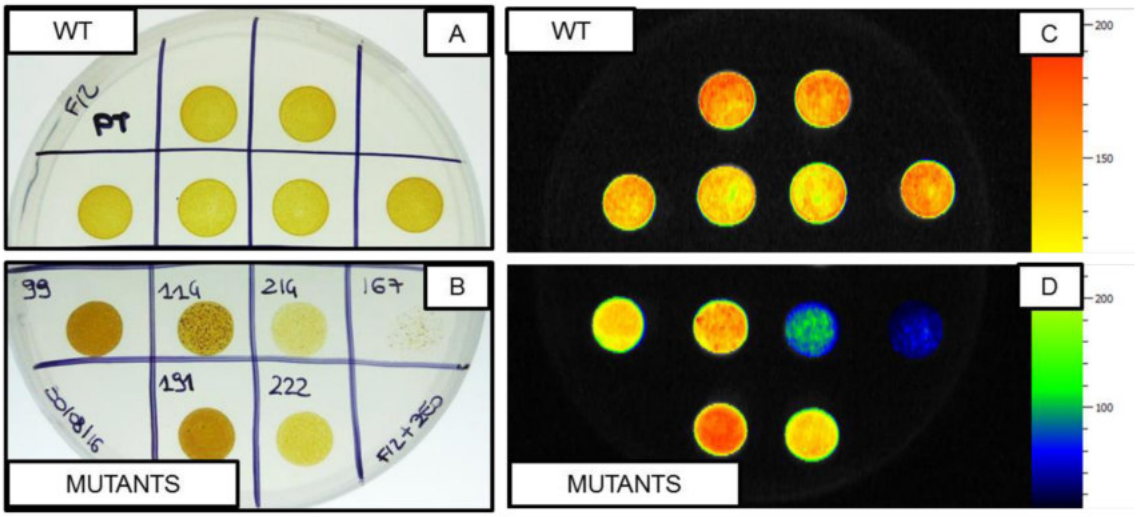

Figure 1: WT and transformed strains after 5 days of growth, inoculated with the same starting OD= 0.2: A- Phaeodactylum tricornutum wild type (WT), B- various KD TP transformed strains, C-F0/area measurement of the wild type and D-F0/area measurement of the mutant strains shown in B.

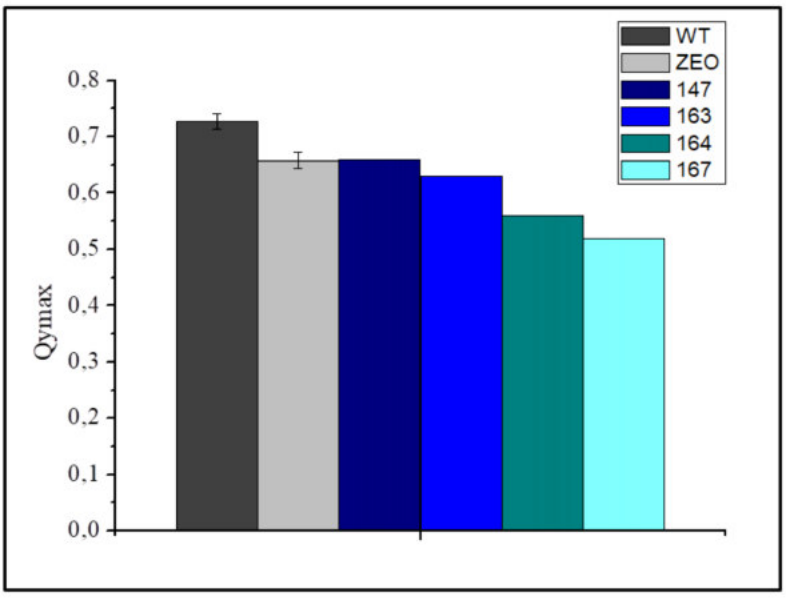

Figure 2: Evaluation of the maximum quantum yield of PSII in the wild type (WT) and different bHLH2 KD lines during the 3rd round of screening. SD in WT and in ZEO resistant lines is the average of 3 colonies.

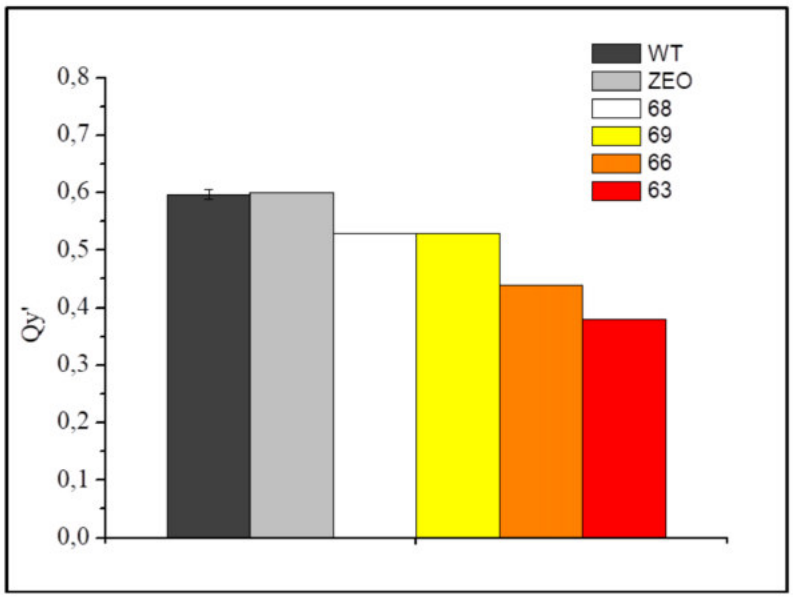

Figure 3: Evaluation of the PSII quantum yield variation in response to the light treatment in the wild type (WT), zeocine resistant lines (ZEO), used as control samples and various bHLH1a KD lines. SD in WT and in ZEO resistant lines is the average of 3 colonies.

These results in any case confirmed the efficiency in the isolation of mutants with a photosynthetic phenotype applying the screening optimized for *N.gaditana*, also to different species.

REFERENCES

Century, Karen, T Lynne Reuber, Oliver J Ratcliffe, and Mendel Biotechnology. 2008. "Regulating the Regulators : The Future Prospects for Transcription-Factor-Based Agricultural Biotechnology Products." *Plant physiology* 147: 20–29.

Perin, Giorgio et al. 2015. "Generation of Random Mutants to Improve Light-Use Efficiency of *Nannochloropsis gaditana* Cultures for Biofuel Production." *Biotechnology for biofuels* 8: 161-174.

Rabara, Roel C, Prateek Tripathi, and Paul J Rushton. 2014. "The Potential of Transcription Factor-Based Genetic." *OMICS* 18(10).

Rayko, Edda et al. 2010. "Transcription Factor Families Inferred from Genome Sequences of Photosynthetic Stramenopiles." *New Phytologist* 188: 52–66.

De Riso, Valentina et al. 2009. "Gene Silencing in the Marine Diatom Phaeodactylum Tricornutum." *Nucleic Acids Research* 37(14).

ABBREVIATIONS

ASII, functional antenna size of PSII
bHLH, basic helix-loop-helix
C, control
Car, carotenoid
CCAP, Culture Collection of Algae and Protozoa
Chl, chlorophyll
DBMIB, dibromothymoquinone
DCMU, 3-(3,4-dichlorophenyl)-1,1-dimethylurea
DMF, N,N'-dimethylformamide
EMS, ethyl methane sulfonate
EPA, eicosapentaenoic acid
ETR, electron transport rate
GMO, genetically modified organism
HL, high light
ID, identifier
LC-PUFA, long chain poly-unsatured fatty acids
LHC, light harvesting complex
LHCX / LHCSR, stress-related light-harvesting complex
LL, low light
ML, medium light
FL, fluctuating light
N, nitrogen
NPQ, non-photochemical quenching
$1O_2$, singlet oxygen
OD, optical density
PAM, pulse-amplitude-modulation
PAR, photosynthetic active radiation
PBR, photobioreactor
PSI, photosystem I
PSII, photosystem II
PSBS, photosystem II subunit S
PUFA, poly-unsatured fatty acids
qE, fast relaxed kinetic of the NPQ (energy dependent NPQ component)
RNAi, RNA interference
ROS, reactive oxygen species
RT, room temperature
RT-PCR, reverse transcriptase polymerase chain reaction
SDS, sodium-dodecyl-sulphate
TAG, triacylglycerol
TEF, total electron flow
TF, transcription factors
TLA, truncated light harvesting
WT, wild type
ZE, zeaxanthin epoxidase
ZEO, zeocin

ACKNOWLEDGMENTS

"L'incontro di due personalità è come il contatto tra due sostanze chimiche; se c'è una qualche reazione, entrambi ne vengono trasformati" (C.Jung)

Ora che questo capitolo volge al termine, ruberò qualche riga per ringraziare tutte le "personalità" che ho incontrato in questi anni. I nomi che ci sono qui hanno dato valore a questo tempo e per questo non posso che dire grazie

Grazie al Prof. Morosinotto, o meglio grazie a Tomas che ha investito tempo e fiducia nel guidarmi in questi anni di dottorato;

Grazie ad Alessandro e Nicoletta per essere stati fonte inesauribile di consigli e sapere in laboratorio, tanto quanto di giornate e serate indimenticabili, fuori dal laboratorio;

Grazie a Giorgio che è stato il mio riferimento costante fin dall'inizio, hai un posto speciale;

Grazie a Diana e Vero perché voi siete state, siete e sarete le mie filles … sempre, il bene che vi voglio è immenso;

Grazie ad Andrea per le sere passate a discutere di qualsiasi cosa. Hai reso il tempo leggero anche nelle giornate più lunghe;

Grazie a Mattia, Mariano, Silvia, Michele, Antonio, Davide e Paola perché siete nel mio cuore, io non posso che essere grata della fortuna che ho avuto nell'incontrarvi;

Grazie a Nicolò, Marco M., Barbara, Simone, Matteo, Raffaella, Marco A, Maddalena, Caterina P, Andrea C, Caterina G, Stefania e a tutti i ragazzi (di sicuro ho saltato qualche nome conoscendomi) che sono passati nel TMslab, con cui abbiamo condiviso un pezzetto di strada. Avete reso questo viaggio indimenticabile;

Grazie ad Anna perché infondo il lab non sarebbe lo stesso senza di lei;

Grazie alla 111 perché hanno reso Padova casa. Le persone belle così sono un regalo;

Grazie a Matteo che è la mia forza;

Grazie a mia sorella che è il mio orgoglio;

E infine ma di certo non per ultimi grazie a mamma, papà che sono la parte migliore di me.